

Some pages of this thesis may have been removed for copyright restrictions.

If you have discovered material in AURA which is unlawful e.g. breaches copyright, (either yours or that of a third party) or any other law, including but not limited to those relating to patent, trademark, confidentiality, data protection, obscenity, defamation, libel, then please read our [Takedown Policy](#) and [contact the service](#) immediately

EXAMINATION VARIABILITY IN SHORT-WAVELENGTH AUTOMATED PERIMETRY.

ROBERT PETER CUBBIDGE

Doctor of Philosophy

THE UNIVERSITY OF ASTON IN BIRMINGHAM

September 1997

This copy of the thesis has been supplied on condition that anyone who consults it is understood to recognise that its copyright rests with the author and that no quotation from the thesis and no information derived from it may be published without proper acknowledgement.

The University of Aston in Birmingham

Examination Variability in Short-Wavelength Automated Perimetry.

Robert Peter Cubbidge

Doctor of Philosophy

1997

The study evaluated sources of within- and between-subject variability in standard white-on-white (W-W) perimetry and short-wavelength automated perimetry (SWAP).

The influence of staircase strategy on the fatigue effect in W-W perimetry was investigated for a 4 dB single step, single reversal strategy; a variable step size, single reversal dynamic strategy; and the standard 4-2 dB double reversal strategy. The fatigue effect increased as the duration of the examination increased and was greatest in the second eye for all strategies. The fatigue effect was lowest for the 4dB strategy, which exhibited the shortest examination time and was greatest for the 4-2 dB strategy, which exhibited the longest examination time. Staircase efficiency was lowest for the 4 dB strategy and highest for the dynamic strategy which thus offers a reduced examination time and low inter-subject variability.

The normal between-subject variability of SWAP was determined for the standard 4-2 dB double reversal strategy and the 3 dB single reversal FASTPAC strategy and compared to that of W-W perimetry. The decrease in sensitivity with increase in age was greatest for SWAP. The between-subject variability of SWAP was greater than W-W perimetry. Correction for the influence of ocular media absorption reduced the between-subject variability of SWAP. The FASTPAC strategy yielded the lowest between-subject variability in SWAP, but the greatest between-subject variability in W-W perimetry. The greater between-subject variability of SWAP has profound implications for the delineation of visual field abnormality.

The fatigue effect for the Full Threshold strategy in SWAP was evaluated with conventional opaque, and translucent occlusion of the fellow eye. SWAP exhibited a greater fatigue effect than W-W perimetry. Translucent occlusion reduced the between-subject variability of W-W perimetry but increased the between-subject variability of SWAP. The elevation of sensitivity was greater with translucent occlusion which has implications for the statistical analysis of W-W perimetry and SWAP.

The influence of age-related cataract extraction and IOL implantation upon the visual field derived by W-W perimetry and SWAP was determined. Cataract yielded a general reduction in sensitivity which was preferentially greater in SWAP, even after the correction of SWAP for the attenuation of the stimulus by the ocular media. There was no correlation between either backward or forward light scatter and the magnitude of the attenuation of W-W or SWAP sensitivity. The post-operative mean deviation in SWAP was positive and has ramifications for the statistical interpretation of SWAP.

Short-wavelength-sensitive pathway isolation was assessed as a function of stimulus eccentricity using the two-colour increment threshold method. At least 15 dB of SWS pathway isolation was achieved for 440 nm, 450 nm and 460 nm stimuli at a background luminance of 100 cdm⁻². There was a slight decrease in SWS pathway isolation for all stimulus wavelengths with increasing eccentricity which was not of clinical significance. Adopting a 450 nm stimulus may reduce between-subject variability in SWAP due to a reduction in ocular media absorption and macular pigment absorption.

short-wavelength automated perimetry, staircase strategy, fatigue effect, age-related cataract, SWS isolation.

To

Patricia, Peter, Julie & Michael

ACKNOWLEDGEMENTS.

I would like to thank my supervisor, Dr John Wild, for his guidance, encouragement and help.

I am also very grateful to the following individuals: Dr John Archer-Hall for his expert assistance in the design and construction of aperture stops for the modified Humphrey Field Analyser; Mrs Rosemary Robinson and Mr Eamon O'Neill for the recruitment of the cataract patients; Mr Derrick Bennett, Mr David Shaw and Mr Mike Hussey for their statistical advice; Mr Ian Pacey for his help in the collection of short-wavelength automated perimetry data for the normal subjects; Professor David Foster for his assistance in obtaining the spectral transmission characteristics of the filters; and Mrs Lynne McCranor for her assistance in the construction of the translucent occluder.

Finally, I am grateful to all the patients and subjects who participated in the clinical studies and to the Department of Vision Sciences, Aston University, for access to the facilities.

	Page
Summary.	2
Dedication.	3
Acknowledgements.	4
List of Contents.	5
List of Figures.	13
List of Tables.	20

LIST OF CONTENTS.

CHAPTER 1. A REVIEW OF AUTOMATED STATIC PERIMETRY.	22
1.1. Introduction.	22
1.2. Historical Perspectives.	23
1.3. Kinetic and Static Stimulus Presentation.	25
1.4. Theoretical and Ergonomic Considerations Related to Perimeter Design.	27
1.4.1. Measurement Units.	28
1.4.2. Dynamic Range and Retinal Adaptation.	28
1.4.3. Stimulus Size and Duration.	31
1.4.4. Stimulus Generation.	33
1.4.5. Bowl Designs.	35
1.5. Examination Strategies.	35
1.5.1. Full Threshold.	35
1.5.2. Suprathreshold.	36
1.5.3. Spatial Configuration of the Test Grid.	38
1.6. Reliability Parameters.	40
1.6.1. Fixation Losses.	40
1.6.2. False-Positive and False-Negative Errors.	42
1.7. Threshold Fluctuation.	43
1.7.1. Short-Term Fluctuation.	43

1.7.2.	Long-Term Fluctuation.	46
1.8.	Graphical Presentation of Perimetric Data.	47
1.8.1.	Numeric Data.	47
1.8.2.	Grey-Scale.	47
1.8.3.	Three-Dimensional Representation.	48
1.8.4.	Probability Plots.	48
1.8.5.	The Glaucoma Hemifield Test.	49
1.8.6.	Bebie Curve.	50
1.9.	Data Reduction of Perimetric Data.	51
1.9.1.	Mean Sensitivity.	51
1.9.2.	Mean Defect and Mean Deviation.	51
1.9.3.	Loss Variance and Pattern Standard Deviation.	53
1.9.4.	Corrected Loss Variance and Corrected Pattern Standard Deviation.	54
1.9.5.	Third Central Moment.	54
1.9.6.	Skewness.	54
1.9.7.	Spatial Correlation.	55
1.9.8.	Defect Volume.	55
1.9.9.	Congruence Index.	55
1.9.10.	Diffuse Loss Index.	56
1.9.11.	Pericecal Index.	56
1.9.12.	Learner's Index.	57
1.10.	Analytical Programs.	57
1.10.1.	STATPAC.	57
1.10.2.	Change Analysis.	58
1.10.3.	Cluster Analysis.	59
1.10.4.	Program DELTA.	59
1.10.5.	PeriData and PeriTrend.	60
1.10.6.	Octosmart.	61
1.10.8.	Artificial Neural Networks.	61

1.11.	Factors Influencing Perimetric Data Acquisition.	63
1.11.1.	Age.	63
1.11.2.	Optical Defocus.	65
1.11.3.	Pupil Size.	65
1.11.4.	Media Opacity.	68
1.11.5.	Pharmacological Agents.	68
1.11.6.	Learning.	68
1.11.7.	Fatigue.	69
CHAPTER 2.	RESEARCH OUTLINE.	70
2.1.	Aims of the Study.	70
2.2.	Rationale.	70
2.3.	Logistics.	73
CHAPTER 3.	THE INFLUENCE OF STAIRCASE STRATEGY ON THE FATIGUE EFFECT IN WHITE-WHITE (W-W) PERIMETRY.	75
3.1.	The Fatigue Effect in Automated Static Perimetry.	75
3.1.1.	Explanation of the Fatigue Effect.	76
3.2.	Staircase Procedures.	77
3.2.1.	Psychophysical Aspects.	77
3.2.2.	Staircase Efficiency.	78
3.2.3.	Standard Perimetry Staircase Strategies.	79
3.2.4.	Fast Perimetry Staircase Strategies.	80
3.2.5.	New Perimetry Threshold Strategies.	83
3.3.	Aims of the Study.	85
3.4.	Materials and Methods.	85
3.4.1.	Sample.	85
3.4.2.	Perimetry.	85
3.4.3.	Statistical Analysis.	90

3.5.	Results.	90
3.5.1.	Global Mean Sensitivity (MS).	90
3.5.2.	Global RMS Short-Term Fluctuation (SF).	90
3.5.3.	Examination Time.	95
3.5.4.	Stimulus Presentations.	95
3.5.5.	Staircase Efficiency (Benefit-Cost).	95
3.6.	Discussion.	100
3.7.	Conclusions.	102
CHAPTER 4.	STAIRCASE STRATEGY VARIABILITY IN SHORT-WAVELENGTH AUTOMATED PERIMETRY.	105
4.1.	Introduction.	105
4.2.	Short-Wavelength Automated Perimetry (SWAP).	106
4.2.1.	SWAP in Ocular Disease.	108
4.3.	The Mechanism of Damage in SWAP.	111
4.3.1.	Selective Nerve Fibre and Ganglion Cell Damage.	111
4.3.2.	S-Cone Vulnerability.	112
4.3.3.	SWS Pathway Redundancy.	113
4.4.	Aims.	114
4.5.	Materials and Methods.	115
4.5.1.	Sample.	115
4.5.2.	Perimetry.	115
4.5.3.	Ocular Media Absorption Assessment.	118
4.5.4.	Forward Light Scatter Assessment.	125
4.5.5.	Statistical Analysis.	127
4.6.	Results.	127
4.6.1.	Mean Sensitivity (MS).	128
4.6.2.	Coefficient of Variation.	137
4.6.3.	Short-Term Fluctuation (SF).	141

4.6.4.	Examination Time.	141
4.6.5.	Stimulus Presentations.	141
4.6.6.	Staircase Efficiency (Benefit-Cost).	147
4.6.7.	Ocular Media Absorption.	147
4.6.8.	Forward Light Scatter.	147
4.7.	Discussion.	152
4.8.	Conclusions.	158
CHAPTER 5. THE INFLUENCE OF EXAMINATION FATIGUE ON SHORT-WAVELENGTH AUTOMATED PERIMETRY.		161
5.1.	Introduction.	161
5.2.	Aims.	161
5.3.	Equipment Modifications.	161
5.4.	Methods.	163
5.4.1.	Perimetry.	163
5.5.	Results.	166
5.5.1.	Global Mean Sensitivity.	166
5.5.2.	Central-Peripheral Mean Sensitivity.	173
5.5.3.	Short-Term Fluctuation.	173
5.5.4.	Examination Time.	173
5.5.5.	Stimulus Presentations.	180
5.6.	Discussion.	180
5.7.	Conclusions.	184
CHAPTER 6. THE INFLUENCE OF AGE-RELATED CATARACT ON SHORT-WAVELENGTH AUTOMATED PERIMETRY.		186
6.1.	Introduction.	186
6.2.	The Normal Human Lens.	186
6.3.	Lens Transparency.	187

6.4.	Ageing of the Human Lens.	187
6.4.1.	Lens Transmission.	188
6.4.2.	Backward Light Scatter.	193
6.4.3.	Forward Light Scatter.	195
6.5.	The Effect of Media Opacity on the Visual Field.	198
6.6.	Aims.	201
6.7.	Sample.	201
6.8.	Perimetry.	202
6.9.	Analysis.	206
6.10.	Results.	206
6.10.1.	Mean Sensitivity (MS).	208
6.10.2.	Mean Deviation (MD_H).	208
6.10.3.	Short-Term Fluctuation (SF).	212
6.10.4.	Pattern Standard Deviation (PSD).	212
6.10.5.	Corrected Pattern Standard Deviation (CPSD).	216
6.10.6.	Ocular Media Absorption.	216
6.10.7.	Forward Light Scatter.	216
6.10.8.	Backward Light Scatter.	223
6.11.	Discussion.	223
6.12.	Conclusions.	226
CHAPTER 7.	QUANTIFICATION OF SHORT-WAVELENGTH SENSITIVITY	
	PATHWAY ISOLATION IN SHORT-WAVELENGTH AUTOMATED	
	PERIMETRY.	227
7.1.	Introduction.	227
7.2.	The Optimum Conditions for SWAP.	233
7.3.	Aims.	235
7.4.	Equipment Modifications and Theoretical Considerations.	235
7.4.1.	Aperture Stop Construction.	239

7.5.	Materials and Methods.	243
7.5.1.	Sample.	243
7.5.2.	Perimetry.	243
7.5.3.	Pre-Receptorial Absorption.	246
7.6.	Results.	250
7.7.	Discussion.	257
7.8.	Conclusions.	262
 CHAPTER 8. SUMMARY OF RESULTS AND CONCLUSIONS AND FUTURE WORK.		 263
8.1.	Summary of Research and Conclusions.	263
8.1.1.	The Influence of Staircase Strategy on the Fatigue Effect in W-W Perimetry.	263
8.1.2.	Staircase Strategy Variability in Short-Wavelength Automated Perimetry.	263
8.1.3.	The Influence of Examination Fatigue on Short-Wavelength Automated Perimetry.	264
8.1.4.	The Influence of Age-Related Cataract on Short-Wavelength Automated Perimetry.	265
8.1.5.	Quantification of Short-Wavelength Sensitive Pathway Isolation in Short-Wavelength Automated Perimetry.	266
8.2.	Future Work.	266
8.2.1.	The Influence of Staircase Strategy on the Fatigue Effect in W-W Perimetry.	266
8.2.2.	Short-Wavelength Automated Perimetry.	267
 REFERENCES.		 270

APPENDIX.

313

A.1. Supporting Publications.

313

LIST OF FIGURES.	Page
1.1. The hill of vision.	26
1.2. Hypothetical frequency-of-seeing curve and scatter around the threshold.	37
1.3. A schematic model of an artificial neural network applied to visual field diagnosis.	62
3.1. The Octopus 1-2-3 perimeter.	86
3.2. Diagram illustrating the right eye spatial location of the stimuli in each Stage of Program G1X.	88
3.3. Group mean of the mean sensitivity as a function of Stage and Phase for the first and second eyes. Error bars represent ± 1 standard error of the mean.	91
3.4. Group mean short-term fluctuation as a function of Stage for the second Phase of the first and second eyes. Error bars represent ± 1 standard error of the mean.	93
3.5. Group mean examination time as a function of Stage and Phase for the first and second eyes. Error bars represent ± 1 standard error of the mean.	96
3.6. Group mean of the mean number of stimulus presentations at each location as a function of stage and phase for the first and second eyes. Error bars represent ± 1 standard error of the mean.	97
3.7. Group mean strategy efficiency as a function of Stage for the second Phase of the first and second eyes. Error bars represent ± 1 standard error of the mean.	98
4.1. The Humphrey Field Analyser 640.	117
4.2. Spectral radiance as a function of wavelength for the 440 nm narrowband stimulus and the broadband yellow background utilised in the commercially available SWAP. The yellow background transmits visible wavelengths above 530 nm.	119
4.3. Spectral radiance as a function of wavelength for the 410 nm and the 560 nm narrowband stimuli employed in the assessment of ocular media absorption.	121

4.4.	The forward light scatter meter and a schematic diagram of the principles of measurement.	126
4.5.	Univariate linear regression of mean sensitivity for Program 30-2 as a function of age for the Full Threshold and FASTPAC strategies in W-W perimetry and SWAP without correction for with absorption and with correction. Note that the dB scales between W-W perimetry and SWAP are not equivalent.	131
4.6.	Univariate linear regression at each individual stimulus location for Program 30-2 as a function of age (dB per year) for the Full Threshold and FASTPAC strategies in W-W perimetry and SWAP without correction for ocular media absorption and with correction. Note that the dB scales between W-W perimetry and SWAP are not equivalent.	132
4.7.	Decibel loss per decade as a function of visual field sector for Program 30-2 for the Full Threshold and FASTPAC strategies in W-W perimetry and SWAP without correction for absorption and with correction. Note that the dB scales between W-W perimetry and SWAP are not compatible.	133
4.8.	Group mean sensitivity at each individual stimulus location of Program 30-2 (± 1 standard deviation) for the Full Threshold and FASTPAC strategies in W-W perimetry and SWAP without correction for absorption and with correction. Note that the dB scales between W-W perimetry and SWAP are not compatible.	134
4.9.	One standard deviation of the group mean sensitivity at each individual stimulus location for Program 30-2 of the young group and the old group, for the Full Threshold and FASTPAC strategies in W-W perimetry and SWAP without correction for absorption and with correction.	136
4.10.	Mean sensitivity as a function of visual field sector for Program 30-2 for the Full Threshold and FASTPAC strategies in W-W perimetry and SWAP without correction for absorption and with correction. Error bars represent ± 1 standard error of the mean. Note that the dB scales between W-W perimetry and SWAP are not compatible.	139

4.11.	One standard deviation of the group mean sensitivity (ie the within-test, between-individual variation in sensitivity) at each stimulus location for Program 30-2 for the Full Threshold and FASTPAC strategies for W-W perimetry and SWAP without correction for absorption and with correction. Note that the dB scales between W-W perimetry and SWAP are not equivalent.	140
4.12.	The coefficient of variation (%) at each individual stimulus location for Program 30-2 for the Full Threshold and FASTPAC strategies for W-W perimetry and SWAP without correction for absorption and with correction.	141
4.13.	Univariate linear regression of examination time for Program 30-2 as a function of age for the Full Threshold and FASTPAC strategies in W-W perimetry and SWAP.	145
4.14.	Univariate linear regression of the number of stimulus presentations as a function of age for the Full Threshold and FASTPAC strategies in W-W perimetry and SWAP.	147
4.15.	Univariate linear regression of ocular media absorption, scaled to 440 nm, as a function of age.	151
4.16.	Univariate linear regression of forward light scatter as a function of age for the three glare angles investigated (3.5°, 10°, and 28°).	152
5.1.	The translucent occluder.	162
5.2.	Summary of the spot photometer measurements to calculate the log unit reduction in luminance when viewing through the translucent occluder.	164
5.3.	The spatial arrangement of the stimulus locations of the custom program (right eye). Diamonds indicate the seed locations.	165
5.4.	Group mean global mean sensitivity as a function of stage for W-W perimetry and SWAP with opaque and translucent occlusion.	167
5.5.	One standard deviation of the group mean sensitivity at each individual stimulus location as a function of stage for W-W perimetry and SWAP with	

	opaque and translucent occlusion. Note that the dB scales between W-W perimetry and SWAP are not compatible.	171
5.6.	Diagram illustrating the spatial arrangement of the division of the visual field into central (inner ring) and peripheral sectors.	174
5.7.	Group mean central and peripheral mean sensitivity as a function of stage for W-W perimetry and SWAP with opaque and translucent occlusion.	175
5.8.	Group mean short-term fluctuation as a function of stage for W-W perimetry and SWAP with opaque and translucent occlusion.	177
5.9.	Group mean examination time as a function of stage for W-W perimetry and SWAP with opaque and translucent occlusion.	178
5.10.	Group mean number of stimulus presentations as a function of W-W perimetry and SWAP with opaque and translucent occlusion.	181
6.1.	Diagram illustrating the sources of light loss in the crystalline lens.	189
6.2.	Spectral transmission as a function of wavelength for the Allergan, IOLAB and Rayner intraocular lenses. Reproduced using data provided by the manufacturers.	204
6.3.	Pre- and post-operative mean sensitivity as a function of cataract severity and type. A slope of unity representing equality between the two measurements is illustrated for reference. Note that the dB scales between W-W perimetry and SWAP are not compatible.	209
6.4.	Pre- and post-operative mean deviation as a function of cataract severity and type. A slope of unity representing equality between the two measurements is illustrated for reference. Note that the dB scales between W-W perimetry and SWAP are not compatible.	210
6.5.	Post-operative change in mean deviation for SWAP against that for W-W perimetry, SWAP uncorrected for ocular media absorption, and SWAP corrected for ocular media absorption. A slope of unity representing equality between the two measurements is illustrated for reference.	211

6.6.	Group numeric total deviation pre- and post-operatively for W-W perimetry, and SWAP uncorrected, and corrected for ocular media absorption scaled to 440 nm.	213
6.7.	Pre- and post-operative short-term fluctuation as a function of cataract severity and type. A slope of unity representing equality between the two measurements is illustrated for reference. Note that the dB scales between W-W perimetry and SWAP are not compatible.	214
6.8.	Pre- and post-operative pattern standard deviation as a function of cataract severity and type. A slope of unity representing equality between the two measurements is illustrated for reference. Note that the dB scales between W-W perimetry and SWAP are not compatible.	215
6.9.	Pre- and post-operative corrected pattern standard deviation as a function of cataract severity and type. A slope of unity representing equality between the two measurements is illustrated for reference. Note that the dB scales between W-W perimetry and SWAP are not compatible.	217
6.10.	Pre- and post-operative absorption scaled to 440 nm as a function of cataract severity and type. A slope of unity representing equality between the two given absorption measurements is illustrated for reference.	218
6.11.	Relationship between change in mean deviation and isolated cataract straylight parameter for W-W perimetry and SWAP, without correction for ocular media absorption and with correction, as a function of cataract severity and type. Note that the dB scales between W-W perimetry and SWAP are not compatible.	220
6.12.	Relationship between pre-operative mean deviation and isolated cataract straylight parameter for W-W perimetry and SWAP as a function of cataract severity and type. Note that the dB scales between W-W perimetry and SWAP are not compatible.	221
6.13.	Relationship between post-operative mean deviation and isolated cataract straylight parameter for W-W perimetry and SWAP as a function of cataract	

	severity and type. Note that the dB scales between W-W perimetry and SWAP are not compatible.	222
7.1.	Stiles displacement rules.	230
7.2.	Humphrey Field Analyser 640 showing the modifications for SWAP and macular pigment absorption assessment, and the stimulus filter holder which is attached to the projection arm of the perimeter.	236
7.3.	Schematic diagram of the auxiliary lighting unit fitted to the modified Humphrey Field Analyser and the ten aperture stops used to modify the background luminance.	237
7.4.	Spectral radiance as a function of wavelength for the Schott OG530 filter in combination with the infra-red absorbing filter. Visible wavelengths above between 530 nm are transmitted and wavelengths above 700 nm are absorbed.	238
7.5.	Reduction in luminance of the upper and lower auxiliary lighting units resulting from the insertion of the aperture stops within the optical path, and the mean reduction in luminance from the combination of the auxiliary lighting units.	244
7.6.	Spatial configuration of the test grid (left eye).	245
7.7.	Spectral radiance as a function of wavelength for the 440 nm, 450 nm and 460 nm narrowband stimulus filters.	247
7.8.	Spectral radiance as a function of wavelength for the broadband red background in combination with the infra-red absorbing filter, and the 570 nm narrowband stimulus filter employed in the assessment of macular pigment absorption. The broadband background transmits visible wavelengths above 645 nm and the infra-red filter absorbs wavelengths beyond 700 nm.	249
7.9.	Group mean threshold versus intensity curves at the fovea for the 440 nm, 450 nm and 460 nm stimuli. Error bars represent ± 1 SD of the mean. Dotted lines represent the magnitude of SWS pathway isolation at 100 cdm ² .	251
7.10.	Group mean threshold versus intensity curves at 2.2 degrees eccentricity for	

	the 440 nm, 450 nm and 460 nm stimuli. Error bars represent ± 1 SD of the mean. Dotted lines represent the magnitude of SWS pathway isolation at 100 cdm^{-2} .	252
7.11.	Group mean threshold versus intensity curves at 5 degrees eccentricity for the 440 nm, 450 nm and 460 nm stimuli. Error bars represent ± 1 SD of the mean. Dotted lines represent the magnitude of SWS pathway isolation at 100 cdm^{-2} .	253
7.12.	Group mean threshold versus intensity curves at 10 degrees eccentricity for the 440 nm, 450 nm and 460 nm stimuli. Error bars represent ± 1 SD of the mean. Dotted lines represent the magnitude of SWS pathway isolation at 100 cdm^{-2} .	254
7.13.	Group mean threshold versus intensity curves at 15 degrees eccentricity for the 440 nm, 450 nm and 460 nm stimuli. Error bars represent ± 1 SD of the mean. Dotted lines represent the magnitude of SWS pathway isolation at 100 cdm^{-2} .	255
7.14.	Group mean threshold versus intensity curves at 20 degrees eccentricity for the 440 nm, 450 nm and 460 nm stimuli. Error bars represent ± 1 SD of the mean. Dotted lines represent the magnitude of SWS pathway isolation at 100 cdm^{-2} .	256
7.15.	Univariate linear regression of group mean SWS pathway isolation at the standard background luminance of 100 cdm^{-2} as a function of stimulus eccentricity for the 440 nm, 450 nm and 460 nm narrowband stimuli. Error bars represent ± 1 SD of the mean.	258

LIST OF TABLES.	Page
3.1. Protocols determining the order of perimetry.	89
3.2. Repeated measures Analysis of Covariance summary table for mean sensitivity.	92
3.3. Repeated measures Analysis of Covariance summary table for the short-term fluctuation.	94
3.4. Efficiency ratios for the 4 dB and dynamic strategies relative to the standard 4-2-1 dB strategy.	99
4.1. Physiological and anatomical identity of the ganglion cell types in the primate retina.	107
4.2. Summary table of the examination protocols assigned to each subject (Std is the Full Threshold, 4-2 dB double reversal staircase strategy, and FP is the FASTPAC, 3 dB single reversal strategy).	116
4.3. Global mean visual field indices (± 1 standard deviation) for the Full Threshold and FASTPAC strategies in W-W perimetry and SWAP. Note that the dB scales between W-W perimetry and SWAP are not compatible.	129
4.4. Summary table for Analysis of Variance of mean sensitivity.	130
4.5. Summary table for Analysis of Variance of the short-term fluctuation.	143
4.6. Summary table for Analysis of Variance of examination time.	144
4.7. Summary table for Analysis of Variance of stimulus presentations.	146
4.8. Summary table for Analysis of Variance of efficiency (benefit-cost).	149
4.9. Benefit-Cost ratios for W-W perimetry and SWAP for the Full Threshold strategy and FASTPAC. Note that the decibel scales between W-W perimetry and SWAP are not compatible.	150
5.1. Percentage decrease in global mean sensitivity with respect to the first stage of each eye, and with respect to the first stage of the second eye for W-W perimetry and SWAP.	169

5.2.	Group mean binocular summation ratios as a function of stage for W-W perimetry and SWAP.	170
5.3.	Percentage decrease of peripheral mean sensitivity compared to central mean sensitivity as a function of stage for W-W perimetry and SWAP.	176
5.4.	Proportionate decrease in examination time (%), with respect to the first stage of each eye and with respect to the first stage of the second eye.	179
5.5.	Proportionate decrease in the group mean number of stimulus presentations (%), with respect to the first stage of each eye and with respect to the first stage of the second eye.	182
6.1.	Group mean pre- and post-operative visual field indices (± 1 standard error). Note that the decibel scales between W-W perimetry and SWAP are not compatible.	207
6.2.	Group mean pre- and post-operative forward light scatter and isolated cataract straylight parameter (± 1 standard error).	219
7.1.	Summary of the characteristics of each individual foveal pi-mechanism.	229
7.2.	Summary of background and stimulus parameters employed for SWAP.	234
7.3.	Summary of the calculations used for the construction of aperture stops.	242
7.4.	Group mean ocular media and macular pigment absorption (± 1 standard deviation).	259

CHAPTER 1. A REVIEW OF AUTOMATED STATIC PERIMETRY.

1.1. Introduction.

Schober (1958) differentiated three concepts; the "object field" which corresponds to the image area on the retina in objective space, the "seen field" representing the subjective perception of the environment, and the "visual field" which characterises physiological excitation of the retina. Clinically however, the visual field is perhaps better defined as all the space that an eye can see at any given time. It has been likened to an island of vision surrounded by a sea of blindness (Traquair 1938).

The peak of the island, or hill of vision, represents maximum sensitivity to light and corresponds to the fovea. The hill declines towards the sea, representing the decrease in light sensitivity towards the periphery of the visual field. The slope of the hill is less steep temporally compared to the nasal side. A physiological blind spot, approximately 5.5° wide and 7.5° high, exists 15° temporal to fixation and 1.5° below the horizontal meridian (Reed and Drance 1972). The blind spot arises due to the convergence of the retinal nerve fibres at the optic nerve head, an area devoid of photoreceptors. The monocular visual field extends to 60° superiorly and nasally, 75° inferiorly, and 100° temporally (Anderson 1992). This area is termed the relative field as it is limited by the orbital bones and the nose. The absolute field is found by moving the head, without altering fixation, to eliminate the constraints of facial anatomy. In perimetry, the monocular central visual field is conventionally defined as the visual field extending out to thirty degrees or less from fixation. The field extending greater than thirty degrees from fixation is defined as the peripheral visual field.

The requirement of the visual field examination is to assess the integrity of the hill of vision. This is accomplished by measuring the minimum light energy necessary to evoke a visual response, defined as the differential light threshold or increment threshold. The reciprocal of the differential light threshold is defined as sensitivity. Departure of the topography of the hill of vision from normal limits represents abnormality in the visual field. An area of reduced sensitivity surrounded by an area of normal sensitivity is termed a relative scotoma. In an

absolute scotoma there is no light perception. A scotoma may also be described as focal loss. An overall loss in sensitivity of the field is termed a depression, or alternatively diffuse loss, whereas loss of the peripheral boundary of the visual field is termed a contraction. Depending upon the site of damage in the visual pathway, characteristic visual field defects are produced. A complete defect in one quadrant of the visual field is termed a quadrantanopia; a complete defect involving one half of the visual field is termed a hemianopia. Hemianopic visual field deficits can either be homonymous or heteronymous. In homonymous visual field defects, the hemianopia affects the same side of the visual field in both eyes. However, in heteronymous hemianopia opposite sides of the visual field are affected. Congruence describes the symmetry of the hemianopias between eyes.

1.2. Historical Perspectives,

The historical foundations of visual field measurement date back to the ancient world. It has been postulated that the biblical story of David slaying Goliath can be interpreted by David's discovery that Goliath had constricted visual fields resulting from pituitary adenoma, a condition associated with gigantism (Griffin 1980). Hippocrates in the 5th Century BC described hemianopic visual field defects deriving from brain disease. Ptolemy in 150 AD is attributed with the first documented measurement of the visual field, although the instrumentation he used is unknown (Atchison 1979), and Galen in the 2nd century AD described central scotomata and constriction of the visual field (Bynke 1983). The physiological blind spot was detected in 1668 by Mariotte (Bynke 1983). Until the mid 19th Century, these phenomena remained little more than scientific observations.

Albrecht von Graefe (1856) was the first to investigate visual fields for the purpose of clinical diagnosis in ocular disease. The instrumentation consisted of a flat blackboard held by the patient and a small piece of chalk on a wire acting as a stimulus. Using this method, he was able to identify small scotomata and hemianopic field defects. The discovery by Aubert and Förster (1857) that the visual field is elliptical in nature and that the extent of the visual field depends upon the angular subtense at the eye led to the introduction of the first commercially

available arc perimeter by Förster in 1869. The practise of perimetry subsequently became widespread during the latter part of the 19th Century.

During the early 20th Century, fundamental developments took place which further advanced the theoretical concepts of perimetry and established it's foundation as a clinical science. Rønne introduced quantitative isopter perimetry in 1909. Ferree and Rand (1922) developed an arc perimeter in which the background and stimulus parameters were carefully controlled. Lauber (1932) and Hartinger (1936) introduced projection perimetry whereby the stimulus could be varied in luminance by the use of filters placed in the optical path of the stimulus. Goldmann (1945a, b) introduced the first bowl perimeter in which the background facilitated a constant state of retinal adaptation throughout the visual field. The instrument incorporated a standardised set of target sizes, together with a calibration system which ensured constant stimulus luminance, and a fixation monitoring device. However, despite this standardisation, the kinetic movement of the stimulus resulted in a high degree of variability arising from both the patient and the examiner.

Sloan (1939) measured contrast sensitivity across the visual field and in the process pioneered static perimetry. Harms and Aulhorn (1959) standardised the conditions for static perimetry in their Tübinger perimeter. Static perimetry had been shown to be a more accurate perimetric technique, (Drance et al 1967; Armaly 1971; Aulhorn and Harms 1967; Greve and Verduin 1977) but was slow to gain acceptance because it was time consuming to perform manually. With the advent of relatively inexpensive and portable computers in the mid 1960's interest developed in the automation of static perimetry. The earliest research into automation centred on computer analysis of the theoretical sensitivity distribution of the visual field (Fankhauser et al 1972). As a result of this work, the first commercially available automated perimeter, the Octopus, was introduced in 1976 (Fankhauser et al 1977). Other innovative perimeters were developed throughout the 1970's but they failed to gain widespread acceptance (Heijl and Krakau 1975a, b; Keltner et al 1979; Greve 1980). During this time further research into the theoretical principles of automated static perimetry was being undertaken (Spahr 1975; Krakau 1978; Fankhauser 1979). In 1985, a new automated

perimeter was introduced, the Humphrey Visual Field Analyser (Heijl 1985) which has become the most widespread automated perimeter in use at present.

1.3. Kinetic and Static Stimulus Presentation.

The principles of kinetic and static perimetry are illustrated in Figure 1.1.

In kinetic perimetry, a circular stimulus of constant luminance is moved towards the hill of vision from non-seeing to seeing until it is seen by the centrally fixating patient. A map is constructed by establishing the distance from fixation that the eye first responds to each of several sizes of stimuli. Lines joining points of equal sensitivity are called isopters. The isopters are analogous to contour lines. In an eye possessing normal sensitivity, small and/or dim stimuli are detected close to the point of fixation, whilst the periphery of the visual field can only detect relatively larger and/or brighter stimuli. In the normal eye, any point within an isopter is supraliminal, ie above threshold, unless the isopter encloses the physiological blind spot. In static perimetry, a circular stimulus of fixed position in the visual field is varied in luminance and/or size until it is detected by the patient. Many positions in the visual field are examined in order to generate a sensitivity profile of the hill of vision.

The kinetic technique has been shown to suffer from a number of limitations. A moving stimulus will be detected more peripherally than a static stimulus because of successive lateral spatial summation which may also result in shallow focal losses being missed (Greve 1973). The magnitude of successive lateral spatial summation is also dependant upon the position in the visual field and upon the sensitivity gradient. Thus, the threshold value for every position is subject to Intra-individual error (Greve 1973). The position of the isopters in kinetic perimetry are subject to influence by patient reaction time (Lynn 1969). Some automated static perimeters have been modified to perform kinetic perimetry (Lynn et al 1991). This has standardised the stimulus velocity but the visual field outcome is still influenced by inter-individual reaction time. The choice of stimulus velocity is equivocal. Greve (1973) suggested a stimulus velocity of 2° per second for the central visual field and 5° for the periphery. Johnson and Keltner (1987) found the optimal stimulus velocity to be 4° per second. It has

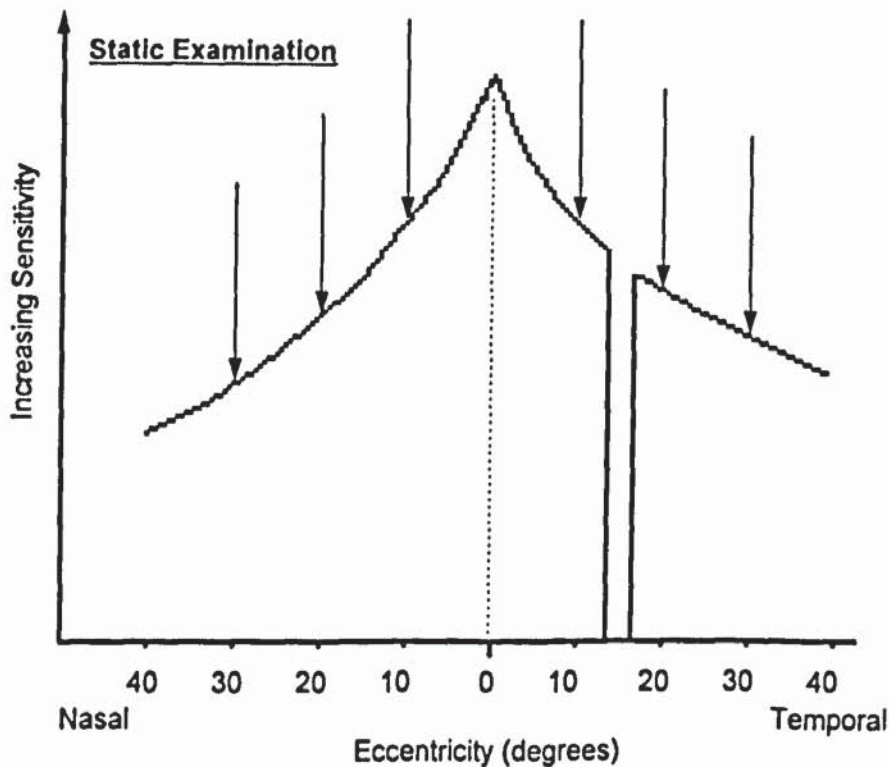
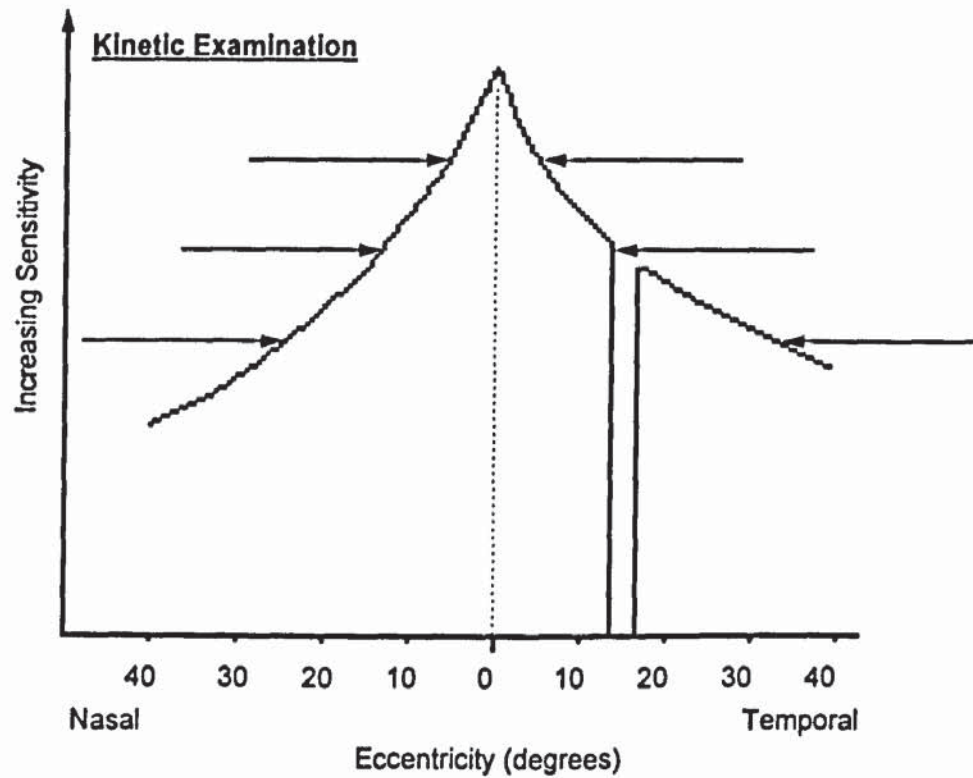


Figure 1.1. The Hill of Vision. In kinetic perimetry (top) a stimulus of fixed luminance is moved towards the hill of vision until it is perceived. Using different stimulus sizes it is possible to construct a contour map of the hill. In static perimetry (bottom) a stimulus of fixed size and location in the visual field is presented at increasing levels of luminance until it is perceived. In this method of testing, a sensitivity profile of the hill of vision is generated.

been suggested that kinetic visual field testing is the method of choice when investigating residual function and in defining areas in the visual field with deep focal loss (Greve 1973; Klewin and Radius 1987).

Static perimetry is independent of the reaction time of the patient and of stimulus velocity (Greve 1975; Trope and Britton 1987). Because manual static perimetry is time consuming, it was not until the advent of automation that thresholds at large numbers of stimulus locations could be obtained within an acceptable time period. Automated static perimetry is more sensitive at detecting visual field loss than manual perimetry (Schmied 1980). Static perimetry is a more sensitive technique than kinetic perimetry for evaluating small isolated areas of focal loss in glaucomatous patients (Drance et al 1967; Armaly 1971, Aulhorn and Harms 1967; Greve and Verduin 1977).

A combination of static and kinetic visual field testing has been advocated by some workers, particularly in glaucoma where between 4% and 11% of patients with a normal central field manifest a glaucomatous peripheral field defect (Aulhorn and Harms 1967; Greve 1973; Miller et al 1989; Ballon et al 1992).

Physiological statokinetic dissociation (SKD) describes a reduced sensitivity to a static perimetric stimulus relative to an identical kinetic stimulus. Hudson and Wild (1992) evaluated this phenomenon in automated perimetry using the Humphrey Field Analyser with Goldmann size I and II stimuli, and a kinetic stimulus velocity of 4 degrees per second. The magnitude of SKD was such that the kinetic technique overestimated the static perimetric profile by approximately 4 dB.

1.4. Theoretical and Ergonomic Considerations Related to Perimeter Design.

A number of principles are fundamental to the interpretation of visual field data for both manual and automated perimetry. These principles have been incorporated into the design of modern-day perimeters and influence the outcome of the visual field examination.

1.4.1. Measurement Units.

The measurement unit used in static perimetry is called the decibel (dB). A value of 0 dB corresponds to the maximum stimulus luminance. Increasing sensitivity is denoted by an increasing value in decibels. One decibel is equal to 0.1 log unit; accordingly 10 dB is equal to a 1 log unit and 20 dB is equal to a 2 log unit attenuation of the maximum possible stimulus luminance (ie a 10-fold and a 100-fold reduction). Sensitivity in dB can be represented by the equation:

$$\text{Sensitivity (dB)} = k + 10 \log \left(\frac{L}{\Delta L} \right) \quad \text{Eqn 1.1.}$$

In the Humphrey Field Analyser, $L = 10 \text{ cdm}^{-2}$ (31.5 asb), and the maximum stimulus luminance, $\Delta L = 3183 \text{ cdm}^{-2}$ (10,000 asb). Thus the constant, $k = 25$. In the Octopus bowl perimeter $k = 24$, in the Octopus 1-2-3, $k = 21$, and in the Dicon $k = 25$.

Because of the variations in the background and maximum stimulus luminances between perimeters, decibels are relative units and cannot be easily compared between instruments. Derivation of conversion formulae between perimeters for thresholds and visual field indices is traditionally derived from empirical data because of the complexity in predicting threshold equivalence theoretically. Anderson and co-workers (1989) compared test patterns with the same spatial configuration in the Dicon, Humphrey Field Analyser, and Octopus perimeters (central threshold, 30-2 and P32 programs respectively) and found the Dicon-Octopus difference to be 3.5 dB, the Dicon-Humphrey difference 6.5 dB, and the Octopus-Humphrey difference to be 3.3 dB. Zeyen et al (1995) derived formulae for conversion between threshold values and visual field indices measured with the Octopus G1X and Humphrey Field Analyser 24-2 programs. They found a 2.2 ± 1.7 dB difference in mean sensitivities between perimeters. Additionally, Wong and associates (1995) found a Dicon-Humphrey difference of 2.47 dB when the FASTPAC threshold algorithm was employed in the Humphrey Field Analyser.

1.4.2. Dynamic Range and Retinal Adaptation.

Fankhauser (1979) defined the dynamic range of a perimeter as "the measurement range over which the neurovisual system can be tested, using specific equipment with a given set of

experimental variables". A large dynamic range is desirable as it facilitates investigation of defect depth within the visual field.

In perimetry, contrast is defined as $\Delta L/L$ is the measure most commonly used for luminance difference threshold. Sensitivity is defined as $L/\Delta L$ where ΔL is the minimum light energy necessary to evoke a visual response and L is the background luminance. The background determines the state of retinal adaptation and therefore influences ΔL . The dynamic range corresponds to the range of the maximum stimulus luminance of the perimeter, and the threshold stimulus luminance of an eye with normal sensitivity (Fankhauser 1979). The Humphrey Field Analyser employs a maximum stimulus luminance of 3183 cdm^{-2} (10,000 asb). The Octopus bowl perimeter and the Octopus 1-2-3 employ stimulus luminances of 318 and 1273 cdm^{-2} (1,000 and 4,000 asb) respectively.

It would seem reasonable to make an assumption that maximising stimulus luminance and minimising background luminance will result in maximum dynamic range. However, very high stimulus luminances result in light scatter around the boundaries of the stimulus (Wilson 1967; Fankhauser and Haerberlin 1980; Dengler-Harles et al 1990; Fankhauser et al 1992). Straylight within the eye and the limitations of the neural system further reduce the efficacy of the stimulus.

Reducing the background, L , increases the dynamic range. Indeed, Fankhauser (1979) found a 5 dB increase in dynamic range when the background luminance was decreased from 10 cdm^{-2} to 1.3 cdm^{-2} . Over an extensive range of luminances the threshold, ΔL , is related to the background intensity, L , by the equation:

$$\frac{\Delta L}{\Delta L_0} = \left(1 + \frac{L}{L_D}\right)^n \quad \text{Eqn 1.2.}$$

where; ΔL_0 , is the absolute threshold, L_D , is a constant, and the exponent, n , has a value between 0.5 and 1. Under photopic conditions, the exponent, n , approaches unity and the increment threshold is said to exhibit Weber Law behaviour. When the exponent, n , is equal to 0.5, the increment threshold obeys the de Vries-Rose Law.

The range of background luminances over which the de Vries-Rose or Weber Law behaviour applies in perimetry is equivocal. Klewin and Radius (1986) found Weber's Law to be most appropriate out to 30° eccentricity, although this finding is disputed by Fankhauser (1986). Weber Law behaviour was also thought to be valid in earlier studies by Aulhorn and Harms (1972) and Greve (1973). However, Fankhauser (1979) showed that the de Vries-Rose Law applied between 1.3 cdm² and 10 cdm² which are the background luminances employed in the Octopus and Dicon perimeters and the Humphrey Field Analyser. Investigations into light and dark adaptation by Barlow (1972), concluded that the background luminances at which Weber's Law and the de Vries-Rose Law are valid show considerable overlap. This conclusion was supported by Flanagan et al (1991) who found that out to 30° eccentricity the de Vries-Rose Law was operative at background luminances of between 1 cdm² and 100 cdm² for Goldmann stimuli sizes I (0.108°), III (0.431°), and V (1.724°). However, for a Goldmann size I stimulus the Law was only true if the stimulus was corrected for the Stiles-Crawford effect at fixation. Weber Law behaviour occurred at background luminances at or above 10 cdm² for Goldmann sizes III and V only.

Adaptation levels which differ from those employed in commercial perimeters have been evaluated in the investigation of ocular disease. Moore et al (1992) demonstrated deeper and more extensive visual field loss in patients with retinitis pigmentosa using scotopic perimetry compared with standard photopic Goldmann perimetry. Drum and co-workers (1986) considered scotopic perimetry a more sensitive technique for the detection of early glaucomatous field loss. Localised scotomata were of equal depth in photopic and scotopic perimetry, but scotopic diffuse loss was greater than photopic diffuse loss by a factor of 2:1 log units. Denis et al (1993) employed a background luminance in the low mesopic range (0.1 cdm²) and were able demonstrate subtle glaucomatous defects which were not present with conventional Goldmann perimetry.

Wilson (1967) demonstrated abnormal spatial summation characteristics in pre-geniculate lesions, spatial and temporal summation abnormalities in post-geniculate lesions when employing a photopic (215 cdm²) adaptation level. In the early stages of third neurone disease

and glaucoma, Shiga (1968) found isopter depression when employing background luminances of 70 cdm⁻² and 223 cdm⁻² compared to isopter enlargement found in normal controls. Elenius and Leinonen (1986) demonstrated visual field loss in progressive cone dysfunction at a background luminance of 200 cdm⁻² which was not present at 10 cdm⁻². However, in glaucoma, Åsman and Heijl (1988) were unable to demonstrate any measurable difference in the magnitude of visual field loss at background luminances of 1, 10 and 100 cdm⁻².

1.4.3. Stimulus Size and Duration.

The effects of spatial and temporal summation on stimulus detection also influence the dynamic range, although to a lesser degree than retinal adaptation.

Spatial Summation.

Spatial summation is defined by Ricco's Law (1887) which assumes complete summation:

$$\Delta L = kA \quad \text{Eqn 1.3.}$$

where ΔL is the increment threshold, k is a constant, and A is the area of the stimulus in degrees squared. The extent to which Ricco's Law applies varies according to the eccentricity of the stimulus, being approximately 30 minutes of arc in the parafoveal region and increasing to 2° at an eccentricity of 35° (Hallett et al 1962). However, Sakitt (1971) suggests that summation may not be complete in these areas. Spatial summation is therefore better described by Piper's Law:

$$\Delta L = kA^{0.5} \quad \text{Eqn 1.4.}$$

Increasing the stimulus size has been shown to result in an increase in dynamic range (Fankhauser 1979; Heijl 1985; Choplin et al 1990). Fankhauser (1979) showed that increasing the stimulus diameter from Goldmann size I to III increased the dynamic range by approximately 12 dB at 50° and 4 dB at fixation, when using a background luminance of 1.27 cdm⁻². The combined effects of reducing background luminance from 12.7 cdm⁻² to 1.27 cdm⁻² and increasing the target size from Goldmann size I to III produced a 17 dB increase in dynamic range at 50° eccentricity.

The Goldmann size III stimulus has become the standard for automated static perimetry. A size III stimulus was selected rather than the size I stimulus employed in kinetic perimetry because it has been shown to be more resistant to the effects of optical defocus (Fankhauser et al 1972; Heijl 1985; Atchison 1987), and lenticular opacity (Radius 1978; Fankhauser 1979; Greve 1980; van den Berg et al 1987; Wood et al 1987a). The use of stimulus sizes other than the Goldmann size III have been advocated by some workers. Zalta and Burchfield (1990) demonstrated significantly greater sensitivity for the Goldmann size I stimulus in the detection of small shallow scotomata when compared to the size III stimulus. Larger stimulus sizes have been shown to be of use in extending the dynamic range of the perimeter in end-stage glaucoma when absolute defects are found using a size III stimulus (Zalta 1991). Use of stimuli smaller than size III result in an increased short-term fluctuation, whilst stimuli larger than size III show similar fluctuation, although greater inter-individual variability (Gilpin et al 1990). Wall et al (1993) also found that Goldmann size III and V targets showed lower variability than a size I target. However, there was greater variability with increasing eccentricity which was lowest for the largest targets. In a further study, Wall et al (1997) measured the frequency-of-seeing psychometric function in ten glaucoma patients using Goldmann size I, III and V stimuli. Intratest variability, defined by the standard deviation of the cumulative Gaussian function of the frequency-of-seeing curve, was lowest for the Goldmann size V stimulus at locations in the visual field demonstrating a defect depth between 10 and 20 dB.

Temporal Summation.

Temporal summation is governed by Bloch's Law (1885):

$$\Delta L = kT \quad \text{Eqn 1.5.}$$

where ΔL , is the increment threshold, k , is a constant and T , is the summation time. This law also assumes complete summation and has been modified to account for the quantum efficiency of photons in stimulating photoreceptors. Barlow (1964) suggested that at high background luminances, Bloch's Law applies because quanta from the background are also involved in stimulus detection. He described Bloch's Law as:

$$\Delta L = \frac{kT^{-1}}{t_m^{0.5}} \quad \text{Eqn 1.6.}$$

where: ΔL , is the increment threshold, k , is a constant, T , is the stimulus duration and t_m , is the minimum summing time.

In modern automated perimeters, the default stimulus duration is between 100 ms (Octopus) and 200 ms (Humphrey Field Analyser and Dicon). Stimulus durations of between 0.5 and 1 second have been proposed in order to eliminate the effects of temporal summation (Aulhorn and Harms 1972; Greve 1973). However, the latency of saccadic eye movements of between 50 and 250 ms (Robinson 1964) encourage saccadic eye movements away from fixation during the examination as well as increasing the overall examination time. Greve (1973) advocated short stimulus durations for the examination of patients with poor fixation. Stimulus duration can be used diagnostically to investigate post-geniculate lesions which exhibit enhanced temporal summation (Wilson 1967).

1.4.4. Stimulus Generation.

A variety of light sources have been used in commercially available perimeters to generate stimuli. These include fibre-optics, light-emitting diodes (LED), and projection systems. Fibre-optics were employed in the now obsolete Fieldmaster and Tubinger 2000 perimeters and were expensive to manufacture and difficult to position accurately within the perimeter bowl.

LED systems are inexpensive to manufacture, are silent in operation and physically robust (Lieberman and Drake 1987). Their light intensity can be varied by means of a high pulse current which enables them to operate at high luminance levels. One of the disadvantages of an LED system is that the stimuli are fixed in geometric size and location within the visual field. Furthermore, large numbers of LED's are required to obtain high spatial resolution of the visual field. Shifting the fixation point may provide increased spatial resolution without increasing the number of LED's (Fankhauser 1979). This approach is employed in the Dicon TKS 4000 perimeter (Li and Mills 1992). Because LED's can be independently controlled, multiple stimulus screening strategies are possible enabling rapid examination of the visual field, a

technique applied in the Henson series of visual field screeners (Henson and Bryson 1986; Henson and Anderson 1989). Another of the principle drawbacks of an LED system is that each LED requires individual calibration, and because of the directional properties of an LED, each needs to be precisely mounted. Indeed, if the LEDs are recessed into the perimeter bowl an impression of "black holes" on the bowl surface may occur (Britt and Mills 1987) which may give rise to local changes in the state of retinal adaptation (Heijl 1985). Additionally, a negative differential threshold may be obtained because the LED luminance is less than the background luminance, although this is thought to be of little clinical significance (Britt and Mills 1987). The "black hole" phenomenon may be eliminated by placing the LEDs behind a diffusing film (Britt and Mills 1987). It should be noted that because of the chromatic nature of LEDs, the results cannot be directly compared with those of projection perimetry (Fankhauser 1979).

Projection systems provide the most versatile form of stimulus generation. The most widely used perimeter, the Humphrey Field Analyser employs a projection system and is able to offer a range of stimulus sizes, intensities and chromaticities. In the Humphrey Field Analyser, the stimulus light source passes through a series of condensing lenses and apertures before it is projected onto the bowl. The stimulus position is varied by means of a series of rotating mirrors controlled by stepping motors giving a maximum possible resolution of 0.2° between adjacent stimuli (Heijl 1985). Stimulus size and chromaticity are controlled by rotating aperture plates placed in the optical path. The stimulus luminance is controlled by a rotating neutral density filter placed in front of the light source. A disadvantage of a projection system is the noise generated by the stepping motors which may lead to an increase in false-positive responses. Aging of projection and LED light sources dictates that they be regularly calibrated. In a projection system this is easily accomplished by self-calibration routines performed when the perimeter is powered up. Neutral density filters are either placed in front of the stimulus thereby ensuring constant stimulus luminance, or the voltage to the stimulus bulb is increased. This latter method may alter the colour temperature of the stimulus.

The advantages of projection and LED technology have been utilised in the Octopus 1-2-3 perimeter. A single 592 nm LED is projected onto the retina using a series of mirrors which vary the location of the stimulus (Octopus 1-2-3 Operating Instructions 1990).

1.4.5. Bowl Designs.

Until the mid 1990's, projection stimuli were traditionally presented onto a hemispherical bowl. In order to facilitate examination of the peripheral visual field this inevitably led to perimeters being large and therefore not easily portable. The Octopus 1-2-3 perimeter achieved reduced physical dimensions by employing a bowl of smaller diameter and projection of the stimulus to infinity. Recently, Humphrey Instruments have designed a new perimeter, the Humphrey Field Analyser II, which incorporates a bowl with an aspheric surface which allows visual field testing to an eccentricity of 60°, and at the same time considerably reduces the size of the instrument (Humphrey Field Analyzer II user's guide, 1994). Conversely, the Dicon and Henson 2000 and 3000 series of perimeters employ a flat surface to present stimuli.

1.5. Examination Strategies.

The mode of strategy employed in static perimetry is governed by the purpose of the examination. Depending on whether the examination requires accurate measurement or screening, full threshold or suprathreshold examination may be undertaken.

1.5.1. Full Threshold.

In a full threshold strategy, sensitivity is measured at each location in the visual field in order to gain an accurate representation of the dimensions of the hill of vision. In manual static threshold perimetry, the thresholds are usually obtained using the "method of limits" (Guilford 1954). In this method, the stimulus is initially presented infraliminally and gradually increased until it is seen by the patient. Automated static perimeters currently employ staircase procedures to measure sensitivity. Cornsweet (1962) evaluated the staircase procedure and found it to be an efficient method of obtaining a threshold as it requires fewer stimuli than other psychophysical methods. However, the number of stimuli required to establish a threshold is greater than that required using the method of limits (Bebié et al 1976a). The frequency-of-

seeing curve describes the probability of seeing a stimulus. The stimulus luminance at which the frequency of perception is 50% is defined as the threshold (Figure 1.2.). The exact nature of the curve is equivocal. It is thought to be either a Gaussian curve, caused by physiological fluctuation of the threshold level, or a Poisson curve, arising from a physical variation of quanta impinging upon a given receptive field (Weber and Diestelhorst 1992). The width of the region in which the curve rises steeply is the standard deviation of the assumed underlying normal distribution and corresponds in most normal observers to the increase in luminance which raises the probability of perception from 16% to 50% or from 50% to 84% (Bebié 1985). The strategies employed to obtain thresholds vary between- and within-instruments and will be discussed more fully in Chapters 3 and 4.

1.5.2. Suprathreshold.

Suprathreshold, or supraliminal, static examination offers a rapid examination of a large number of locations in the visual field (Fankhauser 1979). The ability of this technique to detect glaucoma is in the order of 90% or better (Keltner and Johnson 1981; Dannheim 1987; Johnson et al 1978). Suprathreshold strategies can be divided into three broad classifications.

One Level Strategy.

In this strategy, stimuli of constant luminance are presented at all locations in the visual field. However, the visual field declines in sensitivity with increasing eccentricity from the fovea. It is, therefore, possible that a stimulus which is just suprathreshold in the periphery of the visual field may result in small relative defects being missed at the fovea (Gramer et al 1982).

Gradient-Adapted Luminance Strategy.

In a gradient-adapted suprathreshold strategy, the stimulus luminance is modified to take into account the decrease in sensitivity with eccentricity. This method is dependent upon knowledge of the hill of vision in a standard normal observer. Keltner and co-workers (1979) suggest that this method has a greater sensitivity in detecting focal loss.

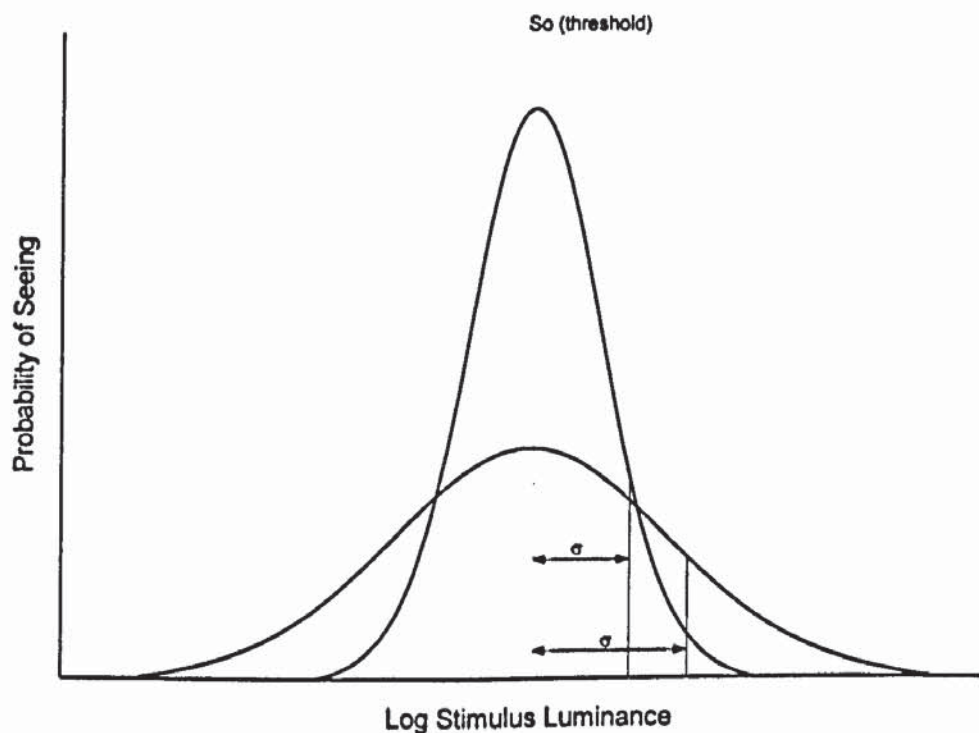
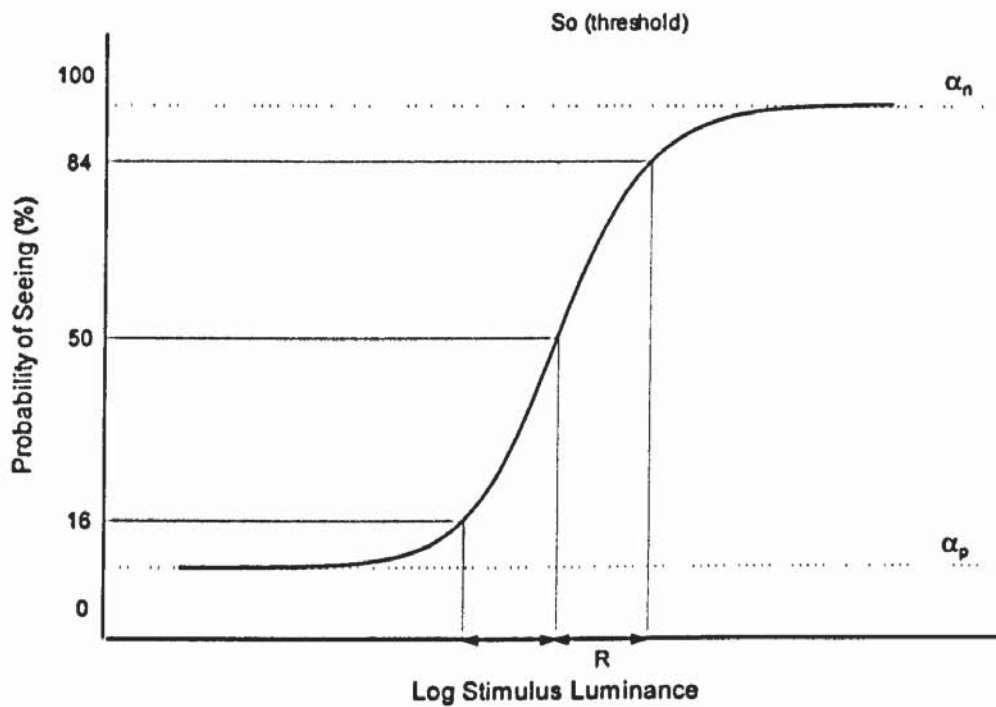


Figure 1.2. Hypothetical Frequency-of-Seeing Curve (top) and Scatter Around the Threshold (bottom). The frequency-of seeing curve is a psychometric function thought to be either a Gaussian or Poisson distribution. The threshold S_0 is defined as the stimulus luminance with a 50% probability of detection. In perimetry, the threshold is determined by presentation of a limited number of stimuli. Repeated measurements of the threshold at the same test location scatter around the real threshold S_0 with a standard deviation σ , dependent upon the threshold strategy employed. R is the standard deviation of the frequency-of-seeing curve and is dependent upon σ . In human observers, the rate of false-positives (α_p) and false-negatives (α_n) never reaches zero or 100%. The size of the transition zone, R can be estimated with knowledge of σ and the number of α_p and α_n (Flammer 1985).

Threshold-Related Gradient-Adapted.

The disadvantage of employing a gradient-adapted approach is that the hill of vision exhibits considerable intra-individual variation in the normal observer. Greve (1972) showed an inter-individual variation in normal sensitivity of approximately 2 dB in individuals of the same age. Heijl (1984), however, suggests that this variation may be as large as 10 dB depending upon patient reliability and physiological factors. To account for this variation between individuals, a threshold-related gradient-adapted strategy, whereby the threshold is primarily obtained at a small number of central locations is the preferred method. The luminance of the subsequent suprathreshold stimuli are based upon these thresholds, set between 4 to 6 dB brighter. A further refinement to this technique is to obtain thresholds at locations where suprathreshold stimuli are not detected. This technique is employed in the Automatic Diagnostic Test of the Humphrey Field Analyser (Haley 1987).

1.5.3. Spatial Configuration of the Test Grid.

The two factors which determine the resolution at which the visual field may be sampled are the number of stimulus locations sampling a given area and the spatial distribution of the locations relative to each other (Greve 1975; Bebié et al 1976b; Fankhauser and Bebié 1979; Johnson and Keltner 1981). Visual field loss in glaucoma primarily occurs in the central field (Werner and Drance 1977; Caprioli and Spaeth 1985). Assuming circular visual field defects, Greve (1975) was able to show that within 30° eccentricity, if 50 regularly distributed stimulus locations were employed a defect of diameter 9° had a 95% probability of detection. For a defect of 7.5° diameter, the detection chance is 100%, and 95% for a 3° diameter defect when employing 452 stimulus locations. However, Greve (1975) describes an optimum situation whereby 150 stimulus locations are examined. At this sampling frequency, the probability of detecting a defect 4° in diameter is 75%. Johnson and Keltner (1981) determined the frequency distributions of scotomata in glaucoma and optic nerve disease for approximately 30,000 locations in the visual field using a high resolution grid consisting of 0.75 by 0.75 degree elements. They found that when more than 140 to 150 stimulus locations were used, both the target density and distribution pattern appeared to have no, or negligible, effect on scotoma detection rate.

Three approaches to inter-stimulus separation exist: systemic sampling, high density sampling in areas of the visual field at risk of damage or a combination of both systemic sampling and high density sampling (Gutteridge 1984).

In systemic sampling, the inter-stimulus separation is constant throughout the visual field. In the Humphrey Field Analyser, the default stimulus separation in full threshold examination is 6°, and is based upon the findings of Fankhauser and Bebié (1979) who reported that the probability of detecting an 8.4° diameter scotoma with a square grid of 6° separation was 100%. Heijl (1993) suggested that the 6° stimulus separation employed in the Humphrey Field Analyser and Octopus perimeters was entirely sufficient to detect early glaucomatous visual field loss. In macular conditions, a higher density sampling of the visual field is desirable. Indeed, in the M1X and M2X strategies of the Octopus perimeter, spatial resolution of 1.4° and 0.7°, has been shown to be beneficial in the detection of macular disease (Kaiser et al 1994). In the Program 30-2 and 24-2 examinations of the Humphrey Field Analyser, stimuli are displaced 3° from the horizontal and vertical midlines, whilst in Programs 30-1 and 24-1 the stimuli are referenced to the midlines. The default Programs G1 and G2 of the Octopus perimeter differ from the 30-2 and 24-2 Programs of the Humphrey Field Analyser in that the stimulus separation is not constant throughout the visual field. Stimulus separation is 2° centrally increasing to 8° in the periphery at 55 degrees. The grid is denser around fixation in order to detect paracentral scotomata (Flammer et al 1987).

By combining both the 30-1 and 30-2 (or 24-1 and 24-2) examinations it is possible to enhance spatial resolution (Heijl 1993). High density sampling of the visual field enhances spatial resolution but at the expense of longer test duration and consequent subject fatigue. A more efficient method is to increase spatial sampling in areas of visual field loss. A novel program, SAPRO, was described whereby the grid changed from coarse to fine resolution in three steps depending upon the presence or absence of reduced sensitivity in the visual field (Haerberlin and Fankhauser 1980). If all the locations measured with the coarse grid were within normal limits, the program ceased. If an area of reduced sensitivity was suspected, the SAPRO program increased resolution in a grid surrounding the suspect area. If the locations within this

grid exhibited reduced sensitivity, the area was examined with a finer grid. The resolution of the fine grid was twice that of the medium grid and four times that of the coarse grid. The spatial separation of the grids was determined by the geometric nature of the grid, being either circular or rectangular (Funkhouser and Fankhauser 1985).

Åsman and co-workers (1988) evaluated the suprathreshold Automatic Diagnostic Test of the Humphrey Field Analyser. This test automatically increases spatial resolution from a 6° inter-stimulus point separation to a 3° separation in areas of the field where a stimulus 6 dB brighter than the expected threshold is not detected with the conventional 6° grid. They found that this spatial enhancement strategy did not improve sensitivity and specificity beyond that achieved by the conventional 6° grid, alone. Furthermore, Heijl (1993) suggested that combination of the Program 30-1 and 30-2 grids would not provide any additional information regarding visual field loss in glaucoma than that obtained by employing one grid alone. High resolution sampling has been found to be diagnostically useful in the detection retinal oedema or the mapping of angioscotoma (Funkhouser and Fankhauser 1985).

1.6. Reliability Parameters.

Automated static perimetry is time consuming and demanding to the patient. Patient inattention during the examination may produce unreliable results. A number of criteria are useful in assessing patient reliability and are easily adopted into the threshold programs of automated static perimeters.

1.6.1. Fixation Losses.

Fixation can be monitored during the course of a perimetric examination by a variety of means. The crudest method is to physically observe the fixating eye, through a telescope or on a television monitor. In the Heijl-Krakau method of fixation monitoring, (Heijl and Krakau 1975a, b), a stimulus of maximum luminance is periodically positioned in the blind spot. If the patient sees this stimulus then a fixation-loss is recorded. The efficacy of the Heijl-Krakau fixation monitoring technique has been questioned by Fankhauser (1993). He argued that reductions in precision will occur when the blind spot is enlarged, or in the presence of pericoecal atrophy.

Furthermore, straylight reflected from the blind spot or arising from the ocular media may result in stimulation of pericoecal receptors (Fankhauser and Haeberlin 1980). For the 30-2 Program of the Humphrey Field Analyser, the number of blind spot stimulus presentations may be as many as 10% of the total number of stimulus presentations in a perimetric examination (Katz and Sommer 1988).

The visual field is usually classed as unreliable if the number of fixation losses exceeds 20%. This value was derived during the development of the Humphrey Field Analyser threshold strategy software because at higher rates of fixation losses, the sensitivity and specificity of the test began to deteriorate (Sanabria et al 1990). Fixation losses greater than 20% have been shown to account for the largest number of unreliable tests in normal subjects, and those with ocular hypertension and glaucoma (Katz et al 1991). Consequently, it has been suggested that the percentage of fixation losses permitted before a visual field examination is classed as unreliable and be increased from 20% to 33% (Johnson and Nelson-Quigg 1993).

Methods which constantly measure fixation during the perimetric examination have been devised for the Octopus 1-2-3 and the Humphrey Field Analyser II perimeters. The Octopus 1-2-3 employs infra-red ocular illumination to produce four corneal reflexes, two on each side of the pupil equator (Octopus 1-2-3 Operating Instructions, 1990). Deviations of gaze and blinking are immediately registered by the perimeter during the course of the examination. If any deviation or prolonged closure of the lids occurs, the examination is temporarily interrupted automatically until the problem is rectified.

The Humphrey Field Analyser II "gaze tracking" system (Humphrey Field Analyzer II user's guide, 1994) employs real-time image analysis to measure the distance between the centre of the pupil and the first corneal reflex (Purkinje I), produced by infra-red lights in the perimeter bowl. This distance is not affected by head movement. A gaze graph is generated for the complete examination which shows upward and downward spikes deviating from a base line. Upward deviations indicate the eye deviated from the fixation target at the time of stimulus presentation, with the magnitude of the spike indicating the degree of deviation, up to an angle

of 10°. Small downward deviations indicate that the gaze tracking system was unable to detect the patient's gaze, whereas large downward deviations illustrate patient blinking. The clinical utility of the gaze tracking system has not been determined to date.

1.6.2. False-Positive and False-Negative Errors.

In order to monitor the patients responses, a number of catch-trials are carried out by the perimeter during the course of an examination. In a false-positive catch-trial, the perimeter produces the noises associated with the presentation of a stimulus but does not present a stimulus. If the patient presses the response button, this indicates patient inattention and a false-positive error is recorded. In a false-negative catch-trial, a stimulus is presented at a suprathreshold level at a location in the visual field where the threshold has already been established. If the patient fails to respond to this stimulus a false-negative error is recorded. A false-positive may also be registered when the catch-trial occurs within the physiological blind spot since the patient would be unable to detect any stimulus (Fankhauser 1993). False-positive and negative rates are unaffected by age, pupil diameter and visual acuity (Katz and Sommer 1988; Bickler-Bluth et al 1989).

A visual field is usually classed as unreliable if the number of false-positive or false-negative answers exceed 33% as it has been found that above this rate the sensitivity and specificity of the test begins to worsen (Sanabria et al 1990). High false-positive rates may give rise to higher mean sensitivity. It has been demonstrated that high false-positive rates occur in inexperienced perimetric observers (Bickler-Bluth et al 1989; Sanabria et al 1990). A positive correlation between false-positive rates and fixation losses has been demonstrated (Reynolds et al 1990). A high false-negative rate may result in reduced mean sensitivity. Katz and Sommer (1990) found that in glaucoma patients who exhibited high false-negative rates, an average 9 dB reduction in mean deviation occurred, against a 7 dB reduction in normals. The number of false-negatives has been shown to be higher in glaucomatous eyes (Katz and Sommer 1988; Reynolds et al 1990).

The ability to estimate false-positive and negative answers statistically from knowledge of the staircase algorithm has been employed to estimate the threshold, negating the need for catch-trials. This method has been demonstrated to give more efficient estimates in normal subjects than traditional catch-trials (Olsson et al 1989; Olsson et al 1995). Another method to estimate the false-positive and negative rate without employing catch-trials has been developed by Wu et al (1994) in which knowledge of the number of stimulus presentations at each location is employed in a noise filtering technique. Recently, Olsson et al (1997) developed a method for improving the estimate of the number of false-positive answers by using information already available in conventional visual field examination, without increasing the overall examination time. False-positive answers were detected during the period between the minimum reaction time of 180 ms (Greve 1973) and the onset of the next stimulus. This information was used to construct a model of patient false-positive behaviour, using maximum likelihood statistical techniques to estimate the frequencies of false-positive answers.

1.7. Threshold Fluctuation.

Due to the nature of the threshold estimation, the measured threshold at a given location in the visual field varies both within a single examination and between examinations.

1.7.1. Short-Term Fluctuation.

Short-term fluctuation (SF) represents the scatter observed when the same threshold is measured repeatedly during a single perimetric examination (Bebié et al 1976b; Flammer et al 1984a,b). It is the average of the local scatter over the entire visual field, determined from the square root of the sum of the local standard deviations averaged over the visual field. In the Octopus perimeter SF is expressed as an unweighted index, the root mean square (RMS) and is calculated as follows:

$$SF = \sqrt{\frac{1}{m} \cdot \sum_{l=1}^m (SD_l)^2} \quad \text{Eqn 1.7.}$$

where, l , is the test location; m , is the number of test locations excluding the blind spot; SD_l , is the standard deviation at the test location, l (Flammer 1986). Determination of RMS SF assumes that variance is constant at all locations in the visual field. However, variance

increases with increase in eccentricity (Heijl et al 1987a). In the Humphrey Field Analyser, double determinations of threshold obtained at ten locations in the visual field are used to calculate a weighted mean of the standard deviations.

$$SF = \sqrt{\left\{ \frac{1}{10} \cdot \sum_{j=1}^{10} s_{2j}^2 \right\} \cdot \left\{ \frac{1}{10} \cdot \sum_{j=1}^{10} \frac{(x_{j1} - x_{j2})^2}{2(s_{2j}^2)} \right\}} \quad \text{Eqn 1.8.}$$

where, x_{j1} , is the first and, x_{j2} , the second threshold value at test location, j . The normal intra-test variance at location, l , is denoted by, s_{2l}^2 . Weighting with $1/s_{2l}^2$ minimises SF in normal subjects (Heijl et al 1987b).

Flammer et al (1984a) reported the SF in a normal population to be a positively skewed distribution. The SF is approximately 0.3 dB greater in the Octopus perimeter than the Humphrey Field Analyser (Brenton and Phelps 1986). This difference may result from the difference in determination of the threshold between the two perimeters. The standard staircase algorithm of the Octopus determines the threshold as the arithmetic mean between the last seen and unseen stimulus. In the Humphrey Field Analyser, the standard staircase algorithm determines threshold as the last seen stimulus. The staircases employed to estimate threshold in perimetry will be discussed further in Chapter 3.

The magnitude of the SF is dependent upon the strategy employed to estimate threshold (Bebié et al 1976b; Weber 1990; Flanagan et al 1993a, b; Weber and Klimaschka 1995). The stimulus and background characteristics have also been demonstrated to influence the SF. Gilpin et al (1990) found the SF to be greater when smaller stimulus sizes are employed. However, the SF has been reported to be independent of stimulus duration (Pennebaker 1992) and of background luminances between 0.0135 cdm^{-2} and 31.5 cdm^{-2} (Crosswell et al 1991).

The SF is not influenced by natural pupil size (Flammer et al 1984b, Rebolleda et al 1992) although small pupils induced by miotic therapy may result in a small increase in the SF (Flammer et al 1984b). Some studies have reported an increase in the SF with increasing age (Haas et al 1986; Chauhan et al 1990). Psychological factors such as the level of perimetric

experience and fatigue are also known to influence the SF (Heijl et al 1989; Searle et al 1991; Hudson et al 1993; Heijl and Bengtsson 1996). The influence of fatigue on the SF will be discussed in greater detail in chapter 3 and 6.

Flammer et al (1984a) and Flammer et al (1985) reported that the SF was independent of visual field location out to an eccentricity of 30°. However, the majority of studies have found that the SF is dependent upon eccentricity (Aulhorn and Harms 1967, Greve and Wijnans 1972, Werner and Drance 1977; Brenton and Phelps 1986; Heijl et al 1987a). The SF is greater around the borders of scotomata (Flammer et al 1984b); small movements in fixation may result in the first and second threshold determination falling within and outside a scotoma respectively (Henson and Bryson 1991; Eizenman et al 1984; Vingrys and Demirel 1993).

The G1, G2 and G1X Programs of the Octopus perimeter estimate the SF from double determinations of threshold at each location in the visual field, obtained over two phases. The 30-2 and 24-2 Programs of the Humphrey Field Analyser estimate SF from double determinations of threshold obtained from ten locations within 21° eccentricity. Bebié et al (1976b) state that when employing ten locations the SF can only be estimated within 44% of the true value at a confidence level of 95%. Flanagan and co-workers (1993c) reported an increase in the magnitude of unweighted SF as the number of locations used to calculate the index was increased. A more accurate estimation of the SF is possible by increasing the number of determinations at fewer locations (Casson et al 1990). However, it is important to obtain an estimate of fluctuation over the entire visual field.

Estimation of RMS SF can be made from a single determination of the visual field. Schulzer et al (1990) fitted a polynomial surface to the Humphrey Field Analyser Program 24-2 visual field from each of three examinations. The polynomial surface was able to better fit the variation in measured field which occurred with increase in eccentricity. The precision in the estimation of the RMS value was found to be $\pm 6.5\%$ at a 95% confidence level, and the SF within $\pm 25\%$ at a 95% confidence level. This suggests that estimating the SF using this method is likely to be

more precise than that obtained using double determinations of threshold from ten locations in the visual field. This estimation technique also serves to reduce examination time.

1.7.2. Long-Term Fluctuation.

The long-term fluctuation (LF) represents the variation observed when the same threshold is measured at a separate examination after the SF has been removed (Flammer et al 1984b). The LF is generally divided into two components; homogeneous, LF(Ho) and heterogeneous, LF(He). The former component represents the uniform fluctuation in threshold, and the latter component the non-uniform fluctuation in threshold. Knowledge of the SF and LF is important when deciding whether significant visual field change has occurred. Brenton and Argus (1987) developed a model for the calculation of the different components of the LF:

$$S_{\text{HOM}}^2 = \left[32 \sum (\bar{y}_l - \bar{y}_-)^2 - 2(S_{\text{HET}}^2) - (S_{\text{STF}})^2 \right] \quad \text{Eqn 1.9.}$$

$$S_{\text{HET}}^2 = \frac{1}{2} \left[\frac{1}{30} \sum_{jk} (\bar{y}_{jk} - \bar{y}_l)^2 - S_{\text{STF}}^2 \right] \quad \text{Eqn 1.10.}$$

where S_{STF} is the variance owing to short-term fluctuation, S_{HOM} is the variance between sessions ie the homogeneous long-term fluctuation, S_{HET} is the variance between location and session ie the heterogeneous long-term fluctuation, j , is the session, k , is the location, $\bar{y}_...$, is the mean threshold for all observations for one subject, $y_{j..}$, is the mean threshold for session, j , for one subject, and, \bar{y}_{jk} , is the mean threshold of repetitions for one subject for session, j , at location, k .

The components of the LF are smaller than the SF. Flammer et al (1984b) found a LF(Ho) of 0.5 dB² and LF(He) of 0.2 dB² in normal subjects. Furthermore, these components were increased in ocular hypertensive and primary open-angle glaucoma patients (LF(Ho) 0.9 dB² and 1.2 dB²; LF(He) 0.4 dB² and 0.5 dB² respectively). An increase of the LF with increasing eccentricity from fixation has been reported by several workers in normal subjects (Heijl et al 1987a; Rutishauser and Flammer 1988) and in glaucoma patients (Boeglin et al 1991; Zulauf et al 1991). Flammer and co-workers (1984b) found the LF(Ho) to be highly correlated with the

LF(He). The SF was also statistically related to the LF(Ho) but the relationship was too weak to predict the LF(Ho) with accuracy. Boeglin et al (1992) found that the LF decreased at sensitivity levels less than 10 dB and increased when sensitivity was greater than 32 dB; they found a 0.7 dB² increase in the LF per decibel decrease in sensitivity. This latter finding is in concordance with the 0.5 dB² increase in the LF with increase in eccentricity reported by Zulauf et al (1991).

Several groups have treated the LF as a single component, calculating the statistical variance of serial values for threshold sensitivity at each stimulus location in the visual field (Rutishauser et al 1989; Katz and Sommer 1987; Heijl et al 1987; Boeglin et al 1991).

1.8. Graphical Presentation of Perimetric Data.

A number of graphical methods have been developed to illustrate the spatial location and severity of a visual field defect.

1.8.1. Numeric Data.

The simplest form of data presentation is a representation of threshold values in decibels arranged in the spatial locations of the test grid. Double determinations of threshold at any given stimulus location are illustrated by the two values of sensitivity. Presentation in this form permits the display of the raw data prior to statistical manipulation. However, the disadvantage is that large amounts of such numeric data makes visual field interpretation difficult.

1.8.2. Grey-Scale.

The grey-scale aims to display perimetric data in a map such that it can be more readily interpreted than raw data. Sensitivity values are represented by shades of grey, ranging from black to white. Sensitivity values are generally banded into 5 dB groupings with increasing greyness denoting decreasing sensitivity. Furthermore, differences in dynamic range between perimeters will result in differences in the shade of grey assigned to a particular sensitivity band. Regions between the locations tested in the visual field are illustrated by interpolation. The interpolation procedure can influence the appearance of the grey-scale display. Weber

and Geiger (1989) studied various mathematical interpolation procedures. "Four points" interpolation involves calculating the mean or median decibel value at the centre of a grid which has a measured point at each of the four corners. It was found to be quickest to perform and gave smooth but inexact outlining of defects. In linear interpolation, a mathematical interpolation is carried out dependent upon the distance from each measured location to the next in an x and y direction. Although a less exact procedure, it produced a more defined outline to a scotoma. A combination of these methods was shown to yield best results.

1.8.3. Three-Dimensional Representation.

Visual field sensitivity can also be expressed three-dimensionally to aid visualisation (Haas et al 1986; Jaffe et al 1986). This type of graphical display does not aid interpretation; sharp elevations, depressions or other irregularities in the visual field can obstruct the view to other parts of the field (Hart and Hartz 1982). When viewing such plots on a computer monitor, this problem can be overcome by employing a rotation algorithm in the software (Hart and Hartz 1982). Due to differing scales applied to the spatial arrangement of stimulus locations, and to sensitivity values, comparison between different three-dimensional plots should be made with caution (Wild et al 1987).

1.8.4. Probability Plots.

Probability plots graphically illustrate the level of statistical probability associated with a given visual field abnormality compared to the normal reference field. Schwartz and Nagin (1985) developed a series of probability displays for visual fields derived from the Octopus perimeter. For single visual fields, percentiles of 0.1, 1, 5, and 10 were calculated from the mean normal values for each decade and stored in a computer. Each measured threshold value was then classified according to its percentile rank from normal values. Comparison of the measured field with the normal reference field resulted in the generation of a percentile probability map. The system was based upon the false assumption that the frequency distribution of the normal values was Gaussian in nature; consequently, probability maps based on this paradigm yield large numbers of falsely significant locations, particularly in the mid-periphery (Heijl et al 1991).

The STATPAC software package in the Humphrey Field Analyser provides probability plots derived from empiric data (Heijl et al 1991). The total deviation plot represents the difference in decibels between the measured results and the age-corrected normal values at each location in the visual field. In a second plot, the values in the former display are translated into pixels. Each pixel is associated with a probability level which indicates the possibility of the location being normal. Four symbols are provided indicating 0.5%, 1%, 2%, and 10% probability. A value of 0.5% at a location indicates that the deviation from normal found at that location occurs in less than 0.5% of normal subjects.

A pattern deviation probability map is also provided in the Humphrey Field Analyser and separates the general reduction in sensitivity which may arise through media opacities, optical defocus or pupillary miosis from the localised reduction in sensitivity. In order to calculate the pattern deviation probability map, locations within 24 degrees of fixation are ranked according to the deviation in sensitivity compared to the age-matched normal population. General sensitivity is calculated from the measured value of the seventh highest deviation (85th percentile) in sensitivity (Heijl et al 1991).

1.8.5. The Glaucoma Hemifield Test.

The Glaucoma Hemifield Test (GHT) was introduced in the Humphrey Field Analyser with the aim of deciding whether visual field loss was compatible with a diagnosis of glaucoma (Åsman and Heijl 1992a). Ten anatomical sectors in the visual field are superimposed on the Program 30-2 test grid, selected according to the normal arrangement of retinal nerve fibres. Five sectors in the upper hemifield mirror five sectors in the inferior field. Probability scores are calculated for each location within the ten sectors according to the pattern deviation probability map. Within each sector, the sum of the probability scores is calculated and the difference compared to the mirror image sector. A visual field is classed as "outside normal limits" if the difference in any of the five corresponding pairs of sectors falls outside the 0.5% or 99.5% confidence limits for that pair of sectors. Visual fields are classified as "borderline" if any sector-pair difference exceeds the 3% confidence limit. If the general height of the field is

below the 0.5% limit, the GHT evaluates the field as a "general reduction in sensitivity". A classification of "abnormally high sensitivity" is associated with a high level of false-positive responses. The general height test is not performed if the visual field has already been classified as "outside normal limits". Åsman (1995) introduced colour-coding of the GHT results which aided the separation of glaucomatous defects from localised or diffuse defects.

Katz et al (1995) evaluated the repeatability of the GHT between two successive visual field examinations in normal subjects, ocular hypertensives, and in glaucoma patients with mild to moderate field loss separated by one year. The GHT yielded a sensitivity of 80.8% and 81.4%, and a specificity of 84.2% and 84.7% in the first examination of ocular hypertensive and glaucoma patients respectively. At the second examination, sensitivity fell to 69.8% in the ocular hypertensives and 80.0% in the glaucoma patients (corresponding specificity 89.5% and 89.9% respectively).

1.8.6. Bebié Curve,

The Bebié curve is a cumulative distribution of the defect depth at each location and is designed to separate normal visual fields from those with early diffuse loss (Bebié et al 1989). The defect depth is sorted into ascending order of severity and plotted as a function of rank. A shaded zone is employed to aid interpretation of the resultant curve. The enclosed region corresponds to the 5th and 95th percentiles. A normal visual field yields a curve above or closely following the 95th percentile line. A curve falling below (ie outside) the 95th percentile line indicates visual field loss. A visual field with purely diffuse loss will mimic the shape of the curve associated with normality, but at a greater overall defect depth. Focal loss is indicated by a steepening of the curve. A clear boundary does not separate diffuse from focal loss on the curve (Funkhouser et al 1992). Furthermore, the Bebié curve does not yield information about the spatial characteristics of the visual field loss (Åsman and Heijl 1992b). Indeed, Kaufmann and Flammer (1989) suggested that the Bebié curve should only be used in conjunction with another type of display which yields spatial information about the field loss.

Asman and Olsson (1995) investigated the effect of test point eccentricity upon the normative limits for cumulative defect curves. They concluded that cumulative curves were of limited value in the detection of pure diffuse loss since the typical central field depressions in early glaucoma may easily be missed with this type of visual field representation.

1.9. Data Reduction of Perimetric Data.

Graphical displays such as grey scales suffer from a number of disadvantages, namely that they inadequately define diffuse visual field loss and changes between a series of visual fields (Flammer 1986). Statistical interpretation of perimetric data does not suffer from these disadvantages. Furthermore, the use of visual field indices is a useful method of data reduction. A wide variety of visual field indices have been developed for the Octopus and Humphrey Field Analyser perimeters to summarise the data reduction at each stimulus location.

1.9.1. Mean Sensitivity.

Mean sensitivity (MS) represents the arithmetic mean of the sensitivity of all stimulus locations tested in the visual field.

$$MS = \frac{1}{m} \cdot \sum_{i=1}^m \bar{x}_i \quad \text{Eqn 1.11.}$$

where, $\bar{x}_i = \frac{1}{n} \cdot \sum_{k=1}^n x_{ik}$

i , is the test location; x , is the measured value; m , is the number of test locations excluding the blind spot; and, n , is the number of threshold replications (independent measurements within the same examination).

1.9.2. Mean Defect and Mean Deviation.

The mean defect (MD_F) is the arithmetic mean of the difference between the measured values and the normal values at the different test locations. This statistic was designed for the Octopus range of perimeters.

$$MD_F = \frac{1}{m} \cdot \sum_{i=1}^m (z_i - \bar{x}_i) \quad \text{Eqn 1.12.}$$

where, m , is the number of stimulus locations excluding the blind spot, z_i , is the age-corrected normal value at test location, i , and, x_i is the measured value. MD_F is sensitive to diffuse visual field loss but is relatively unaffected by focal loss. A positive MD_F represents a loss of sensitivity.

Mean defect is analogous to the mean deviation statistic used in the Humphrey Field Analyser.

Mean deviation (MD_H) is a weighted average deviation from the normal reference visual field:

$$MD_H = \left\{ \frac{1}{m} \cdot \sum_{i=1}^m \frac{(\bar{x}_i - z_i)}{s_{i1}^2} \right\} / \left\{ \frac{1}{m} \cdot \sum_{i=1}^m \frac{1}{s_{i1}^2} \right\} \quad \text{Eqn 1.13.}$$

where, s_{i1}^2 , is the variance of normal field measurements at location, i . Unlike mean defect, mean deviation becomes negative when a visual field defect occurs.

Fluctuation Weighting of Visual Field Indices.

The age-corrected normal threshold values for the Octopus follow a model in which sensitivity decreases linearly by 0.1 log unit per decade. This model of the hill of vision implies that the shape remains unaltered during life and that the normal intra-individual variation is constant across the visual field (Heijl et al 1987a). A more realistic normal reference visual field has been developed by Heijl et al (1987a) based on empiric data gathered from subjects with previous perimetric experience. The model assumes that the normal inter-individual variability of the age-corrected threshold and the intra-individual inter-test variability is not constant across the visual field and is allowed to change with location. The expected sensitivity at each location decreases linearly with age, but not at different rates across the various locations, ie the normal reference field is allowed to change in both height and shape with age.

Funkhouser and Fankhauser (1991) evaluated the unweighted MD_F and weighted MD_H indices. They concluded that weighting of the visual field indices did not provide any benefit in visual field analysis. Heijl et al (1992) disputed the findings of Funkhouser and Fankhauser (1991) arguing that to gain an accurate measure of the average threshold level in a well

defined population, weighting according to variance would increase the precision of the estimate. Furthermore, the sampling errors of the weights were smaller than the variation caused by eccentricity dependence, improving the precision of MD_H in comparison to the corresponding unweighted index. Additionally, they reported that the MD_H index yielded lower test-retest variability.

Åsman and Heijl (1992b) evaluated the unweighted and weighted models in the analysis of glaucomatous visual fields. The weighted model yielded higher sensitivity and specificity than the non-weighted model. Weighting increased the detection of early central and paracentral visual field loss in glaucoma and de-emphasised common examination artefacts in the mid-periphery where normal variability is greater.

1.9.3. Loss Variance and Pattern Standard Deviation.

The loss variance (LV) statistic of the Octopus perimeter describes the non-uniformity in the height of the visual field. It is small if visual field damage is diffuse and is high in the presence of focal loss. It is defined as:

$$LV = \frac{1}{(m-1)} \cdot \sum_{i=1}^m (z_i - MD_F - \bar{x}_i)^2 \quad \text{Eqn 1.14.}$$

The pattern standard deviation (PSD) statistic of the Humphrey Field Analyser is a weighted standard deviation of the pointwise differences between the measured and normal reference visual field. It is analogous to loss variance on the Octopus perimeters.

$$PSD = \sqrt{\left\{ \frac{1}{m} \cdot \sum_{i=1}^m s_i^2 \right\} \cdot \left\{ \frac{1}{m-1} \cdot \sum_{i=1}^m \frac{(\bar{x}_i - z_i - MD_H)^2}{s_i^2} \right\}} \quad \text{Eqn 1.15.}$$

Weighting with $1/s_i^2$ minimises PSD in normal subjects.

Crabb et al (1995) developed a spatial filtering technique to reduce variability in the visual field and then extracted the residual pointwise variability to yield the local spatial variability (LSV). A relationship was found between LSV and PSD; but, unlike PSD, the LSV does not depend upon a comparison with normal values.

1.9.4. Corrected Loss Variance and Corrected Pattern Standard Deviation.

Corrected loss variance (CLV) in the Octopus perimeter aids the separation of real deviations from deviations due to variability. It is defined as:

$$CLV = LV - \frac{1}{n} \cdot (SF)^2 \quad \text{Eqn 1.16.}$$

Pearson and co-workers (1990) studied the relationship between MD_F and CLV and found that in glaucoma patients with early to moderate glaucomatous loss (defined as an MD_F less than 18 dB), CLV significantly co-varied with the MD_F . However, in severe glaucomatous loss (MD_F greater than 18 dB) there was no correlation between MD_F and CLV. Gollamundi et al (1988) advocated the use of a Difference Index given by $\sqrt{CLV} - MD_F$ which was able to differentiate between the severity of glaucomatous visual field loss.

Corrected pattern standard deviation (CPSD) in the Humphrey Field Analyser is analogous to CLV. It is given as:

$$CPSD^2 = PSD^2 - k \cdot SF^2 \quad \text{Eqn 1.17.}$$

where, k, is a constant greater than 1, dependent upon the spatial arrangement of the stimulus locations employed in the calculation of the SF. In Programs 30-2 and 24-2 of the Humphrey Field Analyser, k, is equal to 1.1405. If $CPSD^2$ is less than zero, k, is set to zero because variances are never negative, although their estimates may be.

1.9.5. Third Central Moment.

The third central moment (M3) of the distribution of the deviation the of measured values from the expected values is sensitive to deviations restricted to a very low number of test locations. It may therefore be useful in the detection of very early visual field defects (Flammer 1986). M3 is defined by the equation:

$$M3 = \frac{1}{m} \cdot \sum_{i=1}^m (z_i - MD - \bar{x}_i)^3 \quad \text{Eqn 1.18.}$$

1.9.6. Skewness.

Skewness (Q) is a standardised M3. It is calculated as follows:

$$Q = \frac{M3}{\sqrt{(LV)^3}} \quad \text{Eqn 1.19.}$$

Pearson et al (1989) found the Q statistic to be of little value in glaucoma patients since, as MD_f increases, the sensitivity of the Q statistic decreases.

1.9.7. Spatial Correlation.

Spatial correlation (SC), accounts for the spatial distribution of visual field defects. It is low when defects are dispersed throughout the visual field, and high when defects are clustered (Flammer 1986). It is defined as:

$$SC = \frac{1}{p} \cdot \sum_{(ij)} (z_i - MD - \bar{x}_i) \cdot (z_j - MD - \bar{x}_j) \quad \text{Eqn 1.20.}$$

where, p , is the number of pairs involved in the summation, and, ij , indicates a summation over pairs of adjacent test locations.

1.9.8. Defect Volume.

Defect Volume (DV) is defined as the difference between the volume of the measured visual field (VOL_{meas}) and that of the normal reference field (VOL_{norm}) (van den Berg 1985; Langerhorst et al 1985).

$$DV = VOL_{norm} - VOL_{meas} \quad \text{Eqn 1.21.}$$

1.9.9. Congruence Index.

Weber (1993) developed a congruence index (CI) to objectively and quantitatively assess the similarity of the right and left visual fields. This calculation was based upon the differences in variance at each test location between each field and is defined by the equation:

$$CI = \frac{GV(\Delta L_i)_{expected}}{GV(\Delta L_i)_{true}} \quad \text{Eqn 1.22.}$$

where, L_i , is the local sensitivity of any measured location, i , of the visual field; GM is the global mean; and GV the global variance, of all local sensitivity values in the visual field. If the visual fields between the right and left eyes are dissimilar and independent of each other, then CI is equal to unity. If there is congruence between visual fields, the CI is greater than unity.

The combined congruence index (CCI) is able to differentiate between homonymous and heteronymous congruence (Weber 1993). CCI is defined by the equation:

$$CCI = \log\left(\frac{CI_{ho}}{CI_{he}}\right) \quad \text{Eqn 1.23.}$$

where, CI_{ho} is the homonymous congruence index and, CI_{he} is the heteronymous congruence index. Homonymous congruence is assessed by simple comparison and heteronymous congruence by making a mirror image of the right or left fields. CCI is positive in the case of homonymous congruence and negative in heteronymous congruence.

Weber (1993) suggested that the CI could also be applied to evaluate the similarity between two fields from the same eye during visual field follow-up, or the similarity of a given patient field with a specified normal or abnormal visual field pattern.

1.9.10. Diffuse Loss Index,

The standard index for evaluating diffuse loss is MD. However, the presence of focal loss will influence the value of MD. Langerhorst et al (1989) devised an algorithm, the Individual General Sensitivity Index, which is not influenced by focal loss. Another method of separating diffuse visual field loss from focal loss is the Cumulative Defect Curve (Bebié et al 1989). The boundary between diffuse and focal loss in such curves is not well defined (Funkhouser et al 1992). A refinement to the cumulative defect curve was devised by Funkhouser (1991) in the form of the Diffuse Loss Index; the plateau region of the curve is used to calculate the index which is specified as the mean of the loss values of the plateau.

1.9.11. Pericecal Index,

The Pericecal Index (PI) was derived by Brusini et al (1990) for the purpose of detecting early glaucomatous visual field loss. Twelve locations of the Program 30-2 test grid surrounding the blind spot are used to calculate the index. In a group of 50 patients with early glaucoma, 22% had a statistically significant depressed PI. The sensitivity of the index was found to be greater than for other global visual field indices.

1.9.12. Learner's Index.

The Learner's Index (LI) is designed to detect regions of low sensitivity which may be due to inadequate perimetric experience (Åsman et al 1993). Such visual fields exhibit a depressed mid-peripheral region with a normal central field. Three visual fields were obtained from 74 normal subjects, seven of which exhibited a learning effect. The first visual field was used in the "learning" subjects and the third field in all subjects, to calculate the LI. Each visual field was divided into five concentric zones, and in the learning group the average deviation from the age-corrected normal value was calculated for each zone. The variances and covariances between the results from the five zones were used to determine a linear discriminant function, the LI. A value of zero indicates an entirely normal visual field, and the average "learner" will exhibit a value of approximately one.

Åsman and Heijl (1994) evaluated the LI in 10 eyes of 10 normal subjects and 20 eyes in 20 glaucoma patients, and found that normal subjects who exhibited abnormal GHT results at the first visual field examination were associated with high LI values, which decreased rapidly towards zero with repeated examination. In the glaucoma group, significant GHT results obtained at the first visual field examination were associated with a low LI.

1.10. Analytical Programs.

1.10.1. STATPAC.

STATPAC is a computer program for statistical analysis available on the Humphrey Field Analyser and for use with a personal computer (Heijl et al 1987b). STATPAC contains normal age-corrected threshold values against which the threshold values obtained within a visual field examination are compared. Global visual field indices and probability maps can be generated. Additionally, a number of forms of data reduction are offered for the comparison of serial visual fields. Several visual fields can be printed, compressed in size for Overview analysis. Linear regression of MD_H against time to follow-up can also be plotted and compared to reference lines at the $p < 5\%$ and $p < 1\%$ levels of significance for the normal population contained within the STATPAC database. Box plots, a modified form of histogram, offer an

intermediate form of data reduction; they are calculated from the pointwise differences between the measured and normal field. The maximum, minimum, median, 15th, and 85th percentiles are plotted; 70% of all pointwise differences fall between the upper and lower limits of the box. A normal box is presented on the graphical printout for reference.

STATPAC-2 was introduced in 1991 (Heijl et al 1991). Linear regression of MD_H against time of follow-up was modified to account for learning effects in serial visual field analysis. The first test in a series is ignored if MD_H is significantly deviant from and worse than the trend exhibited at later tests at the 5% significance level. STATPAC-2 also contains the Glaucoma Hemifield Test (described earlier) and the Glaucoma Change Probability Analysis. In the latter analysis, the follow-up field is compared at each stimulus location with the baseline sensitivities. The probability of no change is calculated from an empiric database derived from the repeated testing of patients with stable primary open-angle glaucoma. Glaucoma Change Probability Analysis correlates well with routine clinical evaluation of glaucomatous progression (Morgan et al 1991; Tuulonen and Airaksinen 1991). Tuulonen and Airaksinen (1991) reported that the Statpac 2 Glaucoma Change Probability printout and standard clinical evaluation of progression correlated up to an R² of 0.87.

1.10.2. Change Analysis.

A number of other statistical methods have been developed for change analysis.

Statistical modelling of the visual field may provide information on the nature of visual field progression, either in a consistent or episodic manner. Wild et al (1989a; 1993) proposed topographical and longitudinal models for visual field progression in glaucoma. In the topographical model, a second-order polynomial function described the pointwise value of sensitivity at any stimulus location. The longitudinal model employed a linear function to describe sensitivity. Both components of the model were combined to form a combined model (Wild et al 1993). The combined model exhibited greater precision to describe the pointwise distribution of sensitivity at the nth field. They concluded that the pointwise distribution of

sensitivity can be modelled to an accuracy within 3 dB, within the central thirty degrees from fixation.

The Progressor Program (Noureddin et al 1991; Fitzke and McNaught 1994; Birch et al 1995; Fitzke et al 1996) derives linear regression slopes of change in MD_H against time to follow-up on a pointwise basis. Results are displayed graphically in the form of bar charts at each stimulus location. The length of a bar indicates defect depth, and the colour describes the nature of the slope and the statistical significance. Dark and light bars indicate deterioration ($p < 0.05$ and $p < 0.01$ respectively), yellow bars non-significant regression slopes, and blue bars outliers. Birch et al (1995) compared Progressor with the linear regression of MD_H and the Glaucoma Change Probability programs of the Humphrey Field Analyser. All three algorithms showed concordance in determining whether a visual field series was stable or was showing progression. Similarly, Fitzke et al (1996) showed good agreement between Progressor and glaucoma change probability.

1.10.3. Cluster Analysis.

Cluster analysis is a technique for measuring the spatial relationship between two or more stimulus locations (Chauhan et al 1989). It is based upon the premise that clusters of locations with reduced sensitivity are found with greater frequency in diseased eyes than in normal fields (Heijl and Åsman 1989). The deviation of the measured threshold from the age-corrected normal mean threshold value is calculated for each location and compared as a function of the distance between locations. Clusters are usually analysed according to the approximate nerve fibre distribution of the retina (Heijl and Åsman 1989).

1.10.4. Program DELTA.

The advantage of statistical analysis performed by a computer external to the perimeter is that data can be analysed easily without the need for data transcription and transformation (Fankhauser and Jenni 1981). DELTA was an analytical program developed for the Octopus perimeter (Bebić and Fankhauser 1981). A statistical t-test was performed on the visual field data selected from any two examinations to determine whether a change in MS had occurred

(Fankhauser and Jenni 1981). Hills and Johnson (1988) reported that the t-test was very sensitive to generalised depression of the visual field, but was unable to detect small to moderate localised scotoma.

1.10.5. PeriData and PeriTrend.

PeriData and PeriTrend are PC based programs (DOS and Windows respectively) designed for the transmission, storage, and processing of visual field data from the Humphrey Field Analyser or Octopus range of perimeters (Weber and Kriegelstein 1989; Brusini et al 1991). In addition to the conventional Humphrey Field Analyser and Octopus visual field indices, several new methods have been devised to aid analysis of the visual field. The visual field can be analysed either globally or in hemifields, quadrants, sectors, rings, or according to the arrangement of nerve fibre layers in the retina (Peridata 6.3 α Users Manual).

Stack Bar Histogram.

The stack bar histogram consists of an upper diagram of the relative sensitivity (MD_f or global mean) of the visual field. Beneath this is a grey-scale bar representing the complete visual field. The size of the grey-scale partition is graded according to the frequency at which the different classes of relative sensitivity occur. The advantage of this type of graphical representation is that it facilitates viewing of a number of visual fields sequentially so that any trend may become evident.

Global Analysis of Topographical Trends.

Graphical Analysis of Topographical Trends (GATT) (Weber and Kriegelstein 1989; Weber et al 1989) compares two visual fields by means of an interpolated grey-scale. Characteristic patterns are produced which variously denote stable areas and areas of either improvement or deterioration. In unchanged areas, the appearance of the grey-scale is normal. In changed areas, stripes are produced, the contrast of which is an indication of the degree of change. Vertical stripes indicate an improvement in the visual field, whereas horizontal stripes indicate visual field deterioration. The PeriData program is able to display the results chronologically in either a numeric or graphical format.

1.10.6. Octosmart.

Octosmart is a PC based program designed to evaluate results from the Octopus G1, G1X and G2 Programs objectively (Funkhouser et al 1991). Octosmart aims to standardise visual field interpretation eliminating subjective decisions made by the perimetrist. Several studies have evaluated the performance of Octosmart against that of experienced clinicians. Hirsbrunner et al (1990), and Funkhouser et al (1991) found highly consistent judgements between interpreters and Octosmart only in cases of obvious pathology and concluded that Octosmart was of use in reducing a large number of visual fields into manageable proportions.

1.10.7. Artificial Neural Networks.

Artificial neural networks possess the ability to learn from previous experience. The application of artificial neural networks to visual field analysis is in its infancy but the technique is already showing a high degree of sensitivity and specificity. Error back propagation is currently the most widely implemented of all neural network paradigms (Chester 1993). The principle of a two-layered neural network of this type applied to visual field analysis in glaucoma is illustrated in Figure 1.3. The neural network is exposed to a training set of input data and is also given the correct set of output data. Interconnection weights at the nodes within the network are then adjusted until the network responds correctly. The neural network is then able to receive unknown data and make an appropriate diagnosis.

Using this approach, Kelman et al (1991) were able to produce a neural network which was able to distinguish visual field loss in glaucoma and in optic neuropathy. Nagata and co-workers (1991) trained a neural network to recognise 40 patterns of visual field loss. The computer generated classifications of visual field loss showed 85% concordance with the diagnosis made by ophthalmologists. Spenceley et al (1994) developed a neural network for use with the Henson 2000 Central Field Analyser. In the detection of early glaucomatous loss, the network achieved high sensitivity (0.958) and specificity (0.968). Goldbaum and associates (1994) developed a neural network for the Humphrey Field Analyser. Two experts classified the visual fields against the neural network. The sensitivity of the experts was 59% compared to 67% for the neural network. The corresponding specificity for the experts was 74%

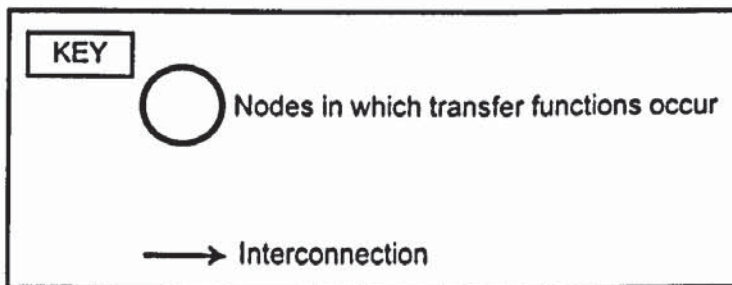
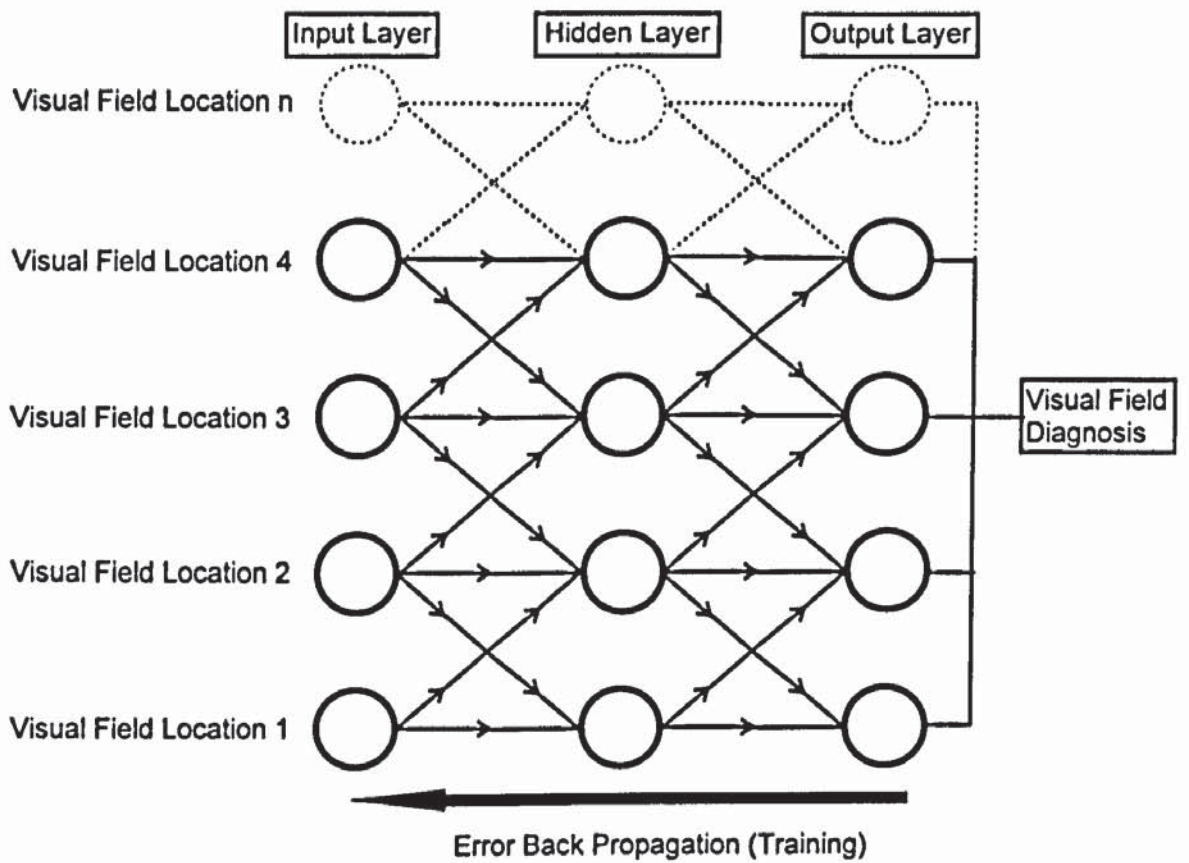


Figure 1.3. A schematic model of an artificial neural network applied to visual field diagnosis.

compared to the neural network which was 71%. The agreement between each observer and the neural network ranged between 72% and 75% which suggested that the data limited sensitivity of the trained observers and the neural network. In conclusion, artificial neural networks are able to distinguish abnormality as well as human observers but their performance is limited by their design which utilises a training data set that has already been classified as normal or abnormal by human observers.

1.11. Factors Influencing Perimetric Data Acquisition.

The acquisition of perimetric data is influenced by a number of extraneous factors which can be classified into three groups: physical, physiological, and psychological factors.

Physical Factors.

The principle limiting physical factors which affect the dimensions of the visual field are the frontal, nasal, zygomatic and maxillary bones surrounding the orbit (see Section 1.1). Facial features such as deep-set eyes and the size of the palpebral aperture may also influence sensitivity (Fisher 1967). The effect of superior lid ptosis reduces sensitivity in the superior visual field (Meyer et al 1993).

Physiological Factors.

1.11.1. Age.

Visual function is known to deteriorate with advancing age for a variety of psychophysical and electrophysiologic functions (Johnson and Choy 1987). Various workers have reported a decrease in sensitivity with increasing age. Haas et al (1986) reported a linear decline in sensitivity of approximately 0.58 dB per decade. Similarly, Brenton and Phelps (1986) reported a linear decline in sensitivity of 0.5 dB per decade at fixation, 0.6 dB per decade within 30° eccentricity and 0.6 dB per decade between thirty and sixty degrees.

Pointwise analysis of the central thirty degrees by Heijl and co-workers (1987a) found that the age decline slope at each location in the visual field is greater in the mid-periphery than

paracentrally. The change in shape of the hill of vision with age has also been corroborated by other workers (Haas et al 1986; Jaffe et al 1986; Flanagan et al 1993a; Okuyama et al 1993).

Differences between the superior and inferior hemifields have also been reported. The rate of decrease in sensitivity with age is faster in the superior field compared to the inferior field (Haas et al 1986; Jaffe et al 1986; Okuyama et al 1993; Flanagan et al 1993a).

The age-related decline in sensitivity to conventional W-W stimuli may partly be due to the reduction in retinal luminance, induced by a reduction in the transmission of the ocular media (Sample et al 1988), and pupil size (Weale 1992). The greatest contribution to the age-related decline in perimetric sensitivity is thought derive from the decline in retinal photoreceptors, retinal neurones, and retinal pigment epithelial cells (Gao and Hollyfield 1992; Curcio et al 1993; Panda-Jonas et al 1995). Panda-Jonas and co-workers (1995) found a linear decline in the total photoreceptors of between 0.2% and 0.4% per year, and in optic nerve fibres a decline of approximately 0.3% per year. This is in concordance with the 0.064 dB per year (0.2%) decline in perimetric sensitivity reported by Zulauf et al (1994).

Photoreceptor loss may be greater in the peripheral rather than in the central retina (Gao and Hollyfield 1992; Panda-Jonas et al 1995), which may account for the greater decline in sensitivity reported in the peripheral visual field when compared to central regions which occurs with advancing age (Haas et al 1986; Jaffe et al 1986; Heijl et al 1987a; Flanagan et al 1993a; Okuyama 1993). Rods appear to be lost at a greater rate than cones (Gao and Hollyfield 1992; Curcio et al 1993; Panda-Jonas et al 1995). There is currently no histological data available regarding the age-related decline of individual long-, medium-, and short-wavelength sensitive cone populations.

The age-related decline in sensitivity for short-wavelength automated perimetry is described in Chapter 4.

1.11.2. Optical Defocus.

Optical defocus has been shown to reduce visual acuity and contrast sensitivity at high spatial frequencies (Campbell and Green 1965; Simpson et al 1986).

In static perimetry, spherical optical defocus attenuates sensitivity (Benedetto and Cyrlin 1985; Atchison 1987; Heuer et al 1987; Herse 1992). The degree of attenuation is not constant across the visual field. Benedetto and Cyrlin (1985) reported that the loss in sensitivity was greater at fixation than at thirty degrees eccentricity for defocus between -2.50 and +10.00 DS. High resolution testing of the central 12 degrees revealed no statistically significant alteration in mean sensitivity for spherical optical defocus within the range of ± 2.00 DS. For blur of +3.00 DS and greater there was a rapid loss in central sensitivity. In a similar study, Heuer et al (1987) reported that +1.00 DS of optical defocus did not significantly alter the threshold at fixation but did so at all other eccentricities. Atchison (1987) also reported that spherical defocus caused a reduction in sensitivity which was greater in the periphery compared to fixation. The attenuation of sensitivity by optical defocus is less pronounced with increase in stimulus size (Sloan 1961; Atchison 1987).

Adams et al (1987a) studied the effect of positive spherical defocus up to +5.00 DS on short-wavelength perimetric thresholds and found that the thresholds were little affected by defocus and eccentricity. Adams et al (1987a) suggested that the Goldmann size V stimulus contained low spatial frequencies and thus dioptric blur had little effect on detection. Indeed, Johnson et al (1993a) also showed that short-wavelength perimetry was resistant to spherical blur between zero and +8.00 DS. They demonstrated that 4 D of spherical blur increased the magnitude of SWS isolation by 0.2 to 0.3 log units.

1.11.3. Pupil Size.

Pupil size determines retinal illumination, and consequently can influence perimetric sensitivity. Retinal illumination, D , in trolands, is given by the following equation which assumes the distance of the nodal point from the retina is 16.7 mm.

$$D = 0.36\tau\lambda sB \qquad \text{Eqn 1.24.}$$

where, τ_λ , is the transmission factor (the ratio of the intensity of light falling on the retina over the intensity of the light falling on the cornea), s , is the area of the pupil in cm^2 , and, B , is the luminance of the extended source of light. The transmission factor, τ_λ , is dependent upon wavelength, varying from 0.1 in the extreme violet where the yellow lens pigment absorbs short wavelengths, to 0.7 in the deep red region of the spectrum. For white light, τ_λ , is equal to 0.5 (Davson 1991).

Under photopic conditions, a change in retinal illuminance due to changes in pupillary diameter would not be expected to alter visual field sensitivity significantly since Weber's Law applies. When perimetry is performed in patients with pupil sizes less than two millimetres in diameter, retinal illuminance is in the mesopic range where Weber's Law no longer applies. Since the background employed in conventional perimetry is in the mesopic range, retinal illuminance should vary with pupil size and therefore significantly affect visual field sensitivity (Lindenmuth et al 1989; Rebolleda et al 1992).

Lindenmuth et al (1989) evaluated the effect of miosis induced by 2% pilocarpine in twenty normal subjects using program 30-2 of the Humphrey Field Analyser. Visual field indices were compared with initial baseline indices derived using natural pupils. Group mean MD_H worsened by 0.67 dB. The deterioration of MD_H was greatest in the peripheral visual field. There was no significant change in SF and foveal threshold.

Webster et al (1993) evaluated the effect of pilocarpine on the glaucomatous visual field. Twenty patients with chronic open angle glaucoma who had not previously undergone miotic therapy were examined with Program 30-2 of the Humphrey Field Analyser. Two percent pilocarpine was applied to one eye 40 minutes before examination and the fellow eye acted as a control. Seventeen of the patients exhibited a deterioration in MD_H , whilst three eyes exhibited an improvement in MD_H following the administering of pilocarpine. No significant changes in PSD were found.

Pupillary dilation would be expected to increase sensitivity due to an increase in retinal illuminance. Wood et al (1988) evaluated the effect of pupil miosis induced by 0.5% thymoxamine and pupil mydriasis induced by 10% phenylephrine in ten normal subjects using the Dicon AP3000 automated perimeter. Sensitivity increased with increase in pupil size. In all drug conditions sensitivity decreased with increasing eccentricity, but decreased at a slower rate in pupillary mydriasis.

Lindenmuth et al (1990) evaluated the effect of pupillary dilation induced with 1% tropicamide in 18 normal subjects. MD_H decreased by an average 0.83 dB, and CPSD worsened by an average 0.60 dB. There was no significant difference in the SF and PSD.

Kudrna et al (1995) evaluated the effect of mydriasis using a combination of 1% tropicamide, 1% proparacaine, and 2.5% phenylephrine in 23 normal subjects using Program 30-2 of the Humphrey Field Analyser. A mean decrease in the foveal threshold of 2.56 dB occurred with mydriasis. The MD_H was greater by 1.43 dB than control eyes, and the SF decreased by 0.19 dB. Their results were at variance with the findings of Wood et al (1988), but were accounted for by the Stiles-Crawford effect and spherical and chromatic aberrations which increase with increase in pupil size. Decreased sensitivity may result from the Stiles-Crawford effect, whereby light rays entering the eye through the centre of the pupil elicit a greater sensation of brightness than light rays that pass through the pupil eccentrically. Spherical and chromatic aberrations may also attenuate visual field sensitivity.

Rebolleda et al (1992) studied 29 eyes of 18 glaucoma patients receiving pilocarpine. Baseline Humphrey Field Analyser Program 30-2 visual fields were obtained prior to the instillation of the 10% phenylephrine. Mean deviation increased by an average 1.89 dB. PSD improved by 1.42 dB and CPSD by 1.73 dB. There was no significant change in foveal threshold or the SF.

1.11.4. Media Opacity,

Absorption of visible wavelengths and light scatter induced by opacity in the ocular media result in attenuation of the threshold. The effect of media opacity on the visual field will be discussed in greater detail in Chapter 6.

1.11.5. Pharmacological Agents.

A number of systemic pharmacological agents can influence the outcome of the visual field. Zulauf et al (1986) studied the effect of a blood concentration of 0.08% alcohol on the visual field. Sensitivity was found to be unaffected by this level of alcohol but the number of false-positive responses increased as a result of decreased patient co-operation. Wild et al (1990) found that for a blood alcohol concentration of 66.9 mg%, MD_H was reduced, whilst the PSD, CPSD, and the number of stimulus presentations were increased. The SF and reliability catch-trials were unaffected.

Drugs which act on the central nervous system (CNS) can also influence the visual field. Haas and Flammer (1985) found that short-term treatment with 5 and 10 mg diazepam had little effect on MS, the SF, and false-positive catch-trials. The effect of antihistamines on the visual field is equivocal. Wild et al (1989b) studied the effect of sedative and non-sedative antihistamines on the perimetric profile. The sedative antihistamine, triprolidine, did not influence the SF but a non-sedative antihistamine, loratadine, was found to increase the SF, although the mechanism was unknown. In a retrospective examination of patients, Mann and co-workers (1989) reported that the that chloroquine (approximately 250 mg day⁻¹) and hydroxychloroquine (approximately 400 mg day⁻¹) had no measurable effect on visual field indices.

Psychological Factors.

1.11.6. Learning.

The presence of a learning effect has been reported by a number of workers. An increase in mean sensitivity has been widely reported, which is maximal between the first and second visual field examinations in normal subjects (Wood et al 1987b; Heijl et al 1989; Marchini et al

1991), ocular hypertensive patients (Wild et al 1989c), and glaucoma patients (Kulze et al 1990; Marra and Flammer 1991; Heijl and Bengtsson 1996). The improvement in sensitivity is non-uniform, the improvement at peripheral locations in the central visual field being greater than at more central locations (Heijl et al 1989; Kulze et al 1990; Heijl and Bengtsson 1996). Heijl and Bengtsson (1996) reported that patients with fields exhibiting moderate glaucomatous loss displayed greater improvements than fields with mild or severe loss. Wood et al (1987b) reported considerable inter-subject variability in the magnitude of the improvement in sensitivity. This variability may exhibit a positively skewed distribution (Heijl et al 1989). The magnitude of the SF decreases as a result of the learning effect (Heijl et al 1989; Wild et al 1989c; Marchini et al 1991; Searle et al 1991; Heijl and Bengtsson 1996).

Marra and Flammer (1991) found the improvement in sensitivity with learning was correlated with refractive error. A greater improvement was shown in patients with high refractive corrections.

1.11.7, Fatigue.

Patient fatigue during the course of visual field examination can result in a non-uniform reduction in sensitivity. The effect of fatigue on the perimetric profile will be discussed in greater detail in Chapters 3 and 5.

CHAPTER 2. RESEARCH OUTLINE.

2.1. Aims of the Study.

The thesis was a continuation of the work previously undertaken within the Department of Vision Sciences, Aston University, Birmingham. It was concerned with the within-subject and between-subject factors which influence conventional white-on-white (W-W) perimetry and short-wavelength automated perimetry (SWAP).

2.2. Rationale.

A considerable proportion of the automated perimetry research carried out within the Department had evaluated within- and between-test alterations in sensitivity (Wood et al 1987b; Wild et al 1989a,c; Wild et al 1991; Dengler-Harles et al 1990; Searle et al 1991; Hudson et al 1993; Moss et al 1993; 1994; 1995; Hudson and Wild 1995). The studies of Searle et al (1991) and Hudson et al (1993) evaluated the progressive decline in within- and between-eye sensitivity which occur during the course of a perimetric examination; a phenomenon termed the fatigue effect. The conclusions from these studies extended those from others (Langerhorst et al 1987; Heijl and Drance 1983; Johnson et al 1988a). The fatigue effect had been assessed using the standard 4-2 dB double reversal staircase strategy. The subsequent introduction of abbreviated staircase strategies provided the opportunity for considerably shorter perimetric examinations although at the expense of increased within- and between-test variability (Flanagan et al 1993a,b; O'Brien et al 1994). The influence of abbreviated staircase strategies on the fatigue effect was unknown. The initial part of the thesis was concerned with the determination of the magnitude and the time course of the fatigue effect during routine perimetric examinations derived using two different abbreviated staircase strategies. The variability of these staircase strategies with respect to the standard staircase strategy was also evaluated. The Octopus 1-2-3 was used for the assessment of within-test alterations in sensitivity since the thresholding of the stimulus locations with this perimeter is divided into eight distinct stages; each location is thresholded sequentially but randomly within each stage.

The remainder of the thesis was concerned with evaluating within- and between-test changes in sensitivity of SWAP, a method of visual field investigation based upon chromatic adaptation of the visual system. SWAP employs a blue stimulus to preferentially stimulate the short-wavelength sensitive (SWS) pathway and a high luminance yellow background to adapt the remaining chromatic pathways and the rods. A number of groups have reported the utility of SWAP in the detection of glaucomatous visual field loss and visual field progression (De Jong et al 1990; Hart et al 1990; Sample and Weinreb 1990, 1992; Sample et al 1993; Johnson et al 1993a,b; Johnson et al 1995).

Previous work undertaken in the Department had been concerned with the use of SWAP for the detection of diabetic retinopathy and of primary open-angle glaucoma (Hudson et al 1993, Moss et al 1995) and with the influence of pre-retinal factors on the outcome of SWAP (Hudson and Wild 1995). Short-wavelength stimuli are attenuated by the ocular media and by the macular pigment. Hudson and Wild (1995) reported that the influence of these components on SWAP exhibited considerable between-subject variability which confounded the interpretation of SWAP. In addition, age-related cataract has also been found to preferentially attenuate SWAP sensitivity compared to standard W-W perimetry (Moss et al 1995). Recently, the stimulus and background parameters utilised in SWAP have been standardised. The standard background luminance is 130 cdm^{-2} less than that employed in previous studies in the Department. Furthermore, the stimulus employed in previous studies was derived using either a narrowband 450 nm stimulus or a broadband OCLI blue. The standard stimulus is a narrowband 440 nm stimulus.

A study was undertaken to evaluate the characteristics of normal sensitivity of SWAP, derived using the standard 440 nm narrowband stimulus and 100 cdm^{-2} yellow background, for the Standard 4-2 dB double reversal staircase strategy and the 3 dB single reversal FASTPAC strategy. The primary aim of this study was to determine the extent of any between-subject differences in sensitivity between SWAP and conventional W-W perimetry. Secondly, the influence of correction of SWAP for ocular media absorption on the magnitude of the between-

subject variation in normal sensitivity was investigated. The final aim of the study was to evaluate the influence of forward light scatter on the outcome of SWAP.

There is a pressing need to evaluate the influence of the fatigue effect in SWAP, which has not been quantified. A study was therefore undertaken to investigate the influence of fatigue on the outcome of SWAP in normals and patients with glaucoma. Several workers have suggested that one of the causal factors to the fatigue effect is the phenomenon of Ganzfeld blankout which is thought to be due to the effects of binocular rivalry, induced by the luminance difference between the tested and occluded eyes (Blake and Overton 1979; Blake 1989). Ganzfeld blankout is prevented under binocular viewing (Bolanowski and Doty 1987) and when the conventional opaque occluder is replaced by a translucent one (Fuhr et al 1990). The second aim of the study was to evaluate the influence of translucent occlusion on the magnitude of the fatigue effect in W-W perimetry and SWAP.

The increase in ocular media absorption with increasing age is undisputed (Said and Weale 1959; Norren and Vos 1974; Johnson et al 1993c; Sample et al 1991 Hudson and Wild 1995). Several studies conducted in the Department have investigated the influence of simulated lens opacity and age-related cataract on the visual field derived using W-W perimetry (Wood et al 1987a; 1989; Dengler-Harles et al 1990; Moss et al 1995). The preferential attenuation of short-wavelengths by crystalline lens has greater implications for SWAP than conventional W-W perimetry. Age-related cataract may be considered as an acceleration of the normal aging process in the crystalline lens. The influence of age-related cataract on SWAP was investigated by Moss et al (1995) who reported a preferential attenuation of SWAP with respect to W-W perimetry. The stimulus and background parameters of SWAP utilised in this study, namely; OCLI broadband blue stimulus, 330 cdm⁻² broadband yellow background, differ from the standard SWAP parameters. A narrowband stimulus filter would be expected to have a greater influence on the outcome of SWAP in patients with age-related cataract than that reported by Moss et al (1995). The aim of this study, therefore, was to investigate the influence of cataract extraction in SWAP derived using the standard parameters. The influence of ocular media absorption and forward light scatter were also studied.

The range of stimulus intensities over which the short-wavelength sensitive pathway is preferentially stimulated determines SWS pathway isolation. The magnitude of SWS pathway isolation has traditionally been quantified utilising the two-colour increment threshold method of Stiles (1959). Previous workers quantified SWS pathway isolation in SWAP from foveal measurements (Sample et al 1990; Johnson et al 1993a). Their methodologies achieved the necessary reduction in background luminance from alterations to the background illumination voltage supply, which theoretically, may alter the state of retinal adaptation due to alterations in the colour temperature of the background. Furthermore, the pupil size was not controlled for the different adaptation levels investigated. A study was undertaken to quantify the degree of SWS pathway isolation with increasing eccentricity, and to evaluate the optimum stimulus wavelength necessary for SWAP. Pupil size was controlled and a system of apertures designed to achieve reduction in background luminance without altering the chromaticity characteristics of the background.

2.3. Logistics.

The research was conducted within the Department of Vision Sciences, Aston University, Birmingham and had approval from the Aston University Human Science Ethical Committee and where applicable from the City Hospitals Health Trust Research and Ethics Committee.

Normal control subjects were recruited from students and staff of the University and from locally situated old age pensioner associations. The nature of the procedures were fully explained both with an information sheet and verbally. Before commencement of each study each subject was requested to sign a consent form.

Cataract patients were recruited from the Birmingham and Midland Eye Centre (formally Birmingham and Midland Eye Hospital) and Selly Oak Hospital, Birmingham by a consultant ophthalmologist who provided confirmation of diagnosis and ensured that all volunteers satisfied the necessary inclusion and criteria of the study. Patients were required to attend the Department for three visits prior to cataract surgery, each visit lasted approximately one hour. Cataract surgery and post-operative follow-up was performed by or under the supervision of

the recruiting consultant ophthalmologist. Each patient was required to attend the Department for three further visits which occurred between six and eight weeks post-operatively.

Modifications to the HFA 640 and recruitment of normal subjects did not present any problems. The recruitment of cataract patients was confounded by a lack of patients meeting the rigid inclusion criteria. A period of approximately 18 months was required to achieve the sample size in this study.

CHAPTER 3. THE INFLUENCE OF STAIRCASE STRATEGY ON THE FATIGUE EFFECT IN WHITE-WHITE (W-W) PERIMETRY.

3.1. The Fatigue Effect in Automated Static Perimetry.

The outcome of a visual field examination is influenced by physiological factors such as pupil size (Rebolleda et al 1992; Webster et al 1993; Kudrna et al 1995), refractive correction (Atchison 1987; Heuer et al 1987; Herse et al 1992) and media opacities (Guthauser and Flammer 1988; Lam et al 1991; Stewart et al 1995), and by psychological factors. A learning effect, whereby sensitivity increases during and between perimetric examinations, has been demonstrated in normal subjects (Wood et al 1987b; Heijl et al 1989; Marchini et al 1991) and in patients with ocular hypertension (Wild et al 1989c) and glaucoma (Kulze et al 1990; Marra and Flammer 1991; Heijl and Bengtsson 1996). The decline in sensitivity which occurs during the course of a perimetric examination is termed the fatigue effect. The fatigue effect has been demonstrated in normal subjects (Heijl 1977; Langerhorst et al 1987; Johnson et al 1988a; Fujimoto and Adachi-Usami 1993; Hudson et al 1993) and patients with ocular hypertension (Heijl and Drance 1983; Langerhorst et al 1987; Hudson et al 1993), glaucoma (Heijl 1977; Heijl and Drance 1983; Langerhorst et al 1987; Johnson et al 1988a; Fujimoto and Adachi-Usami 1993) and optic neuropathy (Johnson et al 1988a; Fujimoto and Adachi-Usami 1993). It is thought that within-eye learning and fatigue effects oppose each other during a perimetric examination until the influence of the learning effect diminishes and the fatigue effect becomes dominant (Brenton et al 1986; Katz and Sommer 1986; Searle et al 1991; Hudson et al 1993).

Fatigue effects have been investigated either by repeated thresholding at a selected number of stimulus locations (Heijl 1977; Heijl and Drance 1983; Langerhorst et al 1987; Johnson et al 1988a; Marra and Flammer 1991; Searle et al 1991; Fujimoto and Adachi-Usami 1993) or in a staged examination of the complete visual field within 30° eccentricity (Hudson et al 1993).

The fatigue effect increases with increasing eccentricity (Johnson et al 1988a; Langerhorst et al 1987; Searle et al 1991; Hudson et al 1993) and is more pronounced in areas adjacent to visual field defects (Heijl 1977; Heijl and Drance 1983; Johnson et al 1988a). Hudson et al

(1993) reported a depression in the hill of vision in normals and ocular hypertensives which was more marked in the inferior field than the superior field and accompanied by localised loss which was greater in the superior and nasal fields. The fatigue effect has not been demonstrated within 10° eccentricity (Fujimoto and Adachi-Usami 1993). Marra and Flammer (1991) were unable to demonstrate a fatigue effect in normal subjects, and in cataract or glaucoma patients for the repeated thresholding of three stimulus locations in one eye for a testing period of between 5 and 8 minutes. An explanation of this finding may be the reduced number of stimulus locations employed in this study.

Searle et al (1991) and Hudson et al (1993) investigated the between-eye fatigue effect. The loss in sensitivity was greater in the second eye examined. Searle et al (1991) reported that the deterioration in MS over time was more pronounced in the superior visual field of the second eye examined. Hudson et al (1993) reported that the change in shape of the hill of vision was more exaggerated in the second eye examined. Furthermore, the introduction of a three minute rest period between eyes was insufficient to overcome the progressive decline in sensitivity. Searle et al (1991) suggested that the order in which the eyes were tested in a perimetry examination was important and that the reduced sensitivity observed in the second eye should be incorporated into the perimeter normative data set.

The magnitude of the fatigue effect is independent of background luminance (Heijl and Drance 1983). Searle and co-workers (1991) reported that the magnitude of the fatigue effect was reduced when the stimulus duration was decreased from 200 ms to 100 ms.

3.1.2. Explanation of the Fatigue Effect.

During the course of a perimetric examination, eye movements are suppressed. The uniform background luminance has zero spatial frequency and therefore induces Ganzfeld blankout or Troxler fading (Barlow and Verrillo 1976; Bolanowski and Doty 1987; Fuhr et al 1990; Gur 1989, 1991). It has been suggested by a several groups that this effect may be the principle factor contributing to the decline in sensitivity during perimetry (Searle et al 1991; Hudson et al 1993). Bolanowski and Doty (1987) showed that Ganzfeld blankout is prevented under

binocular viewing conditions suggesting that the fading phenomenon may be due to the effects of binocular rivalry. The asymmetry in retinal illuminance between the two eyes which occurs when an opaque occluder is used induces Ganzfeld blankout. A translucent occluder retards the onset of Ganzfeld blankout and may therefore reduce the effects of fatigue. Indeed, it has been shown that the MS is greater with such an occluder (Fuhr et al 1990).

Psychological factors may also play a role in the fatigue effect. Perimetry may be considered as a vigilance task since it requires a simple motor response to a randomly presented stimulus against a uniform background. The reduction in sensitivity which occurs during perimetry may result from habituation of the arousal response, and the evoked potentials produced from the repetitive and continuous stimuli which constitute the task (Mackworth 1969). The arousal response describes the change in electroencephalogram from alpha rhythm associated with sleep, to low amplitude desynchronised rhythms associated with arousal. Sokolov (1963) found that arousal results in an increase in sensitivity to a stimulus accompanied by blocking of the alpha response. The decline in sensitivity during perimetry could be explained by decreased vigilance resulting from an increase in habituation due to an increase in alpha wave activity.

3.2. Staircase Procedures.

3.2.1 Psychophysical Aspects.

Fechner (1860) devised the three so called classical methods for estimating the difference threshold; namely the method of constant stimuli, the method of limits, and the method of adjustment. Such methods are non-adaptive, as the stimulus intensities are predetermined and are not influenced by the subject's responses. Conversely, the presentation of the stimulus in adaptive methods is dependent upon the subject's responses from previous trials. Adaptive methods are therefore thought to be more efficient since fewer stimuli are required to estimate the threshold (Cornsweet 1962). Additionally, stimulus intensities presented closest to the threshold yield greater information than those presented farthest from threshold (Taylor 1971).

The classical method of limits may be modified to truncate the presentation of the stimulus after a shift in the response category has occurred, ie the response changes from not-seen to seen or vice versa. This is known as the truncated method of limits, or the simple up-down method. Treutwein (1995) describes the simple up-down method by the equation:

$$X_{n+1} = X_n - \delta(2Z_n - 1) \quad \text{Eqn 3.1.}$$

where, X_n , is the stimulus luminance at presentation, n ; X_{n+1} , is the optimal stimulus luminance; δ , is the fixed step size and, Z , is the response category ($Z_n = 0$ when the stimulus is not seen, and $Z_n = 1$ when the stimulus is seen). The final estimate of the threshold can be determined from the mid-point of the reversal points, or alternatively using the maximum likelihood probability estimate (Dixon and Mood 1948). The stochastic approximation method of Robbins and Monro (1951) are described by:

$$X_{n+1} = X_n - \frac{c}{n}(Z_n - \phi) \quad \text{Eqn 3.2.}$$

where, c , is a constant and, ϕ , is the desired probability on the frequency of seeing psychometric function. When $\phi = 0.5$, the upward and downward steps are of equal size, and asymmetric when $\phi \neq 0.5$. The step size, δ , is proportional to the number of stimulus presentations (c/n), and thus decreases with increasing duration of the staircase procedure.

3.2.2. Staircase Efficiency.

Taylor and Creelman (1967) and Taylor (1971) defined the "sweat" factor, K , to measure the efficiency of a psychophysical procedure. It is given as the product of the variance of the best threshold estimate and the number of trials necessary to obtain that estimate. The benefit/cost ratio may be applied to evaluate the efficiency of a staircase procedure in perimetry (Flanagan et al 1993a; Weber and Klimaschka 1995).

$$\text{Efficiency} = \frac{\text{benefit}}{\text{cost}}$$

where,

$$\text{benefit} = \text{reproducibility} = 1/\text{variance} = 1/SF^2$$

$$\text{cost} = \text{time} = \text{number of stimulus presentations (Q)}$$

Thus,

$$\text{Efficiency} = \frac{1}{(\text{SF}^2 \cdot Q)} \quad \text{Eqn 3.3.}$$

3.2.3. Standard Perimetry Threshold Strategies.

The standard 4-2 dB double reversal staircase procedure employed in perimetry may be considered as an abbreviated stochastic approximation sequence. This method only assumes that the psychometric function governing the frequency-of-seeing is an increasing function. Spahr (1975) evaluated the optimal presentation of stimuli in perimetry in simulation studies. For an up-down staircase, an initial step size of 4 dB followed by a 2 dB step size with a final mathematical correction of 1 dB yielded the best information gain per response. In further simulation studies, Bebié et al (1976b) compared 4-2-1 dB and 2-1-0.5 dB staircase strategies with the method of limits using 4 dB and 2 dB stimulus intervals. The method of limits failed to estimate the true threshold from an average of repeated measurements and the systematic error was highly dependent on the placement of the initial stimulus presentation. Although up-down staircases required more stimuli than the method of limits, they estimated the true threshold with greater accuracy and were independent of the initial stimulus intensity. The reliability of the threshold determinations was slightly increased with the 2-1-0.5 dB strategy but at the expense of a substantial increase in the number of stimulus presentations. The 4-2-1 dB staircase strategy has been adopted in the Octopus range of perimeters. In the standard strategy of the HFA a 4-2 dB staircase design is also employed but without a final mathematical correction of ± 1 dB. The threshold with the HFA is recorded as the last seen stimulus. Johnson et al (1992) evaluated a number of staircase conditions using computer simulations in order to derive the optimum condition. Initial step sizes ranging between 3 and 8 dB, final step sizes between 2 and 4 dB, and the number of reversals (between 1 and 3) were investigated. Response fluctuation information derived from normal subjects was incorporated into the simulation design. For all staircase conditions, there was a reciprocal relationship between accuracy and efficiency. Increases in response fluctuation resulted in an increase in both the number of stimulus presentations and the magnitude and frequency of threshold errors. At low thresholds, the number of reversals at the final step size did not improve

accuracy but at higher levels of threshold accuracy increased. There was no increase in variability of the threshold estimate with increasing number of reversals. The staircase condition with the best accuracy-efficiency compromise was an initial step size of 6 dB, a final step size of 3 dB and a single reversal at the final step. This condition approaches the standard staircase strategies currently employed in automated static perimetry.

3.2.4. Fast Perimetry Threshold Strategies.

A number of faster staircase strategies have been proposed with the specific aim of reducing the overall examination time, whilst striving to maintain accuracy. RIOTS (Real-time Interactive Optimised Test Sequence) (Johnson and Shapiro 1991) was developed with the aid of the KRAKEN simulation program (Shapiro et al 1989). The algorithm was based on the assumption that normal and abnormal visual fields exhibit distinct spatial patterns of sensitivity. RIOTS was a four stage strategy. Initially, thresholds were obtained at 12 seed and two blind spot locations using a modified MOBS (Modified Binary Search) procedure. These thresholds were then used to calculate the expected thresholds at the remaining locations. The stimulus intensities were then presented at the remaining stages, according to a set of heuristic rules dependent upon the spatial arrangement of the threshold with neighbouring stimulus locations, and the rate of false-positive and false-negative responses. Simulation studies demonstrated that the RIOTS procedure was between 1.5 and 2 times faster than the 4-2 dB strategy of the HFA for the normal visual field and two to three times faster in the examination of the abnormal visual field. The accuracy with RIOTS was slightly greater than the 4-2 dB strategy. To date, the RIOTS procedure has not been adopted in commercially available perimeters.

The FASTPAC algorithm of the Humphrey Field Analyser, utilises a 3 dB step size in a staircase which crosses the threshold once. FASTPAC has been studied extensively in normal subjects, glaucoma patients and in simulation studies. Flanagan et al (1993a) studied FASTPAC in 98 normal subjects ranging in age from 23 to 83 years and found no significant difference in global MS compared to the standard 4-2 dB algorithm. Global SF was 0.42 dB greater in FASTPAC whilst the reduction in time was approximately 40%. The improvement in efficiency for FASTPAC was 5%. The relationship of the visual field indices in glaucoma

between the Standard and FASTPAC staircase strategies is equivocal. Flanagan et al (1993b) and O'Brien et al (1994) reported that FASTPAC yielded a lower MD_H than the Standard 4-2 dB algorithm by approximately 1 dB. However, Schaumberger et al (1995) found no statistical difference in MD_H between the two staircase strategies. Flanagan et al (1993b) and Schaumberger et al (1995) reported the SF with FASTPAC to be greater than the Standard 4-2 dB strategy, and this difference increased with increasing severity of visual field defect. This finding is at variance with O'Brien et al (1994) who found no statistical difference in the SF between FASTPAC and the 4-2 dB algorithm. Simulation studies of FASTPAC have found a greater number of threshold errors (defined as the difference between the estimated threshold and the patient's actual threshold) in FASTPAC which may account for the higher SF (Glass et al 1995). FASTPAC underestimated the threshold if the initial stimulus presentation was below the actual threshold and overestimated the threshold if the initial stimulus presentation was above the actual threshold (Glass et al 1995).

Weber (1990) suggested that the step sizes employed to estimate threshold in perimetry should adapt to the size of the physiological threshold zone which is known to depend on sensitivity (Weber and Rau 1992; Chauhan et al 1993; Olsson et al 1993). Weber and Rau (1992) measured the frequency-of-seeing at four locations within eccentricity 21° from fixation in 11 normal subjects, four locations between 29° and 51° in six normal subjects and at various locations out to an eccentricity of 26° from fixation in seven glaucoma patients. The stimulus locations examined in the glaucoma patients were in areas of normal sensitivity and within relative and absolute defects. In the normal subjects, the slope of the threshold zone was steep at the centrally located stimulus locations but flatter and more irregular in peripheral stimulus locations. In glaucoma, the slope of the threshold zone resembled the peripheral curves in normals at all locations tested and the flattest curves were found in regions of low sensitivity. The threshold coefficient was defined as the difference in intensity between the 50% frequency-of-seeing and the 84% frequency-of-seeing. In normals, the mean central threshold coefficient was 2.12 dB; at peripheral locations the mean threshold coefficient was 5.26 dB and was highly correlated with the threshold. In glaucoma patients, the threshold coefficients were higher than other groups (range 2.18 dB to 19.83 dB) and were weakly

correlated with the threshold level. Chauhan and co-workers (1993) examined four to six locations in 22 normals, 12 patients with suspected glaucoma, and 36 patients with glaucoma. The slope of the frequency-of-seeing curve was estimated by calculating the interquartile range corresponding to 25% and 75% frequency-of-seeing. The results were concordant with those of Weber and Rau (1992). Statistically significant differences were found between all groups for the effects of eccentricity, the threshold and the threshold deviation. Olsson et al (1993) used a maximum likelihood method to estimate the frequency-of-seeing in nine normal subjects, 19 patients with glaucoma, and four with cataract. They found that the slope of the frequency-of-seeing curve was strongly dependent on the threshold deviation from the age-corrected normal value.

The dynamic strategy of the Octopus, and Optima strategy in the HFA, employs variable staircase step sizes to estimate threshold. Step sizes of 2, 3, 5, 7, and 10 dB are used, with the largest steps presented in regions of low sensitivity and the smallest steps around regions of normal sensitivity. Weber and Klimaschka (1995) evaluated the dynamic and standard 4-2 dB strategies in 40 eyes of 40 glaucoma patients. Sixteen stimulus locations were examined, comprising the first Stage of Program G1X on the Octopus 1-2-3. A randomised protocol was adopted such that each patient was examined three times each with the dynamic and 4-2 dB strategies. Thresholds obtained at the four primary seed locations were excluded from data analysis since they were measured with a 4-2 dB staircase in both strategies. The number of stimulus presentations for the dynamic strategy was between 34% and 57% of the stimulus presentations necessary for the 4-2 dB strategy. In regions of low sensitivity, a greater number of stimulus presentations was required to estimate threshold, but the number of presentations for the dynamic strategy was not influenced by sensitivity. Variance in regions of low sensitivity was approximately ten times that found in areas of high sensitivity, although the magnitude differed little between strategies. Benefit/cost ratios were found to increase for both strategies with increasing sensitivity. The dynamic strategy was more efficient than the 4-2 dB strategy at all sensitivities.

3.2.5. New Perimetry Threshold Strategies.

The staircase procedures in commercial perimeters are non-parametric since they do not require prior knowledge regarding the nature of the threshold response. Conversely, parametric methods of estimating threshold demand a knowledge of the general form of the psychometric function governing the probability of stimulus detection. Theoretically, they offer a means of reducing the examination time without a loss in accuracy.

QUEST is a threshold estimation procedure which is based upon maximum likelihood probability (Watson and Pelli 1983). After each stimulus presentation with the maximum likelihood method, the most likely value of threshold is determined, which then becomes the stimulus intensity for the next presentation. The final estimate of the threshold is designated as the most likely value of threshold calculated after the last stimulus presentation. QUEST uses the median of the distribution of the probability of thresholds to calculate the stimulus intensity. Zippy Estimation by Sequential Testing (ZEST) is a QUEST procedure but uses the mean rather than the median. Simulations of ZEST show it to be more efficient than QUEST (King-Smith et al 1994). The Zippy Automated Perimetric Procedure (ZAPP) employs the ZEST procedure to estimate the threshold at twelve locations in the visual field (Schaumberger et al 1996). A two-dimensional polynomial surface is then applied to these estimates in order to derive threshold estimates at the remaining locations in the visual field. The number of stimulus presentations with ZAPP was reduced by 8% compared to the standard threshold algorithm. Nevertheless, the test-retest reliability of this algorithm is unproven.

Bayesian posterior mean threshold estimation (BPM) was employed by Olsson (1991) to estimate the threshold in perimetry. The method utilises all responses in the staircase and is capable of providing higher accuracy from the same threshold procedures in current use, or shorter tests with the same accuracy as currently available with conventional staircase procedures. It is assumed that the shape of the frequency-of-seeing curve is dependent upon the rate of false-positive and false-negative responses (Olsson et al 1989). A Gaussian distribution of the deviation of the initial stimulus intensity from the true threshold is specified, in addition to the probability of the staircase. These parameters are then used to estimate the

posterior mean threshold. Olsson et al (1989) obtained 30-2 visual fields in 20 eyes of 10 normals and 24 eyes of 15 patients with glaucoma. For each visual field, the pointwise thresholds were estimated with the BPM procedure and the conventional 4-2 dB double reversal staircase. Each subject was examined on a minimum of four occasions at weekly intervals. In locations where absolute defects were present, the information from the staircases at these points were not used in the BPM estimation. Test-retest variability was significantly lower with BPM method. BPM variance was 27% lower than the standard 4-2 dB strategy in normals and 7% in glaucomatous eyes. The BPM estimate of threshold was approximately 0.1 dB higher than the 4-2 dB threshold estimate.

The Bayesian approach was developed further by Olsson and Rootzén (1994) who employed a Markov random field model to specify the spatial variation of the threshold across the visual field and a prior knowledge of the type of visual field loss in glaucoma. This prior distribution, and the probability that the response button will be pressed yields a posterior distribution for each threshold. The model was applied to simulated and real patients. Between 10% and 30% reductions in the mean square error (MSE) were found between the standard 4-2 dB and the interactive algorithm, with the greatest improvement in normal and borderline visual fields. Although some defective locations were classified as normal in glaucomatous fields, there was good agreement with the defect status measured with the standard 4-2 dB algorithm. Bengtsson et al (1996) compared this interactive threshold algorithm with the standard 4-2 dB and FASTPAC strategies in 20 eyes of 20 normal subjects. The group MSE was 1.59 dB² for the interactive algorithm which was not significantly different from the 4-2 dB algorithm, but significantly lower than FASTPAC (group MSE = 2.61 dB²). The test duration was approximately 50% less with the interactive algorithm compared to the 4-2 dB algorithm and offered equivalent accuracy.

In summary, non-parametric up-down staircases are currently utilised in perimetry. The efficiency of these staircases is a trade-off between examination time and variance. The current "gold standard" is the 4-2 dB staircase with double reversal of threshold. Although the examination is in the order of 15 minutes to complete, the test-retest reliability is high. The

commercially available short staircase strategies employ a single crossing of threshold which is generally agreed to be at the expense of increased variability. A new generation of fast staircase strategies based upon *a priori* decisions relating to the visual field and to the subject responses promises reduced examination time without loss in accuracy.

3.3. Aims of the Study.

The aim was to evaluate the influence of the fatigue effect on the outcome of sensitivity measured with two fast staircase strategies relative to the standard 4-2-1 dB staircase strategy.

3.4. Materials and Methods.

3.4.1. Sample.

The sample comprised 20 clinically normal subjects of (mean age 70.9 years, SD 5.9, range 56 to 82 years). The sample was equally divided between male and female. All subjects were experienced in automated static perimetry. Inclusion criteria comprised a visual acuity of 6/9 or better in either eye, distance refractive error less than or equal to 5 dioptres sphere and less than 2.5 dioptres cylinder, intraocular pressure less than 22 mmHg in either eye, normal optic nerve head appearance, open angles, no systemic medication known to affect the visual field, no previous ocular surgery or trauma, no history of diabetes mellitus and no family history of glaucoma or diabetes mellitus.

3.4.2. Perimetry.

Perimetry was undertaken on both eyes using the Octopus 1-2-3 perimeter (Figure 3.1). The stimulus approximates to a Goldmann size III (0.432°) and is presented against a white 10 cdm^{-2} background (colour temperature 2854 K). The stimulus is generated by a broadband light emitting diode (wavelength 592 nm +78/-32 at 10%), presented for 100 ms. The maximum stimulus luminance of 1273 cdm^{-2} is referenced to 0 dB which yields a dynamic range of 40 dB (Octopus 1-2-3 Operating Instructions). The stimulus and background are projected to infinity

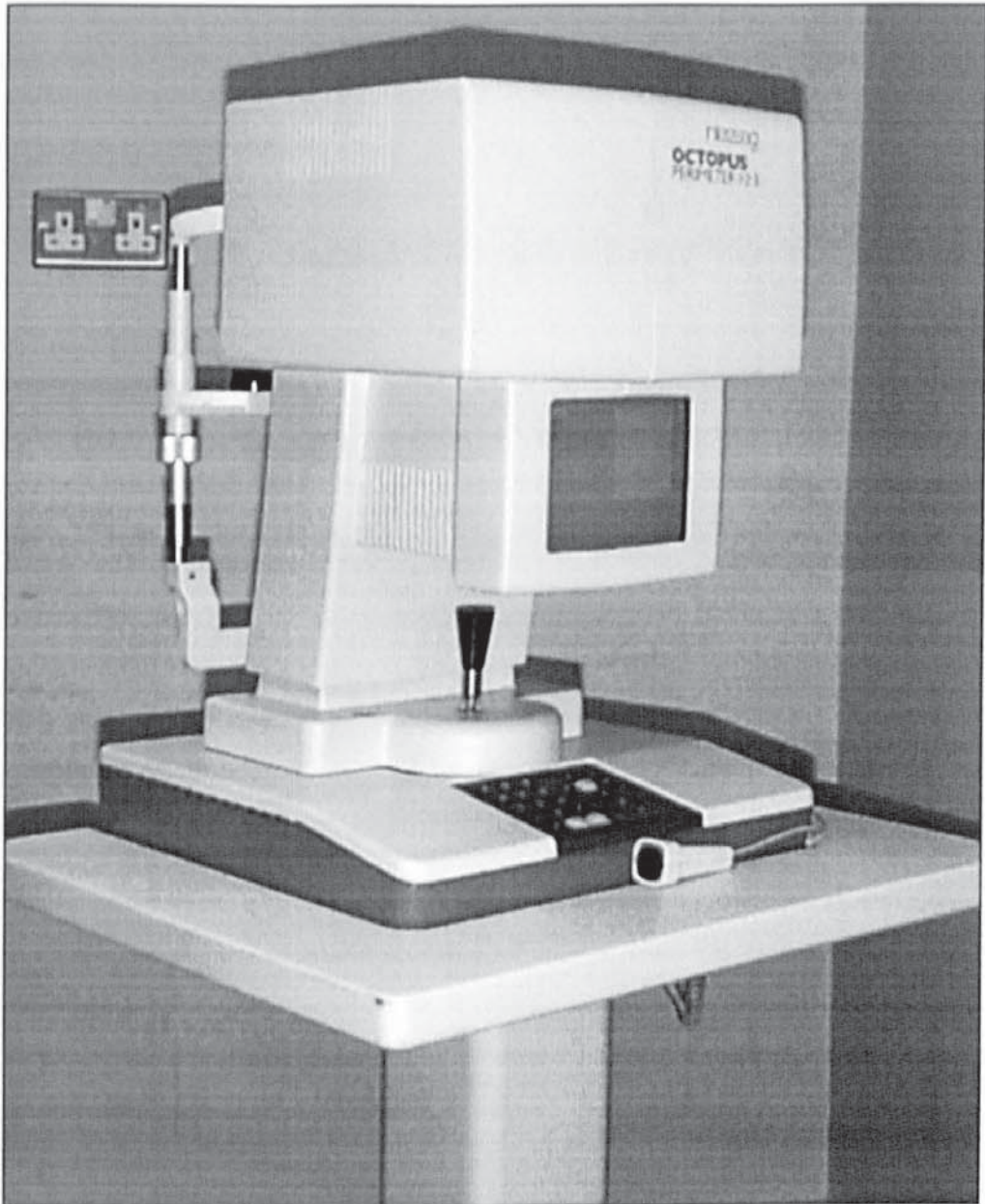


Figure 3.1. The Octopus 1-2-3 perimeter.

which requires correction of the subject's distance refractive error only. Fixation is measured in real-time (section 1.6.1.). Octopus software version 10.08 was employed.

Each subject was examined with programs G1X, eG1X, and dG1X. Program G1X thresholds 59 locations out to an eccentricity of 28°. The examination is divided into two Phases, each consisting of four Stages, facilitating the measurement of within-eye changes in sensitivity. Figure 3.2. illustrates the spatial arrangement of the stimulus locations in each Stage. During the first phase of the examination, thresholds are obtained within each Stage in a random order. A 4-2-1 dB double reversal staircase is employed throughout and each Stage is completed before the commencement of subsequent Stages. In the second Phase, thresholds are obtained with a 2 dB single reversal staircase. The threshold is determined by a ± 1 dB mathematical correction. In the first Stage of each Phase, the thresholds are initially obtained at four seed locations each situated 11.3° from fixation. The initial stimulus luminance is 4 dB above the age-adjusted expected threshold. In the second Phase of the examination, a 2-1 dB staircase is employed; the initial luminance at each stimulus location is based upon the threshold obtained during the first Phase.

The eG1X (4 dB) and dG1X (dynamic) strategies each threshold the same spatial configuration of stimuli as Program G1X but differ in the staircase strategy employed. In the first Stage of Phases 1 and 2, thresholds are obtained at the primary seed locations using a 4-2 dB double reversal staircase. The initial stimulus intensities in Programs eG1X and dG1X are presented 4 dB dimmer than the expected age-corrected value for the G1X Program (personal communication with Interzeag). In Program eG1X, thresholds are obtained at subsequent locations using a staircase with constant 4 dB steps. The threshold is crossed once and is recorded as the mid-point between the last seen and unseen stimulus. In Program dG1X, the thresholds are obtained using dynamic step sizes, the magnitude of which are based upon the sensitivity obtained at the seed points (Weber and Klimaschka 1995). In the second Phase of the 4 dB single step, single reversal and dynamic strategies, the thresholds obtained in the first Phase are used to determine the initial stimulus intensity. A 2 dB staircase

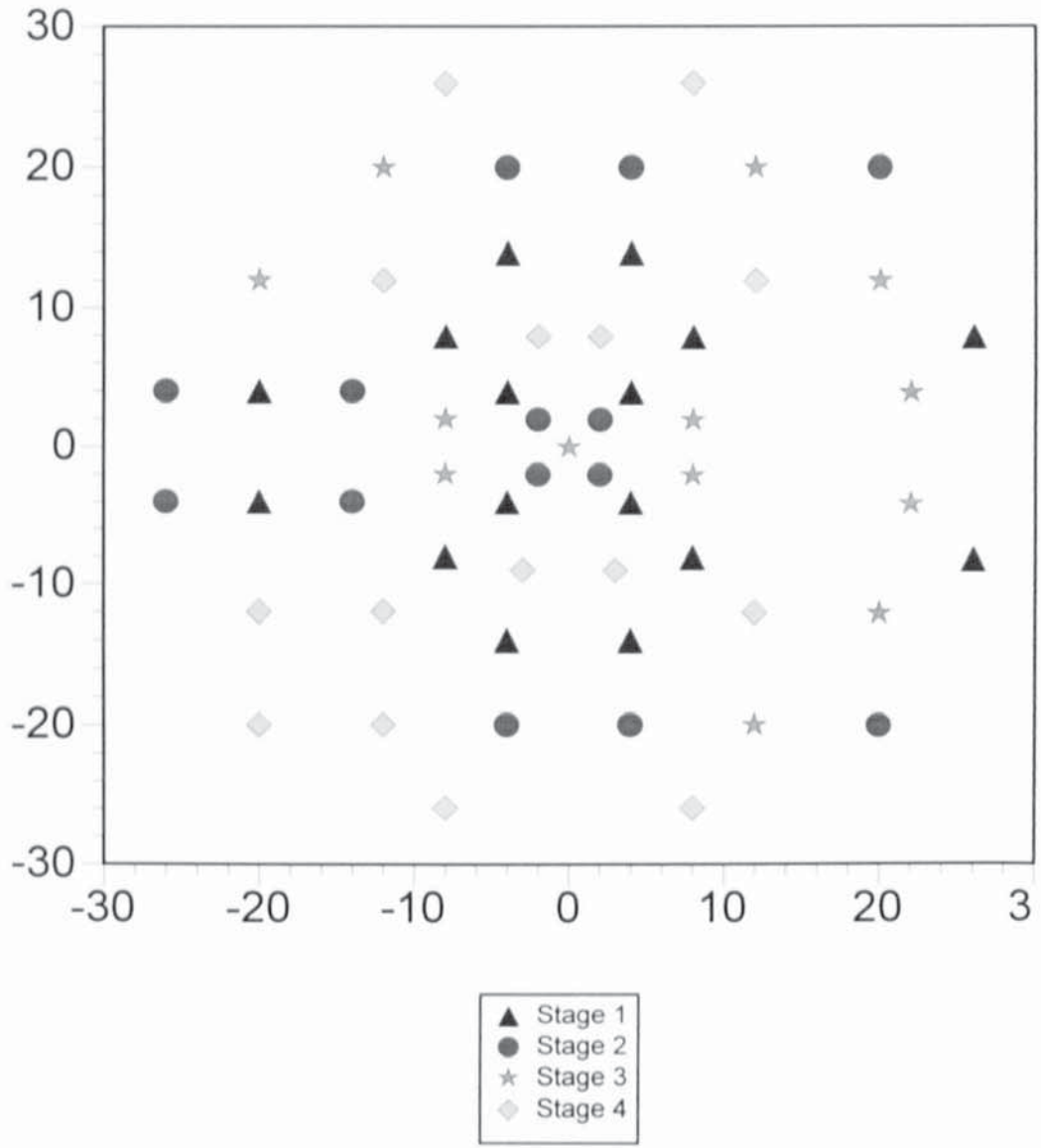


Figure 3.2. Diagram illustrating the right eye spatial location of the stimuli in each Stage of Program G1X.

is used to determine the threshold at the primary locations in Stage 1 of the second Phase (personal communication with Interzeag).

Each subject was examined four times, each visit separated by one week. The first examination consisted of the standard 4-2-1 dB staircase strategy and was undertaken in order to familiarise the subject with the Octopus perimeter. The results of the first examination were discarded. To eliminate order effects, each subject was then assigned one of three protocols which determined the order of subsequent examinations (Table 3.1.).

Protocol	2nd Examination	3rd Examination	4th Examination
A	Standard	4 dB	Dynamic
B	4 dB	Standard	Dynamic
C	Dynamic	4 dB	Standard

Table 3.1. Protocols determining the order of perimetry.

The order of the first eye examined for a given subject was randomly assigned, and was held constant for all examinations. At the end of Phase 1, a one minute rest period was given; a three minute rest period was given between the examination of the two eyes. A period of one week separated the examination with each type of staircase strategy.

During the progress of each examination, the total number of stimulus presentations and the time taken to complete each Stage was noted. The results from Phase 1 cannot be printed without aborting the program. Therefore, the results for the first Phase were documented photographically under the room illumination of the examination using an SLR camera and Ilford FP100 black and white film. The resultant printout at the end of the examination represents the mean of the results from Phase 1 and Phase 2. Prior knowledge of Phase 1 results enabled the calculation of Phase 2 results. Mean sensitivity (MS) was calculated for each Stage, and RMS short-term fluctuation (SF) for Stages 5 to 8 using the equations of Flammer (1986). Mean defect and loss variance could not be calculated because there are

currently no age-adjusted normal values available for the 4 dB and dynamic strategies. Pupil size was measured using the video monitor after correction for the magnification of the optical system. The group mean pupil size was 4.5 mm (SD 0.65).

3.4.3. Statistical analysis.

A repeated measures analysis of covariance (ANCOVA) was carried out for mean sensitivity and short-term fluctuation with staircase strategy, Stage, Phase and eye as within-subject factors, and age as a covariate. The ANCOVA was used in this study to eliminate any effect of differing ages within the sample. Reproducibility which is equal to the reciprocal of the short-term fluctuation squared (variance) was calculated for Phase 2.

3.5. Results.

All visual fields were within the reliability criteria of <20% fixation losses, and <33% false-positive or negative catch trials.

3.5.1. Global Mean Sensitivity (MS).

The global MS for each eye as a function of Stage and Phase, and the associated ANCOVA summary table are illustrated in Figure 3.3. and Table 3.2. respectively. The magnitude of the MS differed between the three strategies ($p < 0.01$). MS became more negative over each successive Stage ($p < 0.001$) and was more pronounced in the second Phase ($p < 0.05$) and in the second eye ($p < 0.01$). The extent of the reduction in sensitivity differed between the three strategies. The standard 4-2-1 dB strategy yielded the lowest MS and the 4 dB strategy the highest. For each stage in the second Phase of the examination in each eye, the global MS was more negative than the corresponding Stage in the first Phase.

3.5.2. Global Short-Term Fluctuation (SF).

The global SF for each eye as a function of Stage and the associated ANCOVA summary table are illustrated in Figure 3.4. and Table 3.3. respectively. In the first eye, the standard and dynamic strategies yielded similar SF's until the last stage when the standard strategy SF was greater than the dynamic strategy SF. In the second eye, the dynamic strategy generally

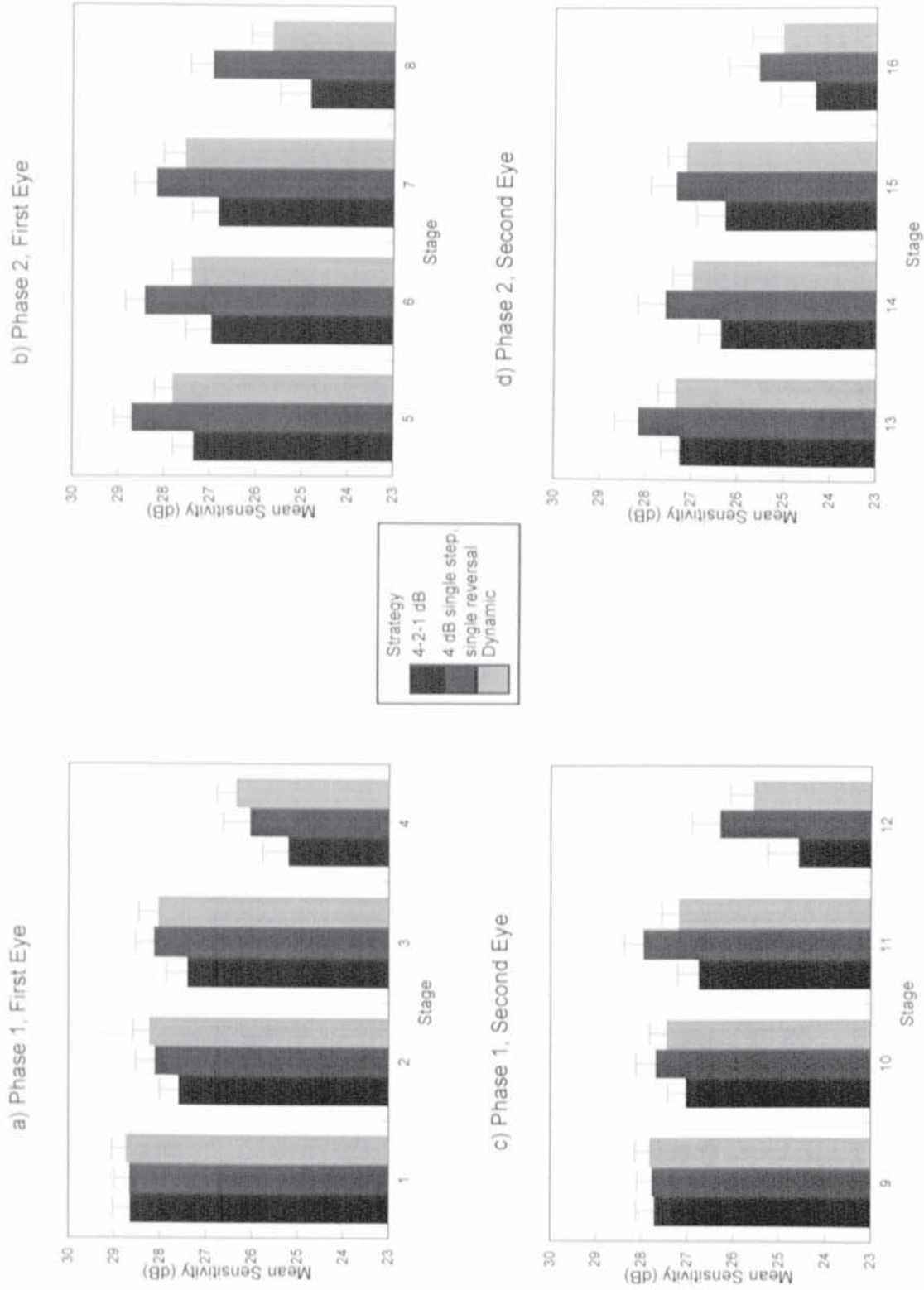


Figure 3.3. Group mean of the mean sensitivity as a function of Stage and Phase for the first eye (top) and second eye (bottom). Error bars represent ± 1 standard error of the mean.

Source	Sums of Squares	Degrees of Freedom	Mean Square	F Value	p Value
Age	69.61	1	69.61	0.50	not significant
Residual	2515	18	139.72		
Strategy	168.60	2	84.30	6.90	<0.01
Residual	464.70	38	12.22		
Stage	841.50	3	280.50	81.07	<0.001
Residual	197.20	57	3.46		
Strategy x Stage	18.63	6	3.11	5.27	<0.05
Residual	66.89	114	0.59		
Eye Order	88.40	1	88.40	10.04	<0.01
Residual	167.20	19	8.80		
Stage x Eye Order	0.15	3	0.05	0.05	not significant
Residual	52.94	57	0.93		
Phase	33.39	1	33.39	5.33	<0.05
Residual	118.80	19	6.25		
Strategy x Phase	19.37	2	9.69	3.52	not significant
Residual	104.40	38	2.75		
Stage x Phase	0.98	3	0.33	0.60	not significant
Residual	31.10	57	0.55		
Strategy x Stage x Phase	7.60	6	1.27	2.15	not significant
Residual	67.60	114	0.59		
Strategy x Stage x Eye Order	10.86	2	5.43	2.56	not significant
Residual	80.65	38	2.12		
Strategy x Stage x Eye Order x Phase	5.15	6	0.86	1.69	not significant
Residual	57.91	114	0.51		

Table 3.2. Repeated measures Analysis of Covariance summary table for mean sensitivity.

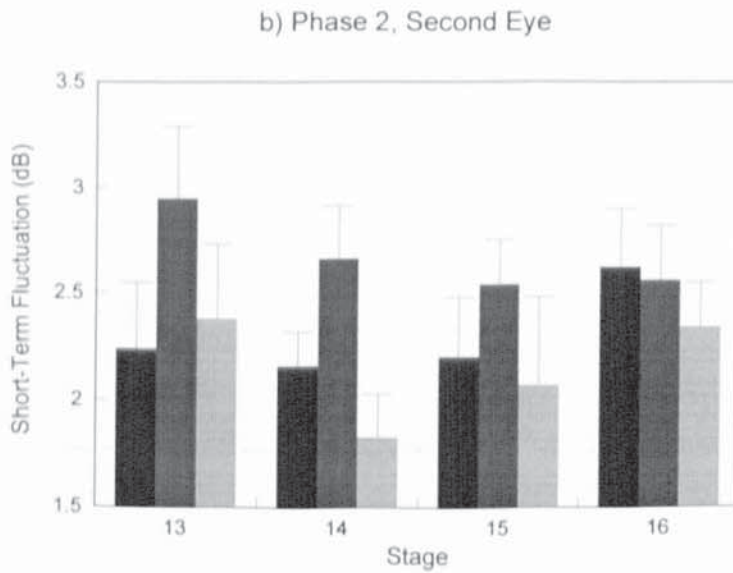
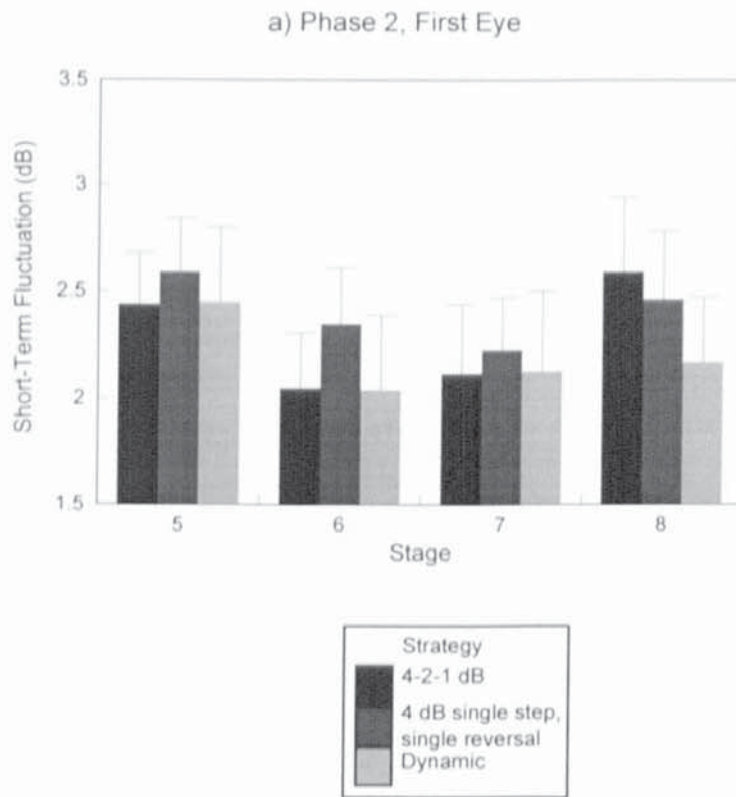


Figure 3.4. Group mean short-term fluctuation as a function of Stage for the second Phase of the first eye (top) and second eye (bottom). Error bars represent ± 1 standard error of the mean.

Source	Sums of Squares	Degrees of Freedom	Mean Square	F Value	p Value
Age	14.46	1	14.46	1.54	not significant
Residual	168.40	18	9.36		
Strategy	11.03	2	5.52	1.15	not significant
Residual	183.30	38	4.82		
Stage	0.10	3	0.33	0.41	not significant
Residual	15.23	19	0.80		
Strategy x Stage	3.22	2	1.61	1.66	not significant
Residual	37.04	38	0.97		
Eye Order	0.73	1	0.73	0.37	not significant
Residual	37.32	19	1.96		
Stage x Eye Order	0.09	1	0.09	0.13	not significant
Residual	12.86	19	0.68		
Strategy x Stage x Eye Order	0.79	2	0.40	0.47	not significant
Residual	32.10	38	0.84		

Table 3.3. Repeated measures Analysis of Covariance summary table for short-term fluctuation.

yielded the lowest SF. The group mean SF of the 4 dB strategy was the highest of the three strategies. Nevertheless, the differences in SF between the three types of strategy did not reach statistical significance.

3.5.3. Examination Time.

The group mean time taken to complete each Stage of the examination is shown as a function of Stage and Phase in Figure 3.5. In the first Phase of the first eye, the 4 dB was 52% and the dynamic strategy 48% faster than the 4-2-1 dB strategy respectively. In the first Phase of the second eye the reduction in time was 54% and 49% for the 4 dB and dynamic strategies respectively. In the second Phase of the examination, the standard strategy was faster than the 4 dB and dynamic strategies in both eyes. In the first eye, the 4 dB strategy was 1% slower and the dynamic strategy 19% slower than the standard strategy. The differences in time between the 4-2-1 dB and dynamic strategies and the 4 dB strategy were more exaggerated in the second eye.

3.5.4. Stimulus Presentations.

The group mean number of stimulus presentations as a function of Stage and Phase is illustrated in Figure 3.6. In the first phase of the first eye examined, the 4 dB and dynamic strategies required 53% and 48% respectively fewer stimulus presentations to obtain a threshold compared to the standard strategy. In the second Phase of the first eye examined, the 4 dB strategy required 2% and the dynamic strategy 16% more stimulus presentations than the standard strategy to obtain a threshold. These differences were similar in the second eye examined.

3.5.5. Efficiency (Benefit/Cost).

The benefit-cost ratios for each strategy are illustrated as a function of Stage and Phase in Figure 3.7. The dynamic strategy showed greater efficiency than both the standard and 4 dB strategies. The efficiency ratios of the 4 dB and dynamic strategies with respect to the standard strategy in each Stage of Phase 2 are summarised in Table 3.4. Unity indicates that the efficiency was the same for the standard and faster strategies. A value greater than unity

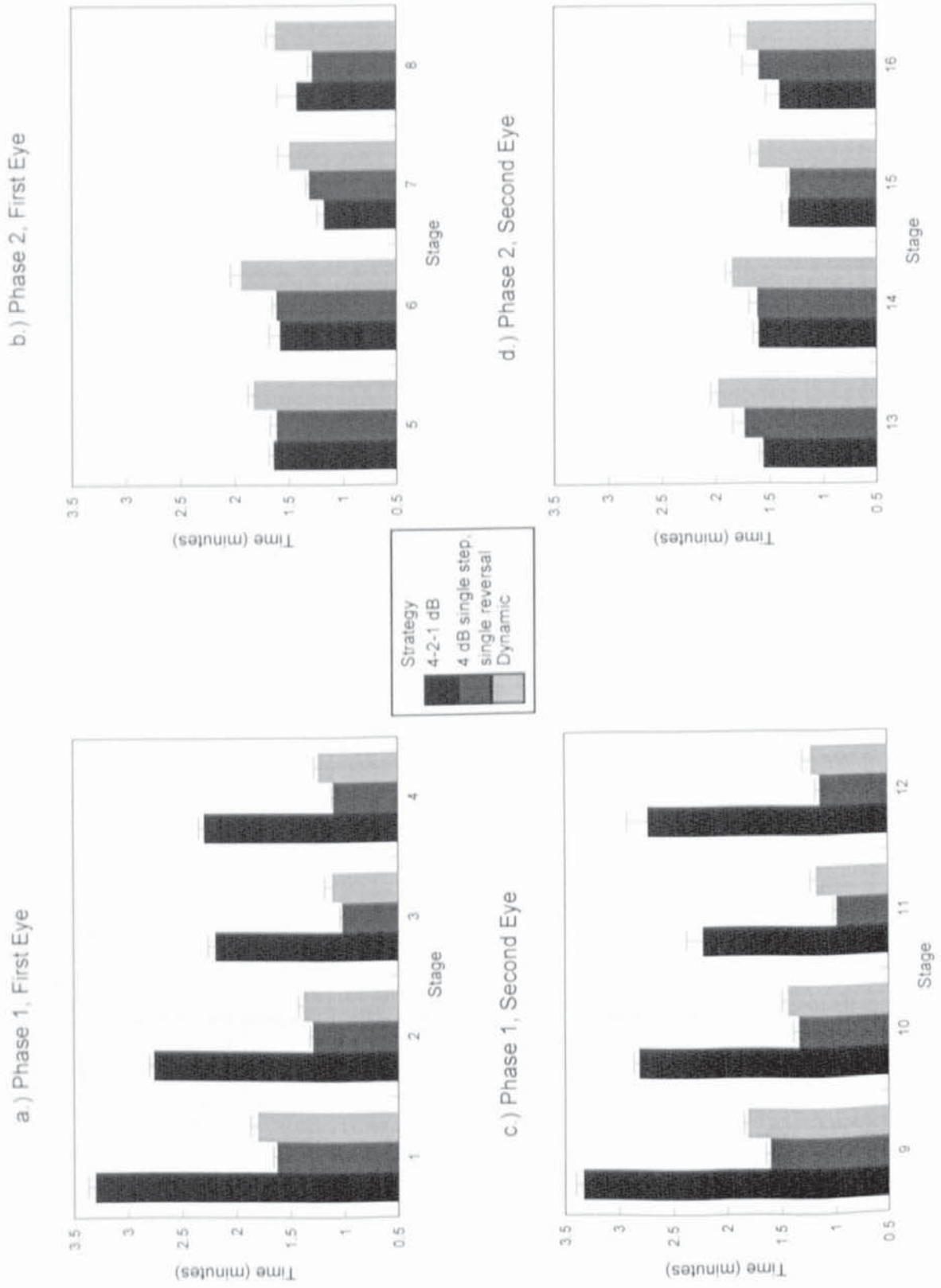


Figure 3.5. Group mean examination time as a function of Stage and Phase for the first (top) and second eye (bottom). Error bars represent ± 1 standard error of the mean.

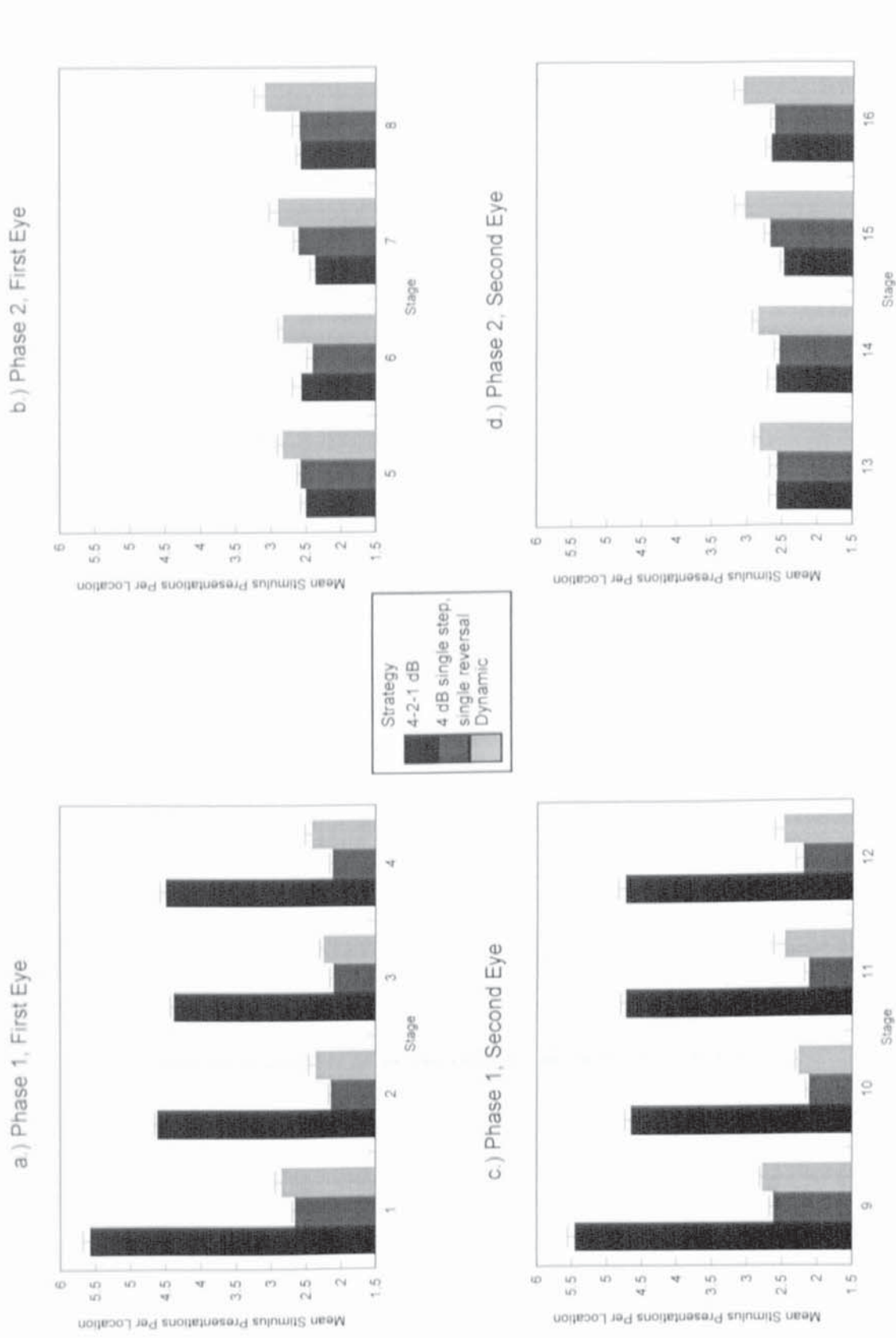
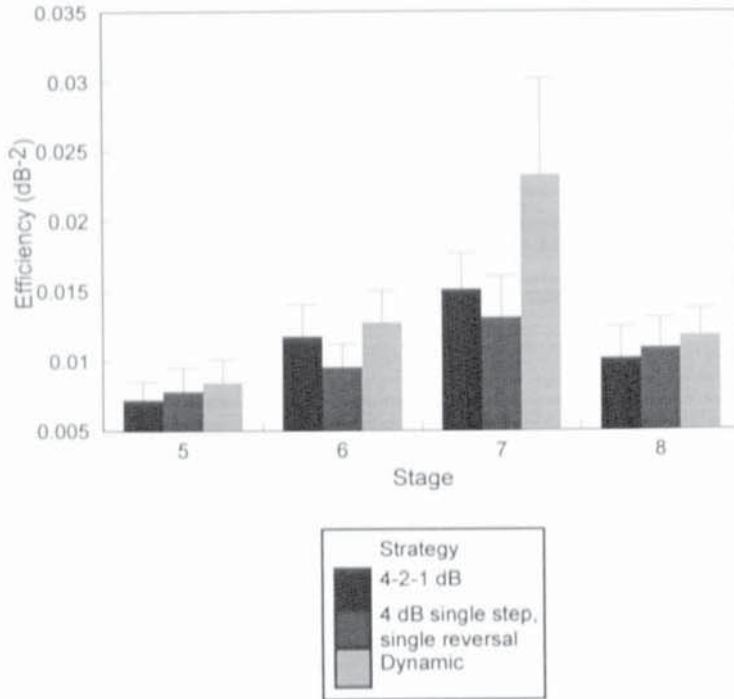


Figure 3.6. Group mean of the mean number of stimulus presentations at each stimulus location as a function of Stage and Phase for the first eye (top) and second eye (bottom). Error bars represent ± 1 standard error of the mean.

a.) Phase 2, First Eye



b.) Phase 2, Second Eye

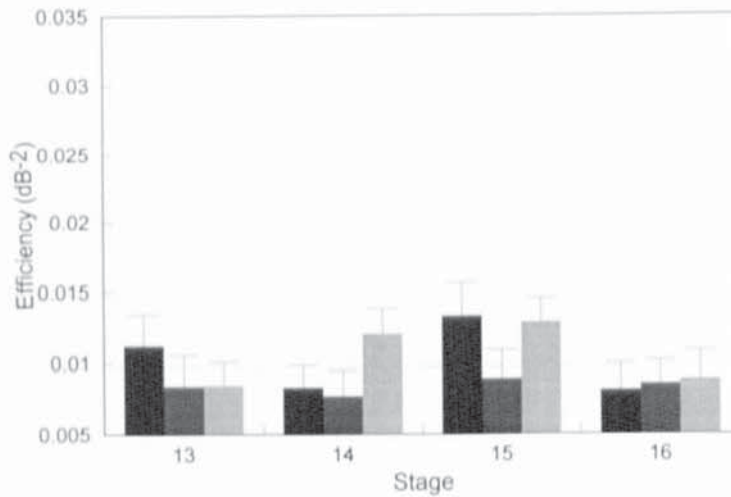


Figure 3.7. Group mean strategy efficiency as a function of Stage for the second Phase of the first (top) and second eye (bottom) examined. Error bars represent ± 1 standard error of the mean.

a) First eye.

Stage	Efficiency (Benefit-Cost) Ratio	
	4 dB	Dynamic
5	1.09	1.17
6	0.82	1.09
7	0.87	1.53
8	1.07	1.15

b) Second eye.

Stage	Efficiency (Benefit-Cost) Ratio	
	4 dB	Dynamic
13	0.75	0.75
14	0.93	1.45
15	0.67	0.97
16	1.05	1.10

Table 3.4. Efficiency (Benefit-Cost) ratios of the 4 dB and dynamic strategies relative to the standard 4-2-1 dB strategy.

favours the 4 dB and dynamic strategies. Conversely, a value less than unity indicates greater efficiency for the standard strategy. In the first eye examined, the dynamic strategy yielded greater efficiency than the standard and 4 dB strategies for all Stages. In the second eye, the dynamic strategy exhibited greater efficiency than the standard in two of the four Stages. The 4 dB strategy was less efficient than the standard strategy.

3.6. Discussion.

The decline in global MS with Stage can be attributed to the effects of fatigue. The results compare well with those of Searle et al (1991) and Hudson et al (1993) who found that the deterioration of sensitivity with time was greater in the second eye. At the completion of Stage 1, the global MS was clinically identical for all the staircase strategies investigated. This would indicate that the fatigue effect did not become apparent until after approximately three and a half minutes of the examination had elapsed. The introduction of a one minute rest period between Phases, and a three minute rest period between eyes increased the global MS relative to the preceding Stage and temporarily arrested the decline in sensitivity. A three minute rest was therefore insufficient to overcome the transfer of the fatigue effect to the second eye. The time required to eliminate the between-eye transfer of fatigue is currently unknown.

The decrease in global MS with Stage was influenced by the duration of the examination. The 4 dB staircase strategy offered the greatest overall saving in time and yielded the highest MS. Conversely, the standard 4-2-1 dB strategy exhibited the longest examination time and the largest reduction in global MS over Stage. The time taken to complete the examination in the dynamic strategy was in between that of the 4 dB and the standard strategies. Global MS was greater than the standard strategy but less than that of the 4 dB strategy.

Cursory examination of the data may lead to a conclusion that the 4 dB staircase strategy is the threshold strategy of choice in a perimetric examination since it was fastest to complete and yielded the highest MS. However the high global MS may have also been due to an overestimation of threshold. A rapid staircase strategy is desirable, but only if it yields clinically

reproducible results. It is known that the FASTPAC strategy, which can be considered analogous to the 4 dB strategy, yields a greater number of threshold errors than the standard 4-2 dB strategy (Glass et al 1995). Furthermore, the number of threshold errors increases as the starting position of the staircase deviates further from the expected threshold (Glass et al 1995). It is conceivable that, as the fatigue effect reduced sensitivity during the course of the examination, the deviation between the estimated and true starting position of the staircase increased as the examination progressed. A greater number of threshold errors would have increased the global MS derived by the 4 dB strategy. Glass and co-workers (1995) also showed that an increased number of threshold errors also increases the short-term fluctuation. It is possible that a combination of an overestimation of threshold and a reduced fatigue effect relative to the other strategies investigated accounts for the high global MS of the 4 dB strategy. The magnitude of the threshold errors with the dynamic strategy is currently unknown. However, the global SF was generally the lowest of the strategies investigated. Because of the relationship between threshold errors and the SF, it is likely that an overestimation of threshold did not have a major influence on the magnitude of global MS in the dynamic strategy.

Since the true threshold and thus the number of threshold errors is unknown, the accuracy of a staircase procedure could not be separated from the reduction in sensitivity induced by fatigue. Nevertheless, it was possible to evaluate the staircase strategies in terms of their efficiency. Despite the higher global MS of the 4 dB strategy, the efficiency was consistently the lowest of all the staircase strategies investigated. Although the dynamic staircase strategy was a little longer in duration than the 4dB strategy, it yielded higher efficiency than the 4-2-1 dB strategy which is considered as the "gold standard" strategy in the Octopus perimeters. The higher efficiency of the dynamic strategy suggests that it may be better able to withstand the effects of fatigue, and may therefore be the staircase strategy of choice for perimetry examinations. Due to the method of calculation, the SF it can only be calculated for the latter Stages of the examination ie in Phase 2. Therefore it was not possible to evaluate the efficiency of the strategies in the early Stages of the examination. The greater efficiency of the

dynamic strategy over the standard strategy compares favourably with the results of Weber and Klimaschka (1995), for the first Stage of Program G1X.

The 4 dB and dynamic strategies offer an approximately 50% reduction in the examination time over the standard strategy. This finding compares favourably with those for other short threshold strategies (Johnson and Shapiro 1991; Flanagan et al 1993a, b; O'Brien et al 1994; Schaumberger et al 1995). At the end of Stage 1 when fatigue was considered to be minimal the mean number of stimulus presentations at each location was slightly greater for the dynamic strategy than for the 4 dB strategy. Subsequently, the number of stimulus presentations for the dynamic strategy continued to increase relative to the 4 dB strategy. As the initial stimulus luminance was identical for the dynamic and 4 dB strategies, the increasing disparity between the two strategies in terms of the number of stimulus presentations may indicate an inefficiency in the staircase procedure, perhaps due to the step sizes chosen for the dynamic strategy not being optimised. Conversely, the effect of fatigue on sensitivity may have altered the nature of the psychometric function governing frequency-of-seeing. It follows that the staircase steps chosen for the dynamic strategy were no longer optimised. As the examination time increased, the mean number of stimulus presentations at each location therefore increased. The nature of how the frequency-of-seeing curve alters under the influence of fatigue is unknown.

3.7, Conclusions.

The objective of any threshold strategy should be to reduce the variability associated with the threshold measurement. One of the principle contributory factors to this variability is the fatigue effect. The primary aim of the development of short staircase strategies is to reduce the fatigue effect via a reduction in overall examination time. This study has shown that although the magnitude of fatigue can be reduced with short staircase strategies it cannot be completely eliminated. Moreover, increased variability may be introduced by threshold errors which are a function of the staircase design.

The functional trade off between variance and time of examination appears to favour the dynamic strategy over the standard double reversal strategy. Further work, however, needs to be conducted on the dynamic strategy with the specific aims of evaluating the threshold errors of the algorithm. With the advent of a new generation of short staircase strategies with improved accuracy (Olsson 1991; Olsson and Rootzén 1994; Bengtsson et al 1996; Schaumberger et al 1996) the effect of fatigue may be minimised to an acceptable level.

The introduction of rest periods into the examination procedure reduced the rate of the decline in sensitivity but was insufficient to eliminate it. The confidence levels currently employed in statistical analysis of visual field data should reflect the difference in sensitivities between the first and second eyes examined. Furthermore, the between-eye fatigue effect reinforces the suggestion that the order of the eye examined during an examination should remain the same at all follow-up examinations.

Other approaches to reducing the fatigue effect may be more appropriate. Reducing the examination time further by decreasing the number of stimulus locations, combined with a short staircase strategy may further reduce fatigue. This has obvious implications for sampling density and the probability of detecting a visual field defect. Alternatively, it has been suggested that the order of stimulus locations should be prioritised in terms of their importance to visual field damage (Zeyen et al 1993), such that clinically important locations will be thresholded prior to other locations thereby reducing the influence of fatigue.

Alternatively, methods have been suggested to increase vigilance and suppress alpha wave activity. Trope (1989) compared the standard fixation method with a method which encouraged saccadic movement during the test. The patients fixated centrally in the conventional manner, but instead of pressing a response button indicating detection of a stimulus the patient moved fixation to the position of the stimulus. Maintaining central fixation indicated that the stimulus was not seen. The sensitivity of the saccadic movement method was 100% and the specificity was 28%. A second method, utilised in the Dicon TKS 4000 perimeter, employs a moving fixation target. This method has been shown to result in an

elevated MS by 2 dB (LI and Mills 1992). A subjective comparison of the Dicon TKS 4000 perimeter with the Humphrey Field Analyser suggested that a greater number of subjects experience fatigue with the Humphrey Field Analyser than with the Dicon (Wong et al 1995). Additionally, continually motivating the patient verbally may increase vigilance.

The influence of fatigue continues to confound the interpretation of perimetric data. The fatigue effect may be eliminated by the development of faster staircase strategies. Alternatively, statistical methods may be sought which are able to correct for the within- and between-eye changes in sensitivity which occur during a perimetric examination.

CHAPTER 4. STAIRCASE STRATEGY VARIABILITY IN SHORT-WAVELENGTH AUTOMATED PERIMETRY.

4.1. Introduction.

The retinal image is sampled by approximately 3.3 million cones and 57.4 million rods (Panda-Jonas et al 1994). The output of the retina is conveyed to the lateral geniculate nucleus (LGN) by approximately 1.1 million nerve fibres (Jonas and Dichtl 1995). The organisation of the visual system is such that some initial processing of visual information must occur within the retinal layers before it is conveyed to the LGN in order to avoid a loss in information. Buchsbaum and Gottschalk (1983) suggested that signals from the cones are transformed in three second-stage retinal mechanisms before they are transmitted through the optic nerve. These mechanisms consist of an achromatic channel which sums the signals from l- (long-wavelength sensitive) cones and m- (medium-wavelength sensitive) cones, a red-green colour opponent channel which conveys the difference between signals from the l- and m-cones, and a blue-yellow colour opponent channel which conveys the difference between s- (short-wavelength sensitive) cone input and the combined input from m- and l-cones.

Distinct laminae are present within the LGN; namely the magnocellular and parvocellular layers. Ganglion cells from the retina which synapse within the magnocellular laminae of the LGN are termed M-cells. Those which synapse within the parvocellular laminae of the LGN are termed P-cells. Animal studies have provided evidence for distinct physiological properties of the M- and P-cells. M-cells exhibit a transient response to visual stimulation (Gouras 1968) and have larger receptive field centres than P-cells (de Monasterio and Gouras 1975). M-cells exhibit high contrast gain which is non-linear, whereas P-cells exhibit a linear low contrast gain (Kaplan and Shapely 1986). Some M-cells also exhibit non-linear spatial summation (Kaplan and Shapley 1982). P-cells demonstrate spectral selectivity (Wiesel and Hubel 1966; de Monasterio 1978). It has been suggested that the M- and P-systems have distinct functional properties within the visual system. M-cells predominantly contribute to motion, luminance and the detection of large patterns, whereas P-cells are primarily responsible for colour, high spatial frequency detection and fine patterns (Merigan and Maunsell 1990; Logothetis et al

1990; Merigan et al 1991). It is now becoming evident from anatomical and psychophysical studies that there may not be a complete segregation of functional properties within the magnocellular and parvocellular pathways. Crook et al (1988) found that for a given eccentricity, M- and P-cells exhibited virtually the same spatial resolution. This finding is in agreement with the fact that the receptive field centre size of M- and P-cells is similar (Blakemore and Vital-Durand 1986; Crook et al 1988; Derrington and Lennie 1984) but is at variance with earlier work by de Monasterio and Gouras (1975). Purpura et al (1990) reported that there is considerable overlap in the luminances over which the M- and P- systems respond; the possibility that the M-system may dominate scotopic vision remains controversial. Merigan and Maunsell (1993) suggested that the M-system is not specialised for motion perception, but is specialised for the transmission of middle and high velocity stimuli. They concluded that their findings did not support the theory of separate sub-systems for specific visual behaviours. Nevertheless, chromatic responses are still believed to be predominantly mediated by the P-system because the spatial and temporal properties of that system are better suited to the processing of spectral information (Merigan and Maunsell 1993). The existence of s-cone input to the luminance channel is controversial (Vos and Walraven 1971; Ingling and Tsou 1977; Smith and Pokorny 1975; Eisner and Macleod 1980; Cavanagh et al 1987). Receptive field studies on primates have shown the existence of four major classes of centre surround P-cells demonstrating cone opponency; +m -l (m-cone excitatory centre and l-cone inhibitory surround), +l -m (l-cone excitatory centre and m-cone inhibitory surround), +s -[ml] (s-cone excitatory centre and inhibitory surround from a combination of m- and l-cones), -s +[ml] (s-cone inhibitory centre and excitatory surround from a combination of m- and l-cones) (Lee 1996). Table 4.1. illustrates the anatomical identity of physiological ganglion cell types in the primate retina: The origin of the yellow input to the blue-yellow opponent mechanism is uncertain. Psychophysical investigations have been unable to state whether it originates in the l-cones, m-cones, or both (Lee 1996).

4.2. Short-Wavelength Automated Perimetry (SWAP).

The rationale for the clinical interest in short-wavelength automated perimetry (SWAP) is based upon studies which have demonstrated colour vision defects in ocular hypertension,

Pathway	Physiological cell type	Anatomical cell type	Bipolar input	Proportion
Magnocellular	On-centre M-cell	Inner parasol	Invaginating diffuse bipolar	5%
	Off-centre M-cell	Outer parasol	Flat diffuse bipolar	5%
Parvocellular	Blue on, yellow off +s -(m) P-cell	Small bistratified	s-cone bipolar	10%
	Blue off, yellow on -s +(m) P-cell	Thought to be large field inner cell	Unknown	5%
	Green and red on-centre cells	Inner midget	Invaginating midget bipolars	30%
	Green and red off-centre cells	Outer midget	Flat midget bipolars	30%
Other	Various transient, non-opponent cells	Other cell types	Unknown	15%

Table 4.1. Physiological and anatomical identity of the ganglion cell types in the primate retina. After Lee (1996).

primary open-angle glaucoma, diabetes and Parkinson's disease (Lakowski et al 1972; Airaksinen et al 1986; Adams 1987b; Sample et al 1988; Lagerlöf 1991; Hardy et al 1992; Huag et al 1995). The nature of the acquired dyschromatopsia suggests that the short-wavelength sensitive (SWS) pathway may be preferentially damaged. The technique of SWAP is based upon chromatic adaptation of the visual system (Stiles 1959). A yellow background differentially desensitises the medium-wavelength sensitive (MWS), and long-wavelength sensitive (LWS) pathways of the visual system. The background is of a high luminance which desensitises the rod photoreceptors. The SWS pathway is rendered more sensitive, mediating the detection of a blue test flash. The background and stimulus characteristics which optimise SWS pathway isolation in short-wavelength automated perimetry are equivocal and are discussed in greater detail in Chapter 7.

4.2.1, Short-Wavelength Automated Perimetry In Ocular Disease.

A number of studies have supported that SWAP is capable of detecting glaucomatous visual field loss at an earlier stage in the disease than conventional W-W perimetry (Heron et al 1988; de Jong et al 1990; Hart et al 1990; Sample and Weinreb 1990; Sample et al 1993; Johnson et al 1993a; Johnson et al 1995).

Initial investigations of SWAP were confined to measurements at a few stimulus locations in the visual field (Heron et al 1988; de Jong et al 1990). Hart et al (1990) compared standard W-W field loss with SWAP defects in 14 normal subjects and 16 patients with primary open-angle glaucoma. Virtually every stimulus location in those areas exhibiting minimal loss with W-W perimetry exhibited a reduction in blue-yellow sensitivity. Locations manifesting a 10 dB or less defect depth with W-W perimetry showed a SWAP defect which was on average 5 dB deeper. W-W defect depths greater than 10 dB exhibited comparable defect depths with SWAP. Glaucomatous eyes revealed a diffuse change in blue-yellow sensitivity over the entire meridian that appeared to be present in areas of the visual field considered normal with W-W perimetry. The extent of focal visual field loss with W-W and SWAP was in good agreement.

Sample et al (1993) followed 25 glaucoma suspect eyes over a period between 12 and 37 months. All W-W visual fields were classified as normal at the completion of the study. Five eyes developed SWAP visual field loss consistent with glaucoma. Four of these five eyes were originally classified as high risk glaucoma suspects. Johnson et al (1993a) followed each eye of 38 patients with ocular hypertension over a five year period. At baseline, all of the ocular hypertensive eyes had normal W-W visual fields; 67 of the 96 eyes were abnormal with SWAP (defined as five or more locations exhibiting sensitivities beyond the 95% confidence limits of normality at least three locations of which were required to be clustered). By the end of the five year period, 5 of the 9 ocular hypertensive eyes who had exhibited abnormal SWAP results in the first year had developed a glaucomatous visual field defect with W-W perimetry. The visual field loss depicted with W-W perimetry occurred in the same general locations as the SWAP defects found at baseline. None of the eyes with normal W-W perimetry and SWAP at baseline had developed glaucomatous visual field loss with W-W perimetry by the end of five years. In ocular hypertensive patients considered as stable, there was little or no change in the number of abnormal visual field locations with either SWAP or W-W perimetry.

Johnson et al (1995) investigated each eye of 232 patients with ocular hypertension, 72 of which were receiving topical medical therapy to lower intraocular pressure. Patients were classified into risk categories according to the classification of Hart et al (1979). Approximately 50% of the patients were classified as low risk. The classification of the patients remaining was equally distributed between moderate and high risk. All patients had normal W-W visual fields. The prevalence of SWAP localised loss was 15.1%. In the low risk category, 10% exhibited SWAP abnormalities. Approximately 20% of patients in the moderate risk category exhibited SWAP abnormalities, and between 20 and 30% high risk patients had SWAP defects. The incidence of SWAP deficits was greater with increase in age. There was also a strong relationship between vertical cup:disc ratio and increase in the size and presence of SWAP deficits. Intraocular pressure and presence of family history of glaucoma did not correlate with the presence of SWAP deficits. It was concluded that the appearance of the SWAP visual field, optic disc evaluation, and age provided the most diagnostically useful information for

determining whether an ocular hypertensive patient would be likely to develop subsequent glaucomatous visual field loss with W-W perimetry.

SWAP may also be useful in the identification of those glaucoma patients with stable visual fields with standard W-W perimetry from those who will develop visual field progression (Sample and Weinreb 1992; Johnson et al 1993b). Sample and Weinreb (1992) examined glaucoma patients twice over a period ranging between 6 and 26 months. SWAP deficits were more extensive than W-W visual field loss. The follow-up visual field exhibited significantly greater visual field progression with SWAP than with W-W perimetry. In a five year longitudinal study, Johnson et al (1993b) reported that SWAP was effective at predicting which patients with early glaucomatous W-W visual field loss were likely to develop visual field progression. Visual field loss with SWAP extended over an area twice as large as that with W-W perimetry in stable glaucoma patients, whilst in patients demonstrating visual field progression with W-W perimetry, SWAP deficits extended over an area three to four times larger than the W-W deficits. The progression of W-W visual field loss occurred in areas of the visual field which had exhibited SWAP abnormality at least three years previously.

SWAP has also been utilised in the investigation of diabetes and neuro-ophthalmic disorders (Lutze and Bresnick 1994; Keltner and Johnson 1995). Lutze and Bresnick (1994) evaluated SWAP in 31 insulin dependent diabetics, 6 diabetics without retinopathy and in 17 normal control eyes. Stepwise linear regression analysis, including age, duration of diabetes and level of retinopathy was significantly correlated with SWAP sensitivity corrected for ocular media absorption. There was no correlation with W-W sensitivity. Localised visual field loss was present with SWAP in 27 diabetics which was correlated with the magnitude of the retinopathy. Keltner and Johnson (1995) reported greater SWAP visual field loss than conventional W-W perimetry in various optic neuropathies including optic neuritis and pseudotumour cerebri.

Many studies of SWAP have corrected sensitivity for the preferential absorption of the short-wavelength stimulus by the ocular media (Sample and Weinreb 1990; Sample and Weinreb 1992; Johnson et al 1993a, b; Sample et al 1993; Lutze and Bresnick 1994; Johnson et al

1995; Keltner and Johnson 1995). Sample et al (1994) evaluated the Glaucoma Hemifield Test in SWAP, with correction for ocular media absorption and without correction in 95 glaucomatous eyes. Ocular media absorption was measured at two stimulus locations (coordinates, 15,0 and 0,15). Sample et al (1994) reported good agreement in glaucoma diagnosis with the Glaucoma Hemifield Test between corrected and uncorrected SWAP. The visual field was classified as abnormal by both methods in 69 eyes and 15 classified as normal by both methods. Eight patients were classified as abnormal by corrected SWAP only, and three as such by uncorrected SWAP. It was concluded that assessment of ocular media absorption was not necessary in SWAP for patients with ocular hypertension and glaucoma.

4.3. The Mechanism of Damage in SWAP.

A variety of mechanisms have been proposed to explain the ability of SWAP to detect visual field loss at an earlier stage than standard W-W perimetry.

4.3.1. Selective Nerve Fibre and Ganglion Cell Damage.

In glaucoma, histological studies have shown that between 40% and 50% of nerve fibres are lost before a visual field defect manifests with standard W-W perimetry (Quigley et al 1982, 1989). Retinal imaging techniques have also provided evidence that nerve fibre atrophy precedes the onset of a W-W visual field defect (Sommer et al 1991). Histological studies, both in primates (Quigley et al 1987) and humans with glaucoma (Quigley et al 1988), show that the larger optic nerve fibres are preferentially lost. The larger ganglion cells are thought to be selectively damaged because they are more vulnerable to mechanical and/or physiological insult and are positioned in the weakest areas of the optic nerve head (Quigley 1987; Radius 1987; Miller and Quigley 1988). Ganglion cell loss in glaucoma has also been demonstrated (Quigley et al 1989; Glovinsky et al 1993; Jonas et al 1995; Wgnanski et al 1995) and correlates well with W-W visual field loss (Quigley et al 1989). Since ganglion cells mediating the short-wavelength sensitive pathway have a larger diameter than other P-cells (de Monasterio 1978; Dacey 1993), it has been postulated that the selective damage of larger ganglion cells would result in preferential damage of the short-wavelength sensitive pathway (Quigley 1994).

However, Morgan (1994) reviewed the literature on selective cell death in glaucoma and concluded that selective cell death may not actually occur, citing the occurrence of cell shrinkage during preparation and the disadvantages of the cell labelling techniques as reasons for previous findings. Indeed, Weber and co-workers (1994) were unable to find differences in LGN cell body size in rhesus monkeys with experimentally induced glaucoma.

Recent psychophysical evidence has suggested that a selective loss of M-cells occurs in glaucoma. Anderson and O'Brien (1997) measured resolution grating acuity to a stationary sinusoidal grating (designed to stimulate P-cells) and to a 30 Hz phase reversing sinusoidal grating (designed to stimulate a higher proportion of M-cells) in eight patients with glaucoma, seven ocular hypertensives and eight normal controls. Peripheral resolution acuity to the stationary grating was significantly reduced in glaucoma patients and some ocular hypertensives, indicating that the underlying ganglion cell density was reduced. There was a greater reduction in resolution acuity for the phase reversal grating, indicating a selective loss of M-cells over P-cells.

4.3.2, S-Cone Vulnerability,

Another explanation for the susceptibility of the short-wavelength sensitive pathway to disease has been proposed by Sperling et al (1980) who demonstrated that s-cones are more vulnerable to photic damage than either m- or l-cones. This evidence had led to the "fragile receptor hypothesis" which states that s-cones are in some way more susceptible to damage by light, chemicals or retinal disease. Hood and Greenstein (1988) evaluated the "fragile receptor hypothesis" psychophysically using probe flashed thresholds to evaluate a two site model for the SWS pathway consisting of the receptors and a post-receptoral site. One patient with congenital stationary night blindness, and one with retinitis pigmentosa fitted the model consistent with loss in sensitivity at the receptor site. Histological studies have been unable to demonstrate cone loss in glaucoma (Wyganski et al 1995).

Greenstein and co-workers (1989) obtained foveal two-colour increment thresholds in 23 patients with retinitis pigmentosa, 14 patients with insulin dependent diabetes, 16 patients with

primary open angle glaucoma, and 11 normal controls. Thirteen of patients with glaucoma, and all the diabetics exhibited a selective loss of sensitivity of the SWS pathway which was greater than the sensitivity loss of the MWS pathway. The diabetics showed a greater reduction of SWS pathway sensitivity than the patients with either retinitis pigmentosa or glaucoma. All but one of the diabetic patients exhibited either normal or slight loss in MWS pathway sensitivity. The pattern of MWS and SWS pathway reduction was similar in patients with retinitis pigmentosa and glaucoma. If SWS pathway vulnerability could be attributed to the cone receptors, then it would be expected that retinitis pigmentosa rather than diabetes or glaucoma would result in more selective loss in the SWS pathway since retinitis pigmentosa affects the photoreceptors and the retinal pigment epithelium. The patients with retinitis pigmentosa did not exhibit greater selective loss than patients with diabetes and glaucoma. Similarly, if the site of SWS vulnerability was at or close to the ganglion cell layer, then patients with glaucoma would be expected to exhibit more selective loss. Greenstein et al (1989) concluded the locus of damage to the SWS pathway occurred at multiple sites.

4.3.3. SWS Pathway Redundancy.

Hood et al (1984) gave other possible causes for s-cone vulnerability. S-cones are less numerous in the retina than m- or l-cones (de Monasterio et al 1981, 1985; Curcio et al 1991,1992) and this paucity may account for the reduced response range of the s-cone pathway. Furthermore, retinal disease may decrease the responsiveness of all cone pathways equally. Because of the differing response functions of the three cone types, an equal change in the response amplitude measured psychophysically would affect the s-cones more than the m- and l-cones, thus appearing to make the s-cones more vulnerable in retinal disease.

Psychophysical studies have suggested that all chromatic pathways are affected in ocular hypertension and glaucoma. Felius et al (1995) measured peripheral (12° from fixation) contrast thresholds to equiluminant stimuli modulated in different colour space directions. The stimuli were variously sensitive to red, green, and blue cones, the red-green and blue-yellow opponent systems, or the achromatic channel. The sample comprised 10 normals, 17 ocular

hypertensive or glaucoma suspect patients and 14 patients with early glaucoma. Deviations in threshold from normal were found in all modulation directions, in all patient groups.

Similarly, Greenstein et al (1996) obtained discrimination thresholds along two equiluminant cardinal colour axes; red-green and blue-yellow, and an achromatic luminance axis. Thirteen patients with suspected glaucoma, 27 patients with primary open-angle glaucoma, and 25 normal controls were evaluated. Mean discrimination thresholds were greater in the patient groups for all cardinal directions and highest in the glaucoma group. Sensitivity reductions were not selective for the SWS pathway. Blue-yellow opponent system loss was accompanied by a similar loss for the red-green opponent system and for the achromatic system.

In summary, a number of studies have shown the utility of SWAP in the detection of visual field loss at an earlier stage than standard W-W perimetry. Visual field defects with SWAP are often more pronounced than those with W-W perimetry. SWAP may be predictive of W-W visual field loss in ocular hypertension, and may also be of use in the diagnosis of diabetic retinopathy and neuro-ophthalmic disorders. The mechanism of visual field loss in SWAP is unknown. Inconsistencies in theories suggesting selective damage to the SWS pathway in glaucoma suggest that a redundancy of the SWS pathway response is probably responsible for the observed reduction in short-wavelength sensitivity. However, the utility of SWAP in a variety of retinal diseases, each with different pathogeneses and aetiologies would suggest that a number of mechanisms of damage to the SWS pathway may be applicable.

4.4. Aims of the Study

The aim of the study was threefold: firstly, to determine the extent of any differences in the characteristics of normal sensitivity between the Full Threshold and FASTPAC algorithms for SWAP compared to W-W perimetry; secondly, to determine the influence of lack of correction for ocular media absorption on the magnitude of the between-subject normal variation in sensitivity derived by SWAP; and thirdly to evaluate the influence of forward light scatter on the between-subject normal variation in sensitivity derived by SWAP.

4.5. Materials and Methods.

4.5.1. Sample.

The sample consisted of 51 normal subjects (24 males) experienced in both conventional and short-wavelength Full Threshold automated perimetry with the HFA. The sample was deliberately chosen such that the age was stratified across all decades. The mean age of the sample was 55.5 years (SD 19.5) and the range 24 to 83 years. The mean pupil diameter was 5.11 mm (SD 1.25) in W-W perimetry and 4.15 mm (1.02) in SWAP.

Inclusion criteria comprised a visual acuity of 6/9 or better in either eye, distance refractive error less than or equal to 5 dioptres sphere and less than 2.5 dioptres cylinder, lenticular changes not greater than NC III, NO III, C I or P I by LOCS III (Chylack et al 1993a), intraocular pressure less than 22 mmHg in either eye, normal optic nerve head appearance, open angles, no history of a congenital colour vision defect, no systemic medication known to affect the visual field, no previous ocular surgery or trauma, no history of diabetes mellitus and no family history of glaucoma or diabetes mellitus.

4.5.2. Perimetry.

The study adopted a two-period cross-over design. The subjects were randomly assigned to one of four sub-groups (Table 4.2) and attended for four visits within a maximum interval of 2 weeks.

At each of the first three visits, one randomly assigned eye of each subject was examined with the Humphrey Field Analyser (HFA) 640 using Software Version 9.31 (Figure 4.1). The HFA incorporated the standard commercially available hardware necessary for SWAP. At the first visit, all subjects underwent conventional W-W perimetry and SWAP using the Full Threshold strategy and Program 30-2 with the foveal threshold option enabled. One half of the sample was examined with W-W perimetry followed by SWAP and the other half with SWAP followed by W-W perimetry. Conventional W-W perimetry was undertaken using the default stimulus parameters of the HFA; namely, a white stimulus size III presented for a stimulus duration of

		Protocol A	Protocol B	Protocol C	Protocol D
<u>Visit 1</u>	Test 1	W-W (Std)	W-W (Std)	SWAP (Std)	SWAP (Std)
	Test 2	SWAP (Std)	SWAP (Std)	W-W (Std)	W-W (Std)
<u>Visit 2</u>	Test 1	W-W (Std)	W-W (FP)	SWAP (Std)	SWAP (FP)
	Test 2	SWAP (Std)	SWAP (FP)	W-W (Std)	W-W (FP)
<u>Visit 3</u>	Test 1	W-W (FP)	W-W (Std)	SWAP (FP)	SWAP (Std)
	Test 2	SWAP (FP)	SWAP (Std)	W-W (FP)	W-W (Std)

Table 4.2. Summary of the examination protocols assigned to each subject (Std is the Full Threshold, 4-2 dB double reversal staircase strategy, and FP is the FASTPAC, single reversal strategy).



Figure 4.1. The Humphrey Field Analyser 640.

200 ms on a 10 cdm² white background. SWAP was similarly undertaken with the default stimulus parameters; namely, a 440 nm narrowband stimulus size V presented for a stimulus duration of 200 ms on a 100 cdm² broadband yellow background. The transmission characteristics of the filters used in SWAP are illustrated in Figure 4.2. At the second visit, the particular order of perimetric examination was maintained for the two groups. However, both groups were each randomly divided into two further categories. One sub-group from each main group was examined with the Full Threshold strategy and one with the FASTPAC strategy. At the third visit, each sub-group was examined with the remaining strategy. The examination of the two visual fields at any given visit was separated by a five minute rest period. For SWAP, subjects looked into the bowl for three minutes prior to testing to ensure retinal adaptation of the MWS and LWS pathways.

Forty seven subjects (mean age 55.53 years; SD 19.83) attended the fourth visit when ocular media absorption and forward light scatter were assessed.

4.5.3. Ocular Media Absorption Assessment.

Ocular media absorption at 410 nm was assessed with a modified HFA 630 (Figure 7.3), using a technique first suggested by Norren and Vos (1974) and later adapted for use in perimetry by Sample et al (1989). The technique is based upon the CIE (Commission Internationale Eclairage) absorption spectrum of rhodopsin. A pair of narrowband stimuli consisting of a short-wavelength and medium-wavelength stimulus may be selected which are equally absorbed by rhodopsin (390 nm and 568 nm, 400 nm and 565 nm, or 410 nm and 561 nm). The difference in scotopic thresholds to these stimuli may be attributed to absorption of the short-wavelength stimulus by the ocular media.

Blocking material was applied to the surround of the perimeter bowl to prevent light leakage from the stimulus projection system onto the bowl surface. A red Cinelux 406 filter (Strand Lighting Ltd, Middlesex, UK) was positioned over the fixation target in order to preserve dark adaptation. A six log unit neutral density gelatin filter was applied over the perimeter monitor to further reduce extraneous light entering the perimeter cupola. The perimeter bowl luminance

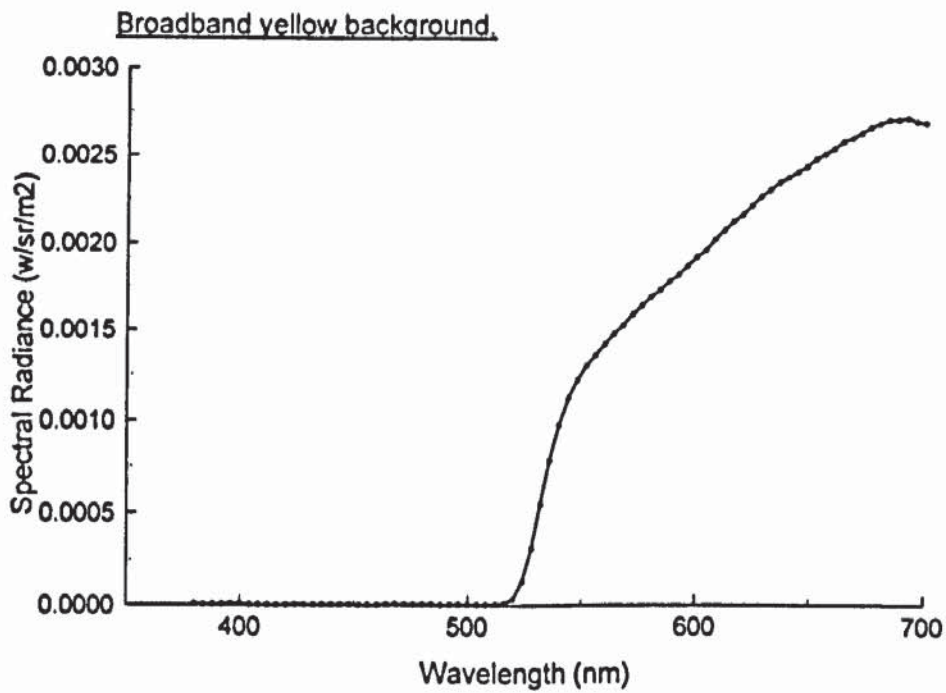
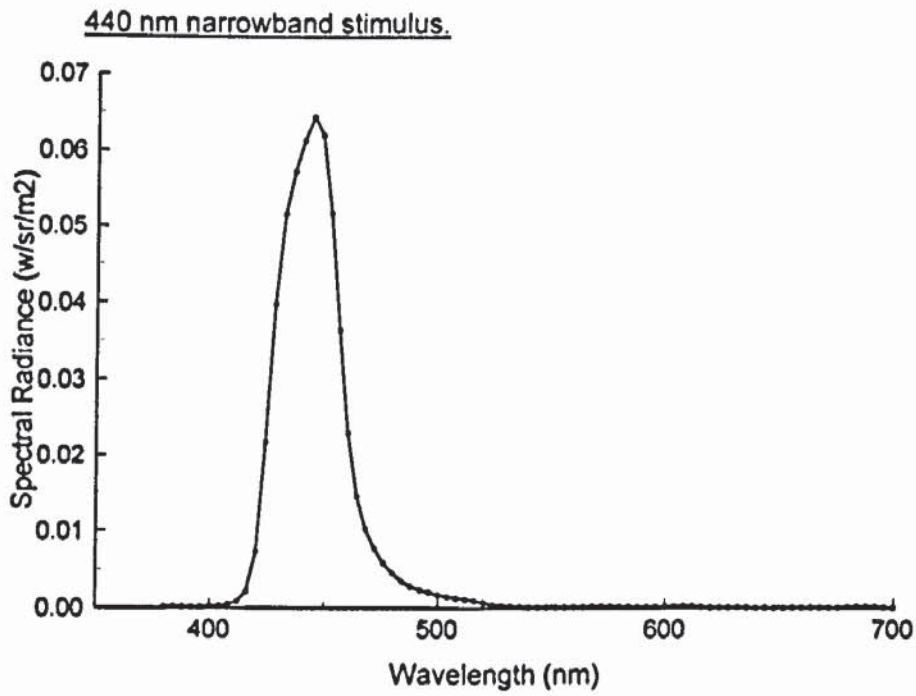


Figure 4.2. Spectral radiance as a function of wavelength for the 440 nm narrowband stimulus (top) and the broadband yellow background (bottom) utilised in the commercially available SWAP. The yellow background transmits visible wavelengths above 530 nm.

was extinguished using the Humphrey Field Analyser's internal software and the stimulus size altered to Goldmann size V, with a stimulus duration of 100 ms. Each subject was dark adapted for a period of thirty minutes prior to commencement of the procedure. Fixation was monitored with the aid of an infra-red source, consisting of an M92 20 W 12 V tungsten halogen lamp (Osram Ltd, Middlesex, UK) mounted behind a Schott RG830 "black light" filter transmitting wavelengths beyond 750 nm. The infra-red assembly was encased within a steel tube and fixed to the frame of the Humphrey Field Analyser such that the infra-red radiation was reflected off the bowl surface and onto the subject. Scotopic thresholds for 410 nm and 560 nm narrowband stimuli (Figure 4.3) were then obtained at four stimulus locations situated at 15 degrees eccentricity in each quadrant of the visual field. This pair of stimuli were selected since the 410 nm stimulus causes the least attenuation of the dynamic range of the perimeter. The stimulus eccentricity was chosen to eliminate the effects of absorption of the short-wavelength stimulus by the macular pigment and also to ensure maximal contribution from the rods. The threshold was obtained three times at each stimulus location for each stimulus wavelength.

The decibel printout from these measurements does not take into account the attenuation caused by the introduction of each narrowband stimulus filter. The true threshold was therefore calculated for the 410 nm and 560 nm stimuli before the measure of ocular media was calculated. Ocular media absorption at 410 nm was scaled to the 440 nm stimulus wavelength employed in SWAP using the equations of Norren and Vos (1974). Knowledge of the maximum stimulus luminance of the 410 nm and 560 nm stimuli was required to perform these calculations. These measurements were carried out using an LMT 3001 spot photometer (LMT Lichtmesstechnik GMBH, Berlin, Germany).

For example, consider a measured decibel value for the 410 nm stimulus of 15 dB, and for the 560 nm stimulus of 35 dB. Using the equation:

$$\text{dB} = k + 10 \log\left(\frac{L}{\Delta L}\right) \quad \text{Eqn 1.1.}$$

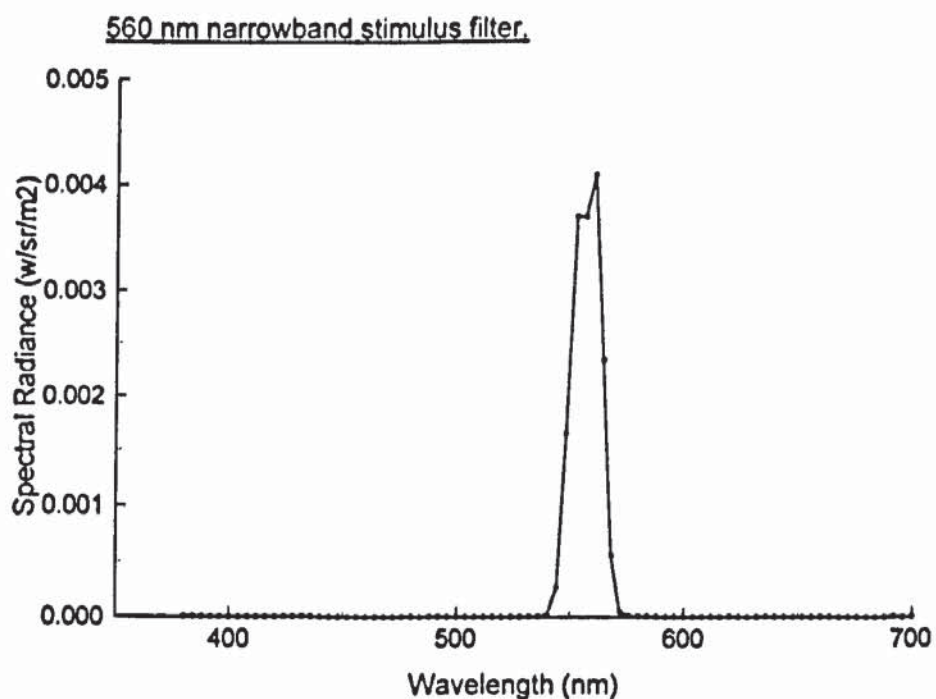
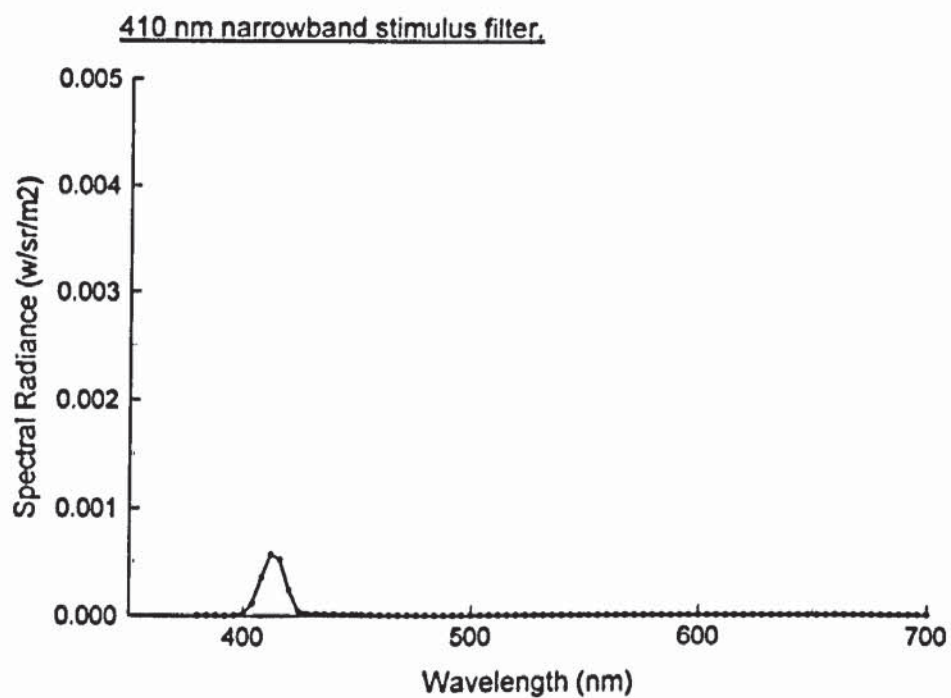


Figure 4.3. Spectral radiance as a function of wavelength for the 410 nm (top) and the 560 nm (bottom) narrowband stimuli employed in the assessment of ocular media absorption.

where, k , is a constant dependent upon the state of retinal adaptation, L , is the background luminance in apostilbs and, ΔL , is the threshold in apostilbs. When the HFA is in default mode, $L = 31.5$ asb and ΔL is 10,000 asb.

Substituting,

$$0 = k + 10 \log \left(\frac{L}{10000} \right)$$

$$0 = k + 10 \log L - 10 \log 10000$$

$$k = 40 - 10 \log L$$

Substituting for, k , into Eqn 1.1. gives:

$$dB = 40 - 10 \log \Delta L \quad \text{Eqn 4.1.}$$

When the perimetry is performed with a given narrowband stimulus filter has been introduced, dB_{printout} is the decibel printout for a given stimulus luminance ΔL_{filter} .

Thus:

$$\Delta L_{\text{filter}} = \log^{-1} \left(\frac{40 - dB_{\text{printout}}}{10} \right) \quad \text{Eqn 4.2.}$$

Substituting for the 410 nm narrowband stimulus filter:

$$\begin{aligned} \Delta L_{410} &= \log^{-1} \left(\frac{40 - 15}{10} \right) \\ &= \underline{316.23 \text{ asb}} \end{aligned}$$

Substituting for the 560 nm narrowband stimulus filter:

$$\begin{aligned} \Delta L_{560} &= \log^{-1} \left(\frac{40 - 35}{10} \right) \\ &= \underline{3.16 \text{ asb}} \end{aligned}$$

When performing colour perimetry, the HFA does not take into account the attenuation caused by the introduction of the narrowband stimulus filter.

The maximum stimulus luminance of the HFA in default mode, ΔL_{\max} , = 10,000 asb
= 4.00 log units

The maximum stimulus luminance of the 410 nm narrowband filter, ΔL_{410} , = 0.1 asb
= -1.00 log units

The maximum stimulus luminance of the 560 nm narrowband filter, ΔL_{560} , = 116.9 asb
= 2.07 log units

The attenuation of the stimulus due to the introduction of a narrowband filter is given as:

$$\Delta L_{\text{att}} = \Delta L_{\max} - \Delta L_{\text{narrowband filter}} \quad \text{Eqn 4.3.}$$

Thus:

The attenuation due to the introduction of the 410 nm stimulus, $\Delta L_{\text{att}410}$
= 4.00 + 1.00
= 5.00 log units

The attenuation due to the introduction of the 560 nm stimulus, $\Delta L_{\text{att}560}$
= 4.00 - 2.07
= 1.93 log units

The true threshold value is given as:

$$\Delta L_{\text{true}} = \Delta L_{\text{theoretical}} - \Delta L_{\text{att}} \quad \text{Eqn 4.4.}$$

Thus:

The true threshold with the 410 nm stimulus, ΔL_{410}
= 2.50 - 5.00 = -2.50 log units
= 0.0032 asb

The true threshold with the 560 nm stimulus, ΔL_{560}
= 0.5 - 1.93 = -1.43 log units
= 0.0372 asb

The true threshold values are then scaled relative to the maximum stimulus luminance of SWAP which is 64.58 asb.

Thus: ΔL_{410} becomes

$$\Delta L_{410\text{scaled}} = 0.0032 \left(\frac{64.58}{0.1} \right)$$

$$= \underline{2.07 \text{ asb}}$$

ΔL_{560} becomes

$$\Delta L_{560\text{scaled}} = 0.0372 \left(\frac{64.58}{116.9} \right)$$

$$= \underline{0.02 \text{ asb}}$$

Under the experimental conditions, the background luminance, L, is assumed to be 0.001 asb.

Therefore, for the 410 nm narrowband filter:

$$\log \left(\frac{L}{\Delta L_{410\text{scaled}}} \right) = \log \left(\frac{0.001}{2.07} \right)$$

$$= \underline{-3.32 \text{ log units}}$$

For the 560 nm narrowband filter:

$$\log \left(\frac{L}{\Delta L_{560\text{scaled}}} \right) = \log \left(\frac{0.001}{0.02} \right)$$

$$= \underline{-1.30 \text{ log units}}$$

The measured difference in sensitivity to the 410 nm and 560 nm stimuli, X, is therefore:

$$X = -1.31 + 3.32$$

$$= \underline{2.01 \text{ log units}}$$

Individual ocular media absorption at 440 nm, OD_{440} , according to the equation of Norren and Vos (1974) is:

$$OD_{440} = 0.27 \left(\frac{X}{0.90} \right) \quad \text{Eqn 4.5.}$$

where, 0.27 is the average "standard observer" ocular media absorption at 440 nm, and 0.90 is the average or "standard observer" difference in ocular media absorption between 410 nm and 560 nm.

Therefore:

$$\text{OD}_{440} = 0.27 \left(\frac{2.01}{0.90} \right)$$

= 0.60 log units = 6.00 dB

Ocular media absorption was expressed as the mean of the four eccentricities tested.

4.5.4. Forward Light Scatter Assessment.

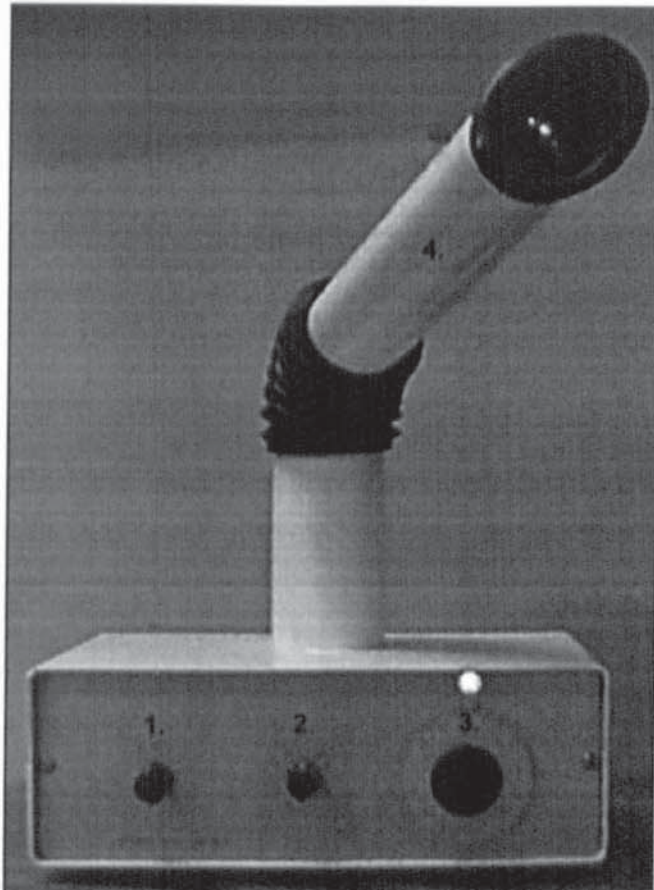
Forward light scatter was assessed using the direct compensation technique of van den Berg (1986) and is defined by the equation:

$$s(\phi) = \phi^2 \cdot \left(\frac{L}{E} \right) \quad \text{Eqn 4.6.}$$

where, s , is the straylight parameter at an angle, ϕ , expressed in log units, E , is the illuminance at the eye resulting from the glare source expressed in lux, and L , is the luminance of the test field expressed in cdm^{-2} .

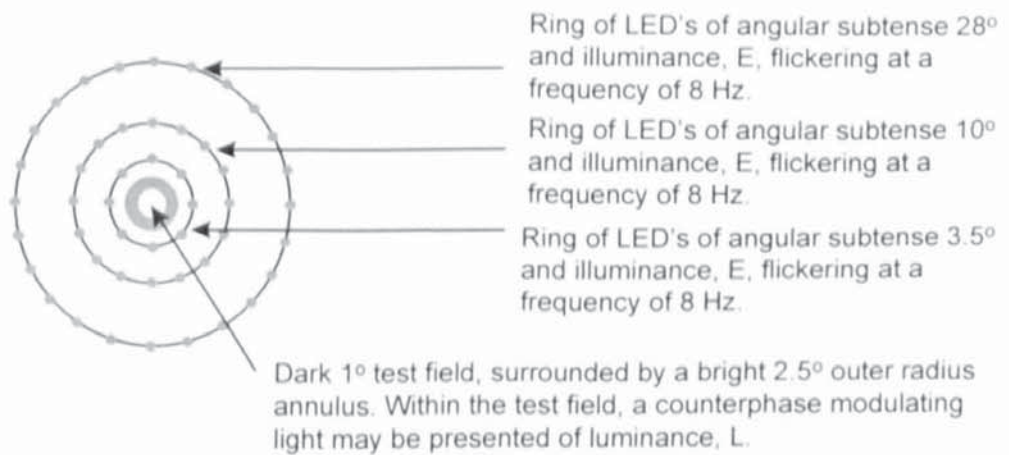
The apparatus used to assess forward light scatter is illustrated in Figure 4.4. Subjects were instructed to fixate the centre of a two degree diameter circular test field. This was surrounded by three independently controlled glare sources of angular subtenses 3.5°, 10°, and 28° respectively. Each glare source was derived from a ring of LED's of wavelength 570 nm (half peak width 30 nm), flickering at a frequency of 8 Hz and of illuminance, E . When the test field was dark it appeared to flicker as a result of entoptic scattering of light from the annular glare source. Within the test field, a light flickering in counterphase with the glare source could be varied in luminance, L , until flicker was not observed by the subject. Fixation errors are assumed to be of minor importance since the test patch and the straylight source are presented virtually simultaneously (van den Berg and IJspeert 1992). To account for differences in flicker sensitivity, the relative modulation depth of the straylight source (and E) could be adjusted.

In each subject forward light scatter was measured ten times at each of the three scatter angles and expressed as the arithmetic mean.



KEY.

1. Glare source selector.
2. Glare source luminance modulation depth adjustment.
3. Test field luminance modulation adjustment.
4. Observation tube.



Forward light scatter, s , at glare angle, ϕ , is defined by:

$$s(\phi) = \phi^2 \cdot \left(\frac{L}{E} \right)$$

Figure 4.4. The forward light scatter meter (top) and a schematic diagram of the principles of measurement (bottom).

4.5.5. Statistical Analysis.

The visual field data corresponding to the Full Threshold and the FASTPAC strategies for conventional W-W perimetry and for SWAP were expressed in terms of the visual field indices mean sensitivity (MS) and unweighted short-term fluctuation (SF); and in terms of the number of stimulus presentations, the examination time, and the staircase efficiency (the benefit-cost ratio - defined by Eqn 3.3). The two stimulus locations immediately above and below the blind spot were omitted from the analysis. The data for each of the five visual field parameters were subjected to a separate Analysis of Variance (ANOVA) appropriate for a two-period cross-over trial. The MS, SF and the benefit-cost ratio were analysed separately for conventional W-W perimetry and for SWAP since the two perimetric measurement scales are not directly comparable. The maximum stimulus luminance associated with 0 dB differs between W-W perimetry and SWAP; however, each dB represents a 0.1 log unit change in stimulus luminance. The type of strategy (Full Threshold or FASTPAC), the type of perimetry (W-W or SWAP), the sequence of the two types of perimetry and the sequence of the two strategies were all considered as within-subject factors. The subjects and the age of the subjects were considered as between-subject factors.

4.6. Results.

All W-W and SWAP visual fields were within the reliability criteria of <33% false-positive or negative catch trials. Fixation losses in W-W perimetry were within the reliability criteria of <20% in all subjects. The Heijl-Krakau method of monitoring fixation was often found to be ineffectual in SWAP because the default Goldmann size V stimulus could be detected by many subjects. This was possibly due to light scatter around the stimulus, and/or the inability of the HFA to accurately position the blind spot. In such cases, the blind spot stimulus was subsequently altered to a Goldmann size III. As a result of the erroneously induced false fixation losses in the early stages of SWAP, some subjects exceeded the <20% reliability criteria for fixation losses. All subjects though were within the <33% fixation loss reliability criteria proposed by Johnson and Nelson-Quigg (1993).

The mean global visual field indices are illustrated in Table 4.3.

4.6.1. Mean Sensitivity (MS).

Table 4.4 illustrates the summary table for the Analysis of Variance of mean sensitivity. For W-W perimetry, the Full Threshold and FASTPAC strategy yielded similar group mean MS's ($p=0.790$) (Table 4.3). MS declined with increase in age ($p<0.001$) and the extent of this reduction in sensitivity was similar for each strategy ($p=0.790$). The results were also independent of the sequence of the strategy ($p=0.836$).

For SWAP, the Full Threshold and FASTPAC strategy also yielded similar group mean MS's ($p=0.065$) (Table 4.3.). MS again declined with age ($p<0.001$) and the extent of the reduction in sensitivity was also similar for each strategy ($p=0.857$). The results were also unaffected by the sequence of the strategy ($p=0.217$).

The decline in MS with increase in age for both W-W perimetry and SWAP was described moderately well by a linear function with the coefficients of determination ranging from 0.39 to 0.51 (Figure 4.5). For W-W perimetry, the slopes were 0.70 dB per decade for the Full Threshold strategy and 0.72 dB per decade for the FASTPAC strategy. For SWAP without correction for ocular media absorption, the slopes were 1.96 dB per decade for the Full Threshold strategy and 1.90 dB per decade for the FASTPAC strategy and with correction 1.46 dB per decade and 1.43 dB per decade respectively. The corresponding slopes of the age-decline in sensitivity at each individual stimulus location are given in Figure 4.6. Figure 4.7 illustrates the regional differences in decibel loss per decade. In W-W perimetry and SWAP the greatest decline in MS with age was found in the superior hemifield, particularly the superotemporal quadrant. The inferotemporal quadrant yielded the lowest decline in MS with age.

The MS and one standard deviation of the MS at each stimulus location for each threshold strategy is plotted in Figure 4.8 for W-W perimetry, for SWAP without correction for ocular media absorption and for SWAP with correction. For W-W perimetry, the mean of the ratio of

	W-W Perimetry		SWAP		SWAP Corrected for Absorption Scaled to 440 nm	
	Full Threshold	FASTPAC	Full Threshold	FASTPAC	Full Threshold	FASTPAC
Mean Sensitivity (dB)	27.97 [2.17]	27.91 [2.28]	23.08 [5.62]	23.67 [5.20]	29.78 [5.02]	30.49 [4.54]
Short-Term Fluctuation (dB)	1.29 [0.35]	1.61 [0.55]	1.60 [0.69]	1.89 [0.63]	1.60 [0.69]	1.89 [0.63]
Number of Stimulus Presentations	461.24 [47.61]	262.16 [14.37]	508.06 [42.91]	297.55 [26.08]	508.06 [42.91]	297.55 [26.08]
Examination Time (minutes)	13.98 [1.42]	8.09 [0.75]	16.08 [1.84]	9.45 [1.07]	16.08 [1.84]	9.45 [1.07]

Table 4.3. Global mean visual field indices [± 1 standard deviation] for the Full Threshold and FASTPAC strategies in W-W perimetry and SWAP. Note that the dB scales between W-W perimetry and SWAP are not compatible.

W-W Perimetry

Source	Degrees of Freedom	Type I Sums of Squares	Mean Square	F-Value	p-Value
Age	1	191.49	191.49	183.05	0.0001
Subject	49	252.43	5.15	4.92	0.0001
Strategy	1	0.08	0.08	0.07	0.7898
Visit	1	0.05	0.05	0.04	0.8363
Age x Strategy	1	0.08	0.08	0.07	0.7893

Tests of Hypotheses using the Type I Mean Square for Subject as an error term

Source	Degrees of Freedom	Type I Sums of Squares	Mean Square	F-Value	p-Value
Age	1	191.49	191.49	37.17	0.0001

SWAP

Source	Degrees of Freedom	Type I Sums of Squares	Mean Square	F-Value	p-Value
Age	1	1416.40	1416.40	557.58	0.0001
Subject	49	1387.91	28.32	11.15	0.0001
Strategy	1	9.04	9.04	3.56	0.0652
Visit	1	3.98	3.98	1.57	0.2165
Age x Strategy	1	0.08	0.08	0.03	0.8570

Tests of Hypotheses using the Type I Mean Square for Subject as an error term

Source	Degrees of Freedom	Type I Sums of Squares	Mean Square	F-Value	p-Value
Age	1	1416.40	1416.40	50.01	0.0001

Table 4.4. Summary Table for Analysis of Variance of Mean Sensitivity.

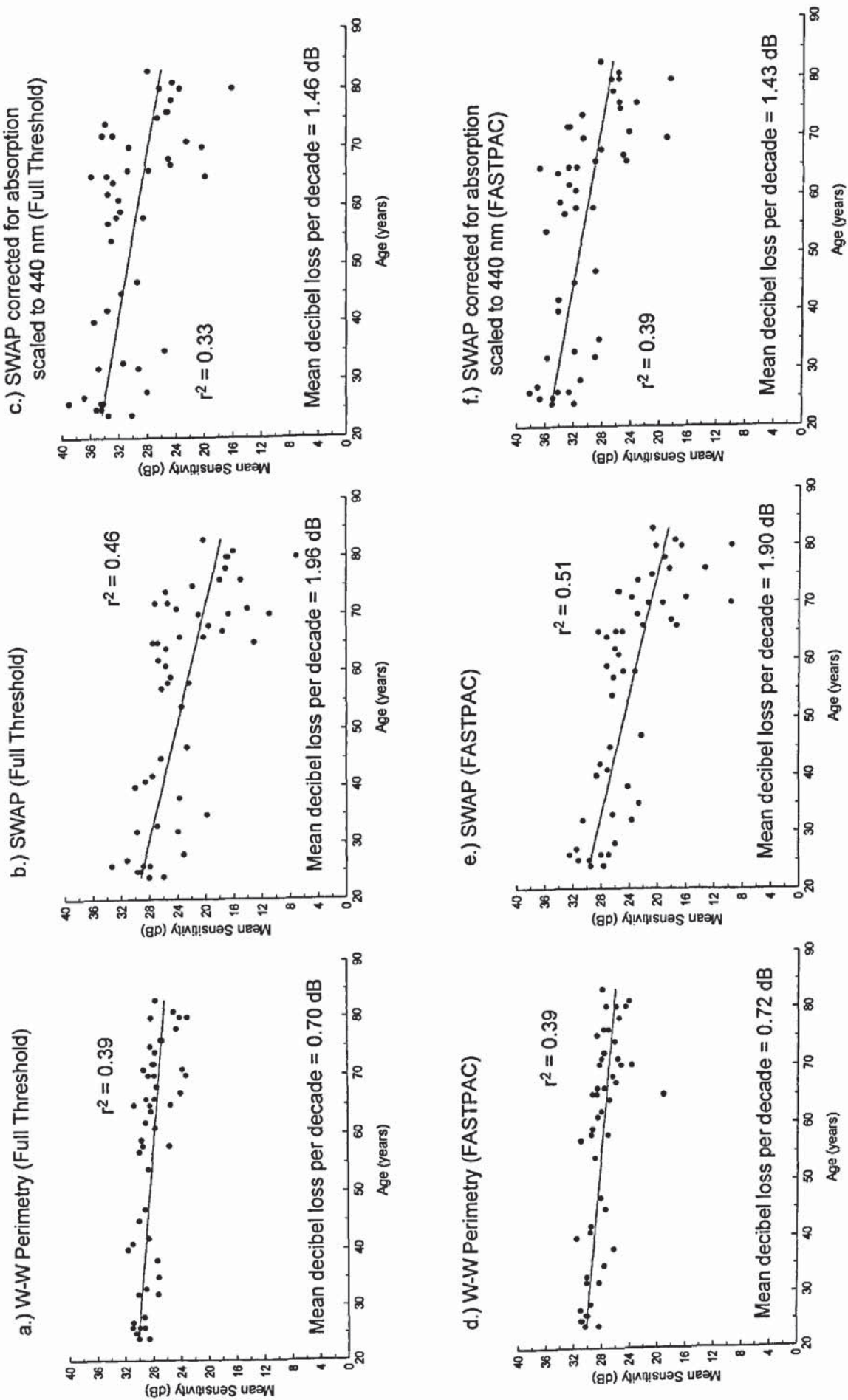
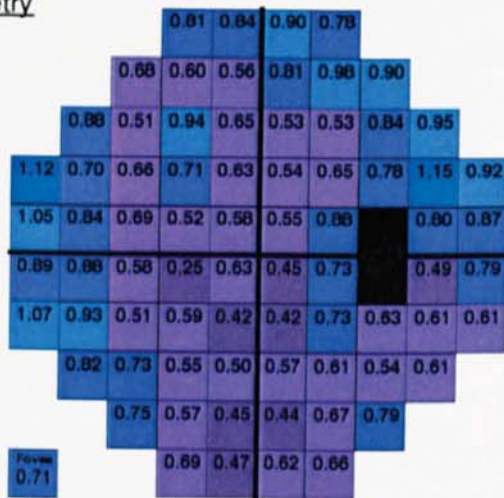


Figure 4.5a-f. Univariate linear regression of mean sensitivity for Program 30-2 as a function of age for the Full Threshold and FASTPAC strategies in W-W perimetry and SWAP. Note the dB scales between W-W perimetry and SWAP are not equivalent.

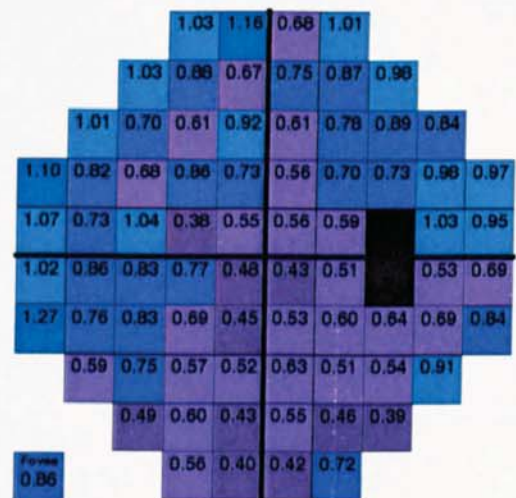
Figure 4.6. Univariate linear regression at each individual stimulus location for Program 30-2 as a function of age (dB per year) for the Full Threshold and FASTPAC strategies in W-W perimetry and SWAP without correction for ocular media absorption and with correction. Note that the dB scales between W-W perimetry and SWAP are not equivalent.

a.) W-W Perimetry

Full Threshold Strategy

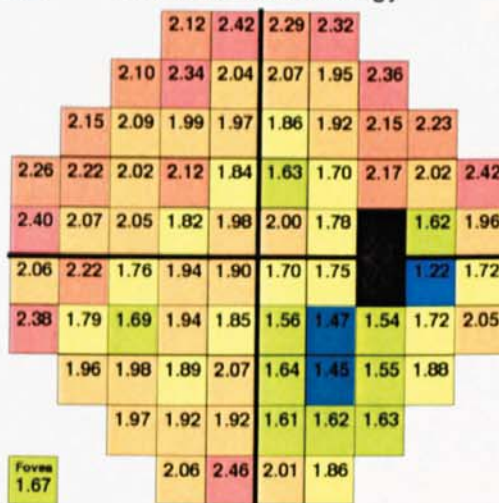


FASTPAC Strategy

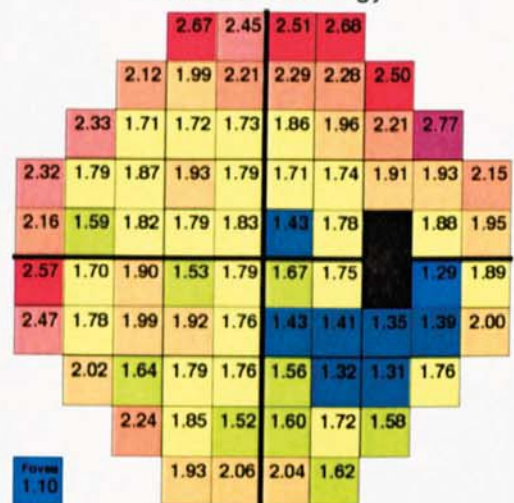


b.) SWAP

Full Threshold Strategy

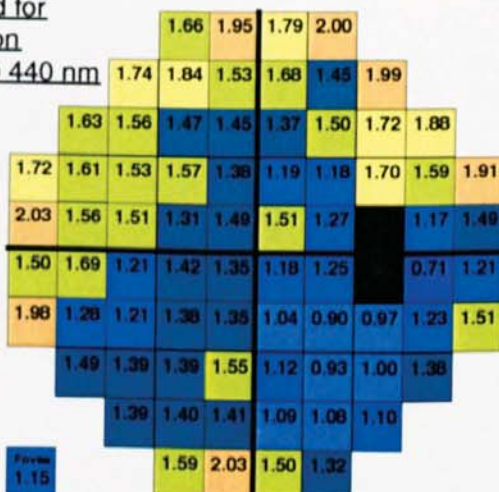


FASTPAC Strategy

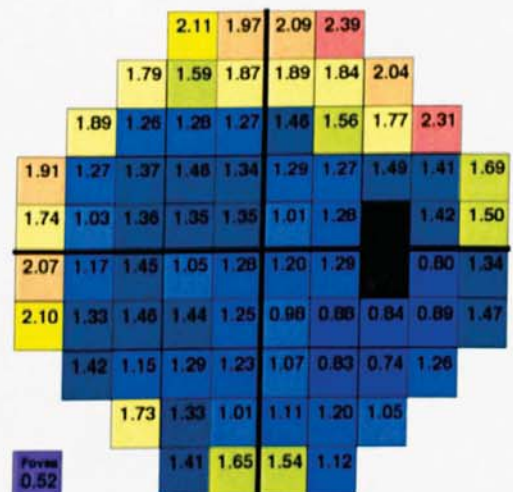


c.) SWAP corrected for absorption scaled to 440 nm

Full Threshold Strategy



FASTPAC Strategy



Group Mean Decibel Loss Per Decade

0.30 - 0.49	0.50 - 0.69	0.70 - 0.89	0.90 - 1.09	1.10 - 1.29	1.30 - 1.49	1.50 - 1.69
1.70 - 1.89	1.90 - 2.09	2.10 - 2.29	2.30 - 2.49	2.50 - 2.69	2.70 - 2.89	

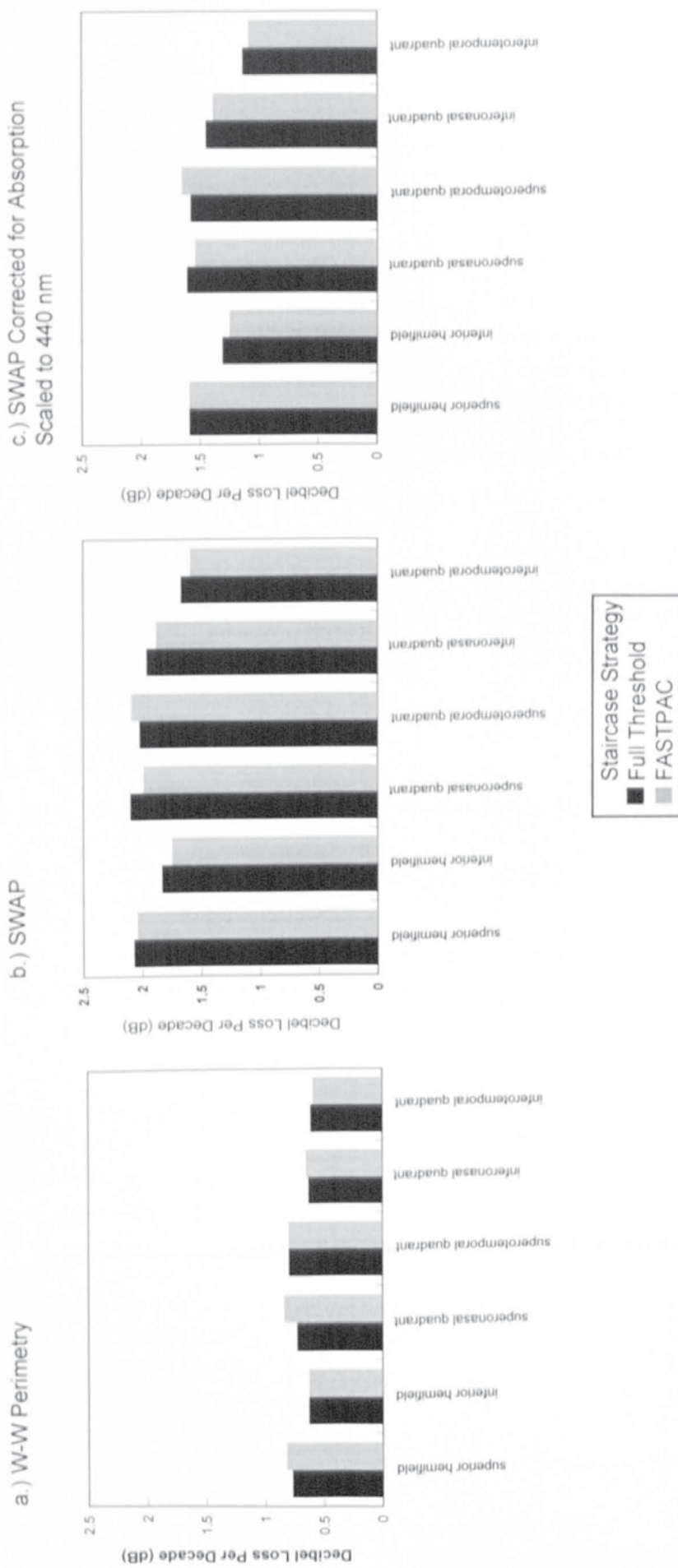
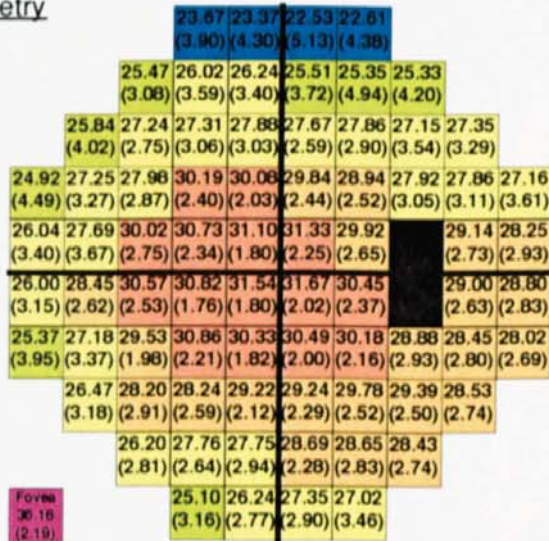


Figure 4.7a-c. Decibel loss per decade as a function of visual field sector for Program 30-2 for the Full Threshold and FASTPAC strategies in W-W perimetry and SWAP. Note that the decibel scales are not compatible between W-W perimetry and SWAP.

Figure 4.8. Group mean sensitivity at each individual stimulus location of Program 30-2 (± 1 standard deviation) for the Full Threshold and FASTPAC strategies in W-W perimetry and SWAP without correction for absorption and with correction. Note that the dB scales between W-W perimetry and SWAP are not compatible.

a.) W-W
Perimetry

Full Threshold Strategy

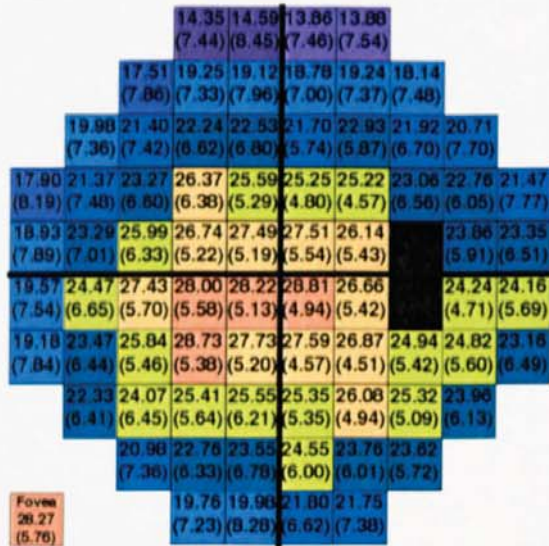


FASTPAC Strategy

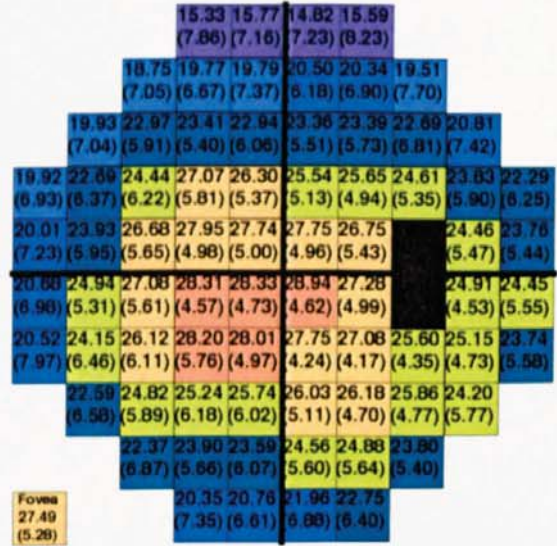


b.) SWAP

Full Threshold Strategy

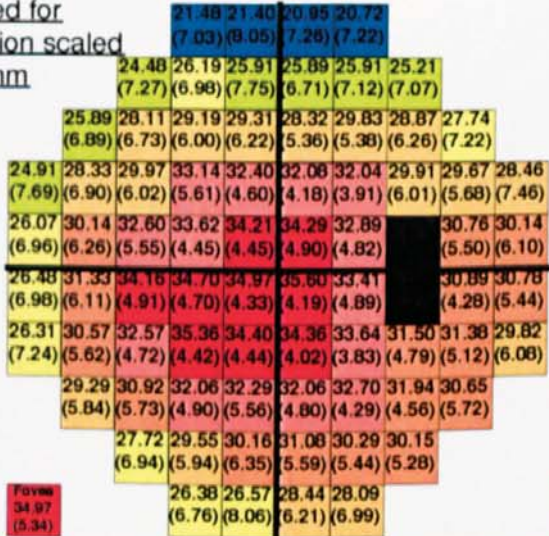


FASTPAC Strategy

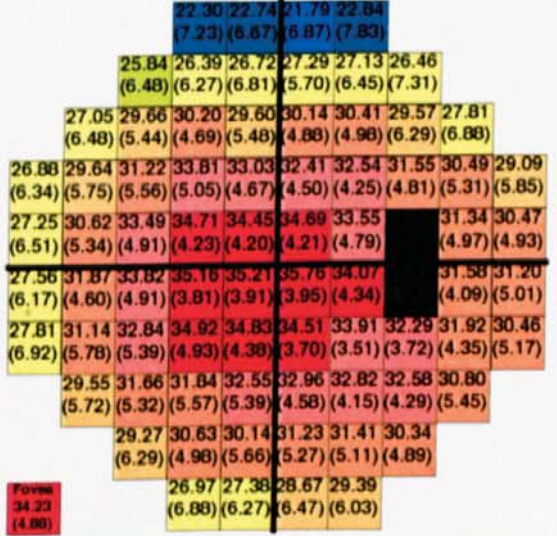


c.) SWAP
corrected for
absorption scaled
to 440 nm

Full Threshold Strategy



FASTPAC Strategy



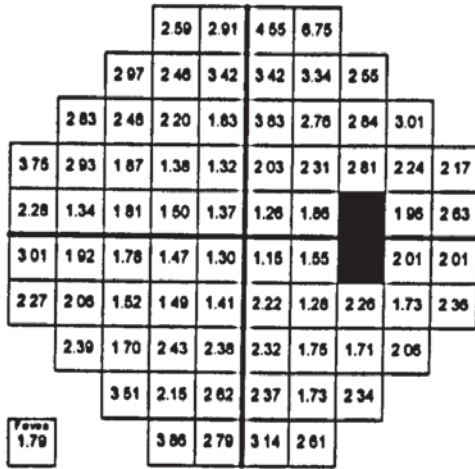
Group Mean Sensitivity (dB)

12.00 - 13.99	14.00 - 15.99	16.00 - 17.99	18.00 - 19.99	20.00 - 21.99	22.00 - 23.99	24.00 - 25.99
26.00 - 27.99	28.00 - 29.99	30.00 - 31.99	32.00 - 33.99	34.00 - 35.99	36.00 - 37.99	

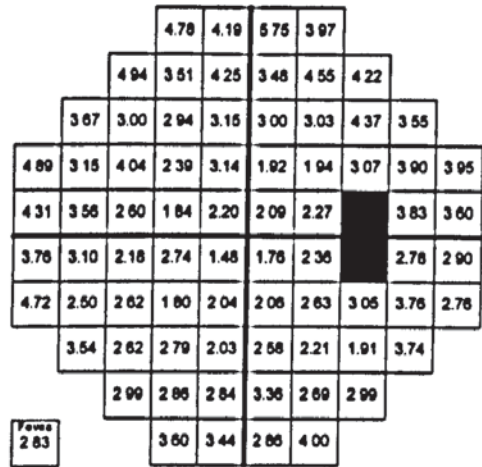
the FASTPAC SD's to the Full Threshold SD's was 1.08 (range 0.77 to 1.54) indicating that the SD's were, in general, slightly larger (8%) for the FASTPAC strategy compared to the Full Threshold strategy; this difference was greatest in the superior field. The SD's for the Full Threshold strategy were on average 1.59 times larger at the extreme peripheral locations than at the paracentral locations and those for FASTPAC 1.81 times larger; the difference between centre and periphery was greatest in the superior field. For SWAP, the mean of the ratio of the FASTPAC SD's to the Full Threshold SD's for SWAP without correction for ocular media absorption was 0.94 (range 0.80 to 1.12) and with correction was 0.92 (range 0.75 to 1.14) indicating that the SD's were in general slightly smaller (6%) for the FASTPAC strategy compared to the Full Threshold strategy; the difference was greatest for the superior field. The SD's at the extreme peripheral locations were greater than the paracentral locations on average by a factor of approximately 1.25 for both the Full Threshold and FASTPAC strategies; the difference between centre and periphery was greatest in the superior field. Correction for ocular media absorption, reduced the magnitude of the SWAP SD's by approximately 10%; the mean of the ratio of the corrected SD's to the uncorrected SD's for the Full Threshold strategy was 0.91 (range 0.82 to 0.97) and for FASTPAC 0.90 (range 0.83 to 0.95).

The sample was divided by age into two groups, each consisting of a random selection of 17 subjects; a young group less than 50 years (mean age 32.5 years, SD 8.0) and an old group greater than 50 years (mean age 68.7 years, SD 7.4). One standard deviation of the mean sensitivity at each individual stimulus location for each threshold strategy in the young and old groups is illustrated in Figure 4.9. For W-W perimetry, the SD's were greater in the young group for both the Full Threshold strategy (range: 0.94 to 4.78 (young group), 1.60 to 5.51 (old group)) and FASTPAC (range: 1.15 to 6.75 (young group), 6.75 to 5.75 (old group)). In SWAP uncorrected for ocular media absorption, the SD's were similar in the Full Threshold strategy and FASTPAC between the young and old groups (range: 3.99 to 8.91 (Full Threshold young group), 4.47 to 8.48 (Full Threshold old group), 4.07 to 8.71 (FASTPAC young group), 3.98 to 8.07 (FASTPAC old group)). Correction of SWAP for ocular media absorption reduced the SD's in the young and old groups for the Full Threshold strategy and FASTPAC. There was a

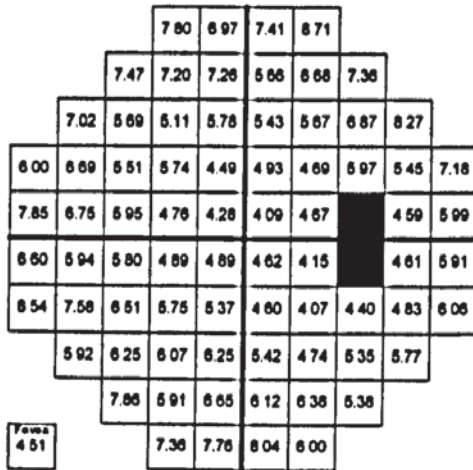
g.) W-W Perimetry (FASTPAC)
Young Group.



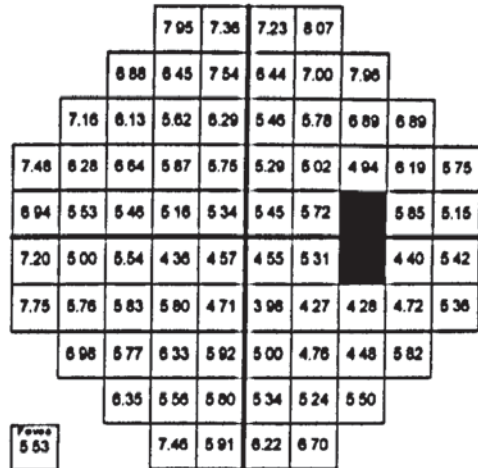
h.) W-W Perimetry (FASTPAC)
Old Group.



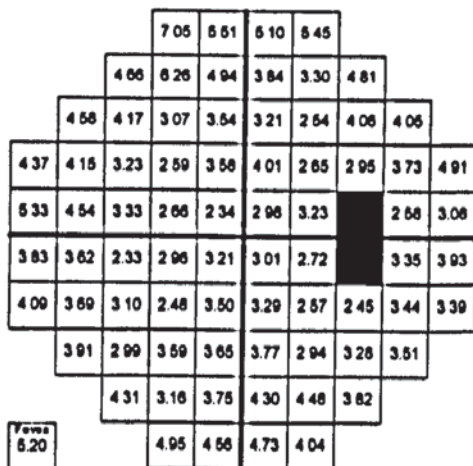
i.) SWAP (FASTPAC)
Young Group.



j.) SWAP (FASTPAC)
Old Group.



k.) SWAP corrected for absorption scaled
to 440 nm (FASTPAC) Young Group.



l.) SWAP corrected for absorption scaled
to 440 nm (FASTPAC) Old Group.

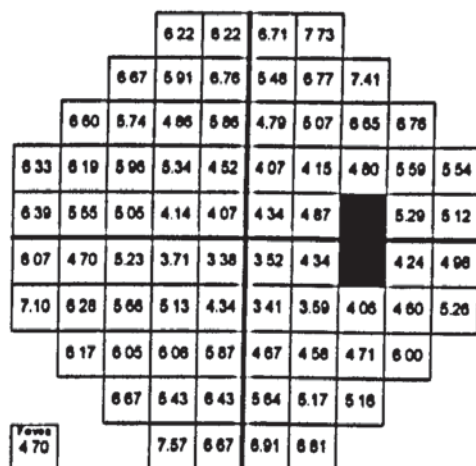


Figure 4.9a-l. Continued.

greater reduction in the SD's of the young group in the Full Threshold strategy (range: 1.71 to 7.37 (young group), 3.64 to 8.78 (old group) and FASTPAC (range: 2.33 to 7.05 (young group), 3.38 to 7.73 (old group)).

Regional differences in group MS are illustrated in Figure 4.10. For W-W perimetry and SWAP, MS was greater in the inferior hemifield and greatest in the inferotemporal quadrant. SWAP yielded more pronounced regional differences in MS than W-W perimetry.

For W-W perimetry, the distribution of group measured sensitivity at each stimulus location was significantly non-Gaussian, negatively skewed and kurtosed at the majority of stimulus locations (Figure 4.11). For SWAP, the distribution at the majority of stimulus locations was Gaussian and in SWAP corrected for ocular media absorption all stimulus locations were Gaussian (Figure 4.11).

4.6.2. Coefficient of Variation.

As W-W and SWAP possess different measurement scales for the stimulus luminance, the difference in the between-subject variability at each stimulus location between the two types of perimetry was expressed in terms of the coefficient of variation (the SD divided by the mean) (Figure 4.12). This statistic enables a comparison between standard deviations derived from distributions which differ in the magnitude of their measurement scales. The coefficient of variation at each stimulus location for SWAP without correction for ocular media absorption was greater than that for W-W perimetry by on average 2.7 times (range 2.0 to 3.9) and 1.9 times greater (range 1.4 to 2.9) with correction. The coefficient of variation for the extreme peripheral locations was greater than at the paracentral locations by a factor of approximately 2.2 for W-W perimetry and also for SWAP regardless of correction for ocular media absorption. However, the difference in SWAP was greater for the Full Threshold strategy than for FASTPAC.

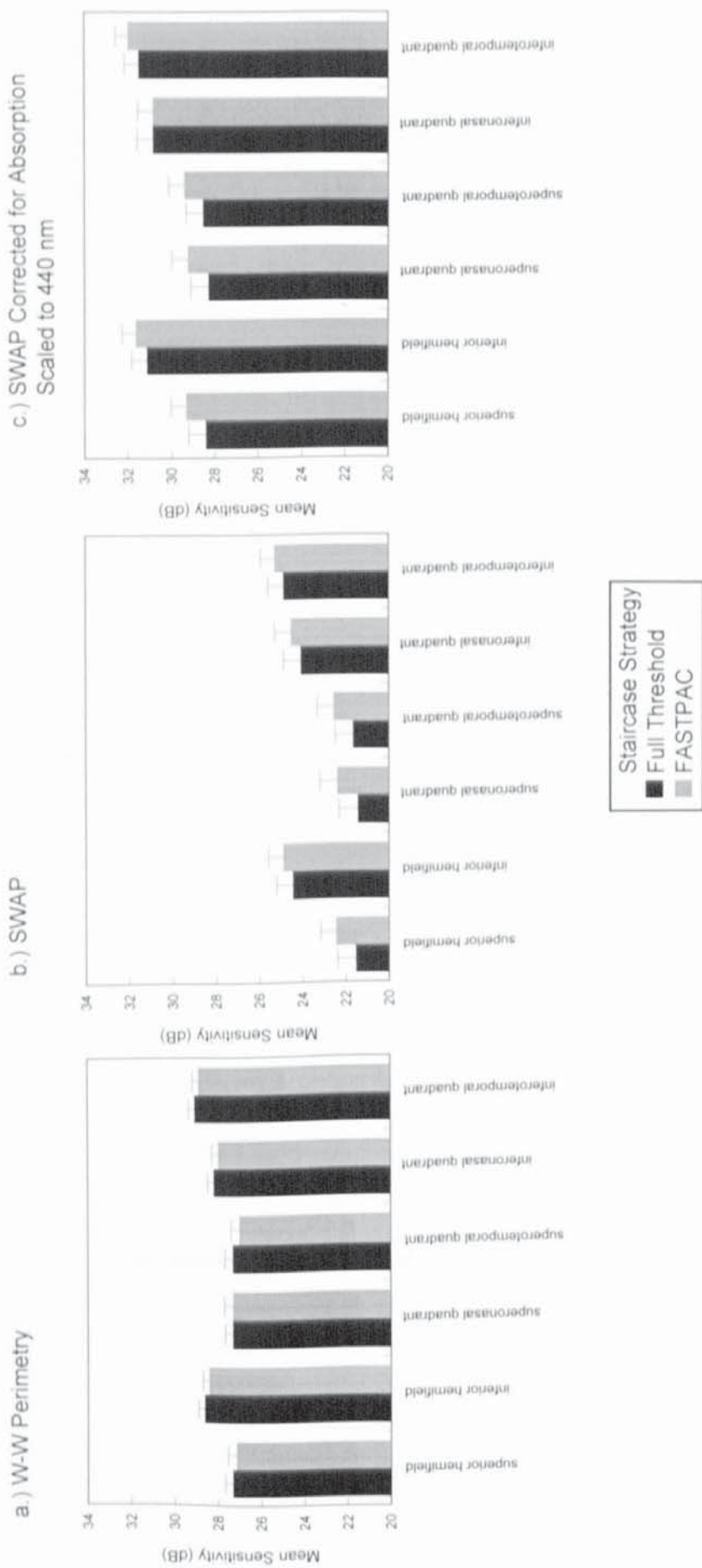
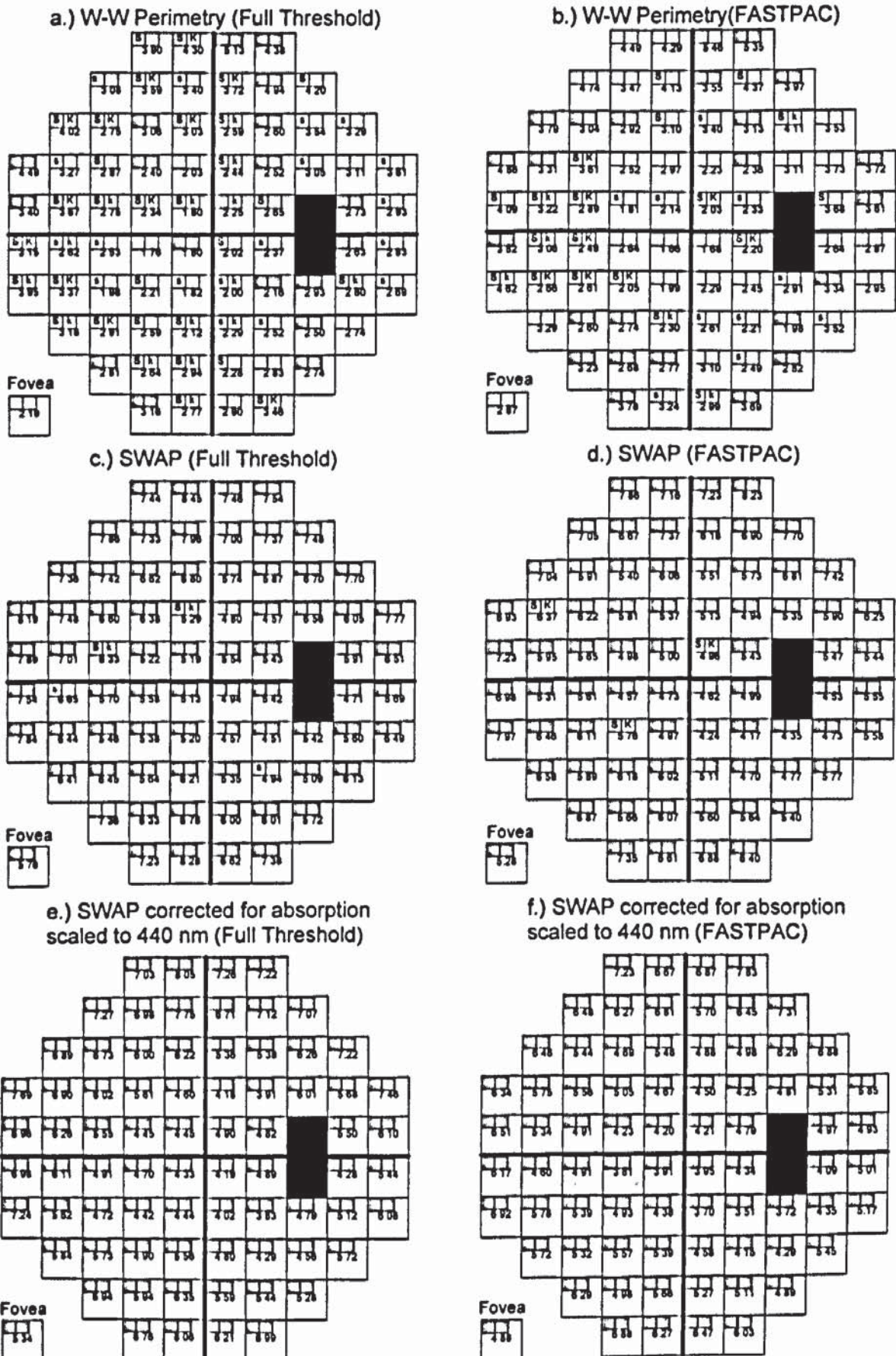


Figure 4.10a-c. Mean sensitivity as a function of visual field sector for the Full Threshold and FASTPAC strategies in W-W perimetry and SWAP. Error bars represent ± 1 standard error of the group mean. Note that the decibel scales are not compatible between W-W perimetry and SWAP.



■ Gaussian distribution of sensitivity	⊖ s = skewness significant at 5%	k = kurtosis significant at 5%
□ Non-Gaussian distribution of sensitivity	⊖ S = skewness significant at 1%	K = kurtosis significant at 1%

Figure 4.11a-d. One standard deviation of the group mean sensitivity (dB) (ie the within-test between-individual variation in sensitivity) at each stimulus location for Program 30-2 for the Full Threshold (right) and FASTPAC(left) strategies for W-W perimetry, SWAP without correction for absorption and SWAP with correction. Note the dB scales between W-W perimetry and SWAP are not equivalent.

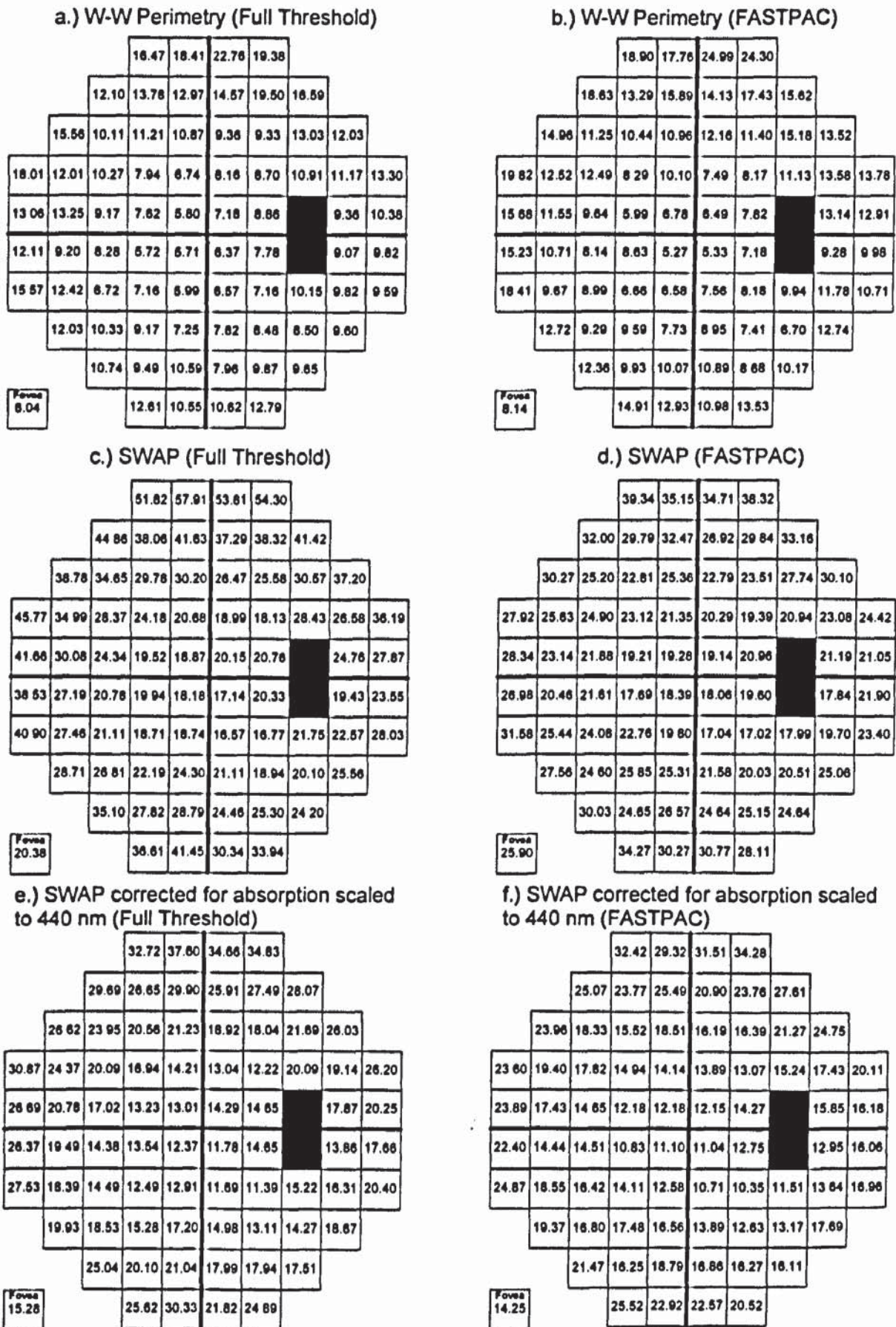


Figure 4.12a-f. The coefficient of variation (%) at each individual stimulus location for Program 30-2 for the Full Threshold (right) and FASTPAC (left) strategies for W-W perimetry, SWAP without correction for absorption and SWAP with correction.

4.6.3. Short-Term Fluctuation (SF).

Table 4.5 illustrates the summary table for the Analysis of Variance of the SF. For W-W perimetry, the group mean SF for the FASTPAC strategy was 24.8% greater than that for the Full Threshold strategy ($p=0.001$) and this effect was independent of age ($p=0.524$) and the sequence of the strategy ($p=0.215$) (Table 4.3).

For SWAP, the group mean SF for the FASTPAC strategy was 15.3% greater than that for the Full Threshold strategy ($p=0.006$) and this effect was independent of age ($p=0.929$) and the sequence of the strategy ($p=0.696$) (Table 4.3).

4.6.4. Examination Time.

Table 4.6 illustrates the summary table for the Analysis of Variance of examination time. Figure 4.13 illustrates examination time as a function of age. The group mean examination time was longer for SWAP than for W-W perimetry ($p<0.001$). The group mean for the SWAP Full Threshold strategy was 15.0% longer compared to that of W-W perimetry and the group mean for the SWAP FASTPAC strategy 16.8% longer than that for the W-W FASTPAC strategy. The group mean examination time was greater for the Full Threshold strategy than for the FASTPAC strategy ($p<0.001$). The group mean examination time for the FASTPAC strategy was 41.2% shorter compared to the Full Threshold strategy in SWAP and 42.1% shorter in W-W perimetry. However, in absolute terms, the difference in the examination time between the Full Threshold strategy and the FASTPAC strategy was greater for SWAP than for W-W perimetry ($p=0.021$). The group mean examination time increased with increase in age ($p=0.001$) but this age effect was independent of the type of perimetry ($p=0.631$) or the type of strategy ($p=0.087$). The order of the type of perimetry ($p=0.831$) and the order of the type of strategy ($p=0.432$) did not influence the examination time.

4.6.5. Stimulus Presentations.

Table 4.7 illustrates the summary table for the analysis of variance of stimulus presentations. Figure 4.14 illustrates the number of stimulus presentations as a function of age. The group mean number of stimulus presentations was greater for SWAP than W-W perimetry ($p<0.001$).

W-W Perimetry

Source	Degrees of Freedom	Type I Sums of Squares	Mean Square	F-Value	p-Value
Age	1	0.10	0.10	0.54	0.4652
Subject	49	12.05	0.25	1.31	0.1723
Strategy	1	2.68	2.68	14.31	0.0004
Visit	1	0.29	0.29	1.58	0.2153
Age x Strategy	1	0.0007	0.0007	0.00	0.9508

Tests of Hypotheses using the Type I Mean Square for Subject as an error term

Source	Degrees of Freedom	Type I Sums of Squares	Mean Square	F-Value	p-Value
Age	1	0.10	0.10	0.41	0.5239

SWAP

Source	Degrees of Freedom	Type I Sums of Squares	Mean Square	F-Value	p-Value
Age	1	0.01	0.01	0.02	0.8885
Subject	49	31.30	0.64	2.50	0.0009
Strategy	1	2.16	2.16	8.47	0.0055
Visit	1	0.04	0.04	0.15	0.6958
Age x Strategy	1	0.0003	0.0003	0.01	0.9203

Tests of Hypotheses using the Type I Mean Square for Subject as an error term

Source	Degrees of Freedom	Type I Sums of Squares	Mean Square	F-Value	p-Value
Age	1	0.005	0.005	0.01	0.9293

Table 4.5. Summary Table for Analysis of Variance of Short-Term Fluctuation.

W-W Perimetry and SWAP

Source	Degrees of Freedom	Type II Sums of Squares	Mean Square	F-Value	p-Value
Subject	50	171.48	3.43	2.75	0.0001
Strategy	1	2002.75	2002.75	1607.49	0.0001
Technique	1	152.02	152.02	122.02	0.0001
Visit	1	0.86	0.86	0.69	0.4068
Test	1	0.01	0.01	0.00	0.9518
Strategy x Technique	1	6.80	6.80	5.45	0.0209
Visit x Test	1	0.32	0.32	0.25	0.6156

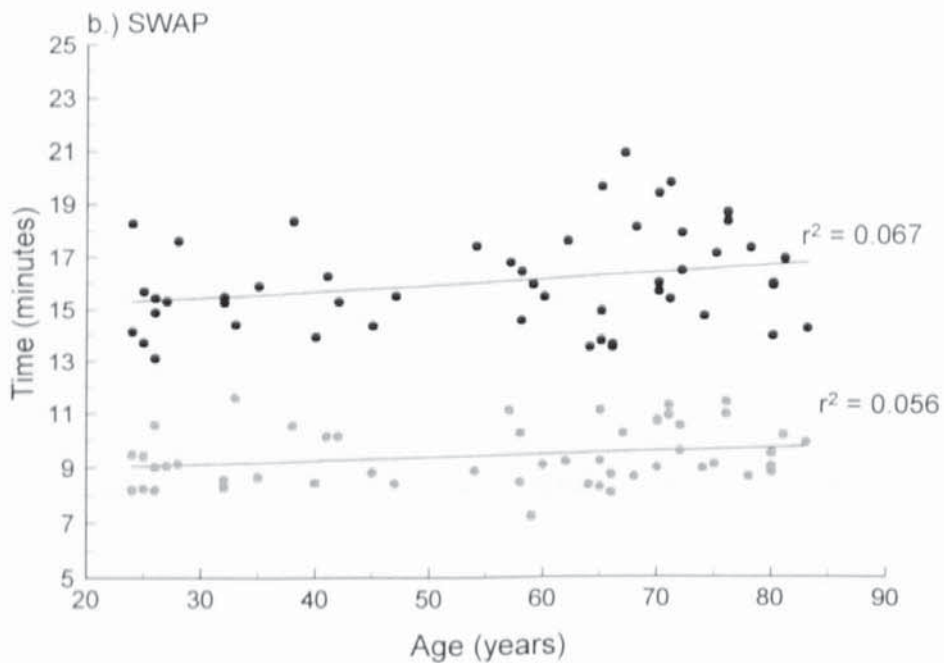
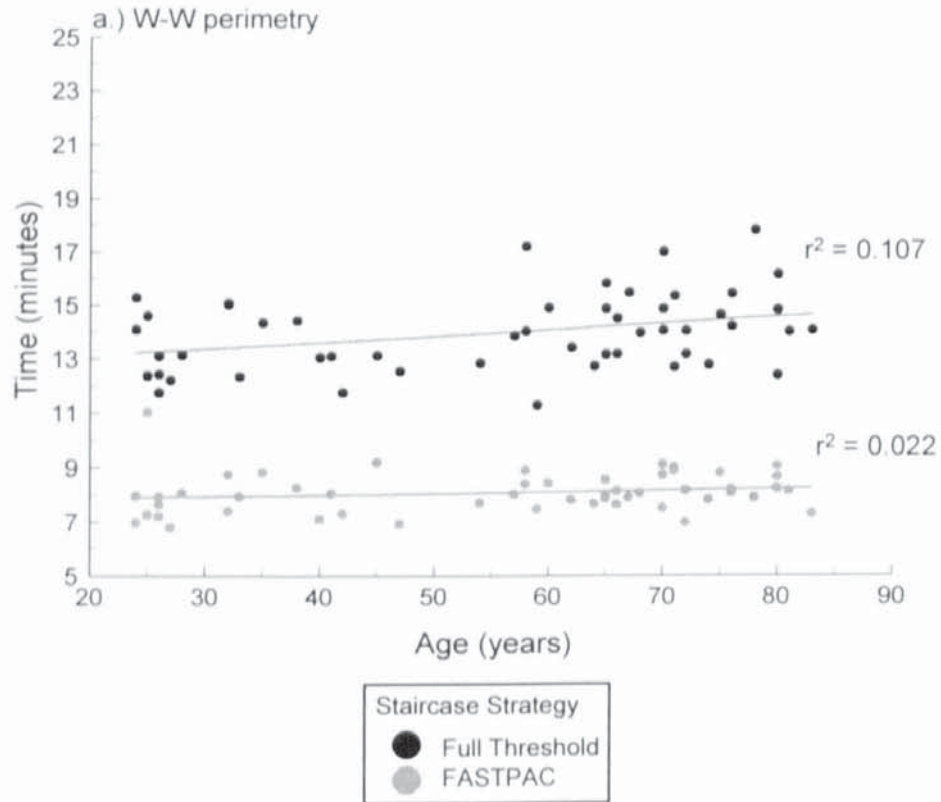


Figure 4.13a & b. Univariate linear regression of examination time for Program 30-2 as a function of age for the Full Threshold and FASTPAC strategies in W-W perimetry (top) and SWAP (bottom).

W-W Perimetry and SWAP

Source	Degrees of Freedom	Sums of Squares	Mean Square	F-Value	p-Value
Subject	50	112255	2245.10	2.48	0.0001
Strategy	1	2139509.64	2139509.64	2364.11	0.0001
Technique	1	86106.14	86106.14	95.15	0.0001
Visit	1	562.19	562.19	0.62	0.4319
Test	1	41.32	41.32	0.05	0.8311
Strategy x Technique	1	1485.45	1485.45	1.64	0.2022
Visit x Test	1	1406.39	1406.39	1.55	0.2145

Table 4.7. Summary Table for Analysis of Variance of Stimulus Presentations.

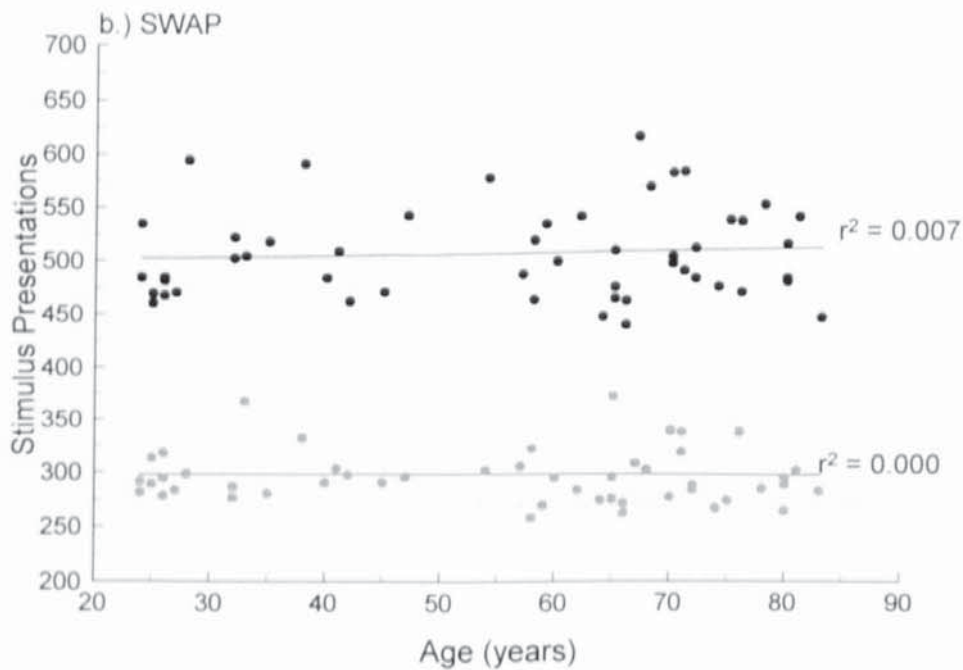
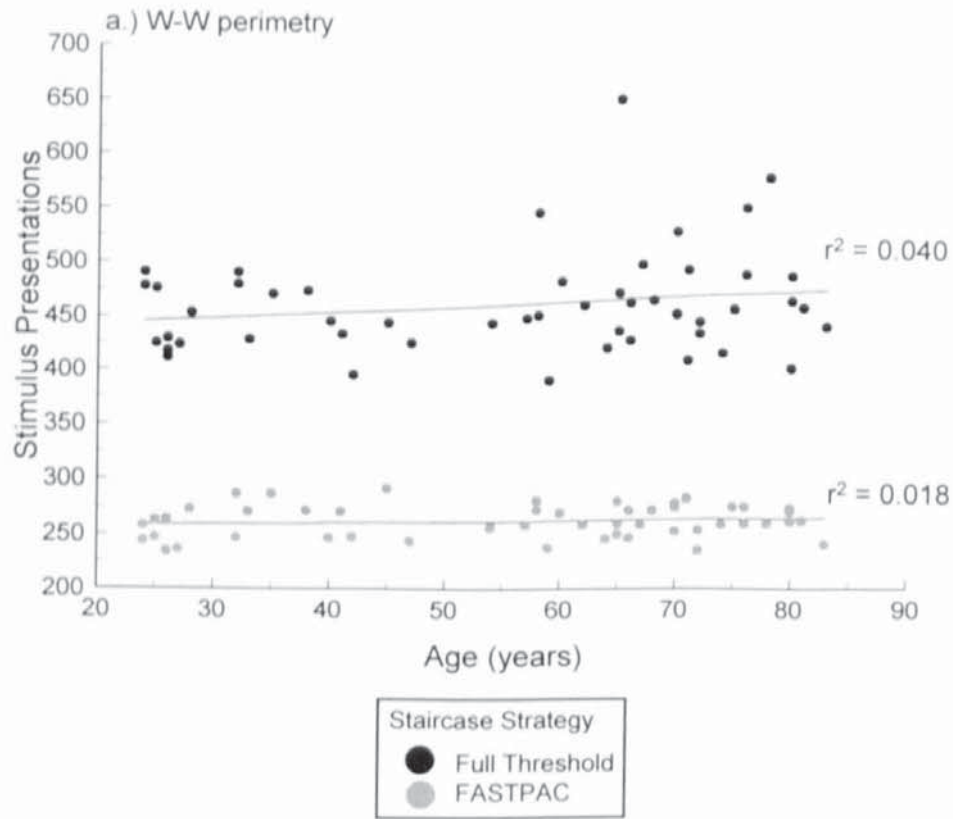


Figure 4.14a & b. Univariate linear regression of the number of stimulus presentations as a function of age for the Full Threshold and FASTPAC strategies in W-W perimetry (top) and SWAP (bottom).

The group mean for the SWAP Full Threshold strategy was 10.2% larger than that for the W-W Full Threshold strategy and the group mean for the SWAP FASTPAC strategy 13.5% larger than that for the W-W FASTPAC strategy. The group mean number of stimulus presentations was greater for the Full Threshold strategy than for the FASTPAC strategy ($p=0.001$). The group mean for the SWAP FASTPAC strategy was 41.4% less than that of the SWAP Full Threshold strategy and the corresponding reduction for W-W perimetry was 43.2%. The reduction in the number of stimulus presentations for the FASTPAC strategy was similar between SWAP and W-W perimetry ($p=0.202$). Age ($p=0.263$), the order of the type of perimetry ($p=0.831$) and the order of the type of strategy ($p=0.432$) did not influence the number of stimulus presentations.

4.6.6. Staircase Efficiency (Benefit-Cost).

Table 4.8 illustrates the summary table for the Analysis of Variance of the staircase efficiency. Table 4.9 illustrates the benefit-cost ratios for W-W perimetry and SWAP for the Full Threshold strategy and FASTPAC. Staircase efficiency appeared to be lower in SWAP than in W-W perimetry. The benefit-cost ratio was more optimal in W-W perimetry for the FASTPAC strategy than for the Full Threshold strategy ($p=0.014$) and this effect was independent of age ($p=0.649$). For SWAP, the benefit-cost ratio was similar between the two strategies ($p=0.138$) and did not vary with age ($p=0.269$).

4.6.7. Ocular Media Absorption.

Figure 4.15 illustrates the magnitude of ocular media absorption at 440 nm as a function of age. Ocular media absorption increased linearly with increasing age. The group mean ocular media absorption was 6.8 dB (SD 1.42 dB).

4.6.8. Forward Light Scatter.

The magnitude of forward light scatter as a function of age is illustrated in Figure 4.16. There was a weak linear increase in forward light scatter with increase in age. There was high inter-individual variation in forward light scatter, which increased with advancing age.

W-W Perimetry and SWAP

Source	Degrees of Freedom	Sums of Squares	Mean Square	F-Value	p-Value
Subject	50	112255	2245.10	2.48	0.0001
Strategy	1	2139509.64	2139509.64	2364.11	0.0001
Technique	1	86106.14	86106.14	95.15	0.0001
Visit	1	562.19	562.19	0.62	0.4319
Test	1	41.32	41.32	0.05	0.8311
Strategy x Technique	1	1485.45	1485.45	1.64	0.2022
Visit x Test	1	1406.39	1406.39	1.55	0.2145

Threshold Staircase Strategy	W-W Perimetry		SWAP	
	Full Threshold	FASTPAC	Full Threshold	FASTPAC
Group Mean Efficiency (dB ⁻²)	0.0017	0.0025	0.0011	0.0013
Standard Deviation (dB ⁻²)	0.0010	0.0022	0.0008	0.0009

Table 4.9. Benefit-Cost ratios for W-W perimetry and SWAP for the Full Threshold strategy and FASTPAC. Note that the decibel scales between W-W perimetry and SWAP are not compatible.

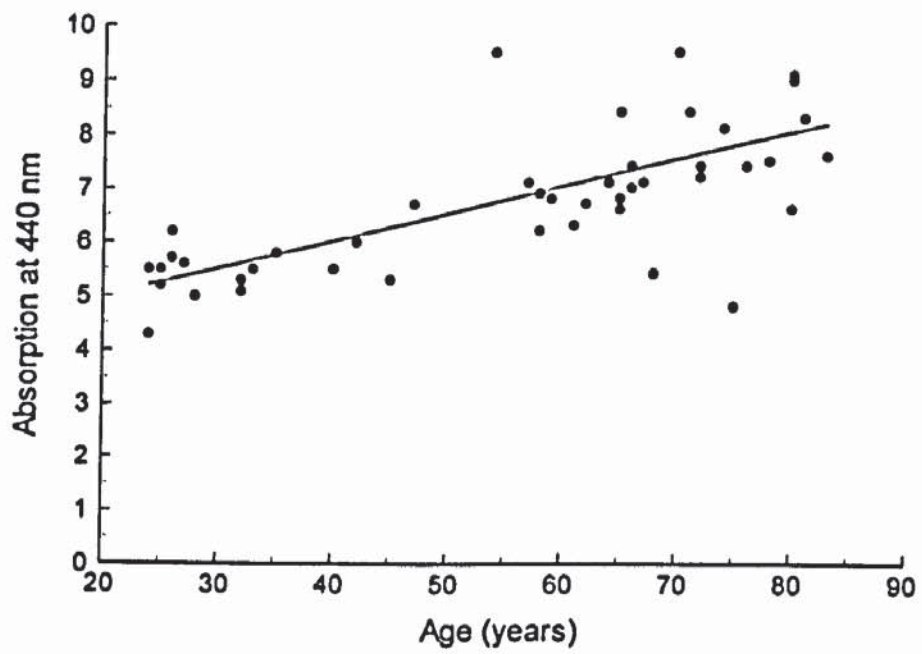


Figure 4.15. Univariate linear regression of ocular media absorption scaled to 440 nm as a function of age.

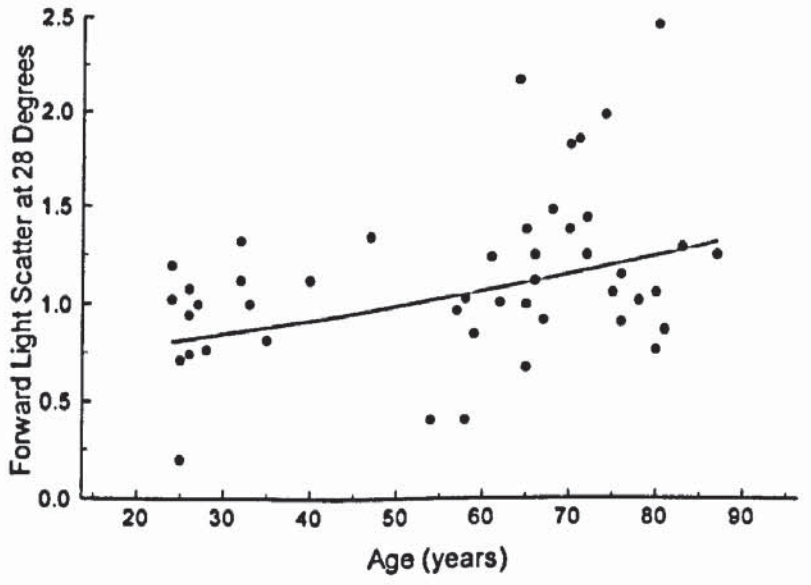
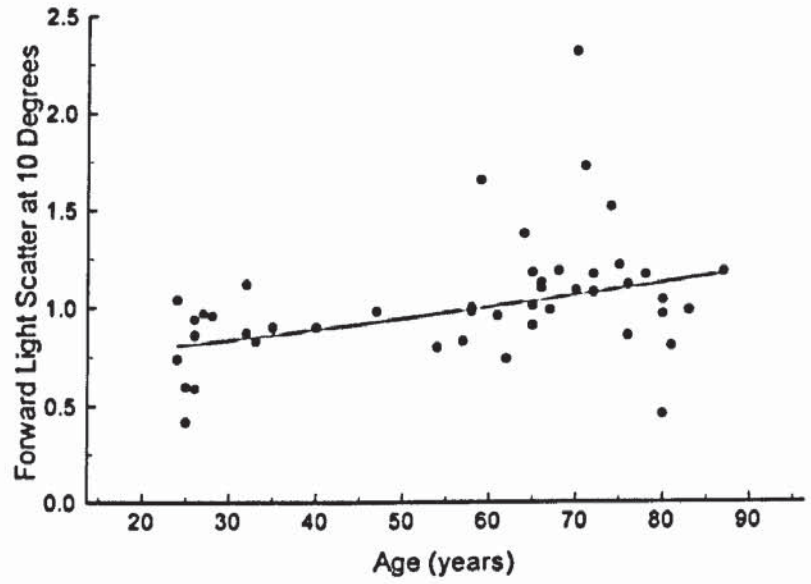
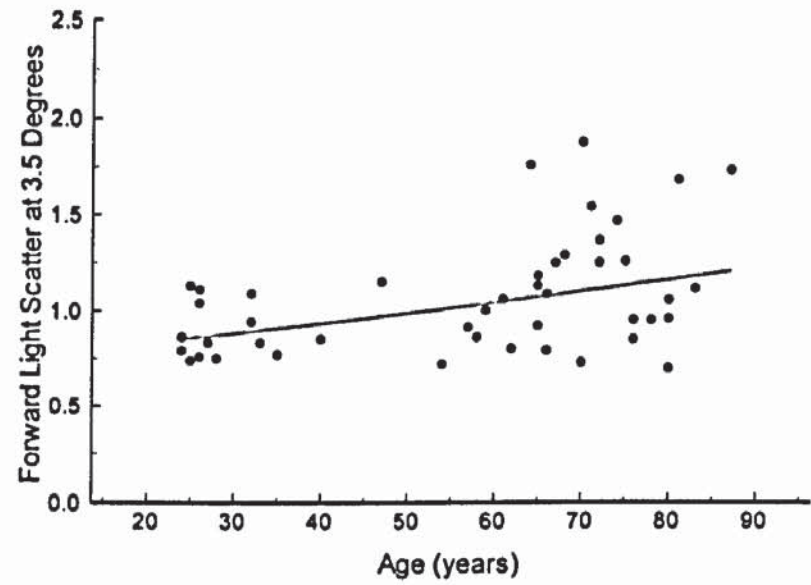


Figure 4.16. Univariate linear regression of forward light scatter as a function of age for the three glare angles investigated (top 3.5°, middle 10°, bottom 28°).

4.7. Discussion.

The similar MS's, increased SF and reduced examination duration for the FASTPAC strategy compared to the Full Threshold strategy in W-W perimetry are comparable with a previous study (Flanagan et al 1993a). The proportionate difference between the two strategies in SWAP for MS and for SF was almost identical to that for W-W perimetry. The apparent increased SF for SWAP compared to W-W perimetry should be approached with caution due to the difference in the respective measurement scales. Nevertheless, when considered in terms of the SWAP scale normalised relative to that for W-W perimetry, the increased magnitude of the SF for SWAP is unequivocal and is in agreement with other studies (Nelson-Quigg et al 1990; Moss et al 1995; Wild et al 1995). The increased SF may be due to the greater physiological variability around the threshold in SWAP; however, the nature of the psychometric function in SWAP has yet to be quantified.

The 15-17% increase in the duration of the SWAP examination together with the increased SF compared to that of W-W perimetry has profound implications for the clinical use of SWAP. The more optimal benefit-cost ratio of the FASTPAC strategy in W-W perimetry has been reported previously (Flanagan et al 1993a) and FASTPAC has been advocated as the strategy of choice in the examination of individuals with a low index of suspicion of field loss (Flanagan et al 1993a). However, in patients with deep visual field loss, the 3dB step single crossing of threshold with FASTPAC may result in an examination time which exceeds that with the 4-2dB staircase of the Full Threshold strategy. For SWAP, there was no difference in the benefit-cost ratio between the two strategies. This indicates that any saving in the examination time is at the expense of an increased short-term fluctuation and vice versa. However, the FASTPAC strategy should still be considered as the strategy of choice with SWAP for the examination of patients with a low index of suspicion of field loss due to the substantial saving of time compared to the Full Threshold strategy. In cases of expected or confirmed visual field loss, the Full Threshold strategy would theoretically be more advisable due to the inherent lower SF but would be susceptible to a greater within- and between-eye fatigue effect resulting from the longer examination time (Hudson et al 1993). The FASTPAC strategy underestimates the

depth and area of field loss compared to the Full Threshold strategy in W-W perimetry and a similar finding may be present for SWAP (Flanagan et al 1993b).

The increase in the number of stimulus presentations and in the SF compared to W-W perimetry suggests that the Full Threshold and the FASTPAC strategies are not the most appropriate staircase design for SWAP. Strategies whereby the step sizes are optimised for the blue-yellow frequency-of-seeing curve may achieve the desired reductions in the number of stimulus presentations and in the SF thereby increasing the staircase efficiency (Nelson-Quigg et al 1990; Weber 1990; Hudson et al 1993; Olsson et al 1994; Weber and Klimaschka 1995). Alternatively, the longer examination time for SWAP may be due to the increased difficulty of the detection task which is more dependent upon the low spatial frequency content of the blue stimulus compared to the high spatial frequency content of the white stimulus. Ganzfeld blankout, induced by the difference in retinal luminance between the occluded and tested eyes (Fur et al 1990; Gur et al 1991) and which is greater in SWAP due to the increased bowl luminance, may further contribute to increased difficulty of the detection task.

The findings for ocular media absorption, if scaled to 450nm, can be compared with those derived from the data of Johnson et al (1988b; 1989) who employed a similar measurement procedure. The value for ocular media absorption at 450nm, extrapolated to an age of 0 years, was 0.30 log units in the current study, compared with approximately 0.23 log units derived from the Johnson data. The similarity of the two values is striking given the differences between the two methodologies in terms of the wavelengths of the scotopic stimuli, the length of the dark adaptation and the inherent large between-individual variation in the derived measure of ocular media absorption interacting with any differences in the characteristics between the two samples. The precise nature of the relationship between ocular media absorption and age is equivocal. The finding of a linear function is in accord with some studies (Werner 1982; Zeimer et al 1987; Savage et al 1993); however, others have described a bi-phasic relationship (Sample et al 1988; Johnson et al 1989b; Cook et al 1994; Delori and Burns 1996). The linear function present in the current study is likely to be due to the exclusion of subjects with nuclear colour and opacity exceeding LOCS grade III.

The magnitude of the decline in W-W MS with increase in age for the Full Threshold strategy lies within the range reported previously for the HFA of 0.6-0.7 dB per decade (Heijl et al 1987a). However, the slopes are less steep than those found by Flanagan et al (1993a) for the FASTPAC and Full Threshold strategies, namely 0.8 dB per decade and 0.9 dB per decade respectively. The magnitude of the age-decline in MS for SWAP is influenced by the transmission characteristics of the blue stimulus filter. A slope of 1.5 dB per decade, which reduced to 1.0 dB per decade following correction for the effects of ocular media absorption, has been found for a broadband stimulus with a dominant wavelength of 470 nm and a slope of 2.2 dB per decade (which decreased to 1.6 dB per decade) for a broadband stimulus with a cut-off at 450 nm. However, these values can only be qualitatively compared due to the differing transmission characteristics of the blue stimulus influencing the ranges of stimulus luminance and hence the dB scale.

The age-decline in W-W sensitivity at each individual stimulus location compares favourably with that of Heijl and colleagues (1987a); the hill of vision declines more rapidly with increase in eccentricity indicating a depression and a steepening of the hill of vision with age. The age-decline for SWAP corrected for ocular media absorption increased with increase in eccentricity and was more pronounced in the superior field, beyond approximately 9° eccentricity, than in the inferior field. The greatest contribution to the decline in perimetric sensitivity with increase in age is thought to be due to decreases in the photoreceptor population, retinal neurones, and retinal pigment epithelial cells (Gao and Hollyfield 1992; Curcio et al 1993; Panda-Jonas et al 1995). Indeed, Panda-Jonas et al (1995) reported a correlation between the decrease in photoreceptors and in optic nerve fibres with increase in age and the age-related decline in W-W perimetric sensitivity. The greater magnitude of sensitivity in the inferior visual field in W-W perimetry and SWAP, may be explained by the greater importance of the inferior visual field to higher order mammals (Lehmann and Skrandies 1979) and the postnatal development of the visual system which adapts to match the occurrence of stimuli to its visual input (Blakemore and Cooper 1970).

A knowledge of the distribution of sensitivity within the normal population at each stimulus locations is a fundamental requirement for the designation of visual field loss in W-W perimetry. The extent of the deviation of the measured sensitivity from the corresponding age-corrected normal sensitivity is compared with the prediction limits for normality and a statistical probability level assigned to the deviation. In the HFA, the probability analysis is weighted for the increase in the deviations which occur with increasing eccentricity (Heijl et al 1987b). The distribution of normal sensitivity for W-W perimetry with the HFA is considered to be non-Gaussian (Heijl et al 1987a,b), and the confidence limits within the STATPAC analytical package are based upon empirically determined values (Heijl et al 1987b). In the current study, the majority of stimulus locations for W-W perimetry also exhibited a negatively skewed non-Gaussian distribution. However, the distribution of normal sensitivity for SWAP without correction for ocular media absorption was Gaussian at virtually all the stimulus locations and the distribution for SWAP with correction, Gaussian at all stimulus locations.

The inherent larger coefficient of variation for SWAP both with and without correction for ocular media absorption, indicates that the deviations from the mean associated with a given level of statistical significance when measured in units of SD are considerably further from the mean in SWAP than in W-W perimetry regardless of whether the distributions are Gaussian or non-Gaussian. This finding has profound implications for the statistical interpretation of the SWAP visual field since the reduction in sensitivity required to indicate abnormality will be proportionately larger for SWAP than for W-W perimetry. As a consequence, field loss for W-W perimetry could conceivably be identified, statistically, prior to the corresponding SWAP deficit.

The reason for the smaller SD's in SWAP for the FASTPAC strategy compared to the Full Threshold strategy is difficult to explain. The finding may well be an artefact secondary to a more pronounced within-test fatigue effect in SWAP than in W-W perimetry for the Full Threshold strategy compared to FASTPAC and to a proportionately greater susceptibility of SWAP to the effects of between-test fatigue.

Correction for ocular media absorption reduces the extent of the normal between-subject variability of SWAP, and hence the magnitude of a given confidence limit, by approximately 10%. However, when considered in terms of the coefficient of variation (Figure 4.8), the reduction is approximately one third.

The increased between-subject normal variability for SWAP might be expected to increase with increase in age due to the greater effects of absorption and of neuronal loss. The SD's for both the Full Threshold and FASTPAC strategies at each stimulus location for W-W perimetry for the 17 subjects aged less than 50 years were approximately distributed in the ratio 2:3 compared to 17 subjects randomly selected from those aged greater than 50 years. The corresponding SD's for SWAP, uncorrected for ocular media absorption, were equivalent between the two groups. However, when corrected for ocular media absorption, the SD's again became approximately distributed in the ratio 2:3 between the two age groups. Correction for ocular media absorption thus reduced the SD of the younger age group rather than that of the older group indicating a greater underlying between-subject variability in the SWAP hill of vision for the older age-group. The importance of the correction for ocular media absorption may be under-emphasised as a result of the restriction of the inclusion criteria in the study to patients with lenticular changes not greater than NCIII, NOIII, CI or PI by LOCS III. Clearly any reduction in the normal between-subject variability arising from the correction of ocular media absorption has to be considered in the context of the clinical viability of the psychophysical measurement technique employed in the study and emphasises the need for a more rapid objective procedure such as that developed by Johnson and colleagues (1993c). One consequence of the lack of correction for ocular media absorption is that a patient with an ocular media clearer than that expected for their age and a normal pattern deviation would be expected to yield a less negative MD_H . A pseudophakic patient with a normal visual field to SWAP may yield a positive MD_H .

The proportionately greater between-subject variability with increase in eccentricity will necessitate the application of a greater weighting function across the field for SWAP than for W-W perimetry. The influence of the larger between-subject variability at the extreme

peripheral locations of the central field in SWAP could also be partially reduced by the use of Program 24-2 which would also simultaneously reduce the examination time.

The wider confidence intervals together with the lower sensitivity in the superior hemifield compared to the inferior hemifield for SWAP may also render the Glaucoma Hemifield Test used in W-W perimetry less appropriate for the identification of focal loss with SWAP. Alternative analyses which use spatial filtering methods to reduce the variability in the visual field and which extract the local spatial variability may assume more importance for SWAP since the techniques do not depend upon a knowledge of normal sensitivity and are responsive to changes in the shape of the hill of vision (Crabb et al 1995; Fitzke et al 1995).

Forward light scatter increased with age and increasing glare angle, findings concordant with other workers (Ijspeert et al 1990; van den Berg 1995). Ijspeert et al (1990) and van den Berg (1995) also found considerable inter-individual variation in the magnitude of forward light scatter, but found a stronger correlation with age than in this study which was probably due to the larger sample sizes in these studies. Forward light scatter induces a veiling glare, reducing the luminance contrast between the stimulus and the background. The attenuation of W-W perimetry arises because light scatter causes the stimulus and background to merge together such that the sharp edges of the stimulus are lost. The SWAP stimulus in addition to the loss in luminance contrast, also exhibits a change in chromaticity towards the yellow background (Moss and Wild 1994). Since forward light scatter increased with age and eccentricity of the glare source, i.e. the stimulus, it may have been a contributory factor to the decline in perimetric sensitivity with age, and the intra-individual decrease in sensitivity with increasing eccentricity.

Lenticular fluorescence may have contributed to an underestimation of the degree of forward light scatter observed in SWAP. Lenticular fluorescence is due to the emission characteristics of fluorophores present in the lens. A blue fluorophore or fluorophores of excitation waveband between 340-360 nm (emission at 420-440 nm), and a green fluorophore or fluorophores of excitation waveband between 420-435 nm (emission at 500-520 nm) have been found in the human lens (Lerman et al 1976). The SWAP stimulus transmits at wavelengths between 410

nm and 450 nm (Figure 4.2) and is likely to have induced lenticular fluorescence with an emission wavelength of 500-520 nm, potentially acting as a source of veiling glare. Since forward light scatter increases with the angle of the glare source, peripheral stimuli in SWAP may have resulted in greater veiling glare than stimuli presented more centrally. The wavelength of the LED's in the forward light scatter meter is 570 (± 30) nm; consequently it may have underestimated forward light scatter in SWAP. The concentration of the lens fluorophores increases with advancing age (Spector et al 1975) and may contribute to the steeper decline in SWAP sensitivity with age.

The greatest decline in sensitivity with age in SWAP was found in the nasal visual field and in particular the superior nasal quadrant. In W-W perimetry the greatest decline in sensitivity was found in the superior temporal quadrant. Their findings are concordant with those of this study. The relatively flattened profile of the SWAP hill of vision paracentrally has been observed previously and can be attributed to further absorption of the SWAP stimulus by the macular pigment (Wild and Hudson 1995). This may be thought of as little importance clinically since the paracentral stimulus locations are of little importance in the detection of glaucoma. However, this finding may be more significant in the investigation of maculopathies using examination grids which evaluate the central ten degrees. The combined effect of ocular media absorption and macular pigment absorption may attenuate the dynamic range of SWAP in elderly patients, or diabetics such that it is not a viable technique in such cases. Furthermore, macular pigment absorption shows considerable inter-individual variability (Pease et al 1987; Werner et al 1987) which may further increase SWAP variability and confound statistical interpretation of the short-wavelength visual field.

4.8. Conclusions.

SWAP is limited clinically by the increased between-subject variability in normal sensitivity, and thus the confidence limits for normality, compared to W-W perimetry. The proportionately greater between-subject variability with increase in eccentricity of SWAP will necessitate the application of a greater weighting function across the visual field than that applied in W-W perimetry. Alternative methods of analysing the SWAP visual field such as spatial filtering

methods which reduce the variability in the visual field and extract the local spatial variability without knowledge of the normal sensitivity may be required (Crabb et al 1995; Fitzke et al 1995).

A reduced number of stimulus locations avoiding those which exhibit high variability may increase the sensitivity and specificity of SWAP, whilst at the same time reducing the examination time and the fatigue effect. The use of Program 24-2 would eliminate many of the peripheral stimulus locations which exhibit high variability and would simultaneously reduce examination time. A reduction in variability in SWAP might be achieved by increasing the stimulus duration from the default 200 ms. It would be expected that increased temporal spatial summation would occur simultaneously increasing the dynamic range of SWAP but would lengthen the examination time. The influence of stimulus duration on SWAP has not been quantified.

Correction of SWAP for absorption of the stimulus by the ocular media is also advisable since the confidence limits for normality are reduced resulting in an increase in specificity and sensitivity of SWAP. Moreover, serial examination with SWAP without correcting for absorption may yield false indications of visual field progression since an increase in absorption is likely to occur with follow-up time. However, the measurement of ocular media absorption requires an additional examination time of approximately one hour. Non-invasive methods of measuring absorption may be appropriate such as the Lens Absorption Monitor (Johnson et al 1993c) and could be incorporated into the design of perimeters. Absorption of the short-wavelength stimulus by macular pigment should be considered when conducting visual field examinations which evaluate the central ten degrees, since further attenuation of the SWAP occurs (Wild and Hudson 1995), thereby reducing the dynamic range of the perimeter.

Because of the longer duration of visual field examination in SWAP, fatigue is more likely to influence the visual field outcome than in W-W automated perimetry. Consequently, the FASTPAC strategy may be more appropriate in SWAP in normal subjects. The advent of new faster strategies may reduce the inter- and intra-test variability of SWAP.

CHAPTER 5. THE INFLUENCE OF EXAMINATION FATIGUE ON SHORT-WAVELENGTH AUTOMATED PERIMETRY.

5.1. Introduction.

The influence of examination fatigue in W-W perimetry was reviewed in Chapter 3. However, the influence of examination fatigue in SWAP is unknown.

It has been suggested that one of the factors contributing to the progressive decline in sensitivity in W-W perimetry is Ganzfeld blackout (Fuhr et al 1990; Hudson et al 1993). This effect describes the loss in visual perception which occurs when a homogenous field is viewed monocularly and is present when the difference in retinal illuminance between the two eyes exceeds approximately 0.75 log units (Bolanowski and Doty 1987). Translucent occlusion minimises Ganzfeld blackout in W-W perimetry (Fuhr et al 1990) but the influence of translucent occlusion on the fatigue effect in SWAP is unknown.

5.2. Aims.

The primary aim of the study was to identify the magnitude and type of examination fatigue present in the normal eye using SWAP. The secondary aim was to evaluate the use of translucent occlusion on any fatigue effect.

5.3. Equipment Modifications.

A translucent occluder was constructed from a CR39 plano lens blank of diameter 70 mm. The lens was cut using a standard lens edging machine into a shape suitable for use as an occluder. Both sides of the lens were then abraded with glass paper until the lens was uniformly opaque. Two holes were then drilled into the surface of the lens to which elastic thread was attached. Silicone padding was attached to the periphery of the occluder to allow adequate clearance of the eye lashes. The translucent occluder is illustrated in Figure 5.1. The homogeneity of the transmittance was verified by measuring the transmission through the occluder when mounted to the HFA using an LMT L1003 spot photometer (LMT Lichtmesstechnik GMBH Berlin, Germany). The luminance of the HFA 640 bowl was

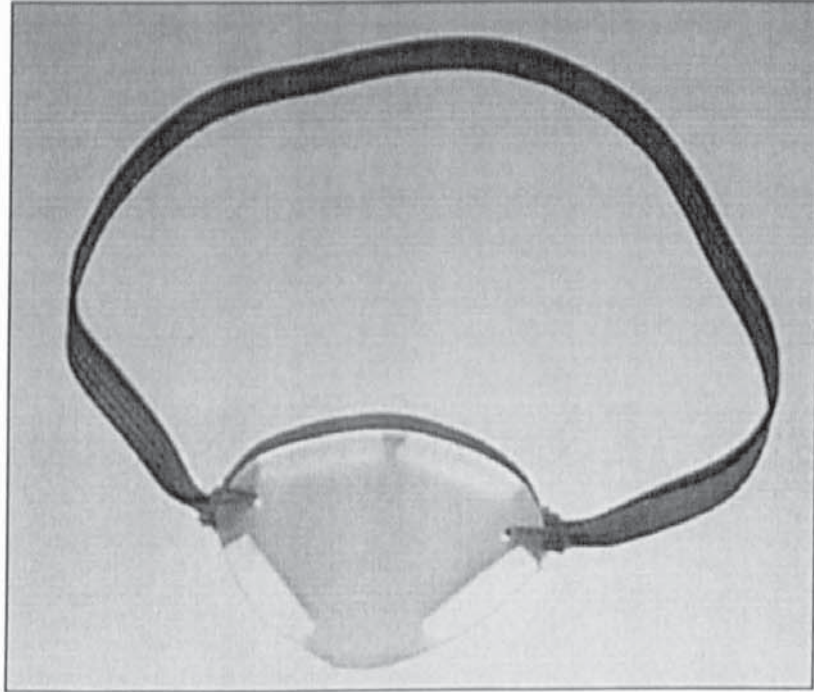


Figure 5.1. The translucent occluder.

measured through the centre of the occluder and two centimetres above, below, left and right of the centre. The occluder produced a 0.66 log unit reduction in light intensity (Figure 5.2.). Scattering of the white Goldmann size III and blue Goldmann size V stimuli by the occluder prevented detection of the maximum stimulus luminance.

5.4. Methods.

The sample consisted of 20 normal subjects of mean age 70.45 years (SD 7.00), with an age range between 58 and 83 years. Nine subjects were male. Subjects met the inclusion criteria described in Section 4.5.1. All subjects were experienced at Full Threshold W-W perimetry and SWAP.

5.4.1. Perimetry.

Perimetry was undertaken using a Humphrey Field Analyser 640 which had been modified using the commercially available upgrade to perform SWAP. Software version 9.31 was used throughout. Each subject was examined using a custom program which consisted of 26 stimulus locations out to an eccentricity of 21° from fixation (Figure 5.3) and the standard 4-2 dB double reversal staircase strategy.

Both eyes were examined at each of four visits, with each visit lasting approximately one hour. The order of the eye examined within a subject was assigned at random and remained constant for all remaining visits. At each visit, either W-W perimetry or SWAP was undertaken, using either the standard opaque occluder or the translucent occluder. The order of type of perimetry was randomised. The near correction, appropriate for the viewing distance of the perimeter fixation target was employed for all perimetry.

Each subject was examined with the custom program three times for each eye. A one minute rest period separated each program (stage) and a five minute period separated eyes. The custom program was designed such that the overall duration of the three examinations would approximate to the duration of Program 30-2. A three minute adaptation period was given before commencement of SWAP to allow for adaptation of the MWS and LWS pathways.

Luminance through the translucent occluder (cdm^{-2}).

	2.15	
2.27	2.12	2.19
	2.21	

Log luminance through the translucent occluder (cdm^{-2}).

	0.33	
0.36	0.33	0.34
	0.34	

Log background luminance of the HFA 640 = 1.00 cdm^{-2}

Log reduction in luminance through the translucent occluder (cdm^{-2}).

	0.67	
0.64	0.67	0.66
	0.66	

Mean log unit reduction in transmission through the translucent occluder = 0.66 log units.

Figure 5.2. Attenuation of the background luminance by the translucent occluder for each of five locations (the centre of the occluder and two centimetres above, below, left and right of the centre).

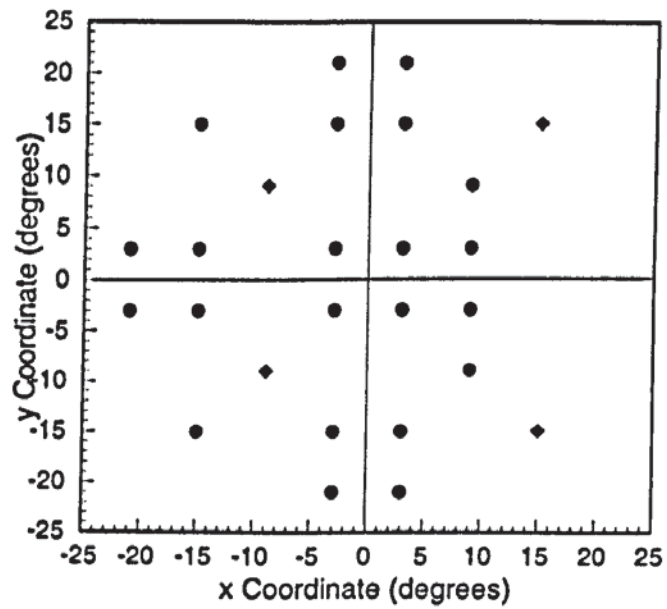


Figure 5.3. The spatial arrangement of the stimulus locations of the custom program (right eye). The diamonds indicate the seed locations.

Where possible, this adaptation period was incorporated into the rest periods introduced into the examination. The subject was instructed to keep both eyes open for the duration of the examination regardless of the type of occluder.

5.5. Results.

The number of fixation losses and false-positive and -negative catch trials were totalled for the three stages in each eye. All W-W and SWAP visual fields were within the reliability criteria of <33% false-positive or negative catch trials. Fixation losses in W-W perimetry were within the reliability criteria of <20% in all subjects. The Heijl-Krakau method of monitoring fixation was found to be ineffectual in five subjects because the default Goldmann size V stimulus could be detected. This was possibly due to light scatter around the stimulus, and/or the ability of the HFA to accurately position the blind spot. In such cases, the blind spot was initially replotted with the default Goldmann size V stimulus. If fixation losses still occurred, the blind spot stimulus was altered to a Goldmann size III. As a result of the erroneously induced false fixation losses, some subjects exceeded the <20% reliability criteria for fixation losses. All subjects though were within the <33% fixation loss reliability criteria proposed by Johnson and Nelson-Quigg (1993). All 20 subjects reported Ganzfeld blankout when the opaque occluder was used, which was not apparent with translucent occlusion. Five subjects reported that wearing the translucent occluder made perimetry more uncomfortable, particularly with SWAP.

5.5.1. Global Mean Sensitivity.

The group mean global MS as a function of stage is illustrated in Figure 5.4 for W-W perimetry and for SWAP. There was a progressive reduction in the magnitude of MS with stage for both W-W perimetry and SWAP which was greater in the second eye. The second eye examined yielded a lower MS than each of the corresponding stages of the first eye examined in W-W perimetry and SWAP. The disparity was more pronounced in SWAP. The introduction of a one minute rest period between stages did not appear to prevent the decline in sensitivity. The introduction of a five minute rest period between eyes elevated sensitivity at the first stage of the second eye relative to the last stage of the first eye investigated.

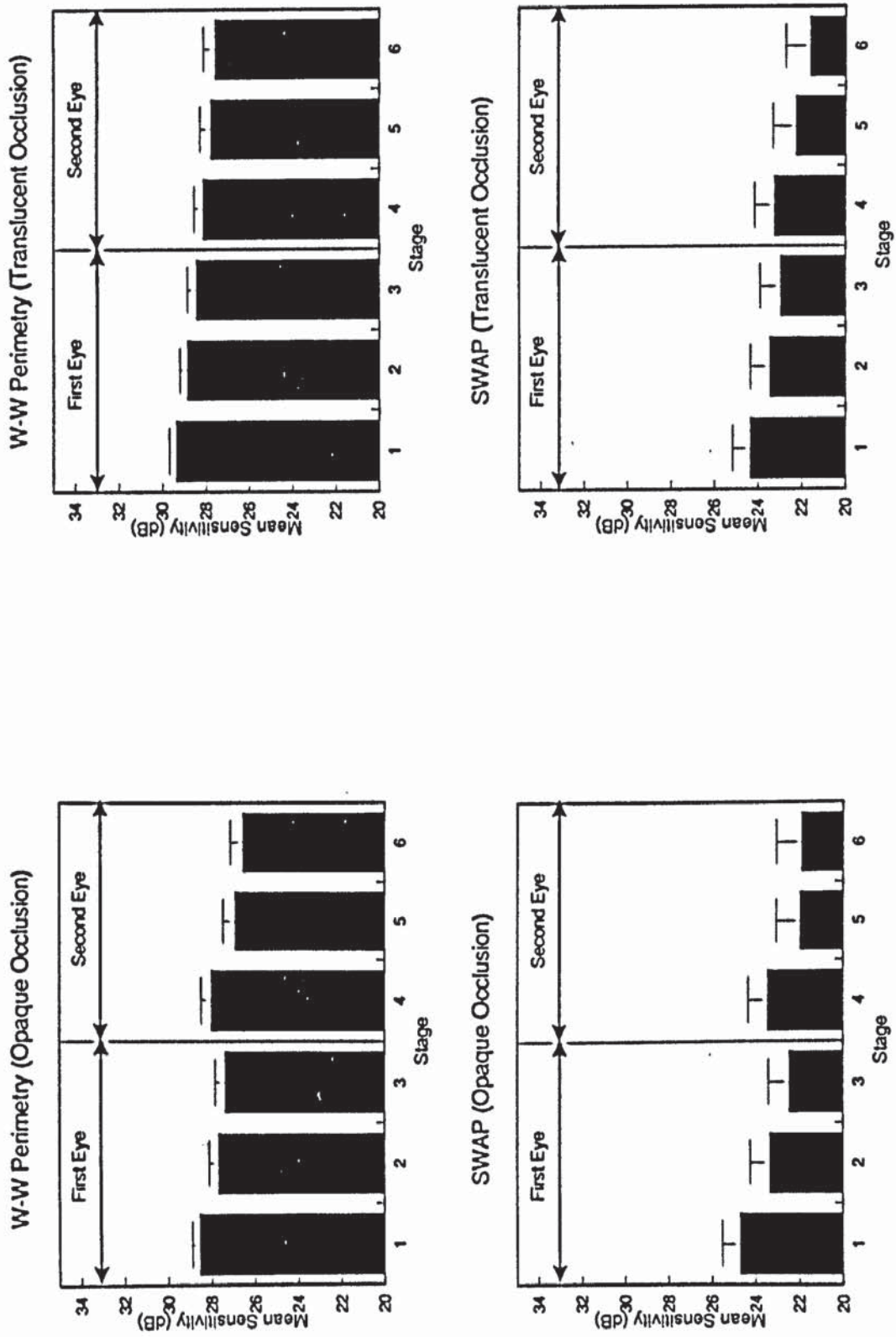


Figure 5.4. Group mean global mean sensitivity as a function of stage for W-W perimetry (top) and SWAP (bottom) with opaque (left) and translucent (right) occlusion. Error bars represent ± 1 standard error of the mean. The vertical line separating stages 3 and 4 delineates examination of the first and second eyes. Note that the decibel scale varies between W-W perimetry and SWAP.

Table 5.1 illustrates the proportionate decrease in global MS from stages 2 to 6, relative to the first stage, and the proportionate decrease in global MS of the latter two stages relative to the first stage of the second eye in both W-W perimetry and SWAP. The reduction was greatest for SWAP regardless of the type of occlusion. The magnitude of the reduction in global MS was greater for the second eye. The proportionate decrease in global MS with stage was greater with opaque occlusion than translucent occlusion for both W-W perimetry and SWAP. The standard error of the proportionate decrease in MS with stage, increased over stage for W-W perimetry and SWAP, regardless of the type of occlusion indicating greater between-subject variation in the tolerance to the fatigue effect.

In order to evaluate further the sensitivity difference between perimetry conducted with opaque occlusion and translucent occlusion, "summation ratios" were calculated by dividing the mean sensitivity with translucent occlusion by the mean sensitivity with opaque occlusion. A "summation ratio" greater than unity indicated that the global MS was greater with translucent occlusion, whilst a value less than unity indicated that global MS was greater with opaque occlusion. Table 5.2 illustrates the group mean "summation ratios" for each stage with W-W perimetry and SWAP.

MS was slightly greater with translucent occlusion than opaque occlusion for all stages, indicating that binocular summation occurred at all stages of the examination. The degree of binocular summation remained relatively constant over all stages of the examination in W-W perimetry and SWAP.

Figure 5.5 illustrates one standard deviation of the group mean sensitivity at each individual stimulus location as a function of stage for W-W perimetry and SWAP. For W-W perimetry and SWAP, the SD's were greatest at the peripheral stimulus locations. The magnitude of the SD's increased as a function of stage and were greatest in the second eye. In W-W perimetry, translucent occlusion generally yielded similar or smaller SD's compared to opaque occlusion, particularly for stages 1 to 3. Conversely, SWAP with translucent occlusion generally yielded similar or higher SD's than SWAP with opaque occlusion.

	Proportionate Decrease in Mean Sensitivity (%) Relative to the First Stage of the First Eye			
	W-W Perimetry (Opaque Occluder)	W-W Perimetry (Translucent Occluder)	SWAP (Opaque Occluder)	SWAP (Translucent Occluder)
Stage 2	3.08 (0.79)	1.72 (0.60)	5.70 (1.53)	3.88 (1.10)
Stage 3	4.13 (0.81)	3.14 (0.66)	11.36 (2.67)	5.99 (1.50)
Stage 4	1.84 (1.11)	4.22 (0.71)	5.01 (1.87)	4.62 (1.54)
Stage 5	5.79 (1.17)	5.47 (0.91)	11.45 (2.56)	8.99 (2.29)
Stage 6	7.11 (1.38)	6.15 (1.24)	11.86 (2.82)	11.79 (2.69)

	Proportionate Decrease in Mean Sensitivity (%) Relative to the First Stage of the Second Eye			
	W-W Perimetry (Opaque Occluder)	W-W Perimetry (Translucent Occluder)	SWAP (Opaque Occluder)	SWAP (Translucent Occluder)
Stage 5	4.01 (0.64)	1.30 (0.73)	6.96 (1.60)	4.69 (1.54)
Stage 6	5.36 (0.95)	2.03 (1.00)	7.44 (1.94)	7.65 (2.15)

Table 5.1. Proportionate decrease in global mean sensitivity (± 1 standard error of the mean), expressed as a percentage, with respect to the first stage of the first eye (top) and with respect to the first stage of the second eye (bottom).

a.) First Eye

Stage	Binocular Summation Ratio W-W Perimetry	Binocular Summation Ratio SWAP
1	1.035 (0.009)	1.010 (0.021)
2	1.106 (0.059)	1.025 (0.029)
3	1.071 (0.023)	1.058 (0.036)

b.) Second Eye

Stage	Binocular Summation Ratio W-W Perimetry	Binocular Summation Ratio SWAP
4	1.017 (0.011)	1.008 (0.023)
5	1.045 (0.010)	1.046 (0.027)
6	1.051 (0.009)	1.028 (0.035)

Table 5.2. Group mean binocular summation ratios (± 1 standard error of the mean) as a function of stage in the first eye (top) and in the second eye (bottom), for W-W perimetry and SWAP.

5.5.2. Central-Peripheral Mean Sensitivity.

Figure 5.7 illustrates the MS for the central and peripheral stimulus locations in the visual field (defined by Figure 5.6). Table 5.3. illustrates the proportionate difference, expressed as a percentage, between the central and peripheral MS as a function of stage for W-W perimetry and SWAP. For all perimetry types, the central MS was greater than the peripheral MS. The proportionate difference between central and peripheral MS increased as a function of stage for W-W perimetry and SWAP, indicating a greater rate of decline in sensitivity at peripheral stimulus locations. Translucent occlusion yielded similar differences between central and peripheral MS compared to opaque occlusion for W-W perimetry and SWAP.

5.5.3. Short-Term Fluctuation.

Unweighted SF was calculated using the four seed locations illustrated in Figure 5.3. Figure 5.8 illustrates the group mean SF as a function of stage for W-W perimetry and SWAP. The magnitude of the SF was generally greater in SWAP than W-W perimetry, regardless of the type of occlusion. The proportionate difference in the SF as a function of stage could not be calculated because several subjects yielded an SF of zero. However, the magnitude of the SF did not appear to alter materially as a function of stage.

5.5.4. Examination Time.

Group mean examination time as a function of stage for W-W perimetry and SWAP is illustrated in Figure 5.9. Table 5.4. illustrates the proportionate difference in the examination time, expressed as a percentage, as a function of stage for W-W perimetry and SWAP. In the first eye, the examination time for W-W perimetry decreased with stage regardless of the type of occlusion. In the second eye, the W-W perimetry examination time increased with stage using opaque occlusion but did not alter materially with stage using translucent occlusion. In SWAP, examination time also increased with stage in the first eye with both opaque and translucent occlusion. In the second eye, the SWAP examination time did not in general alter materially with stage. Examination time with SWAP was longer than W-W perimetry, regardless of the type of occlusion employed. With opaque occlusion, the examination with SWAP was on average 8.7% longer than W-W perimetry, whereas with translucent occlusion,

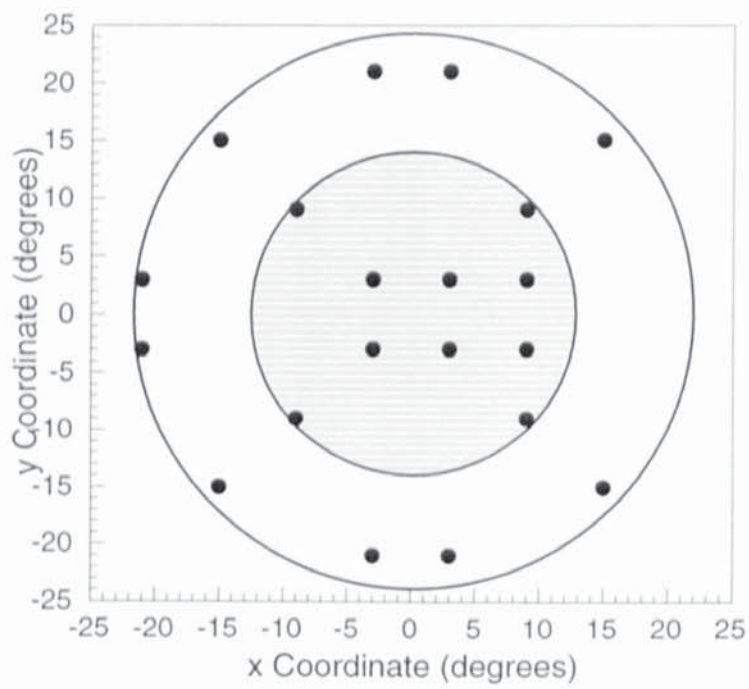


Figure 5.6. Diagram illustrating the spatial arrangement of the division of the visual field into central (inner ring) and peripheral sectors. Note that for the purposes of the calculation, the intermediate stimulus locations were omitted (see Figure 5.3).

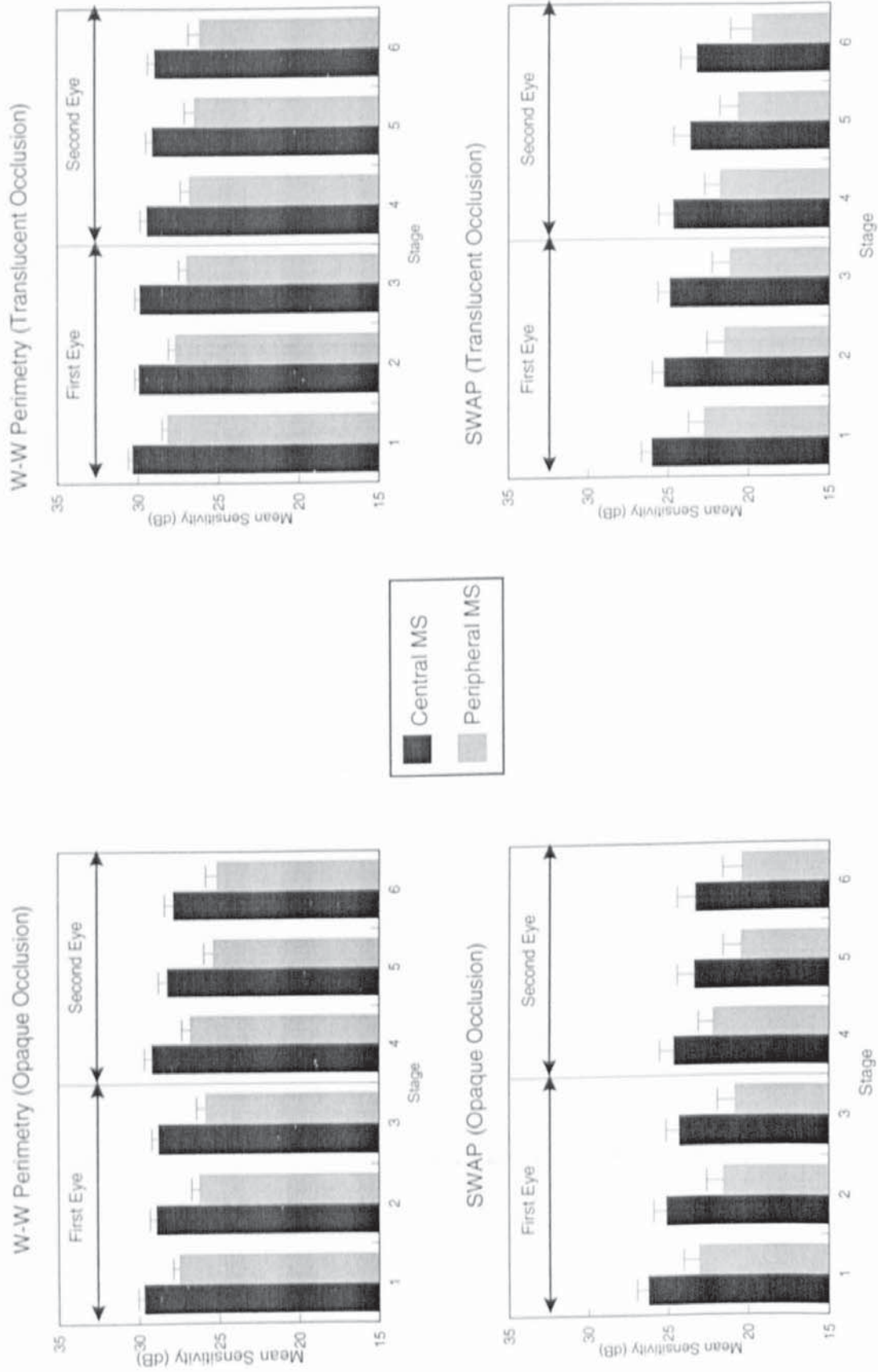


Figure 5.7. Group mean central and peripheral mean sensitivity as a function of stage for W-W perimetry (top) and SWAP (bottom) with opaque (left) and translucent (right) occlusion. Error bars represent ± 1 standard error of the mean. The vertical line separating stages 3 and 4 delineates examination of the first and second eyes. Note that the decibel scale varies between W-W perimetry and SWAP.

Stage	W-W Perimetry (Opaque Occlusion)	W-W Perimetry (Translucent Occlusion)
First Eye		
1	7.34 (0.82)	7.14 (0.69)
2	9.36 (1.12)	7.59 (0.91)
3	10.19 (1.36)	9.80 (1.06)
Second Eye		
4	8.13 (1.47)	8.75 (1.76)
5	10.06 (1.32)	8.97 (1.82)
6	9.76 (1.60)	9.70 (1.85)

Stage	SWAP (Opaque Occlusion)	SWAP (Translucent Occlusion)
First Eye		
1	12.78 (1.69)	13.18 (2.03)
2	14.78 (2.02)	15.74 (2.48)
3	15.13 (2.26)	15.69 (2.41)
Second Eye		
4	10.03 (1.58)	11.40 (2.34)
5	12.64 (2.08)	12.59 (2.42)
6	12.82 (2.07)	15.62 (3.33)

Table 5.3. Percentage decrease of peripheral mean sensitivity compared to central mean sensitivity (± 1 standard error of the mean) as a function of stage for W-W perimetry (top) and SWAP (bottom).

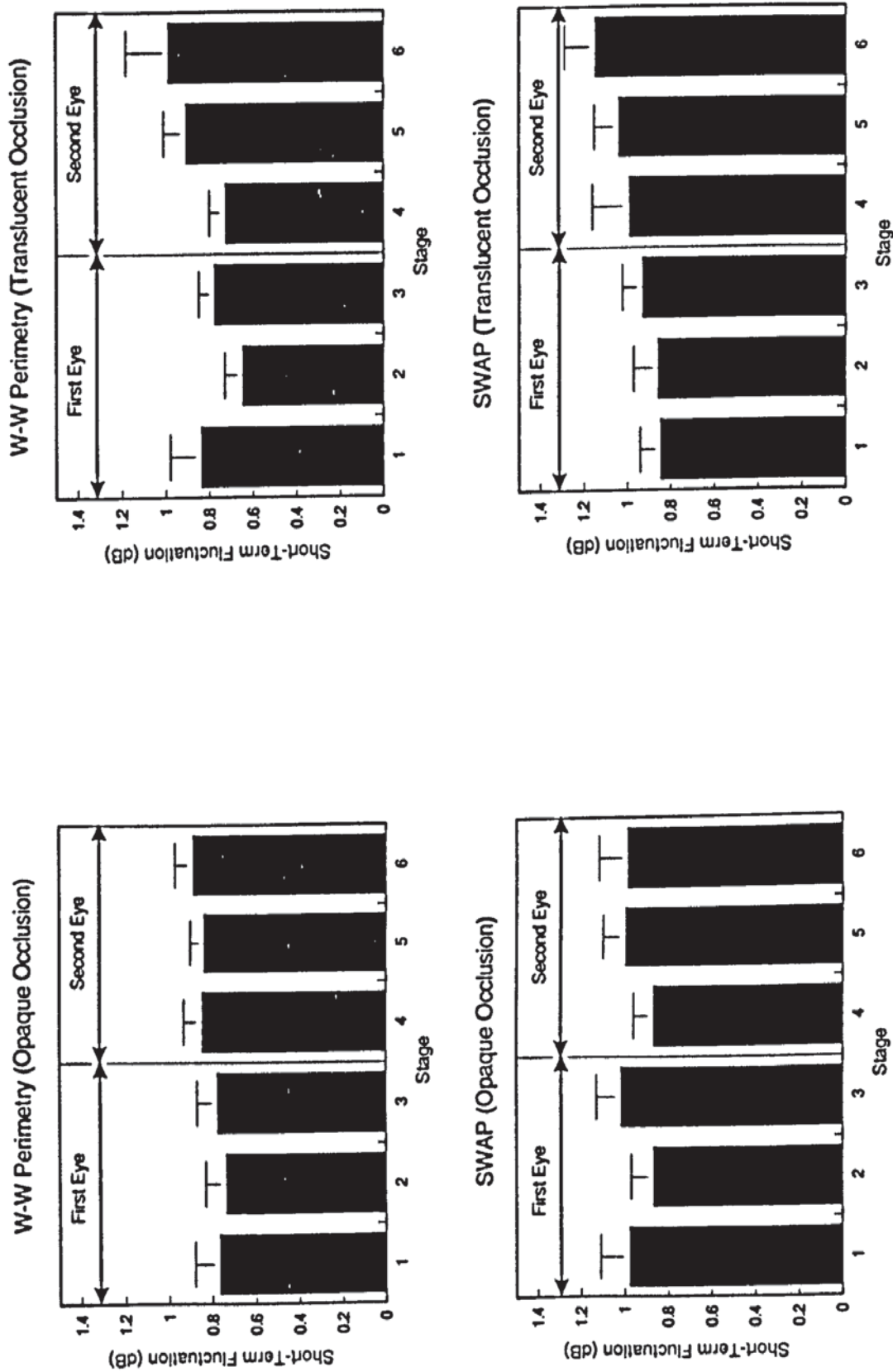


Figure 5.8. Group mean short-term fluctuation as a function of stage for W-W perimetry (top) and SWAP (bottom) with opaque (left) and translucent (right) occlusion. Error bars represent ± 1 standard error of the mean. The vertical line separating stages 3 and 4 delineates examination of the first and second eyes. Note that the decibel scale varies between W-W perimetry and SWAP.

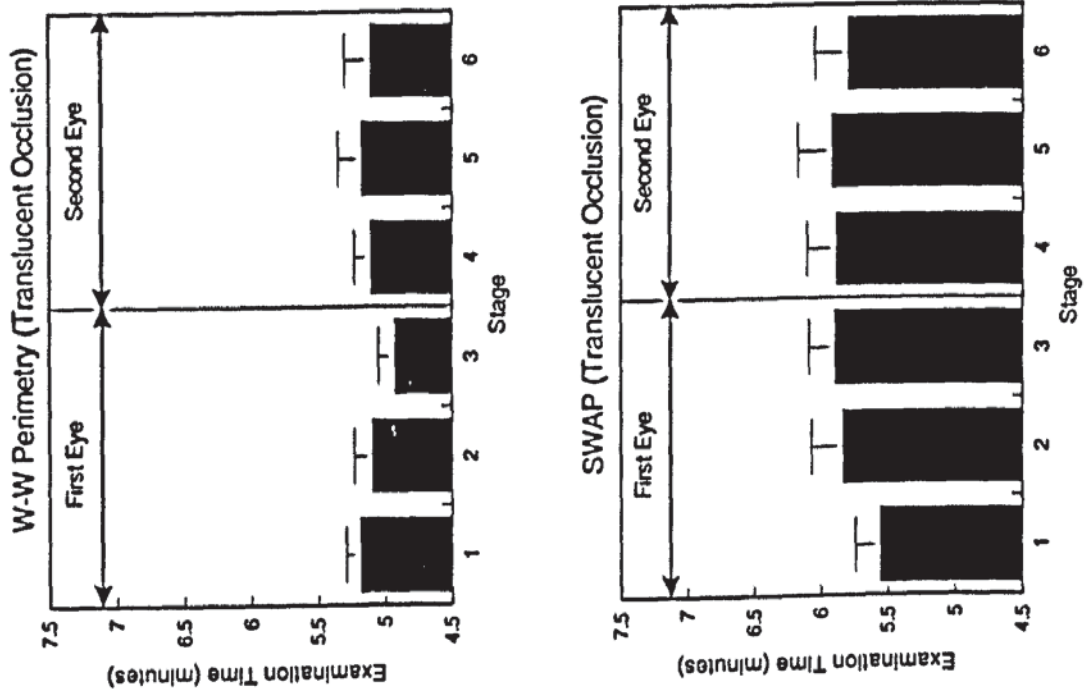


Figure 5.9. Group mean examination time as a function of stage for W-W perimetry (top) and SWAP (bottom) with opaque (left) and translucent (right) occlusion. Error bars represent ± 1 standard error of the mean. The vertical line separating stages 3 and 4 delineates examination of the first and second eyes.

	Proportionate Difference in Examination Time (%) Relative to the First Stage of the First Eye			
	W-W Perimetry (Opaque Occluder)	W-W Perimetry (Translucent Occluder)	SWAP (Opaque Occluder)	SWAP (Translucent Occluder)
Stage 2	-3.81 (4.19)	-1.09 (3.04)	5.18 (4.45)	5.31 (2.95)
Stage 3	-4.72 (4.11)	-4.60 (2.63)	8.95 (3.43)	7.12 (3.47)
Stage 4	-2.65 (3.67)	-1.62 (3.55)	3.62 (4.17)	6.80 (3.45)
Stage 5	2.24 (4.05)	-0.08 (2.87)	6.60 (4.35)	6.81 (3.76)
Stage 6	8.24 (6.77)	-0.71 (4.47)	5.75 (5.55)	5.10 (4.25)

	Proportionate Difference in Examination Time (%) Relative to the First Stage of the Second Eye			
	W-W Perimetry (Opaque Occluder)	W-W Perimetry (Translucent Occluder)	SWAP (Opaque Occluder)	SWAP (Translucent Occluder)
Stage 5	5.59 (3.21)	1.60 (2.88)	3.60 (2.75)	0.86 (3.29)
Stage 6	10.82 (4.47)	0.10 (3.01)	2.86 (4.38)	-1.37 (2.71)

Table 5.4. Proportionate decrease in examination time (± 1 standard error of the mean), expressed as a percentage, with respect to the first stage of the first eye (top) and with respect to the first stage of the second eye (bottom).

the examination time with SWAP was on average 14.1% longer than W-W perimetry. In W-W perimetry, translucent occlusion decreased the examination time compared with opaque occlusion by on average 3.7%. In SWAP, the type of occlusion did not materially influence the examination time.

5.5.5. Stimulus Presentations.

The group mean number of stimulus presentations as a function of stage for W-W perimetry and SWAP is illustrated in Figure 5.10. Table 5.5 illustrates the proportionate difference in the number of stimulus presentations, expressed as a percentage, as a function of stage for W-W perimetry and SWAP. In the first eye, the number of stimulus presentations for W-W perimetry decreased with stage regardless of the type of occlusion. In the second eye, the number of stimulus presentations for W-W increased with stage using opaque occlusion but did not alter materially with stage using translucent occlusion. In SWAP, the number of stimulus presentations increased with stage in the first eye with both opaque and translucent occlusion. In the second eye, the number of stimulus presentations for SWAP did not alter materially with stage. With opaque occlusion, SWAP required a 7.4% greater number of stimulus presentations than W-W perimetry and with translucent occlusion, SWAP required 9.1% more stimulus presentations.

5.6. Discussion.

The results indicate a small, but nevertheless, progressive overall depression of the hill of vision during the course of the examination in W-W perimetry and SWAP which can be attributed to the fatigue effect (Figure 5.4 and Table 5.1). The results for W-W perimetry are in agreement with other studies (Heijl and Drance 1983; Langerhorst et al 1987; Johnson et al 1988a; Searle et al 1991; Hudson et al 1993). The rate of decline in sensitivity over stage was greater in SWAP than in W-W perimetry and can be attributed to the increased duration of SWAP. The greater decrease in the peripheral MS compared to the central MS as a function of stage in W-W perimetry and SWAP, indicated that a steepening in the hill of vision also occurred as a result of the fatigue effect (Table 5.3). The steepening of the hill of vision for W-W perimetry is in agreement with the results of Johnson et al (1988a) who reported that the

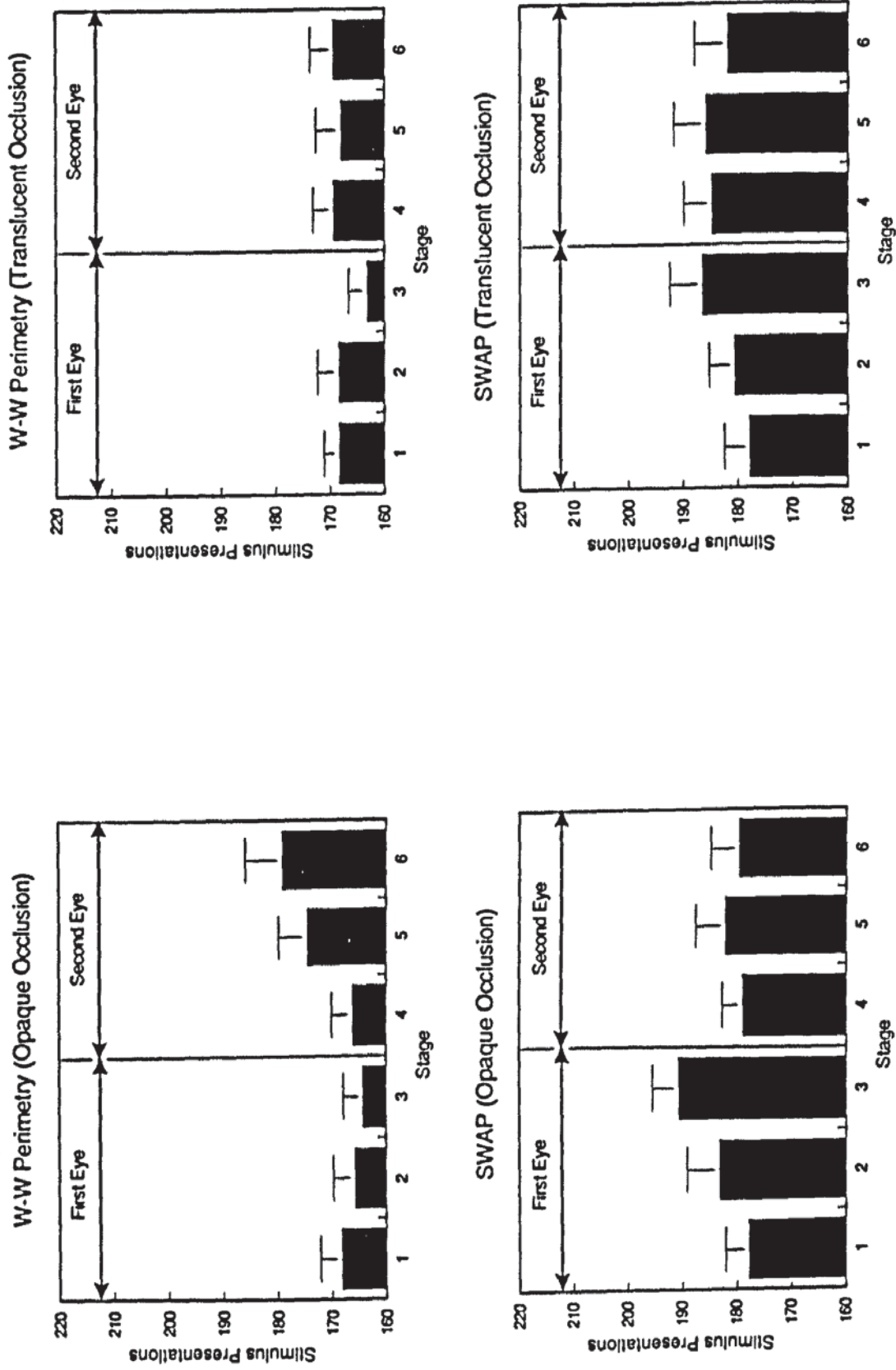


Figure 5.10. Group mean number of stimulus presentations as a function of stage for W-W perimetry (top) and SWAP (bottom) with opaque (left) and translucent (right) occlusion. Error bars represent ± 1 standard error of the mean. The vertical line separating stages 3 and 4 delineates examination of the first and second eyes.

	Proportionate Difference in the Number of Stimulus Presentations (%) Relative to the First Stage of the First Eye			
	W-W Perimetry (Opaque Occluder)	W-W Perimetry (Translucent Occluder)	SWAP (Opaque Occluder)	SWAP (Translucent Occluder)
Stage 2	-0.87 (2.67)	0.53 (2.76)	3.71 (3.56)	1.93 (2.30)
Stage 3	-1.61 (2.69)	-2.78 (2.18)	7.83 (2.66)	5.32 (2.97)
Stage 4	-0.62 (2.51)	-0.69 (1.76)	1.54 (2.93)	4.66 (3.13)
Stage 5	3.94 (2.55)	0.06 (2.68)	2.95 (3.15)	4.78 (2.92)
Stage 6	7.19 (4.59)	1.07 (2.75)	1.60 (2.94)	2.92 (3.70)

	Proportionate Difference in the Number of Stimulus Presentations (%) Relative to the First Stage of the Second Eye			
	W-W Perimetry (Opaque Occluder)	W-W Perimetry (Translucent Occluder)	SWAP (Opaque Occluder)	SWAP (Translucent Occluder)
Stage 5	5.22 (2.58)	-0.39 (2.45)	1.85 (2.29)	1.16 (3.15)
Stage 6	8.00 (3.64)	0.38 (2.09)	0.77 (2.78)	-1.29 (2.63)

Table 5.5. Proportionate decrease in the group mean number of stimulus presentations (± 1 standard error of the mean), expressed as a percentage, with respect to the first stage of the first eye (top) and with respect to the first stage of the second eye (bottom).

greatest reduction in sensitivity occurred between 15 and 20 degrees eccentricity. Similarly, Hudson et al (1993) reported that in normals and ocular hypertensives, the greatest reduction in sensitivity was observed in the superior and nasal visual field. The influence of a one minute rest between stages and a five minute rest between eyes did not eliminate the fatigue effect. The transfer of the fatigue effect to the second eye has been reported previously (Searle et al 1991; Hudson et al 1993).

Searle et al (1991) and Hudson et al (1993) hypothesised that Ganzfeld blankout may be the principle contributory factor to the fatigue effect. This hypothesis is supported by the reduction in the decline in MS with stage when using translucent occlusion for both W-W perimetry and SWAP. The contribution of Ganzfeld blankout to the fatigue effect appeared to be uniform across the visual field because the difference between the central and peripheral MS's was not influenced by the type of occlusion. Translucent occlusion reduced the magnitude of the decline in sensitivity with stage rather than eliminate it. Other factors such as psychological and physical fatigue are therefore likely to be additional components of the fatigue effect. The fatigue effect was greater in SWAP than W-W perimetry, even after Ganzfeld blankout was prevented with translucent occlusion. Ganzfeld blankout is thought to derive from binocular rivalry which is considered to be cortical in origin (Blake and Overton 1979; Blake 1989). Although the translucent occluder prevented detection of the stimulus by the occluded eye, vision was considered binocular because simultaneous vision occurred. The degree of binocular rivalry is influenced by the difference in retinal luminance between the two eyes (Bolanowski and Doty 1987). Employing the standard opaque occluder, the difference in retinal illuminance between the two eyes was greater in SWAP than in W-W perimetry and would therefore be expected to induce greater Ganzfeld blankout. Bolanowski and Doty (1987) and Fuhr et al (1990) reported that Ganzfeld blankout was eliminated when the difference in retinal illuminance was less than 0.75 log units. The increase in mean sensitivity with translucent occlusion can be explained by summation in the visual pathway; such a concept has been reported previously (Fuhr et al 1990; Pardhan 1997).

Translucent occlusion reduced the between-subject variability for W-W perimetry but increased the between-subject variability of SWAP (Figure 5.5). The increase in the between-subject variability for SWAP may have resulted from the increased background luminance relative to W-W perimetry. Indeed, several subjects reported that the translucent occluder made SWAP more uncomfortable. The perceived increase in luminance of the SWAP background may have resulted in an increased veiling glare and consequent reduction in the visibility of the stimulus, thereby increasing between-subject variability. The reduction in the fatigue effect with translucent occlusion supports the conclusion that this type of occluder should be employed for W-W perimetry and SWAP. However, this finding should be approached with caution because the increased sensitivity with translucent occlusion may influence statistical analysis of the visual field in terms of the MD_H and the total deviation plot. In W-W perimetry, the current STATPAC database was derived using opaque occlusion. In SWAP, the increase in normal sensitivity using translucent occlusion would effectively increase the dynamic range of SWAP because the higher sensitivity would increase the range of useable stimulus luminances. Nevertheless, the generally increased magnitude of the SD's in SWAP using translucent occlusion (Figure 5.5) suggests greater between-subject variability. Therefore, the advantage of increased dynamic range in SWAP would be negated by the greater confidence levels defining visual field abnormality, and by the longer examination time.

5.7. Conclusions,

The fatigue effect in SWAP was greater than W-W perimetry and resulted both in a progressive overall depression and a steepening of the hill of vision. Translucent occlusion was shown to reduce the fatigue effect and the between-subject variability in W-W perimetry but currently, should not be advocated for routine use in perimetry because of the implications for the delineation of visual field abnormality. The increase in the between-subject variability of SWAP with the translucent occluder together with the increased examination time outweighs the advantages of a reduction in the fatigue effect and an increased dynamic range. Therefore, translucent occlusion could not be advocated for SWAP. Translucent occlusion does not eliminate the fatigue effect in W-W perimetry or SWAP. Other approaches to reducing the components of fatigue must remain paramount in visual field investigation. Shorter staircase

strategies which reduce the overall examination time without loss of accuracy would obviously be useful in this respect. In addition, the new SITA strategies (Bengtsson et al 1997) which use mathematical approaches to adjust the thresholds obtained in the latter stages of a visual field examination could be modified to account for the influence of fatigue.

CHAPTER 6. THE INFLUENCE OF AGE-RELATED CATARACT ON SHORT-WAVELENGTH AUTOMATED PERIMETRY.

6.1. Introduction.

Cataract is the commonest cause of age-related vision loss in the world (Kupfer 1984; Klein and Klein 1982). Estimates of the incidence of cataract vary due to differences in examination techniques, sample characteristics, and decisions relating to the definition of cataract. Hirvelä et al (1995) found an incidence of 64.4% of a population between the ages of 70 and 95 years. Klein and co-workers (1992) reported an incidence of 47% between the ages of 43 and 84 years with a greater prevalence in females.

6.2. The Normal Human Lens.

The lens is a transparent avascular biconvex structure, enclosed by an outer elastic basement membrane called the capsule. A single layer of epithelial cells is attached to the anterior surface of the capsule as far as the equator. Equatorial cells undergo mitosis and the resultant cells (lens fibres) elongate, passing anteriorly between the epithelium and previous layers of cells, and posteriorly along the inner surface of the posterior capsule. Cell division forces older lens fibres inwards towards the lens nucleus. The newer lens fibres constitute the cortex. As the lens fibres proceed towards the nucleus they gradually lose their nuclei, mitochondria, and other intracellular organelles.

Biochemically the lens is dehydrated and contains approximately 66% water and 33% protein. Eighty-five percent of the proteins are water soluble consisting of α -crystallin (15%), β -crystallin (55%), and γ -crystallin (15%). The high protein concentrations of uniform distribution within the lens fibres yields a high refractive index. α -crystalline is thought to be involved in the transformation of epithelial cells into lens fibres (Delcour and Papacontstantinou 1972). The remaining insoluble proteins derive from cytoskeletal material and plasma membranes, also called albuminoid (Cotlier 1987).

The lens contains higher concentrations of K^+ ions and lower concentrations of Na^+ , and Cl^- ions than the surrounding aqueous and vitreous humours. Electrolytic balances are principally maintained by the high negative resting membrane potential of the lens which is approximately -75 mV. The resting membrane potential maintains high concentrations of K^+ and Cl^- ions within the lens. Na^+ ions are continually diffusing down a concentration gradient from the surrounding aqueous and vitreous into the lens. Na^+ is actively extruded by a Na^+-K^+ pump regulated by the enzyme $Na^+,K^+-ATPase$ found in the epithelial cells. The energy requirements of the lens are derived from glucose which diffuses into the lens from the surrounding aqueous and vitreous. Due to the lack of cellular organelles within the cortex and nucleus only a small portion of respiration occurs via the Krebs cycle, hexose monophosphate shunt, oxidative phosphorylation and the sorbitol pathway. The principle metabolic requirements of the lens are met by the Embden-Meyerhof pathway (glycolysis), accounting for approximately 70% of lens metabolism (Cheng and Chylack 1984).

6.3. Lens Transparency,

The tightly packed cellular structure, combined with the lack of intracellular organelles and regular arrangement of the lens fibres mediates lens transparency. The lack of birefringence in the lens indicates a lack of optical anisotropy (Bettleheim 1975). Maurice (1957) developed a theory for corneal transparency in which light passes through the regular lattice structure of the stroma causing diffraction. Diffracted light rays interfere by destructive interference allowing undiffracted rays to pass through unhindered. The model of corneal transparency can be applied to the lens since it is composed of a regular arrangement of lens fibres. Goldman and Benedeck (1967) showed that for diffraction to occur, it is only necessary for the collagen fibres of the cornea (or protein molecules in the lens) to be separated by a distance which is small compared to the wavelength of light.

6.4. Ageing of the Human Lens,

Studies using Scheimpflug slit-lamp photography show that the lens becomes thicker sagittally with advancing age as a result of an increase in cortical width (Brown 1974). In latter life, the cortex represents approximately one third of the total lens thickness (Davson 1991). The

difference between the visible light energy incident on the lens and that which is transmitted is termed extinction (Trokel 1962). Light energy may be lost by absorption and scatter (Figure 6.1). Light scatter may be sub-divided according to the direction of scatter; backward and forward. Changes in light transmittance and light scatter occur with advancing age. Cataract may therefore, be considered as an acceleration of the ageing process.

6.4.1. Lens Transmission.

Spectral transmission in the human crystalline lens is non-uniform in the visible spectrum due to the presence of a water soluble yellow pigment with absorption maxima at 365 and 260 nm (Cooper and Robson 1969). This results in preferential absorption of short wavelengths (Weale 1954). The reduction in transmission primarily occurs at wavelengths below 450 nm (Said and Weale 1959; Norren and Vos 1974; Beems and van Best 1990; Savage et al 1993; Delori and Burns 1996).

Direct spectrophotometry measurements of crystalline lens transmission have been made on excised lenses (Boettner and Wolter 1962; Weale 1954; 1988; Mellerio 1971; 1987). Lenticular fluorescence has also been employed to estimate ocular media absorption (Zeimer and Noth 1984; Zeimer et al 1987; Teesalu et al 1997). This method assumes that there is a direct relationship between crystalline lens fluorescence at the posterior and anterior poles for fluorescence excited at approximately 460 nm and emitted at approximately 530 nm. This posterior-anterior fluorescence ratio has been directly correlated with spectrophotometry measurements of excised lenses (Zeimer et al 1987).

The disadvantage of analysing human-eyes in-vitro is that post-mortem changes to the crystalline lens may occur which influence measurement. In-vivo measurements of transmission are preferable, and facilitate greater sample sizes, but generally are only able to assess the ocular media as a whole. However, the contribution of the cornea and aqueous and vitreous humours is considered to be small in comparison to the contribution from the crystalline lens (Boettner and Wolter 1962; Alpern et al 1965; Ruddock 1972; Wyszecski and Stiles 1982; Weale 1992; Beems and van Best 1990).

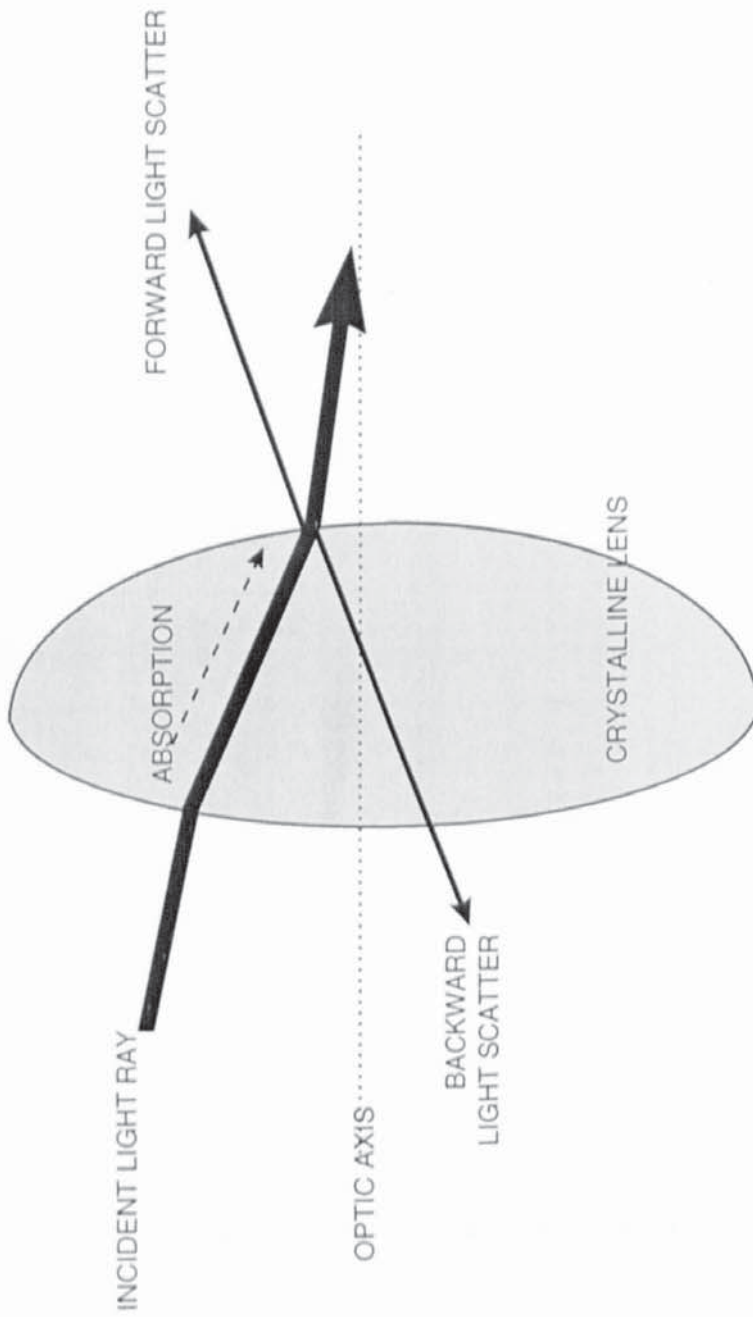


Figure 6.1. Diagram illustrating the sources of light loss in the crystalline lens.

Various psychophysical methods have been devised to assess ocular media absorption. Wright (1951), Weale (1954) and Werner and Hardenbergh (1983) estimated crystalline lens density from comparisons of phakic, pseudophakic and aphakic eyes. Alpern et al (1965) measured the fundus reflectance at chorioretinitis scars which were devoid of significant choroidal pigment. Werner (1982) assessed ocular media absorption by subtraction of the log scotopic spectral sensitivity function from the human rhodopsin absorption spectrum. The spectral sensitivity function was derived from visually evoked cortical potential amplitudes and thus enabled measurement of lenses between the ages of one month and 70 years. A psychophysical matching procedure using a bipartite field was employed by Coren and Girgus (1972) and Savage et al (1993).

Tan (1971) compared scotopic sensitivity as a function of wavelength with the rhodopsin spectrum in normal and aphakic observers. Differences in the sensitivity spectra between the two groups were attributed to the optical density of the crystalline lens. Norren and Vos (1974) suggested a method for measuring ocular media absorption using the CIE rhodopsin spectrum and derived a lens density spectrum for the standard observer. Ocular media absorption can be assessed by determining scotopic sensitivity to two narrowband wavelengths which are equally absorbed by rhodopsin (400 nm and 565 nm, 410 nm and 561 nm, or 390 nm and 568 nm). Any difference in sensitivity can be attributed to ocular media absorption. The technique of Norren and Vos has been applied to the Tübinger perimeter (Johnson et al 1988b, 1989, 1993; Adams et al 1991; Lewis et al 1993) and the Humphrey Field Analyser (Sample et al 1986; 1988; 1989; 1993; Sample and Weinreb 1989, 1990, 1992; Weinreb and Sample 1991; Hudson and Wild 1993; Moss et al 1995) and has become the standard method of assessing ocular media absorption in SWAP. The procedure applied to the Humphrey Field Analyser is described more fully in Section 4.5.3.

Said and Weale (1959) assessed ocular media absorption by measuring the intensity of the 3rd and 4th Purkinje images for a series of wavelengths. This involved densitometric analysis of photographic plates and was therefore time consuming. Johnson et al 1993c; Nelson-Quigg et al 1994) adapted this technique in the Lens Absorption Monitor (LAM) which enabled objective

measurement of the spectral transmission of the ocular media in approximately two seconds. An intensified charged coupled device (ICCD) video camera measured the intensity of the 4th Purkinje image at different narrowband wavelengths (410, 420, 430, 450, 470, 500, 530, and 550 nm). Rapid sampling of the image at 60 Hz minimised intensity variations in the image induced by head movements. Johnson and co-workers (1993c) compared the LAM procedure with two psychophysical measurement techniques; the difference in scotopic sensitivity method applied in the Tübinger perimeter and the bipartite field matching procedure of Savage et al (1993). The LAM demonstrated greater test-retest reliability than the psychophysical techniques but yielded lower estimates of lens density. These differences were possibly due to the influence of pupil size, since each of the techniques investigated employed different light adaptation conditions and did not control for pupil size.

Weale (1971) considered the increase in optical density of the crystalline lens with increase in age to result from an increase in the total lens thickness since little change in the photometric density per unit-pathlength of the lens was observed. Spector et al (1975) isolated an age-dependent polypeptide which was associated with increasing yellow pigmentation in the lens. The increase in lens yellowing with advancing age was proposed as the cause of decreased lens transmittance. Indeed, Lutze and Bresnick (1994) found increased ocular media absorption in a group of diabetic patients with increased yellowing of the lens compared to normal controls. Nevertheless, Mellerio (1987) found no increase in light loss in the cortex with age but an increase in light loss per unit-pathlength. With advancing age, the cortex increases in thickness (Brown 1974) and the light loss only occurs because of this change in thickness. In the nucleus, the pathlength does not increase with age. Therefore, Mellerio concluded that the increase in lens density is due to the increased pathlength and not due to pigment accumulation. Crystalline lens fluorescence may also be associated with decreased lens transmission with age. Lerman and Borkman (1976) described two age-related compounds which developed in the lens nucleus. The first absorbed light between 340 and 360 nm and the second, which appeared after the first decade of life, absorbed light between 415 and 435 nm. The second compound had an emission at 500 to 520 nm and was thought to contribute to lenticular brunescence in advanced nuclear cataracts. Teesalu et al (1997) determined a lens

transmission index from the ratio between posterior and anterior autofluorescence peaks and reported a significant linear correlation of mean sensitivity in SWAP in normals.

The increase in the optical density of the crystalline lens with advancing age is undisputed. Large inter-individual variations in the magnitude of ocular media absorption have been observed within a given age and as a function of increasing age (Coren and Girgus 1972; Werner 1982; Sample et al 1988; Hudson and Wild 1993; Johnson et al 1993c; Savage et al 1993; Cook et al 1994; Delori and Burns 1996; Teesalu et al 1997). As much as one log unit of variation for a given age has been observed by some workers (Boettner and Wolter 1962; Johnson et al 1993c). Furthermore, differences between magnitudes of ocular media density may be due to differing methodologies between studies. These differences may be attributed to the large inter-individual variation in optical density (Werner 1982; Johnson et al 1993c) but may also be influenced by the interaction of pupil size with optical pathlength through the lens. Weale (1992) proposed that greater ocular media absorption would be observed in subjects with small pupil sizes since light would pass through relatively thicker regions of the crystalline lens. Nelson-Quigg et al (1994) reported that pupil size influenced measurement of ocular media absorption using the Lens Absorption Meter. The measurement of ocular media absorption using the difference in scotopic sensitivity technique in the Humphrey Field Analyser is not thought to be influenced greatly by pupil size. Sample et al (1988) calculated that a 0.06 log unit increase in ocular media absorption would result from a reduction in pupil diameter from 7 mm to 2 mm.

The exact nature of the increase in lenticular optical density is equivocal. A linear increase in the optical density of the crystalline lens has been proposed by Said and Weale (1959), Ruddock (1965), Mellerio (1971; 1987), Werner (1982; 1988) Zeimer et al (1987), Savage et al (1993) and Teesalu et al (1997). Conversely, a non-linear increase in optical density with age has been proposed (Coren and Girgus 1972; Pokorny et al 1987; Sample et al 1988; Johnson et al 1988b; Johnson et al 1993c; Hudson and Wild 1993; Cook et al 1994; Delori and Burns 1996). Sample et al (1988) demonstrated a non-linear optical density beyond the age of 70, but a number of patients with cataract were included in the sample. Similarly, Pokorny et al

(1987) found two slope functions describing the change in optical density with age; one function describing the relationship between 20 and 60 years and the other greater than 60 years:

20-60 years

$$T_L = T_{L_1}[1 + 0.02(A - 32)] + T_{L_2} \quad \text{Eqn 6.1}$$

>60 years

$$T_L = T_{L_1}[1.56 + 0.0667(A - 60)] + T_{L_2} \quad \text{Eqn 6.2}$$

where A is the subject's age and T_L is the total lens transmission function; T_{L_1} is the portion of lens transmission which is unstable after the age of 20; T_{L_2} is the portion of the total lens transmission which is stable after the age of 20. Pokorny and co-workers (1987) suggested that the component T_{L_1} was influenced by the age of the observer and the component T_{L_2} was not influenced by age. Tan (1971) also suggested that the crystalline lens spectral optical density function was influenced by two factors. The first resulted in an increase in optical density at ultra-violet wavelengths and was attributable to an increase in cellular material within the lens as a consequence of growth. The second factor increased optical density as a result of increased yellowing of the lens with increasing age.

6.4.2. Backward Light Scatter.

Backward light scatter may be assessed using objective or subjective methods. Wolf and Gardiner (1965), Siegelman et al (1974). The Scheimpflug slit-lamp method of assessing backward light scatter uses densitometric analysis of a photographically documented section of the crystalline lens (Sasaki et al 1992; Khu and Kashiwagi 1993). The Scheimpflug system has been utilised in the quantification of the influence of lens opacity on the conventional W-W visual field (Guthauser et al 1987).

The Interzeag Opacity Lens Meter (OLM) 701 was developed by Flammer and Bebié (1987) with the specific aim of measuring the influence of cataract on the visual field. A modulated 1.5

mm diameter light beam of 700 nm is pulsed for 500 ms on the crystalline lens and is back scattered in all directions. The amount of red light reflected back into a detector is analysed and expressed as a numeric output on a scale from 0 to 100 with an increasing number denoting greater opacity. The measurement is dependent upon the degree of pigmentation of the fundus, non-Caucasian subjects yielding lower scores than Caucasian subjects (Elliott and Hurst 1989). Furthermore, measurement in subjects with a pupil diameter of less than 4 mm may reduce the efficacy of the instrument due to absorption of the scattered light by the iris (Clarke et al 1990). Elliott and Hurst (1989) reported a high correlation between Logmar visual acuity and the OLM in normal eyes and nuclear cataracts.

Subjective measures of backward light scatter entail assessing the appearance of the crystalline lens using a slit-lamp-biomicroscope. In the Lens Opacities Classification System II (LOCS II) the slit-lamp appearance of the crystalline lens is compared with a photographic reference sheet enabling grading of nuclear status (five categories), cortical status (seven categories), and posterior sub-capsular status (seven categories) (Chylack et al 1989). LOCS II shows high intra-observer agreement (Chylack et al 1989) and is capable of detecting progressive changes in lens opacity (Maraini et al 1989; Magno et al 1993). However, for posterior sub-capsular opacities misclassification often occurs, particularly as the existence of coexisting opacities increases (Maraini et al 1989). The Lens Opacities Classification System III (LOCS III) developed by Chylack and co-workers (1993a) aims to overcome the limitations of LOCS II: namely, the small, and therefore coarse, scale for nuclear colour (NC); the under representation of the early stages of nuclear opalescence (NO) and posterior sub-capsular cataract (P); the unequal scaling intervals between each of the cataract grades; the lack of standardisation of colour grading; and the large 95% tolerance limits for grading since LOCS II employs an integer scale. LOCS III consists of six slit lamp images for grading NC and NO, five retroillumination images for grading cortical cataract, and five retroillumination images for grading P. Cataract severity is graded on a decimal scale with each standard possessing regularly spaced intervals, thus reducing the 95% tolerance limits from 2.0 for each class found with LOCS II to 0.7 for NO, and NC, 0.5 for C and 1.0 for P with LOCS III. LOCS III demonstrates higher reproducibility than LOCS II (Chylack et al 1993b) and reduced intra- and

inter-observer variability in grading posterior sub-capsular opacities. In advanced cortical and nuclear opacities inter-observer agreement is higher than LOCS II and intra-observer agreement is good (Khu et al 1994).

6.4.3. Forward Light Scatter.

The point spread function (PSF) describes the distribution of a point source of light on the retina. The PSF can be divided into two parts; a central portion up to 10' arc in diameter and a peripheral portion termed straylight, which occurs beyond 1° eccentricity. The terms straylight and forward light scatter are synonymous. Van den Berg (1995) proposed four main sources of intra-ocular straylight; the cornea, the crystalline lens, translucency of the ocular wall and fundus reflectance. These sources combine additively with age according to the equation:

$$s(\theta) = s_{\text{cornea}}(\theta) + s_{\text{lens}}(\theta) + s_{\text{wall}}(\theta) + s_{\text{fundus}}(\theta) \quad \text{Eqn 6.3}$$

The corneal component is independent of age (van den Berg and Tan 1994). The lenticular component is dependent on age and the remaining components upon pigmentation (van den Berg 1995). In a young adult, the lenticular component is thought to contribute 50% of the straylight, the cornea 30% and the remaining components 20% (Vos 1984).

Forward light scatter may be assessed using the equivalent veil technique. Consider a glare source situated at a glare angle, θ , from a test object; the glare source produces both an illuminance at the observer's eye, E_{gl} (lm m^{-2}), and a light veil of luminance, L (cdm^{-2}), which masks the test object. L , is said to be the equivalent veiling luminance, L_{eq} . The relationship between E_{gl} , and L_{eq} describes the glare function, $f(\theta)$;

$$f(\theta) = \frac{L_{eq}}{E_{gl}} \quad \text{Eqn 6.4}$$

Proportionality between L_{eq} and E_{gl} may be taken as evidence for straylight as the cause for the masking effect and a lack of proportionality as evidence for a neural cause (Vos 1984). Early studies concluded that the ratio L_{eq}/E_{gl} was constant for any glare angle (Holladay 1926; 1927; Stiles 1929; Stiles and Crawford 1937). Later studies disputed these findings and it is

now evident that the ratio L_{eq}/E_{gl} does not remain constant for all glare angles (Schouten and Ornstein 1939; Stiles 1930; Fry 1954; Vos 1984). Straylight also exhibits angular dependency for glare angles greater than approximately one degree. Theoretical studies by Stiles (1930) and Fry (1954) of intraocular light scattering found that the ratio L_{eq}/E_{gl} declined with glare angle according to an inverse square relationship ($1/\theta^2$). Other workers have reported different angular functions for a variety of glare angles and these functions have been reviewed by Vos (1984). Many studies have used the Stiles-Holladay approximation (Stiles 1929; Stiles and Crawford 1934; Vos 1984; van den Berg 1986; Ijspeert et al 1990) given by;

$$\frac{L_{eq}}{E_{gl}} = \left(\frac{10}{\theta^2}\right) \cdot \cos \theta \quad \text{Eqn 6.5}$$

The factor, $\cos \theta$, is often omitted from this equation since it is not thought to be relevant for angles of less than 30 degrees (Vos 1984). Vos (1984) determined the veiling luminance, L_{eq} , at various glare intensities, E_{gl} , using a test stimulus presented for approximately 40 milliseconds. Other studies have derived L_{eq} from the difference in contrast threshold of a sinusoidal grating with and without a glare source (Paulsson and Sjöstrand 1980; Abrahamsson and Sjöstrand 1986; Wood et al 1987a; 1989; Elliott et al 1989; Dengler-Harles et al 1990). Yager et al (1992) examined the hypothesis of Paulsson and Sjöstrand (1980) and Abrahamsson and Sjöstrand (1986) that the light scatter factor (LSF) is defined by the following equation:

$$LSF = \left(\frac{L_{eq}}{E_{gl}}\right) \cdot \left[CF \cdot \left(\frac{M_2}{M_1}\right) - 1\right] \quad \text{Eqn 6.6}$$

where, M_1 , is the contrast threshold without a glare source and, M_2 , the contrast threshold in the presence of a glare source. CF, is a correction factor derived empirically to account for changes in the pupil size due to the introduction of a glare source. Yager et al (1992) calculated LSF at two different values of L_{eq}/E_{gl} and found that LSF did not remain constant, which would be expected if the hypothesis was true. deWaard et al (1992) also demonstrated

a non-linear relationship between forward light scatter, measured using the direct compensation technique, and LSF measured with and without a glare source using the Vistech MCT8000. Nevertheless, Whitaker et al (1994) measured contrast thresholds for three values of L_{gl} and E_{gl} with and without a glare source and concurred with the Paulsson and Sjöstrand equation. However, their measurements were made at high adaptation levels where contrast thresholds are independent of luminance.

The direct compensation method of measuring forward light scatter (van den Berg 1986) enables in-vivo measures of forward light scatter to be made at different glare angles (Section 4.5.4).

$$s(\phi) = \phi^2 \cdot \left(\frac{L}{E}\right) \quad \text{Eqn 6.7}$$

where, L , is the compensating luminance modulation of the central fixation target, ϕ , is the scattering angle and, E , is the illuminance of the straylight source at the pupil plane. The measurement is repeated several times at each glare angle and the straylight parameter at each angle expressed as the arithmetic mean of these measurements. Using this technique, forward light scatter has been demonstrated to increase with advancing age (van den Berg 1986; Elliott et al 1991). An increase in forward light scatter has also been demonstrated in the presence of cataract (deWaard et al 1992), corneal dystrophy, hypopigmentation (IJspeert et al 1990; van den Berg 1991, 1993; Elliott et al 1991) and in contact lens wear (Elliott et al 1991). Forward straylight using this technique decreases with scattering angle (IJspeert et al 1990; van den Berg 1995). Van den Berg (1996) described this relationship by the equation:

$$\text{straylight intensity} = s0^p \quad \text{Eqn 6.8}$$

where, s , is a constant and the power, p , approximates to -2. In elderly eyes and in cataract, p , is approximately the same and the constant, s , increases. Intraocular lens implantation has been shown to result in an increase in forward light scatter (Witmer et al 1989; Hard et al 1993). The influence of forward light scatter in SWAP has been studied in cataract simulation studies (Moss and Wild 1994) and in cataract patients (Moss et al 1995).

Wolf (1960), Elliott and Hurst (1989) and Dengler-Harles (1991) demonstrated a linear relationship between backward light scatter and disability glare in normal subjects. Backward light scatter measured with the OLM correlates poorly with forward light scatter in cortical and posterior sub-capsular cataracts, although moderately with nuclear cataract (deWaard et al 1992). Similarly, Mitchell and Hurst (1993) found little correlation between backward light scatter measured with the Scheimpflug camera and the direct compensation measurement of forward light scatter. Van den Berg (1995) proposed that the relationship between glare and forward light scatter is complex, concluding that glare testing has merit for evaluating the nature of a patient's visual impairment, whereas forward straylight measurement yields information regarding the quality of the optic transfer function. The laws governing the relationship between the two phenomena are unknown.

6.5. The Effect of Media Opacity on the Visual Field.

The effect of cataract on the conventional W-W visual field has been widely studied. Simulation studies have employed a variety of methods to simulate cataract. Heuer et al (1988) utilised ground glass diffusers placed in front of the eye of normal subjects. Using both the Octopus perimeter and the Humphrey Field Analyser, they found a general reduction in sensitivity which increased as the opalescence of the diffuser increased. They concluded that the reduction in perimetric sensitivity occurred as a result of light scatter of the stimulus, effectively reducing the perceived stimulus luminance. Budenz and co-workers (1993) also employed ground glass diffusers to simulate cataract in a group of glaucomatous subjects. Areas of the visual field considered to be normal before introduction of the diffuser and areas of visual field damage both underwent a general reduction in sensitivity after introduction of the diffuser. Budenz et al (1993) suggested that glaucomatous progression of the visual field could be detected in patients where cataract and glaucoma co-exist by subtraction of the change in visual field sensitivity in relatively normal areas of the visual field and comparing it with the change in sensitivity in scotomata. If the change in sensitivity in a scotoma was greater than that in the normal areas of the field then it could be attributed to glaucomatous progression. Other methods of simulating cataract include neutral density filters and diffusers

(Eichenberger et al 1987) and orthoptic occluders (Niesel et al 1978, Niesel and Wiher 1982; Uner-Bloch 1987). Niesel et al (1978) and Niesel and Wiher (1982) recorded a general reduction in sensitivity across the visual field, whereas Eichenberger et al (1987) and Uner-Bloch (1987) recorded an increase in loss variance as the degree of simulated cataract increased. In glaucoma patients, simulated cataract has been reported to increase the MD_F and decrease CLV as result of the disappearance of small scotomata (Uner-Bloch 1987). Wood et al (1987a) simulated cataract using various concentrations of polystyrene microspheres suspended in solutions of distilled water. The visual field was studied with the Dicon LED Autoperimeter and the Octopus projection perimeter. A general reduction in sensitivity was reported, which increased as the degree of light scatter increased. The Dicon perimetric profile exhibited greater attenuation centrally, whereas the Octopus perimetric profile exhibited greater attenuation peripherally. It was suggested that the larger stimulus size of the Octopus perimeter (0.43°) relative to the Dicon perimeter (0.28°) may saturate the central visual field rendering it relatively insensitive to light scatter. This finding was concordant with Greve (1979) who reported that cataract flattened the hill of vision as a result of a depression in central sensitivity. Wood et al (1989) evaluated this model in patients with nuclear and non-nuclear cataract. The group with non-nuclear cataract exhibited results in agreement with the model, but the group with nuclear cataract exhibited a reduction in sensitivity which was greater in the central visual field for both the Octopus and Dicon stimuli. Dengler-Harles et al (1990) applied the model of Wood et al (1987a) to a sample of glaucoma patients. A linear increase in MD_F and a curvilinear decrease in LV was reported with increase in light scatter, indicating that the depth and/or area of focal loss decreased. Their findings could be attributed either to the greater influence of light scatter in areas of the visual field exhibiting high sensitivity compared to areas of reduced sensitivity, or that areas of the visual field adjacent to scotomata might be responsible for the detection of a stimulus as a result of light scatter.

The effect of age-related cataract extraction and intraocular lens implantation on the W-W visual field has also been studied in normals (Guthauser and Flammer 1988; Lam et al 1991) and in glaucoma (Stewart et al 1995; Chen et al 1996, Smith et al 1996). Guthauser and

Flammer (1988) reported a diffuse depression in visual field sensitivity with the Octopus perimeter. Central visual field sensitivity exhibited a significantly greater reduction in sensitivity than peripheral regions. Lam et al (1991) reported a small but significantly greater improvement in threshold in the central visual field with the Humphrey Field Analyser following cataract extraction. Chen and co-workers (1996) reported a significant improvement in MD_H , PSD and SF post-operatively, but a worsening in CPSD in glaucoma patients. The foveal threshold was affected more severely than other stimulus locations. Similarly, Smith et al (1996) reported a significant post-operative improvement in MD_H and a worsening in CPSD. They suggested that the worsening in CPSD resulted from areas of the visual field less affected by glaucoma yielding a greater improvement in sensitivity than that of the damaged areas. Conversely, Stewart et al (1995) found no significant improvement in MD_H and PSD in 24 patients with chronic open-angle glaucoma despite a significant improvement in visual acuity. They suggested that the lack of improvement in the visual field indices could be explained by the hypothesis that patients with glaucoma-related ganglion cell loss were more dependent upon spatial summation for light perception. The refractive blur induced by cataract may have resulted in an enhanced spatial summation of ganglion cells. Cataract extraction would result in a clearer image and a reduced spatial summation and therefore, reduced ability to detect a dimmer stimulus.

The influence of simulated cataract using polystyrene microspheres on the visual field derived by SWAP was studied by Moss and Wild (1994). The degree of perimetric attenuation was diffuse and increased with increasing forward light scatter. Preferential attenuation of the short-wavelength perimetric profile occurred compared to W-W perimetry. The influence of age-related cataract on the SWAP visual field was investigated by Moss et al (1995). Cataract resulted in a general reduction in sensitivity for both W-W perimetry and SWAP but was proportionately greater in SWAP. The SWAP MD_H was greater for posterior sub-capsular cataract whereas the W-W MD_H was greater for anterior cortical cataract. This phenomenon was explained by the smaller pupil size in SWAP yielding a greater reduction in visual performance for centrally located opacities such as posterior sub-capsular cataract, and the relatively greater pupil size in W-W perimetry yielding maximal reduction in visual performance

for anterior cortical opacities. The loss in luminance contrast of the SWAP stimulus together with a change in chromaticity of the stimulus towards the yellow background may have resulted in greater attenuation of SWAP. Alternatively, any preferential forward light scattering of short-wavelength stimuli may have resulted in the greater attenuation of SWAP.

6.6. Aims.

The influence of pseudophakia on SWAP has not been investigated. Furthermore, the previous study of the influence of age-related cataract on SWAP employed a broadband OCLI blue stimulus presented against a 330 cdm⁻² yellow background (Moss et al 1995). The recently standardised SWAP parameters utilised in the Humphrey Field Analyser possess a narrowband 440 nm stimulus presented against a 100 cdm⁻² yellow background. The influence of age-related cataract on the SWAP derived using these parameters has not been quantified. The primary aim of this study was to investigate the effect of age-related cataract on the standard SWAP parameters. The secondary aim was to investigate the influence of pre- and post-operative ocular media absorption on SWAP.

6.7. Sample.

The sample comprised 19 subjects with age-related cataract but otherwise normal eyes. The mean age of the sample was 74.58 years (SD 6.60), ranging in age between 57 and 84 years. Twelve subjects were male. Pre-operatively, all subjects underwent a full ophthalmological examination in which direct ophthalmoscopy, slit-lamp examination of the lens and Goldmann applanation tonometry were performed. The level of cataract was graded using the LOCS III system (Chylack et al 1993a). The sample comprised 13 patients with predominantly nuclear opacity, one patient with predominantly cortical opacity and five patients with approximately equal gradings of nuclear, cortical and posterior sub-capsular opacity. All subjects were within the pre- and post-operative inclusion criteria of intraocular pressure less than 21 mmHg, distance refractive error less than ± 3.00 DS and ± 3.00 DC, absence of a congenital tritanopic colour vision defect, a negative family history of glaucoma, absence of previous ocular surgery or trauma, and absence of medication with known ocular or central nervous system side effects. Pre-operative Snellen visual acuity ranged between 6/12 and 6/60. Post-operative

Snellen visual acuity ranged between 6/7.5 and 6/5. Sixteen patients underwent extracapsular cataract extraction and the remaining three patients underwent phakoemulsification.

6.8. Perimetry.

Perimetry was undertaken using the Humphrey Field Analyser 640 with the commercially available hardware and software (version 9.31) upgrade necessary for SWAP. The default stimulus and background conditions were employed for both W-W perimetry and SWAP; namely a Goldmann size III stimulus of 200 ms duration presented against a background of 10 cdm⁻² for W-W perimetry and a Goldmann size V stimulus of 200 ms presented against a background of 100 cdm⁻² for SWAP. Each subject was examined using Program 24-2 and the Standard 4-2 dB double reversal staircase strategy, which estimates the threshold at 56 locations within 24° eccentricity.

The eye which was to undergo cataract extraction underwent visual field examination, three times pre-operatively and three times post-operatively. Each visit lasted approximately one hour. At each of the first two pre-operative visits, a single W-W and short-wavelength visual field was obtained. The patient's near refractive correction was employed for all perimetry. Fifteen minutes separated the two visual field examinations within each visit. Prior to the commencement of SWAP, each patient underwent a three minute adaptation period to allow adequate isolation of the SWS pathway. The order of W-W perimetry and SWAP was randomised between subjects to eliminate order effects, but remained constant within a subject for all visits. At the third perimetry visit, ocular media absorption was assessed using the difference in scotopic sensitivity method, and forward light scatter assessed using the direct compensation technique described in Chapter 4.

Following routine surgery and uneventful post-operative recovery, each subject underwent an identical perimetric protocol between six and eight weeks post-operatively. The IOLAB intraocular lens (IOL) was used in ten patients, the Rayner IOL was used in six patients and the Allergan IOL in the remaining three patients. Ocular media absorption was assessed post-operatively since the IOL's incorporated UV filters and consequently possessed reduced

transmission at the SWAP stimulus peak wavelength of 440 nm. The procedure used to calculate ocular media absorption was modified to account for the greater absorption of the 410 nm stimulus by the IOL (Figure 6.2).

The absorption of each IOL at the stimulus wavelengths utilised in the assessment of ocular media absorption (410 nm and 560 nm) was derived from the spectral transmission curves of each IOL (Figure 6.2). The attenuation caused by the introduction of each narrowband filter was then recalculated to account for the further attenuation caused by the IOL. Consider the calculation of ocular media absorption in the presence of the Allergan IOL:

The maximum stimulus luminance of the HFA in default mode, ΔL_{\max} , = 10,000 asb
= 4.00 log units

The spectral transmission of the Allergan IOL at 410 nm is 36.92%. Therefore, the absorption at 410 nm is 63.08%. The maximum stimulus luminance of the 410 nm narrowband filter, ΔL_{410} , = 0.1 asb.
= -1.00 log units

The further attenuation of the maximum stimulus luminance caused by the introduction of the IOL, ΔL_{IOL} , is:

$$0.1 - \left(\frac{63.08}{100} \cdot 0.1 \right)$$

= 0.037 asb
= -1.43 log units

The attenuation of the stimulus, ΔL_{att} , caused by the introduction of a narrowband stimulus filter in the presence of an IOL is:

$$\Delta L_{\text{att}} = \Delta L_{\max} - \Delta L_{\text{IOL}}$$

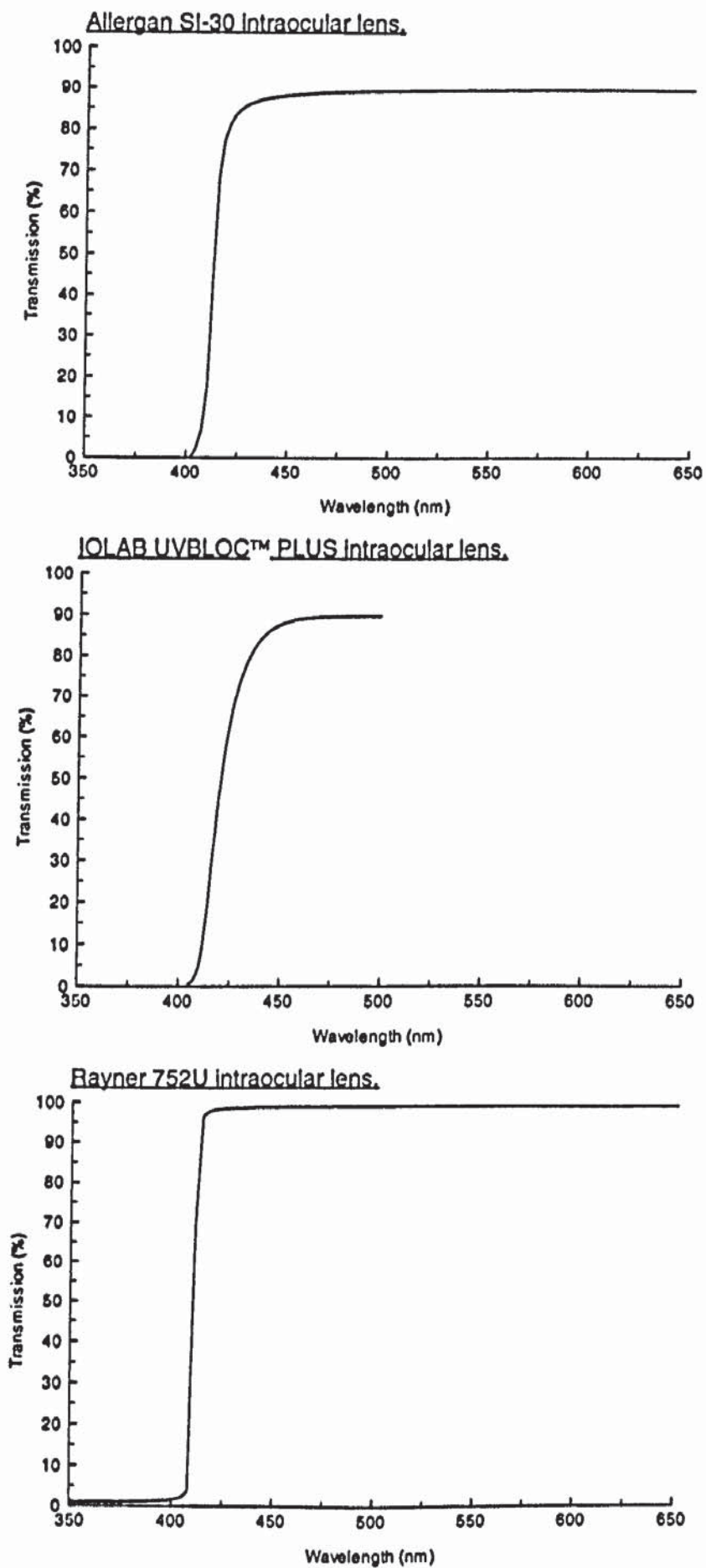


Figure 6.2. Spectral transmission curves for the Allergan (top), IOLAB (middle) and Rayner (bottom) intraocular lenses. Reproduced using data provided by the manufacturers.

$$= 4.00 + 1.43$$

$$= \underline{5.43 \text{ log units}}$$

Similarly, the maximum stimulus luminance of the 560 nm narrowband filter, ΔL_{560} , = 116.9 asb.

$$= \underline{2.07 \text{ log units}}$$

The spectral transmission of the Allergan IOL at 560 nm is 91.37%. Therefore, the absorption at 560 nm is 8.63%. The maximum stimulus luminance of the 560 nm narrowband filter, ΔL_{560} , = 116.9

$$= \underline{2.07 \text{ log units}}$$

ΔL_{IOL} , is:

$$116.9 - \left(\frac{8.63}{100} \cdot 116.9 \right)$$

$$= 106.81 \text{ asb}$$

$$= \underline{2.02 \text{ log units}}$$

The attenuation of the stimulus, ΔL_{att} , caused by the introduction of a narrowband stimulus filter in the presence of an IOL is:

$$\Delta L_{att} = \Delta L_{max} - \Delta L_{IOL}$$

$$= 4.00 - 2.02$$

$$= \underline{1.98 \text{ log units}}$$

Ocular media absorption was then calculated according to the remaining steps outlined in Section 4.5.3.

6.9. Analysis.

The visual fields obtained at the initial perimetry visit, pre-operatively were excluded from data analysis in order to reduce the effects of learning. Similarly, the first post-operative visual field examination was excluded to exclude any learning effect arising from the different appearance of the background and stimulus. The mean sensitivity and the unweighted Indices mean deviation, short-term fluctuation, pattern standard deviation and corrected pattern standard deviation were calculated from the visual fields obtained at each of the visits. The two stimulus locations immediately above and below the blind spot were omitted from the analysis.

Forward straylight parameters derived from 47 normal subjects (mean age 55.53 years; SD 19.83) were used to calculate the group mean straylight parameter for each of the three glare angles for each of three age groups; 60 to 69, 70 to 79 and 80 to 89 years.

The difference between the straylight parameter of each cataract patient and that of the mean of the corresponding age-matched normal group was then calculated. This procedure yields a measure of the isolated cataract straylight parameter (ICSP) (de Waard et al 1992). The index is analogous to the MD_H visual field index. A positive ICSP represents greater forward light scatter than the age-matched normal observer.

6.10. Results.

All W-W and SWAP visual fields were within the reliability criteria of <33% false-positive or negative catch trials. In W-W perimetry, one patient pre- and post-operatively exceeded the <33% reliability criteria for fixation losses proposed by Nelson-Quigg et al (1993). In SWAP, one patient pre-operatively and two patients pre-operatively exceeded the <33% reliability criteria for fixation losses.

The group mean visual field indices pre- and post-operatively are illustrated in Table 6.1.

Visual Field Index	Pre-Operative			Post-Operative		
	W-W Perimetry	SWAP	SWAP corrected for absorption at 440 nm	W-W Perimetry	SWAP	SWAP corrected for absorption at 440 nm
MS (dB)	21.92 (0.58)	12.31 (1.20)	20.34 (1.19)	25.44 (0.41)	23.29 (0.90)	27.37 (0.97)
MD _H (dB)	-5.78 (0.62)	-8.05 (1.23)	-9.05 (1.45)	-2.48 (0.35)	2.04 (0.95)	-1.49 (0.96)
SF (dB)	1.55 (0.13)	2.01 (0.18)	2.01 (0.18)	1.54 (0.12)	1.91 (0.12)	1.91 (0.12)
PSD (dB)	2.52 (0.19)	3.45 (0.19)	3.45 (0.19)	2.94 (0.28)	3.73 (0.26)	3.73 (0.26)
CPSD (dB)	1.75 (0.23)	2.42 (0.30)	2.42 (0.30)	1.90 (0.34)	2.98 (0.31)	2.98 (0.31)

Table 6.1. Pre- and post-operative visual field indices (group mean ± 1 SE). Note that the decibel scales between W-W perimetry and SWAP are not compatible.

6.10.1. Mean Sensitivity (MS).

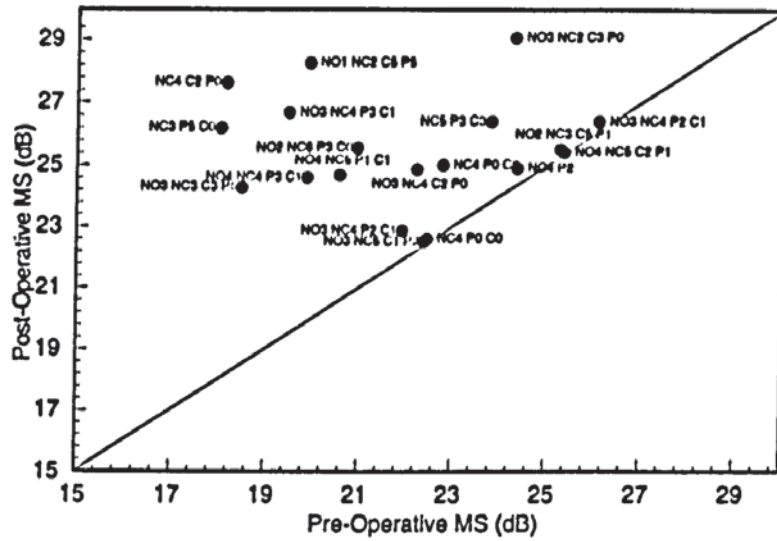
Pre- and post-operative MS as a function of cataract severity and type is illustrated in Figure 6.3. The pre- and post-operative group mean MS for W-W and SWAP with and without correction for ocular media absorption is illustrated in Table 6.1. There was less improvement in MS post-operatively in W-W perimetry than SWAP. Six subjects yielded no clinical improvement in MS for W-W perimetry, whereas all subjects exhibited an improvement in SWAP MS with and without correction for ocular media absorption. The group mean post-operative improvement in W-W MS was 3.52 dB (SD 3.15). The group mean post-operative improvement in SWAP MS was 10.98 dB (SD 3.43) which decreased to 7.03 dB (SD 3.15) after correction for ocular media absorption.

6.10.2. Mean Deviation (MD_H).

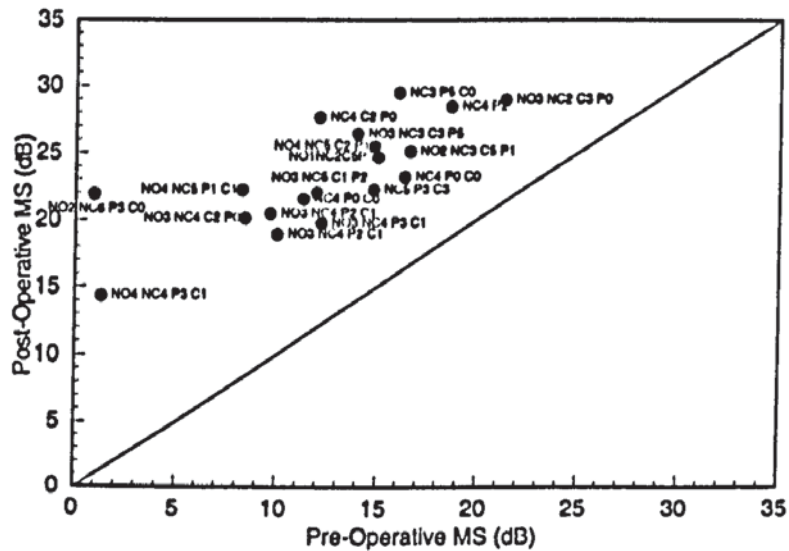
Figure 6.4 illustrates the pre- and post-operative MD_H as a function of cataract severity and type. The pre- and post-operative group mean MD_H for W-W and SWAP with and without correction for ocular media absorption at 440 nm is illustrated in Table 6.1. Three patients exhibited little change in MD_H post-operatively for W-W perimetry whilst one patient exhibited a slight deterioration. For SWAP, all patients exhibited an improvement in MD_H post-operatively; 12 of the patients yielded a positive SWAP MD_H prior to correction for ocular media absorption. Six patients yielded a positive SWAP MD_H post-operatively after correction for ocular media absorption. The group mean post-operative improvement in W-W MD_H was 3.30 dB (SD 2.90). The group mean post-operative improvement in SWAP MD_H was 10.88 dB (SD 3.41) which decreased to 7.55 dB (SD 4.05) after correction for ocular media absorption at 440 nm.

Figure 6.5 illustrates the post-operative change in MD_H for W-W perimetry and SWAP with and without correction for the influence of ocular media absorption as a function of cataract severity and type. Although the decibel scales differ between W-W perimetry and SWAP, one decibel represents a 0.1 log unit change in stimulus intensity. The MD_H indices for W-W perimetry and SWAP represents the average deviation in decibels from the corresponding age-corrected normal value. Thus, changes in MD_H for W-W perimetry and for SWAP can be compared quantitatively. The post-operative change in MD_H was preferentially greater in

a.) W-W Perimetry



b.) SWAP



c.) SWAP corrected for absorption scaled to 440 nm

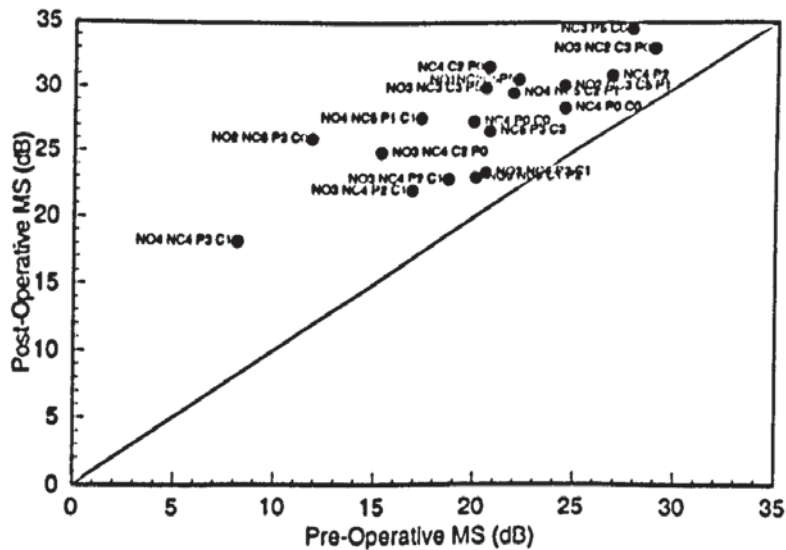


Figure 6.3a-c. Pre- and Post-operative mean sensitivity as a function of cataract severity and type. A slope of unity representing equality between the two given measurements is illustrated for reference. Note that the decibel scales between W-W perimetry and SWAP are not compatible.

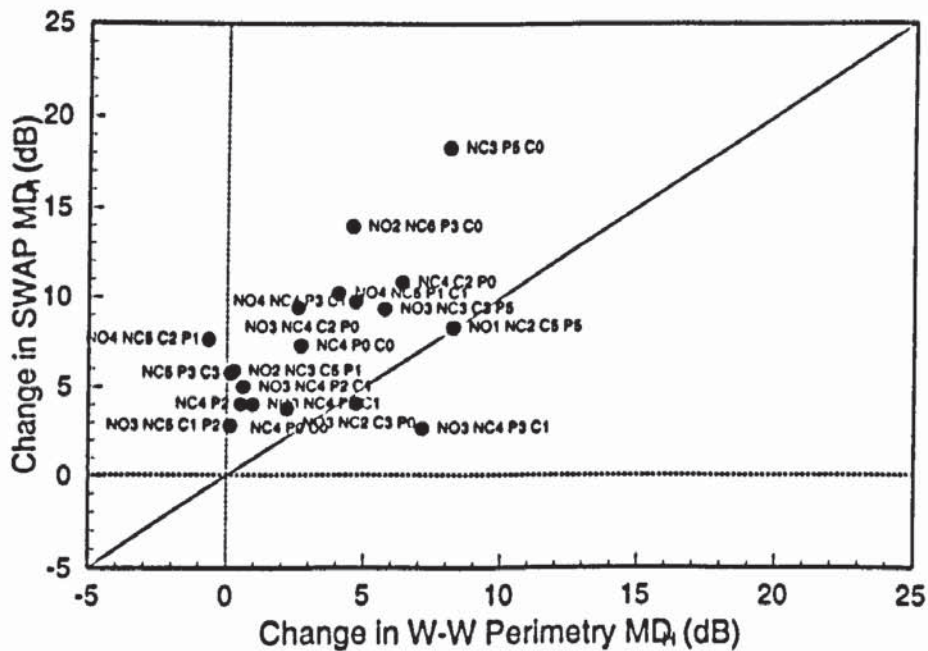
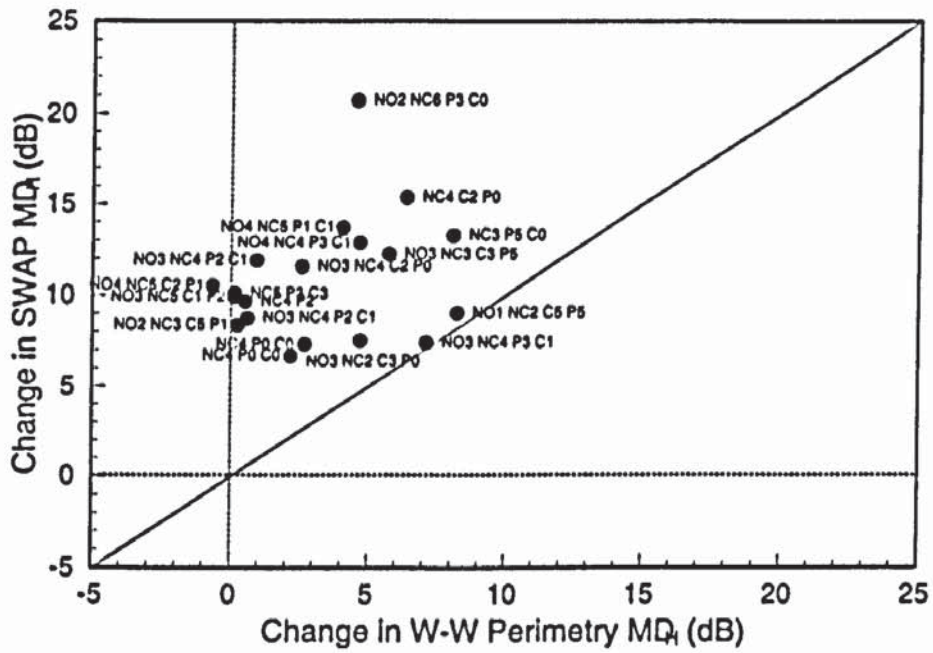


Figure 6.5. Post-operative change in mean deviation for SWAP against that for W-W perimetry (top, SWAP uncorrected for ocular media absorption; bottom, SWAP corrected for ocular media absorption). A slope of unity representing equality between the two given measurements is illustrated for reference.

SWAP than for W-W perimetry. Correction of SWAP for the effects of ocular media absorption reduced the extent of this preferential improvement in MD_H.

Figure 6.6 illustrates the group mean pointwise total deviation pre- and post-operatively. The pre-operative reduction in W-W and short-wavelength sensitivity was slightly greater at central stimulus locations than at peripheral stimulus locations. The post-operative improvement in total deviation was smallest for W-W perimetry. SWAP uncorrected for ocular media absorption yielded the greatest post-operative improvement in total deviation. Post-operatively, the total deviation was positive at all stimulus locations for SWAP uncorrected for ocular media absorption. The post-operative change in total deviation was smaller when SWAP was corrected for ocular media absorption and was negative at all but one stimulus locations.

6.10.3. Short-Term Fluctuation (SF).

Figure 6.7 illustrates the pre- and post-operative SF as a function of cataract severity and type. The pre- and post-operative group mean SF for W-W and SWAP with and without correction for ocular media absorption is illustrated in Table 6.1. W-W perimetry SF was greater pre-operatively in seven patients and greater post-operatively in twelve patients. In SWAP, five patients exhibited no change in SF pre- and post-operatively, five patients yielded greater SF post-operatively and nine patients yielded greater SF pre-operatively. Globally, cataract extraction yielded no difference in W-W perimetry SF and a 0.1 dB reduction in SWAP SF.

6.10.4. Pattern Standard Deviation (PSD).

Figure 6.8 illustrates pre- and post-operative PSD as a function of cataract severity and type. The pre- and post-operative group mean PSD for W-W and SWAP is illustrated in Table 6.1. W-W perimetry yielded a mean post-operative increase in PSD of 0.42 (SD 1.4), whilst SWAP yielded a mean post-operative increase in PSD of 0.28 (SD 1.43). The W-W PSD was greater pre-operatively in seven patients and greater post-operatively in eleven patients. One patient the W-W PSD was unchanged post-operatively. In SWAP, the PSD was greater pre-operatively in eight patients and greater post-operatively in eight patients. The SWAP PSD was unchanged post-operatively in three patients.

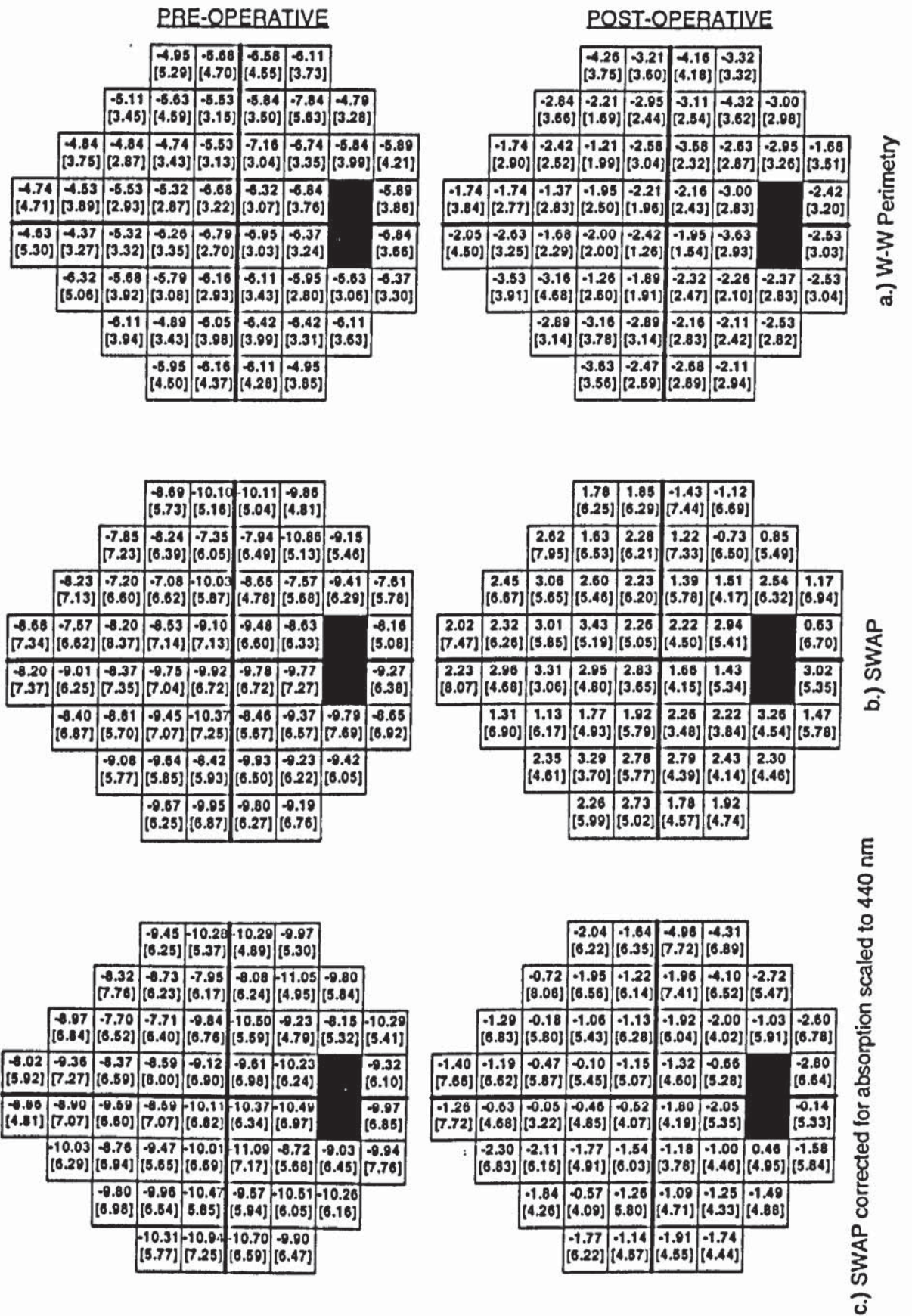
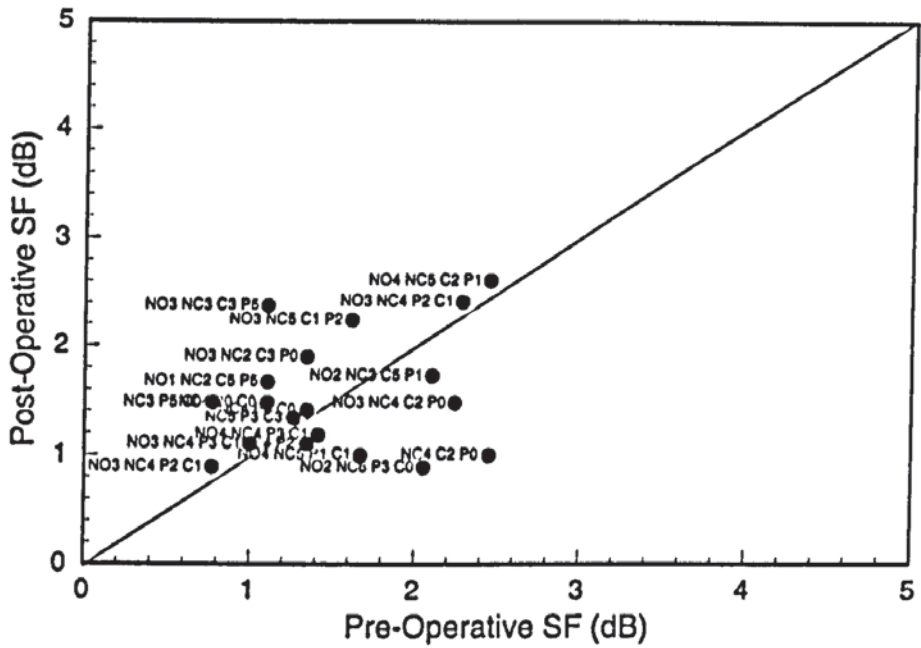


Figure 6.6. Group numeric total deviation pre- (left) and post-operatively (right) for W-W perimetry (top) and SWAP uncorrected (middle) and corrected for the influence of ocular media absorption at 440 nm (bottom). Bracketed numbers indicate ± 1 standard deviation of the group mean.

a.) W-W Perimetry



b.) SWAP

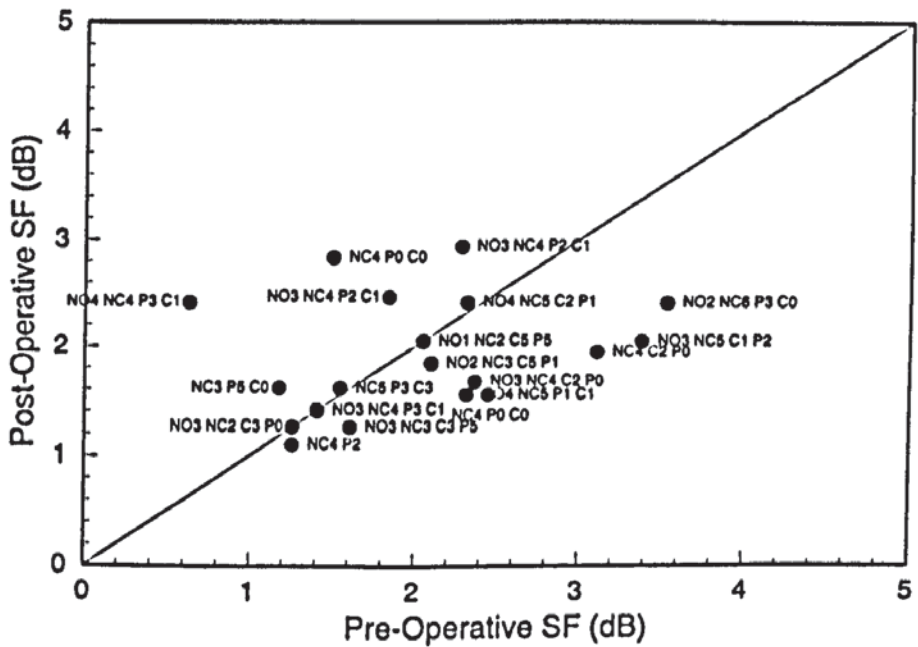
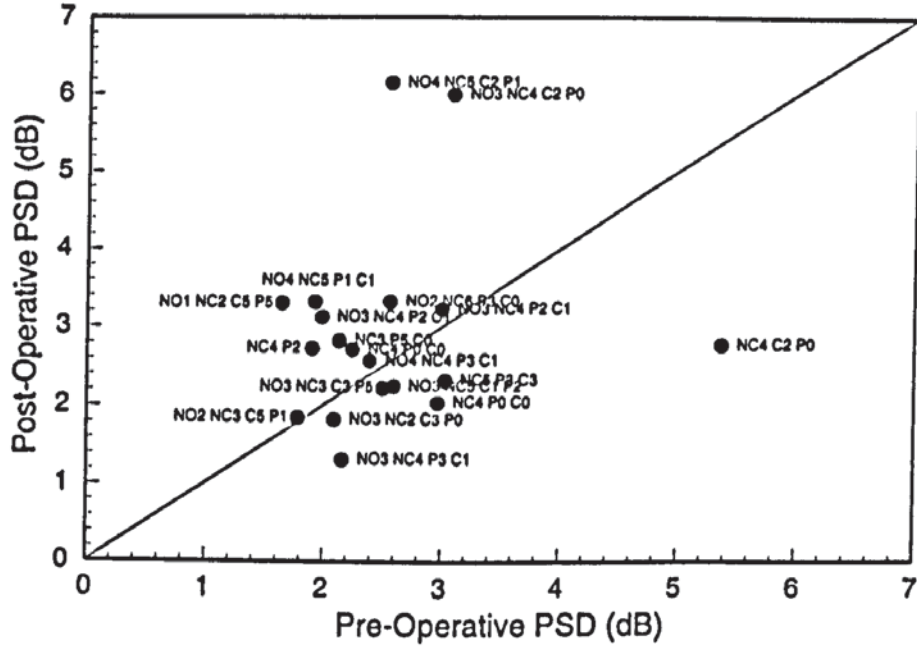


Figure 6.7a & b. Pre- and post-operative short-term fluctuation as a function of cataract severity and type. A slope of unity representing equality between the two given measurements is illustrated for reference. Note that the decibel scales between W-W perimetry and SWAP are not compatible.

a.) W-W Perimetry



b.) SWAP

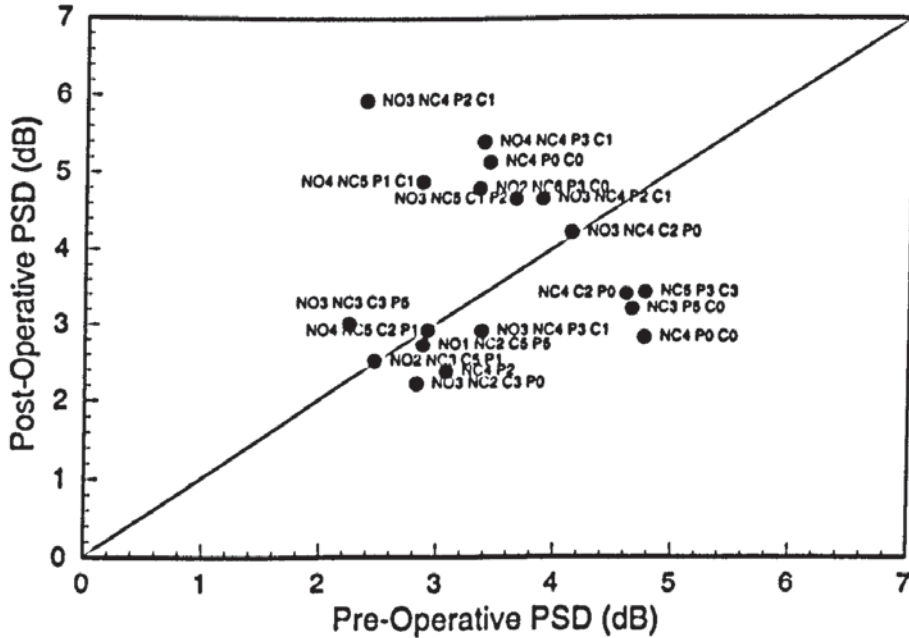


Figure 6.8a & b. Pre- and post-operative pattern standard deviation as a function of cataract severity and type. A slope of unity representing equality between the two given measurements is illustrated for reference. Note that the decibel scales between W-W perimetry and SWAP are not compatible.

Three patients in W-W perimetry and twelve patients in SWAP yielded a PSD which was greater than expected in a normal population. These patients exhibited a pattern of visual field loss which was consistent with the presence of a fatigue effect at peripheral stimulus locations.

6.10.5. Corrected Pattern Standard Deviation (CPSD).

Figure 6.9 illustrates pre- and post-operative CPSD as a function of cataract severity and type. The pre- and post-operative group mean CPSD for W-W and SWAP is illustrated in Table 6.1. W-W perimetry yielded a mean post-operative increase in CPSD of 0.15 (SD 1.66), whilst SWAP yielded a mean post-operative increase in CPSD of 0.56 (SD 1.97). For W-W perimetry, CPSD was greater pre-operatively in five patients and greater post-operatively in fourteen patients. For SWAP, CPSD was greater pre-operatively in eight patients, greater post-operatively in ten patients and unchanged in one patient. Nine patients in W-W perimetry and twelve patients in SWAP yielded a CPSD which was greater than expected in a normal population. These patients exhibited a pattern of visual field loss which was consistent with the presence of a fatigue effect at peripheral stimulus locations.

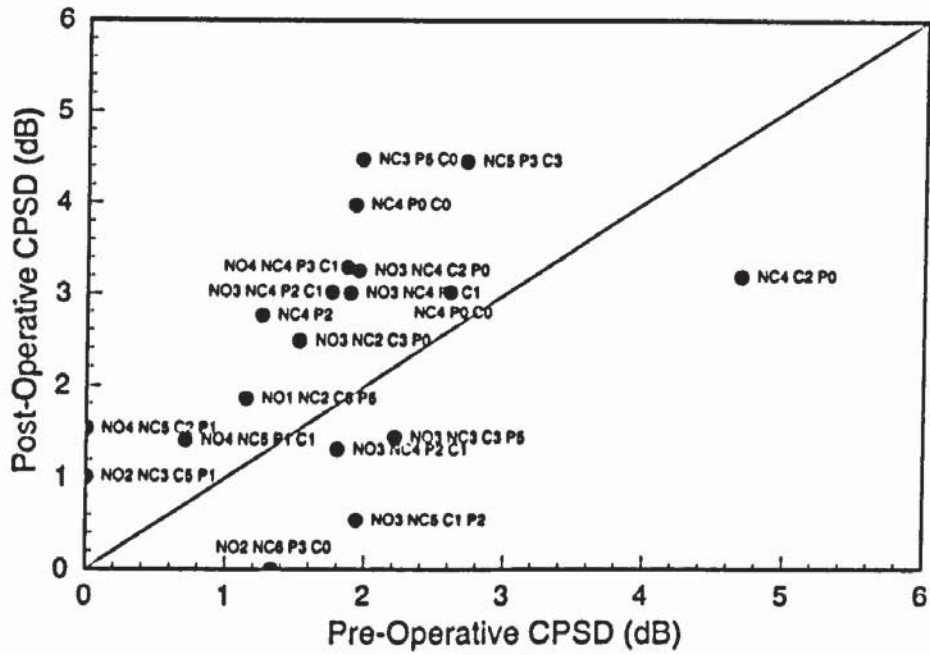
6.10.6. Ocular Media Absorption.

Figure 6.10 illustrates the pre- and post-operative ocular media absorption scaled to 440 nm as a function of cataract severity and type. Ocular media absorption was greatest pre-operatively in all patients. The group mean absorption at 440 nm was 7.80 dB (SD 1.15) pre-operatively, and 4.01 dB (SD 1.17) post-operatively. The post-operative group mean reduction in ocular media absorption at 440 nm was 3.78 dB (SD 1.71).

6.10.7. Forward Light Scatter.

The group mean pre- and post-operative forward straylight parameters and corresponding ICSP are illustrated in Table 6.2. Group mean forward light scatter was greatest pre-operatively and reduced post-operatively by 0.44 log units (Table 6.2). The group mean post-operative ICSP did not clinically deviate from the age-matched normal value (Table 6.2). There was no correlation between pre- and post-operative MD_H and pre- and post-operative ICSP (Figures 6.11 and 6.12). Figure 6.13 illustrates the change in MD_H and ICSP as a function of

a.) W-W Perimetry



b.) SWAP

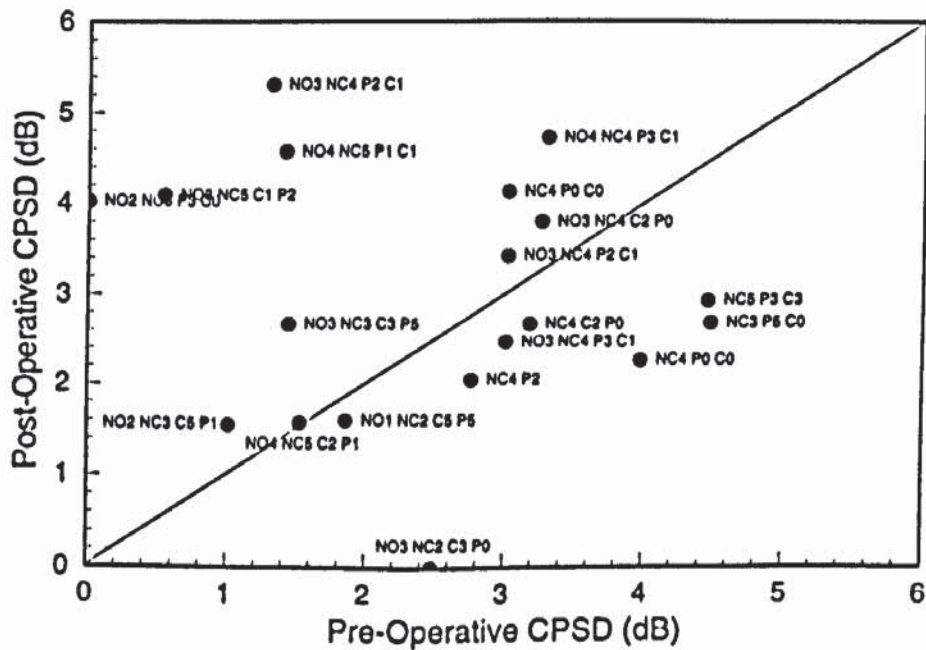


Figure 6.9a & b. Pre- and Post-operative corrected pattern standard deviation as a function of cataract severity and type. A slope of unity representing equality between the two given measurements is illustrated for reference.

	Forward Straylight Parameter (log units)	ICSP (log units)
Pre-Operative	1.76 (0.06)	0.50 (0.07)
Post-Operative	1.32 (0.06)	0.06 (0.07)

Table 6.2. Group mean (± 1 SE) pre- and post-operative forward light scatter and isolated cataract straylight parameter.

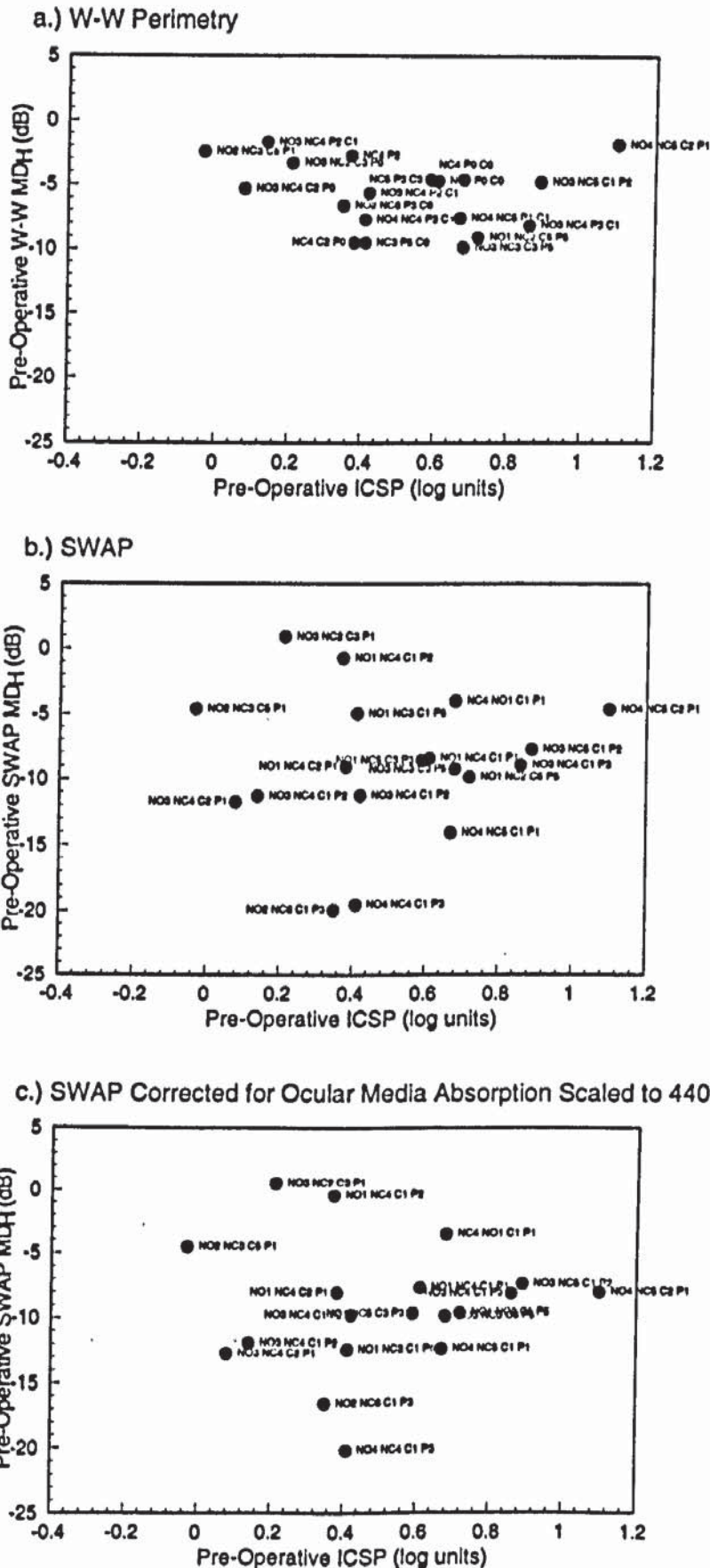


Figure 6.11a-c. Relationship between pre-operative mean deviation and isolated cataract straylight parameter for W-W perimetry (top) and SWAP without correction for absorption (middle) and with correction (bottom) as a function of cataract severity and type. Note that the decibel scales between W-W perimetry and SWAP are not compatible.

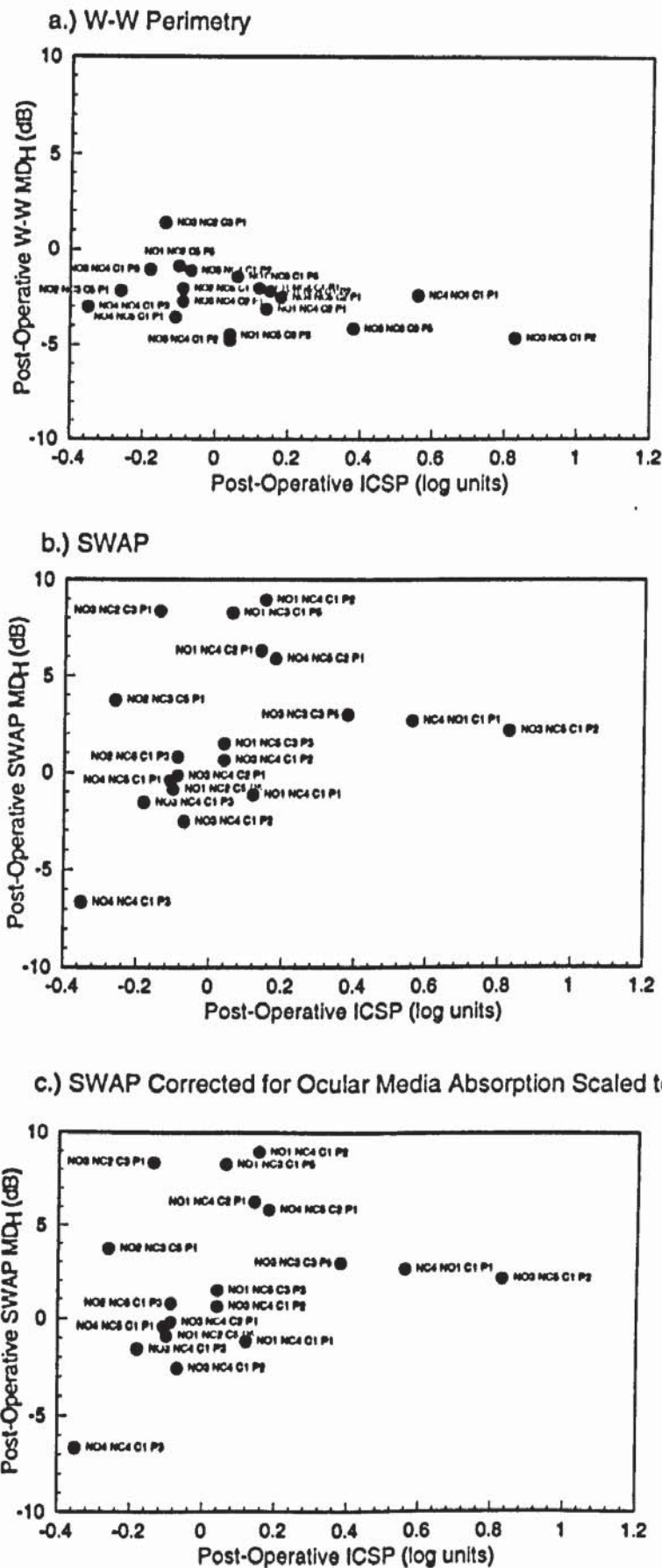


Figure 6.12a-c. Relationship between post-operative mean deviation and isolated cataract straylight parameter for W-W perimetry (top) and SWAP without correction for absorption (middle) and with correction as a function of cataract severity and type. Note that the decibel scales between W-W perimetry and SWAP are not compatible.

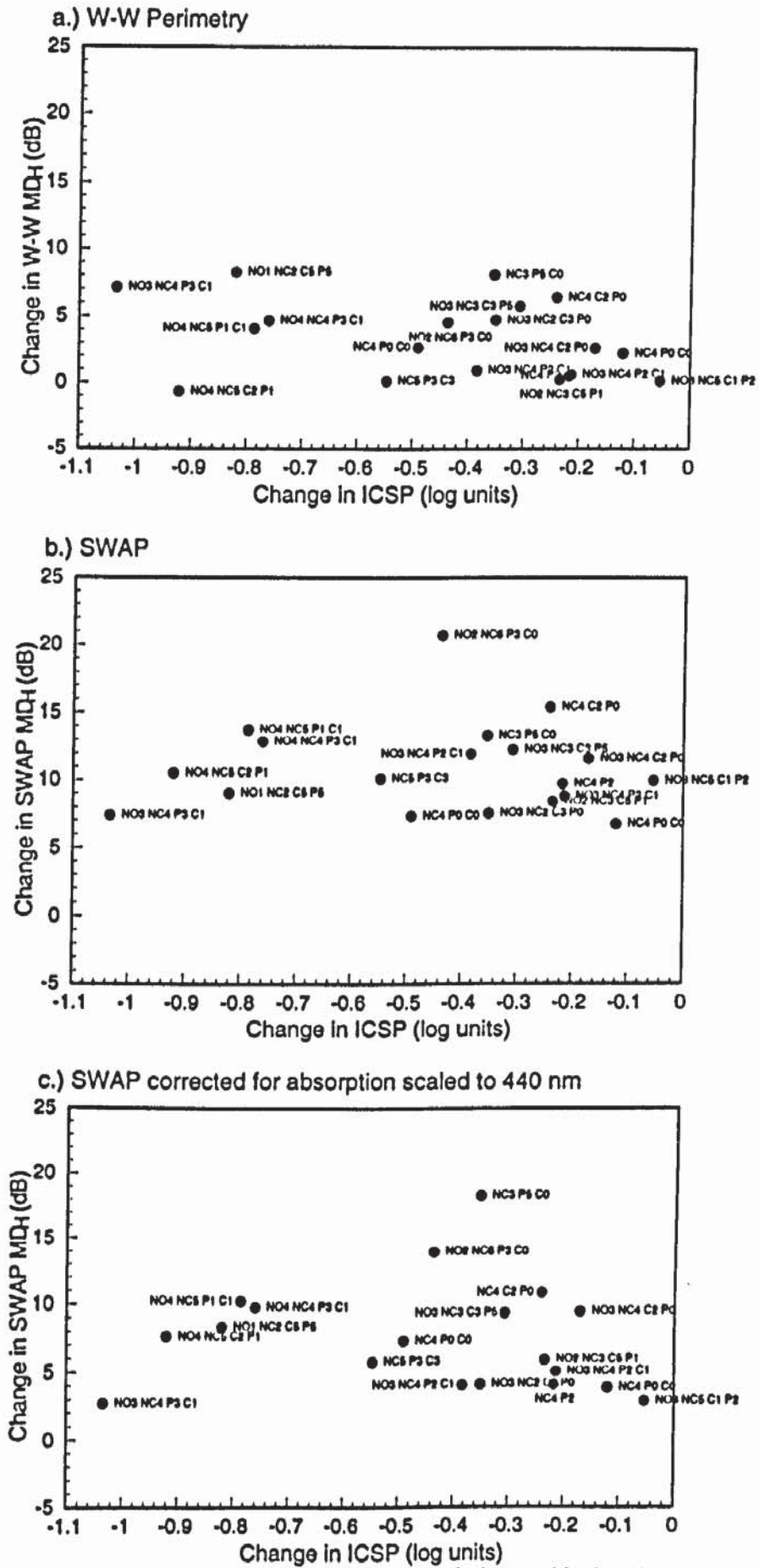


Figure 6.13a-c. Relationship between change in mean deviation and isolated cataract straylight parameter for W-W perimetry (top) and SWAP without correction for absorption (middle) and with correction (bottom). Note that the decibel scales between W-W perimetry and SWAP are not compatible.

cataract severity and type. The improvement in ICSP did not correlate with the post-operative improvement in MD_H for either W-W perimetry or SWAP.

6.10.8. Backward Light Scatter,

There appeared to be no correlation between backward light scatter, defined by LOCS III and the magnitude of ocular media absorption at 440 nm. Additionally, there was no correlation between the magnitude of pre-operative MS, MD_H, SF, PSD and CPSD and backward light scatter defined using the LOCS III classification (Figures 6.3-5; 6.7-9).

6.11. Discussion.

The influence of age-related cataract on the W-W and SWAP profile was a profound general reduction in sensitivity across the visual field. The attenuation was preferentially greater in the short-wavelength visual field.

The general reduction in W-W sensitivity induced by age-related cataract is concordant with other studies (Guthauser and Flammer 1988; Wood et al 1989; Lam et al 1991; Moss et al 1995) and is thought to be attributable to a reduction in luminance contrast between the stimulus and background, occurring as a result of forward light scatter (Moss et al 1995). The greater attenuation of the short-wavelength visual field could be attributed to the combined effect of forward light scatter inducing a reduction in luminance contrast between the stimulus and background and a shift in chromaticity of the blue stimulus towards that of the yellow background (Moss et al 1995). Effectively, the stimulus becomes less blue and more yellow.

Correction for ocular media absorption reduced the magnitude of the perimetric attenuation of SWAP. However, the resultant attenuation was still greater than that of W-W perimetry. The greater attenuation of SWAP may have been due to additional forward light scattering, not quantified by the forward light scatter meter which employs medium wavelength stimuli. Nevertheless, studies have shown that forward light scatter does not exhibit wavelength dependency (Whitaker et al 1993). The influence of the autofluorescence phenomenon, whereby short-wavelength stimuli are transmitted as visible wavelengths (Occhipinti et al

1986; Larsen and Lund-Andersen 1991; Siik et al 1993), may have induced greater forward light scatter since the degree of autofluorescence is known to increase in age-related cataract (Siik et al 1993). Lenticular autofluorescence has been used to quantify ocular media absorption in SWAP (Teesalu et al 1997), but the influence of autofluorescence on forward light scatter in SWAP has not been quantified.

Backward light scatter, defined by LOCS III did not appear to influence the degree of attenuation of W-W or short-wavelength perimetric sensitivity. Moss et al (1995) reported that SWAP MD_H was greatest in posterior sub-capsular cataract, whereas cortical cataract influenced W-W MD_H more than other cataract morphologies. These differences were attributed to the smaller pupil size in SWAP which arose from the 330 cdm² background luminance used by Moss et al (1995). Furthermore, as the severity of cataract increased, greater attenuation in sensitivity occurred in for both W-W perimetry and SWAP. The lower SWAP background luminance of 100 cdm², in combination with the greater degree of cataract severity of the patients in this study may account for the lack of correlation between the degree of backward light scatter and the magnitude of attenuation in both W-W perimetry and SWAP. The relationship between backward and forward light scatter in age-related cataract is likely to be a complex one. Indeed, in a study of excised human cataractous lenses, van den Berg (1996) reported that lenticular absorption obscures the true degree of forward light scattering.

The lack of clinical improvement in post-operative MD_H in W-W perimetry of four patients may have resulted from greater forward light scatter due to the introduction of the IOL. An increased forward light scatter has been reported by Witmer et al (1989) and Hard et al (1993). The four patients yielded a positive post-operative ICSP which indicates greater forward light scatter than expected for age.

The post-operative SWAP MD_H uncorrected for the effects of ocular media absorption was positive in all patients. This finding was not surprising, since the absorption characteristics post-operatively can be considered equivalent to a young adult crystalline lens (Said and Weale 1959; Powers et al 1981). Since ocular media absorption increases with age, the

difference between the measured sensitivity and the age-corrected sensitivity for SWAP would be expected to be greater in a pseudophakic observer than in a phakic observer of the same age.

The finding of a greater post-operative PSD and CPSD has been reported previously for W-W perimetry in glaucoma (Chen et al 1996; Smith et al 1996). The reduced magnitude of PSD and CPSD pre-operatively may have resulted from forward light scatter increasing the degree of spatial summation across the visual field. Therefore, any small depressions in the shape of the hill of vision may have been lost.

The influence of cataract on the SWAP visual field has profound implications for the statistical interpretation of SWAP. The wider confidence limits of SWAP due to greater between-subject variability (Chapter 4) may lead to a total deviation probability not reaching statistical significance. Similarly, the high positive total deviation of SWAP post-operatively, may also lead to a total deviation probability not reaching statistical significance. Patients with cataract may not be suitable for serial analysis of the visual field since the accelerated absorption of short-wavelengths may influence confidence limits and may yield diminishing focal loss. These problems may be overcome by adopting different methods for analysing SWAP. Statistical methods which extract the local spatial variability may be more effective in the identification of focal visual field loss (Crabb et al 1995; Fitzke et al 1995).

The influence of SWS isolation on cataract is unknown. It would be expected that the degree of SWS isolation would be reduced and extend over a different decibel range than in normal subjects. When attenuation exceeds 1.5 log units (15 dB) in normal subjects, SWS isolation may be lost (Johnson et al 1993a; Sample et al 1993, Sample et al 1997) and SWAP would stimulate the MWS pathway. Therefore, the diagnostic advantage of SWAP would be lost. Furthermore, since both SWAP and W-W perimetry would be stimulating the luminance pathway, W-W perimetry may be a more viable technique since it inherently exhibits less between-subject variability.

6.12. Conclusions.

It is clear that age-related cataract attenuates SWAP to a greater degree than W-W perimetry. There is likely to be a complex interaction between the magnitude of absorption, forward and backward light scatter and their influence on the perimetric attenuation of SWAP. Methods may be sought which quantify forward light scatter using short-wavelength stimuli. There is also a need to quantify the influence of lens autofluorescence on forward light scatter in SWAP. Contrast sensitivity measurement as opposed to Snellen visual acuity may provide an insight into the mechanism of SWAP attenuation since the W-W stimulus is composed of high spatial frequencies whereas the SWAP stimulus is composed of predominantly low spatial frequencies. The reduced dynamic range of SWAP induced by age-related cataract may not be sufficient to detect and quantify focal loss.

CHAPTER 7. QUANTIFICATION OF SHORT-WAVELENGTH SENSITIVE PATHWAY ISOLATION IN SHORT-WAVELENGTH AUTOMATED PERIMETRY.

7.1. Introduction.

SWAP is a clinical application of the two-colour increment threshold procedure of Stiles (1939). As was discussed in Chapter 4, a high luminance, broadband yellow background simultaneously saturates the MWS (medium-wavelength sensitive) pathway, LWS (long-wavelength sensitive) pathway, and the rods, whilst a blue stimulus stimulates the SWS (short-wavelength sensitive) pathway.

In the two-colour increment threshold method, the eye is adapted to a uniform field of wavelength, μ , and luminance, M_μ , which extends over the given retinal area. A test stimulus of wavelength, λ , of approximately 1° diameter is applied to the adapting field and the smallest detectable increase in stimulus luminance is termed the increment threshold, N_λ . Two-colour increment thresholds may be evaluated by any one of three methods. Plotting $\log N_\lambda$ as a function of λ for a fixed value of μ and M_μ yields a threshold versus wavelength curve (tv λ). Determining $\log N_\lambda$ as a function of $\log M_\mu$, whilst λ and μ remain constant, yields a threshold versus radiance (tvr) curve. The terms radiance and intensity are synonymous and such functions are more commonly referred to as threshold versus intensity (tvi) curves. Determining the value of the field radiance required to raise the increment threshold, N_λ to a fixed multiple of the value when $M_\mu = \text{zero}$ and λ remains constant, yields field radiance versus field wavelength curves (fv μ).

Employing a variety of background and stimulus conditions, Stiles (1939) produced a series of foveal tvi curves which described three functions termed π (pi) mechanisms with maximum sensitivities in the red, green and blue regions of the spectrum. For the i th component pi-mechanism, the increment threshold N_λ is defined by the equation:

$$\frac{1}{N_{i\lambda}} = \pi_{i\lambda} \zeta_i(M_\mu \Pi_{i\mu}) \quad \text{Eqn 7.1.}$$

where:

$$\Pi_{i\mu} = \frac{1}{M_\mu} \quad \text{Eqn 7.2.}$$

The function $\zeta_i(x)$ defines the shape of the tvi curve of the pi-mechanism. When M_μ equals zero, $\pi_{i\lambda}$ is the absolute threshold. This represents the test spectral sensitivity of the pi-mechanism. When M_μ is equal to unity, $\Pi_{i\mu}$, represents the field spectral sensitivity of the pi-mechanism. In the middle or rising portion of the tvi curve, the Weber-Fechner Law applies.

Thus:

$$\frac{N_\lambda}{M_\mu} = \text{constant} \quad \text{Eqn 7.3.}$$

Further studies by Stiles (1959) revealed the presence of seven foveal pi-mechanisms, namely; π_1 , π_2 , and π_3 with spectral sensitivity peaks in the short-wavelength region of the spectrum; π_4 and π'_4 whose spectral sensitivity peaked in the medium-wavelength region; and π_5 and π'_5 whose spectral sensitivity peaked in the long-wavelength region. A scotopic pi-mechanism, attributed to the rods, was termed π_0 . The spectral sensitivity and corresponding Weber-Fechner fraction define each individual pi-mechanism (Table 7.1). The pi-2 mechanism is not evident in every observer and covers a range of thresholds not thought to be greater than 0.4 log units (Wyszecki and Stiles 1982; Watkins 1969).

Characteristic changes in the nature of the pi-mechanisms, defined by tvi curves, occur as λ and μ are varied. These are referred to as Displacement Rules (Stiles 1939). A change in the stimulus wavelength, λ , when the adapting field wavelength, μ , remains constant will result in a shift of the tvi curve parallel to the ordinate axis by an amount determined by the relative spectral sensitivity of the mechanism under study (Figure 7.1). Alternatively, a change in the adapting field wavelength, μ , whilst the stimulus wavelength, λ , remains constant will result in displacement of the tvi curve by an amount which is also fixed by the relative spectral sensitivity of the mechanism under study (Figure 7.1). The assumption that the shape of the tvi curve must remain constant when the stimulus wavelength is changed is termed field

Cone Type	Pi-Mechanism	Wavelength of Maximal Spectral Sensitivity (nm)	Weber-Fechner Fraction
s	π_1	440	8.7
s	π_2	between 440 & 480	unknown
s	π_3		440
m	π_4	540	1.9
m	π'_4	540	unknown
l	π_5	575	1.8
l	π'_5	587	unknown

Table 7.1. Summary of the characteristics of each individual foveal pi-mechanism derived using data from Enoch (1972).

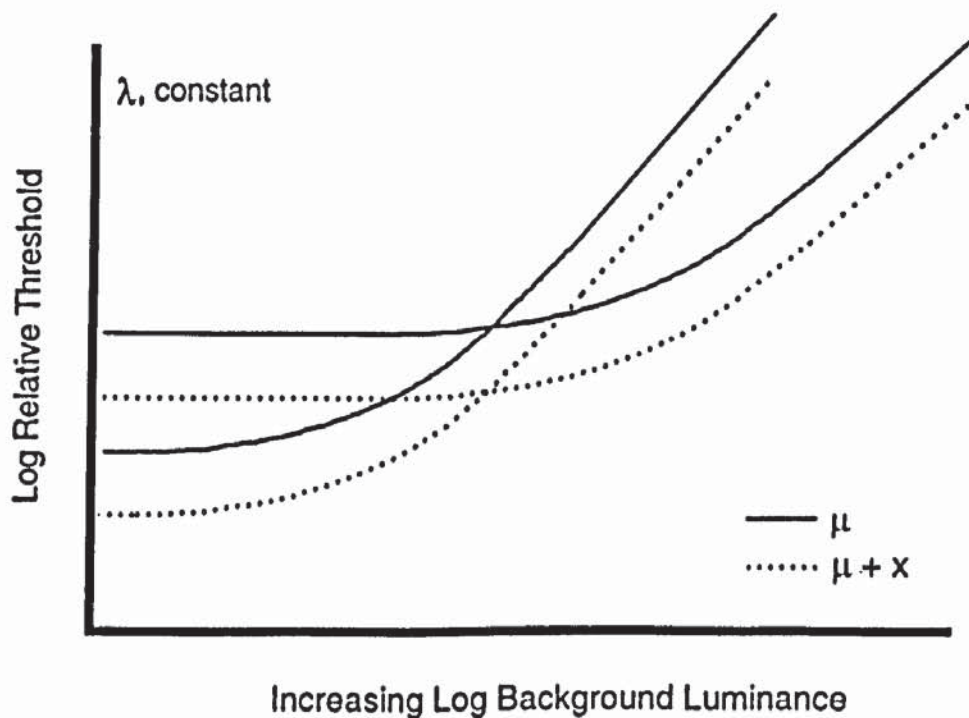
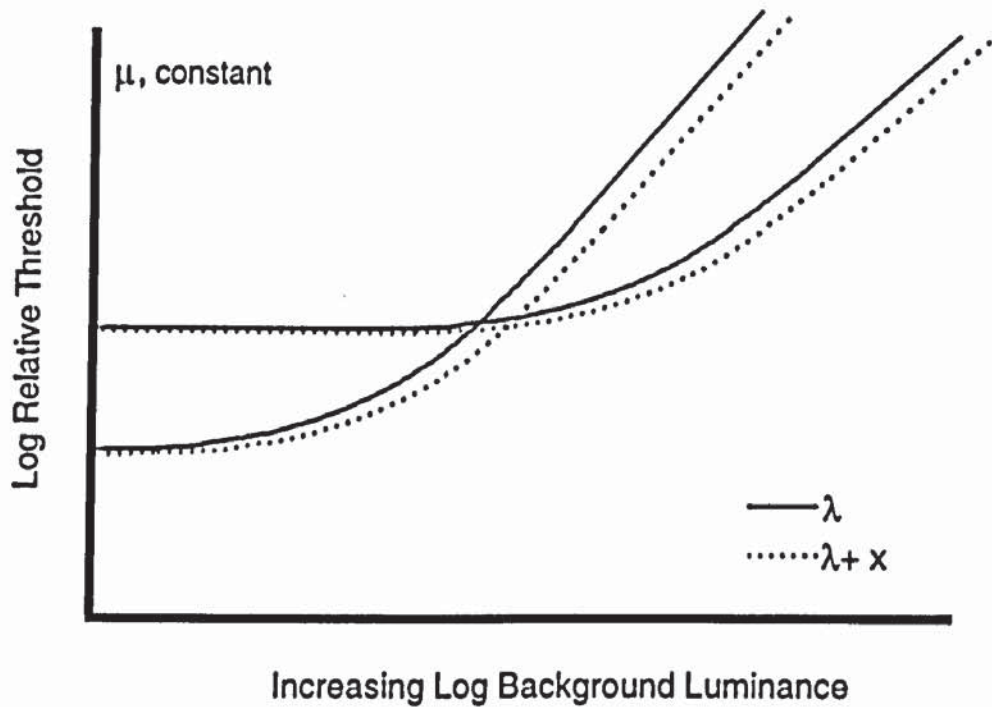


Figure 7.1, Stiles Displacement Rules. The top figure illustrates the lateral shift which occurs in a tvi function when the stimulus wavelength, λ , is increased, whilst the adapting wavelength, μ , remains constant. The bottom figure illustrates the downward shift which occurs in a tvi function when the adapting wavelength, μ , is increased, whilst the stimulus wavelength, λ , remains constant.

univariance. Correspondingly, the assumption that the shape of the tvl curve must remain constant when the adaptation wavelength is changed is termed test univariance (Sigel and Brousseau 1982).

Univariance predicts that any physiological function, for example a tvl curve, controlled by a single class of photoreceptor must have a shape which is independent of the wavelength of the stimulus (Augenstein and Pugh 1977). If pi-mechanisms are independent, univariant mechanisms, then adapting fields will act additively in controlling the sensitivity of the mechanisms (Boynton et al 1966; Pugh 1976). Clearly, the number of foveal pi-mechanisms is in conflict with the established Trichromacy theory of colour vision. The pi-mechanism must therefore, be a feature of the neural processing of colour (Wyszecki and Stiles 1982). Further evidence to support this hypothesis derives from studies which demonstrate that some pi-mechanisms are non-additive and do not exhibit field or test univariance (Pugh 1976).

A series of unified theories have been proposed to explain the nature of the SWS mechanisms (pi-1 and pi-3), the MWS mechanisms (pi-4 and pi-4') and the LWS mechanisms (pi-5 and pi-5') (Pugh 1976; Augenstein and Pugh 1977; Pugh and Mollen 1979; Sigel and Brousseau 1982; Wandell and Pugh 1980a, b).

Pugh (1976) reported that when two adapting fields, μ_1 and μ_2 , of wavelengths less than 500 nm were combined, pi-1 was additive, but when a short-wavelength adaptation field, μ_1 , of wavelength less than 500 nm was mixed with a long-wavelength field, μ_2 , of wavelength greater than 550 nm, pi-1 was strongly non-additive. Augenstein and Pugh (1977) reported that the time course of the pi-1 adaptation was not spectrally univariant. Pugh and Mollen (1979) developed a unified model to account for the nature of the pi-1 and pi-3 mechanisms in which the detection signal passed sequentially through two gain stages: the first controlled by the s-cones alone; the second controlled by an opponent signal generated either by the m-, or the l-cones, or both. The gain of the pathway was the product of the attenuation factors at the first and second sites.

Sigel and Brousseau (1982) demonstrated that the π_4 mechanism did not exhibit test and field univariance when a stimulus duration of 10 ms was employed. A unified model was constructed to explain the nature of the π_4 and π_4' mechanisms which stated that the detection of a stimulus was dependent upon the output of an achromatic process which summed the signals from all three classes of cone. The resultant attenuation of cone signals was determined from the degree of stimulation by the field for each class of cone, such that the sum of the three adapted signals generated a steady-state achromatic signal which was due to the adapting field. When the test stimulus plus steady state response exceeded a criterion level, detection occurred. The model suggested that for a stimulus duration of 10 ms, stimuli of any wavelength greater than 500 nm were detected through the achromatic system, corresponding to π_4 , π_4' and π_5 . For stimulus durations of 200 ms and wavelengths of between approximately 500 nm and 600 nm, only π_4 and π_4' were mediated through the achromatic pathway.

Wandell and Pugh (1980a) showed that for a stimulus wavelength of 667 nm and duration 10 ms, Displacement Rules and field additivity applied such that a single t_v function defined the action of the l-cones. Stimulus detection therefore, was thought to originate from a single class of cone. However, when the stimulus duration was increased to 200 ms (Wandell and Pugh 1980b) failures in univariance and field additivity occurred, π_5 mediated detection at low field intensities, and π_5' mediated detection on high intensity fields. A model with two-detection pathways was constructed to explain these conflicting results. The detection signal passed through both pathways with the more sensitive of the two pathways mediating stimulus detection. The first site was univariant and termed the field-additive pathway and the second pathway was chromatically opponent, receiving signals from all classes of cones. At low background intensities, only the field-additive pathway adapted. When moderate or intense backgrounds were employed, the second site adapted in addition to the field-additive pathway resulting in attenuation of the signals.

7.2. The Optimum Conditions for SWAP.

The choice of background and stimulus conditions employed in SWAP must be chosen to ensure maximal isolation of the SWS pathway, whilst allowing an adequate dynamic range. The background and stimulus conditions which achieve optimal isolation of the SWS pathway are equivocal and are summarised in Table 7.2.

The background luminance required to suppress rod activity is equivocal. Aguilar and Stiles (1954) reported that background luminances of between 120 cdm^2 and 300 cdm^2 were required to ensure saturation of the rod system, whilst Yeh and co-workers (1989) found that an adaptation level of greater than approximately 140 cdm^2 (for a pupil diameter of 3 mm) was necessary to ensure SWS pathway isolation in the normal eye. Sample and Weinreb (1990) advocated employing a background luminance of 80.9 cdm^2 , arguing that greater adaptation levels serve only to increase SWS thresholds rather than increase the magnitude of SWS isolation. The background luminance utilised in the commercially available SWAP is 100 cdm^2 , transmitting visible wavelengths above 530 nm (Figure 4.2).

The choice of stimulus filter for SWAP is also equivocal. A narrowband wavelength stimulus filter guarantees isolation of the SWS pathway but attenuates the dynamic range of the perimeter due to the reduced spectral transmission of the filter. In order to increase the dynamic range, some workers have advocated the use of a broadband wavelength blue filter because the spectral transmission of such filters is greater than for narrowband filters (Adams et al 1991; Johnson et al 1991, 1993a, b; Moss et al 1994, 1995; Johnson and Keltner 1995; Wild et al 1995). Nevertheless, it has been argued that such a broadband stimulus does not guarantee isolation of the SWS pathway and, in the presence of an SWS deficit, may stimulate the MWS pathway (Sample and Weinreb 1990). Furthermore, thresholds obtained with a narrowband filter may be less susceptible to shifts in the peak retinal wavelength due to advancing cataract (Sample et al 1996). The stimulus adopted in the commercially available SWAP is a narrowband 440 nm filter (Figure 4.2).

	Yellow Background Filter	Blue Stimulus Filter	Background Luminance (cd/m ²)	Magnitude of SWS Isolation (log units)
Adams et al (1991); Johnson et al (1991, 1993a, b); Johnson and Keltner (1995)	Schott OG530	OCLI broadband	200	1.5
Sample et al (1990, 1993, 1994); Weinreb et al (1991)	Wratten # 12	440nm narrowband	89	1.5
Heron et al (1988)	Schott OG530	Wratten 47B broadband	500	unknown
Hudson (1993a)	Schott OG530	460nm narrowband	330	1.4
Moss et al (1994; 1995); Wild et al (1995)	Schott OG530	OCLI broadband	330	1.4

Table 7.2. Summary of background and stimulus parameters employed for SWAP.

The increase in spatial summation with increasing stimulus size is greater for short-wavelengths than for other wavelengths (King-Smith and Carden 1976). Indeed, Adams et al (1991) reported little, or no, SWS pathway isolation when stimulus sizes smaller than Goldmann size IV were employed. Temporal summation is maximal for the pi-1 and pi-3 mechanisms at 200 ms (King-Smith and Carden 1976; Friedman et al 1984). The conventional stimulus size in SWAP is a Goldmann size V (1.724°) of 200 ms duration.

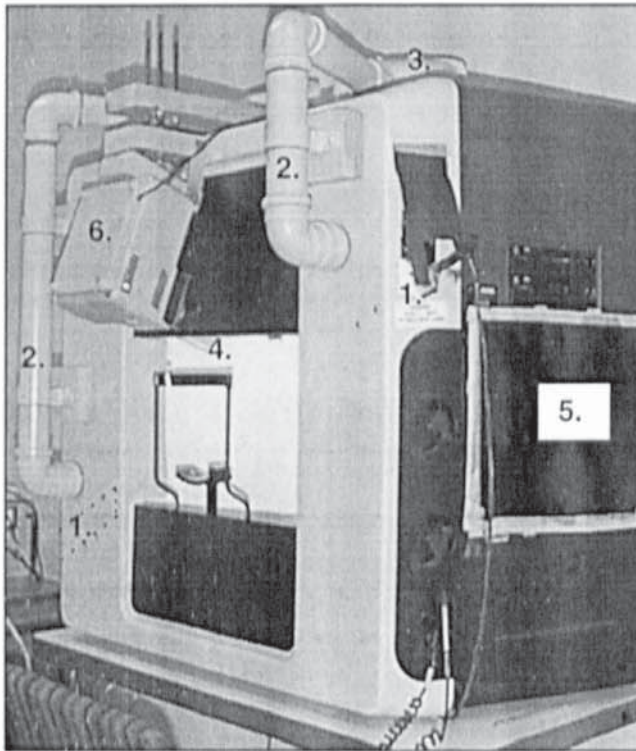
7.3. Aims.

Previous investigations of the magnitude of SWS pathway isolation have only been determined at the fovea (Sample et al 1990; Johnson et al 1993a). Early glaucomatous visual field loss occurs beyond the foveal region (Hart and Becker 1982, Mikelberg and Drance 1984, Caprioli et al 1987). It is therefore, important to establish the characteristics of the SWS pathway across the visual field. The aim of this study was twofold, to quantify the magnitude of SWS pathway isolation with increasing eccentricity and to evaluate the standardised background and stimulus conditions in order to establish whether they achieved optimal isolation of the SWS pathway.

7.4. Equipment Modifications and Theoretical Considerations.

In order to obtain the perimetric data necessary for construction of the tvl curves, further modifications were made to the HFA 640 initially modified by Hudson and Wild (1993) and illustrated in Figure 7.2. This comprised two auxiliary lamp housings, illustrated in Figure 7.3, each containing an ELE/ELT 80 Watt/30 Volt tungsten-halogen bulb (General Electric Co, Cleveland, Ohio, USA); an infra-red absorbing filter which protected the filters beyond; a Schott OG530 filter which provided a broadband yellow background (Figure 7.4) and an opal diffusing filter which was fitted flush with the perimeter cupola surface ensuring uniform illumination over the surface. Each bulb was operated at a reduced voltage of 28.5 Volts in order to extend the life span of the bulb. A stabilised power unit (Farnell Instruments Ltd, Wetherby, West Yorkshire, UK) supplied each bulb. Each lamp housing was constructed of aluminium alloy which acted as a heat sink. A ventilation system directed cool air over each lamp housing and further dissipated the heat generated by the bulbs. Concave spherical

Humphrey Field Analyser 640 showing the modifications made for SWAP and macular pigment absorption assessment.



KEY.

1. Auxiliary lighting unit providing yellow background for SWAP.
2. Ventilation duct.
3. Ventilation fan dissipates the heat generated from the auxiliary lighting unit.
4. Infra-red light source for monitoring fixation at low bowl luminances.
5. Removable neutral density filter covering television monitor, used to reduce the ambient room illumination at low background luminances.
6. Auxiliary lighting unit providing red background for macular pigment absorption assessment.

Stimulus filter holder.

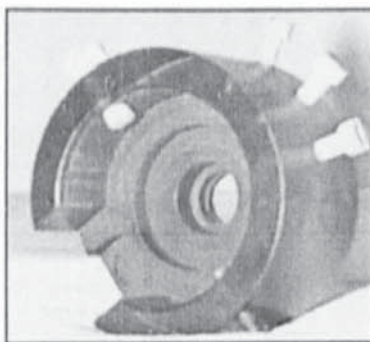
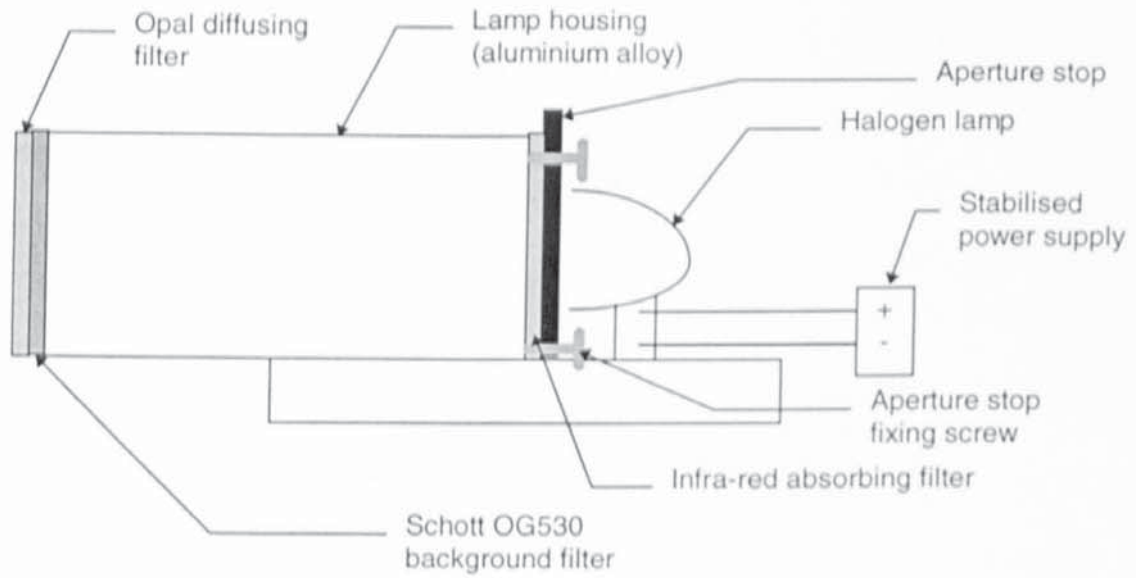


Figure 7.2. Humphrey Field Analyser 640 showing the modifications for SWAP and macular pigment absorption assessment (top) and the stimulus filter holder (bottom) which is attached to the projection arm of the perimeter.

Schematic diagram of the auxiliary lighting unit.



Apertures used to modify the background luminance.

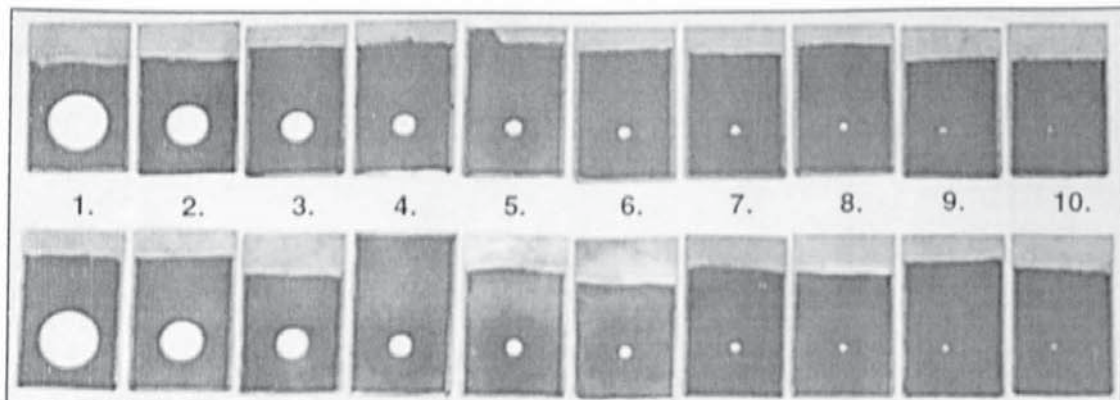


Figure 7.3. Schematic diagram of the auxiliary lighting unit fitted to the modified Humphrey Field Analyser (top) and the ten apertures used to modify the background luminance (bottom).

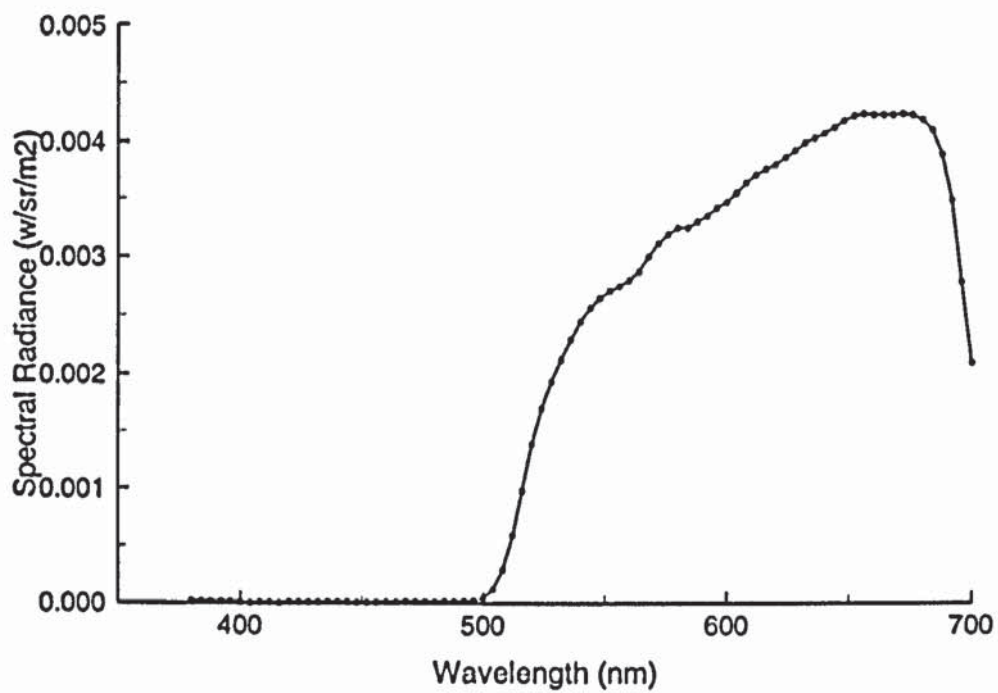


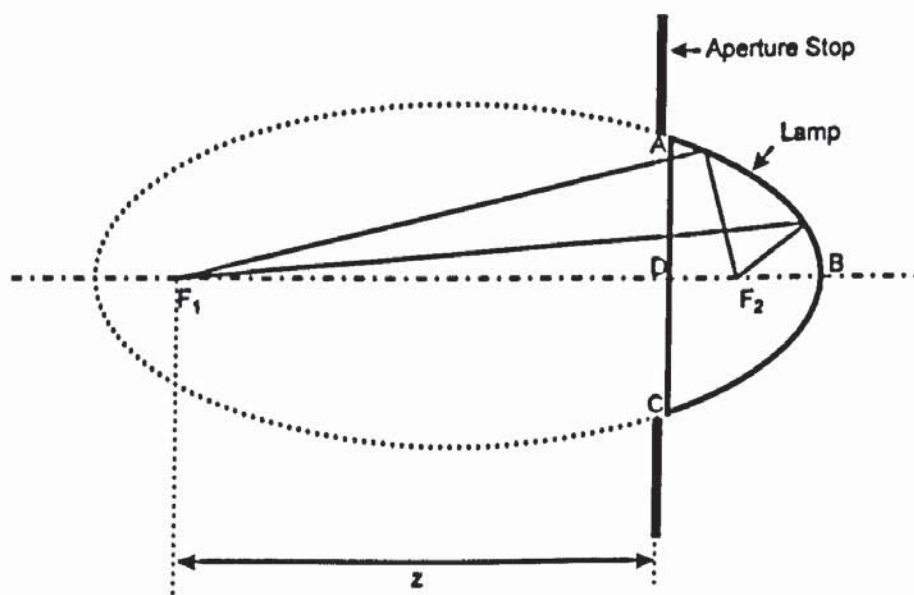
Figure 7.4. Spectral radiance as a function of wavelength for the Schott OG530 in combination with the infra-red absorbing filter. Visible wavelengths above 530 nm are transmitted and wavelengths above 700 nm are absorbed.

reflectors were installed into the stimulus projection system to increase the dynamic range of the perimeter.

Previous workers have achieved the necessary variation in background luminance by altering the voltage supply to the lighting units (Sample et al 1990; Johnson et al 1993a). This approach suffers from the disadvantage that variation in the colour temperature of the bulbs alters the spectral distribution of the background, thereby preferentially inducing a change in the adaptation level of the MWS and LWS pathways. Neutral density filters are commonly used in psychophysical techniques which evaluate tvf functions (Pugh and Mollen 1979; Wandell and Pugh 1980a, b; Sigel and Brousseau 1982) and would ensure that the colour temperature of the background is constant over the range of background luminances employed. However, they could not be used in this study due to difficulties incorporating them into the existing illumination system. Instead, the background luminance was varied by introducing a series of aperture stops into the illumination system. Manufactured from metal, they were unaffected by the heat generated by the bulbs and all possessed the same thickness, making them easy to install within the illumination system. A further advantage of adopting an aperture stop system was that unlike neutral density filters, aperture stops are not spectrally dependent.

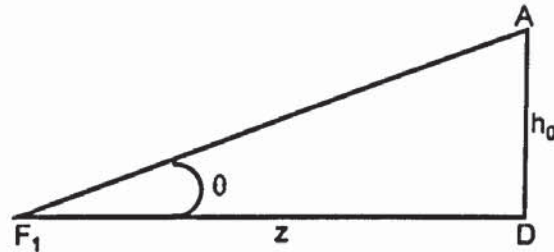
7.4.1. Aperture Stop Construction.

Consider the diagram below:



where, ABC, represents the plane of the lamp front, F_1 , is the image of the lamp filament, F_2 , is the lamp filament. The distance, F_1D , is equal to the distance, z . The distance between the plane of the aperture stop and the silvered portion of the lamp's surface is negligible.

Simplifying:



where, z , is the distance from the image of the filament to the plane of the aperture stop and, h_0 , is the radius of the lamp reflector. By measurement, $z = 80$ mm and, $h_0 = 21.4$ mm.

$$\tan \theta_0 = \frac{h_0}{z} \quad \text{Eqn 7.4.}$$

$$\theta_0 = \underline{15^\circ}$$

The light transmitted by any aperture stop is proportional to the solid angle, ω , which the stop subtends at F_1 , the first focus of the reflector, i.e. the image of F_2 in the middle of the filament.

Thus:

$$\omega = 2\pi (1 - \cos \theta) \quad \text{Eqn 7.5.}$$

Let the quantity, m , = $\frac{\omega}{2\pi}$

Thus:

$$m = 1 - \cos \theta \quad \text{Eqn 7.6.}$$

When no aperture stop is in place,

$$m_0 = 1 - \cos \theta_0$$

$$= 1 - \cos 15$$

Ten aperture stops were constructed from 0.38 mm brass sheet, drilled using commercially available tools. Each successive aperture stop, numbered N_1 to N_{10} , was designed to reduce

the background luminance of the HFA of the previous aperture stop by half, ie in 0.3 log unit steps. The quantity, n , defines the required reduction in luminance for each aperture stop:

$$n = 2^N \quad \text{Eqn 7.7.}$$

Therefore, the radius of each aperture stop can be calculated as follows:

Rewriting Equation 7.6 for any aperture stop:

$$m_N = \frac{1 - \cos 15}{n}$$

Then:

$$1 - \cos \theta_N = \frac{1 - \cos 15}{n}$$

Rearranging:

$$\cos \theta_N = \left(1 - \frac{1 - \cos 15}{n} \right)$$

$$\theta_N = \cos^{-1} \left(1 - \frac{1 - \cos 15}{n} \right)$$

Rewriting Equation 7.4 for any aperture stop:

$$\tan \theta_N = \frac{h_N}{z}$$

$$h_N = z \tan \theta_N$$

Substituting for θ_N :

$$h_N = 80 \tan \left[\cos^{-1} \left(1 - \frac{1 - \cos 15}{n} \right) \right] \quad \text{Eqn 7.8.}$$

Table 7.3 summarises the values of, n , and, h , for each aperture stop and the calculated diameters required for manufacture of each aperture stop. Each aperture stop was painted with heat resistant black paint to ensure absorption of any straylight within the illumination system. A series of screws were inserted into each of the two auxiliary lighting unit to enable the placement of each aperture stop. A schematic diagram of an auxiliary lighting unit, and the ten aperture stops are illustrated in Figure 7.3.

Aperture number	Reduction in luminance (log units)	Multiple reduction in luminance, n	Aperture stop radius, h (mm)	Aperture stop diameter, D (mm)
1	0.3	2	12.48	24.96
2	0.6	4	8.74	17.48
3	0.9	8	6.15	12.30
4	1.2	16	4.34	8.68
5	1.5	32	3.07	6.14
6	1.8	64	2.17	4.34
7	2.1	128	1.53	3.06
8	2.4	256	1.08	2.16
9	2.7	512	0.76	1.52
10	3.0	1024	0.54	1.08

Table 7.3. Summary of the calculations used for the construction of aperture stops.

The aperture stop system was evaluated by mounting each auxiliary lighting unit on an optical bench and measuring the luminance with a mini spot photometer. Figure 7.5 illustrates the reduction in luminance for each aperture stop. Deviation from the expected luminance values for each of the two auxiliary lighting units was observed at low luminance levels and was probably due to inaccuracies in the manufacture of the tungsten-halogen bulbs, the filaments being incorrectly aligned. Nevertheless, this deviation was not present in the graph of mean luminance which was equivalent to that obtained when the aperture stops were in situ within the perimeter, because the cupola evenly distributes the light over the entire surface. The background luminance of the perimeter was measured using an LMT L1003 spot photometer (LMT Lichtmesstechnik GMBH Berlin, Germany) and the luminance of each background resulting from the introduction of the aperture stops calculated using the mean log unit reduction in luminance derived in Figure 7.5.

7.5. Materials and Methods.

7.5.1. Sample.

The sample comprised seven normal subjects of mean age 26.8 years (SD 1.8), ranging in age between 25 and 29. Five subjects were female. All subjects were experienced at short-wavelength Full Threshold automated static perimetry. All subjects met the inclusion criteria previously described in Section 4.5.1.

7.5.2. Perimetry.

The Humphrey Field Analyser background illumination system was extinguished using internal software commands, and the stimulus size altered to Goldmann size V. The default stimulus duration of 200 ms was used at all background luminances. A custom Full Threshold program was designed to measure the threshold at six stimulus locations including the fovea, which is illustrated in Figure 7.6.

One eye of each subject was examined seven times, each visit separated by between one and two weeks. In order to prevent changes in the pupil diameter over the range of luminances

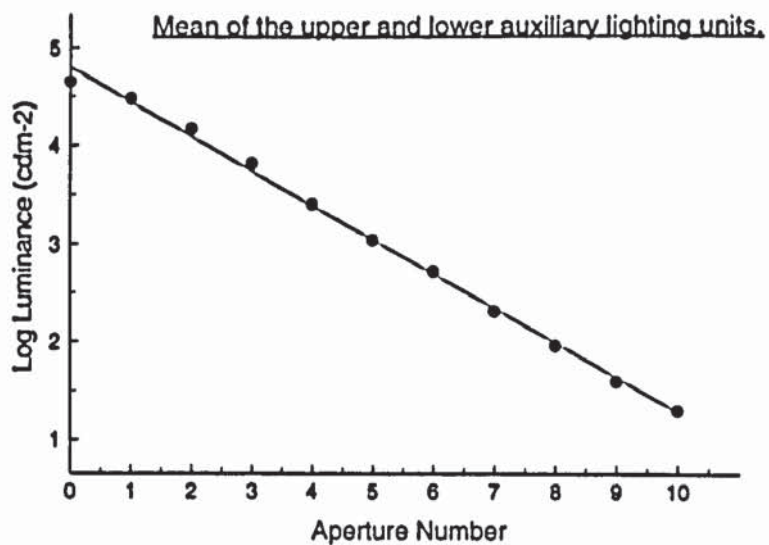
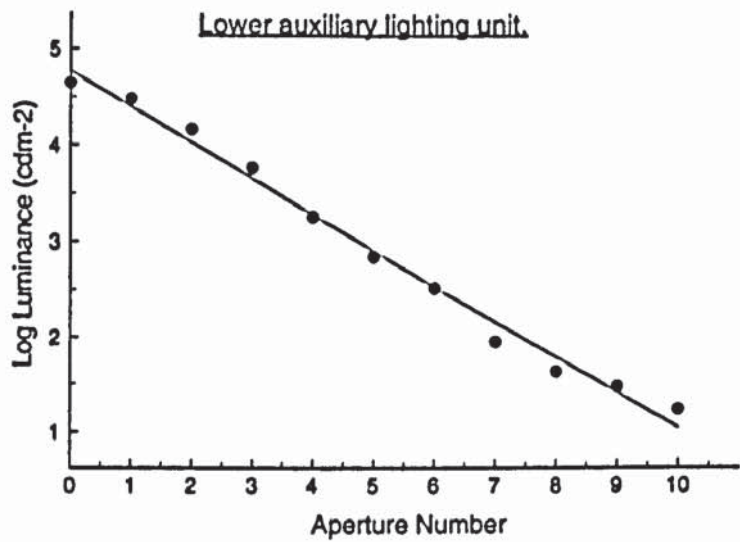
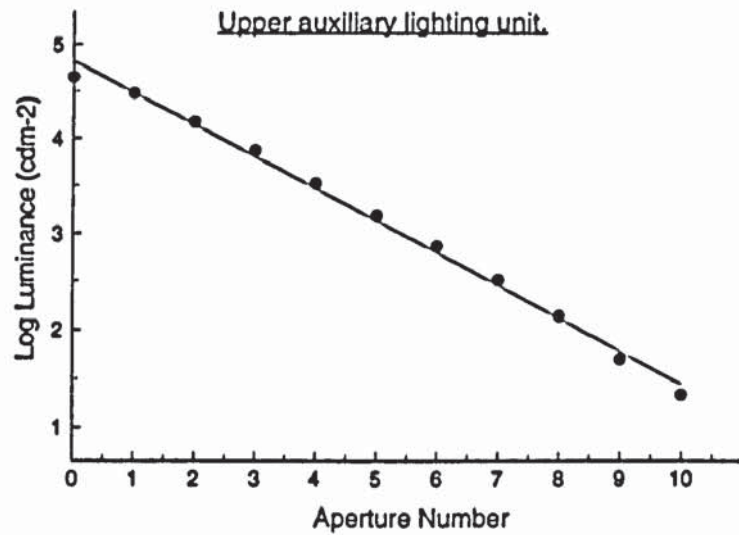


Figure 7.5. Reduction in luminance of the upper (top) and lower (middle) auxiliary lighting units resulting from the insertion of the aperture stops within the optical path. The bottom graph illustrates the mean reduction in luminance from the combination of the auxiliary lighting units.

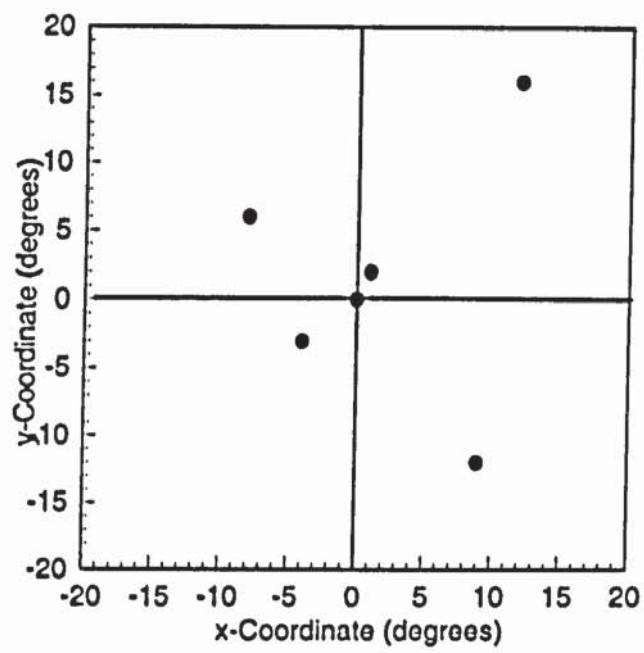


Figure 7.6. Spatial configuration of the test grid (left eye).

investigated, the left pupil was dilated forty minutes prior to the commencement of each examination by instilling one drop of 0.5% Tropicamide Hydrochloride into the lower conjunctival sac (punta closed). The mean pupil diameter was 6.55 mm (SD 0.40 mm) and was unresponsive to light throughout the examination. At the first six perimetry visits, two background adaptation levels were investigated for each of three stimulus conditions. One adaptation level was investigated at the final perimetry visit. The aperture stops selected for examination were randomised between the visits. The lowest adaptation level was examined first at each examination in order to reduce the time required to adapt the MWS and LWS pathways. Adaptation times varied between three minutes for the highest adaptation level and thirty minutes for the lowest adaptation level. The stimulus conditions were randomised for each adaptation level and consisted of 440 nm (Half-Peak Width (HPW) 10 nm), 450 nm (HPW 15 nm) and 460 nm (HPW 10 nm) narrowband stimuli (Figure 7.7). The duration of each perimetry visit was approximately 90 minutes. In order to reduce the influence of fatigue on the measured thresholds, frequent rest periods were introduced. The near refraction compatible with the degree of cycloplegia was employed throughout and was frequently checked during the examination since Tropicamide induces short-duration cycloplegia.

7.5.3. Pre-Receptorial Absorption.

At a separate perimetry visit, ocular media and macular pigment absorption were assessed under cycloplegia.

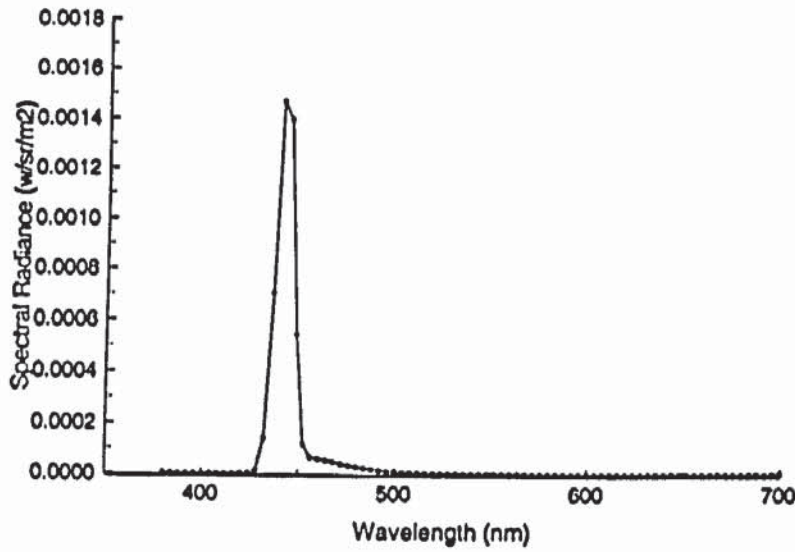
Ocular Media Absorption.

The procedure for assessing ocular media absorption is described in full in Section 4.5.3.

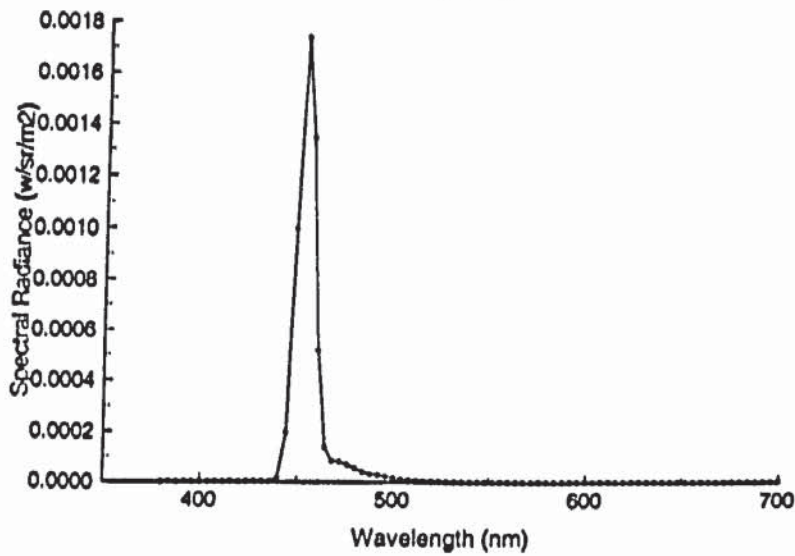
Macular Pigment Absorption.

Macular pigment is located within the receptor axon and the inner plexiform layers of the macula (Snodderly et al 1984a). It is primarily composed of short-wavelength absorbing carotenoids, mainly zeaxanthin which is dominant at the centre of the fovea and leutin, with minor constituents which have yet to be isolated (Snodderly et al 1984a). The elongated molecular structure of zeaxanthin and leutin results in dichroism, whereby the absorption of

440 nm narrowband stimulus filter.



450 nm narrowband stimulus filter.



460 nm narrowband stimulus filter.

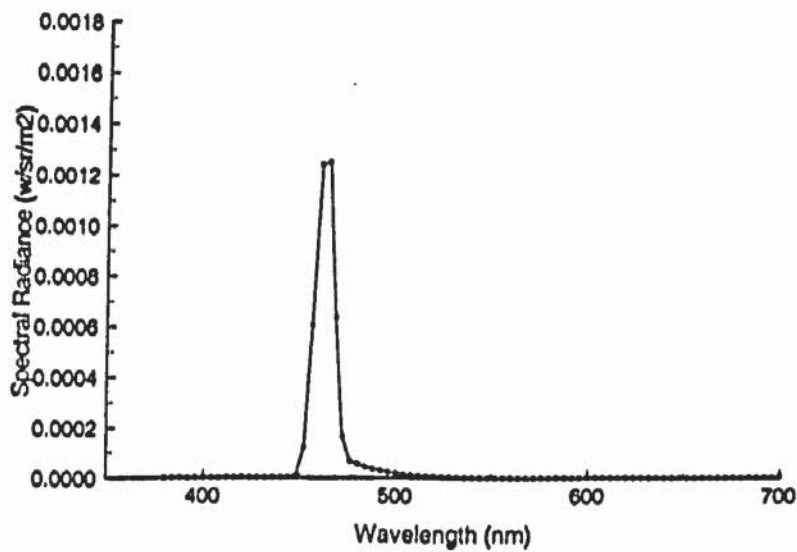
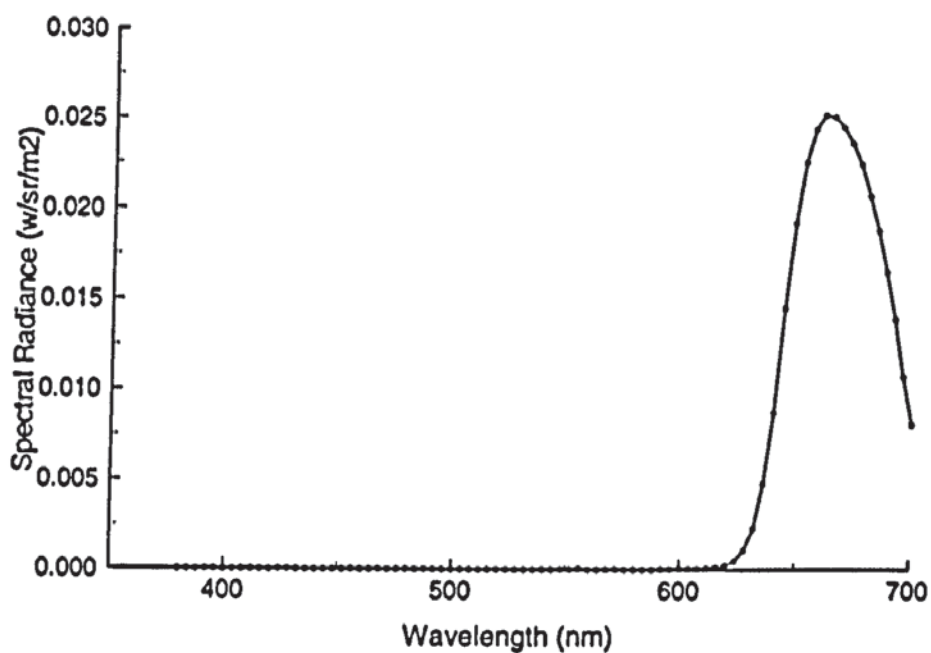


Figure 7.7. Spectral radiance as a function of wavelength for the 440 nm (top), 450 nm (middle) and 460 nm (bottom) narrowband stimulus filters.

polarised light is dependent upon the angle of incidence relative to the axis of the molecule (Bone and Landrum 1984). The zeaxanthin and leutin molecules are regularly arranged such that the molecular axes are aligned tangentially in concentric circles around the macula (Bone and Landrum 1984; Bone et al 1992). Macular pigment exhibits greatest density at the foveola and gradually decreases with eccentricity until it reaches a constant level at approximately 4° from the fovea (Snodderly et al 1984b). Macular pigment density does not vary significantly between eyes (Hammond et al 1992). High between-subject variability in macular pigment density has been reported which is not related to age (Werner et al 1987).

Pease and Adams (1983) developed a method for measuring macular pigment absorption *in vivo*, based upon measuring the spectral sensitivity function for the MWS pathway. This technique was adapted for use with the modified HFA (Wild and Hudson 1995). A light box was mounted above the forehead rest of the HFA. This comprised an ELC 250 W, 24 V tungsten halogen lamp (General Electric, Cleveland, Ohio, USA) mounted behind a series of infra-red absorbing filters, cooled by a squirrel cage fan (Figure 7.2). A red adapting field of diameter 26° and luminance 425 cdm^{-2} was produced from the combination of the light box and the two auxiliary lamp housings, each incorporating a Schott RG645 broadband filter (Figure 7.8). The transmission characteristics of this filter allowed adaptation of the LWS pathway. A 25 Hz flicker wheel was positioned in the optical path of the HFA stimulus between the stimulus bulb and the aperture plate. A relay coil allowed the flicker wheel to be reset when not in use, preventing the stimulus light path from becoming hindered. Each subject was adapted to the red field for approximately three minutes prior to commencement of the procedure. Using a custom threshold program, a Goldmann size V stimulus flickering at 25 Hz of duration 1300 ms, measured MWS pathway sensitivity at the fovea and eccentricities of 5.5° and 8° for each of the three short-wavelength stimuli and a 570 nm narrowband stimulus (Figure 7.8). The 25 Hz flicker excluded stimulus detection by the rods and s-cones. The difference in measured sensitivities between 5.5° and 8° eccentricity for the each short-wavelength stimulus relative to a value of zero at the fovea is attributable to absorption by the macular pigment. Macular pigment absorption was calculated for each subject using the equation:

Schott RG645 broadband background filter in combination with an infra-red absorbing filter.



570 nm narrowband stimulus filter.

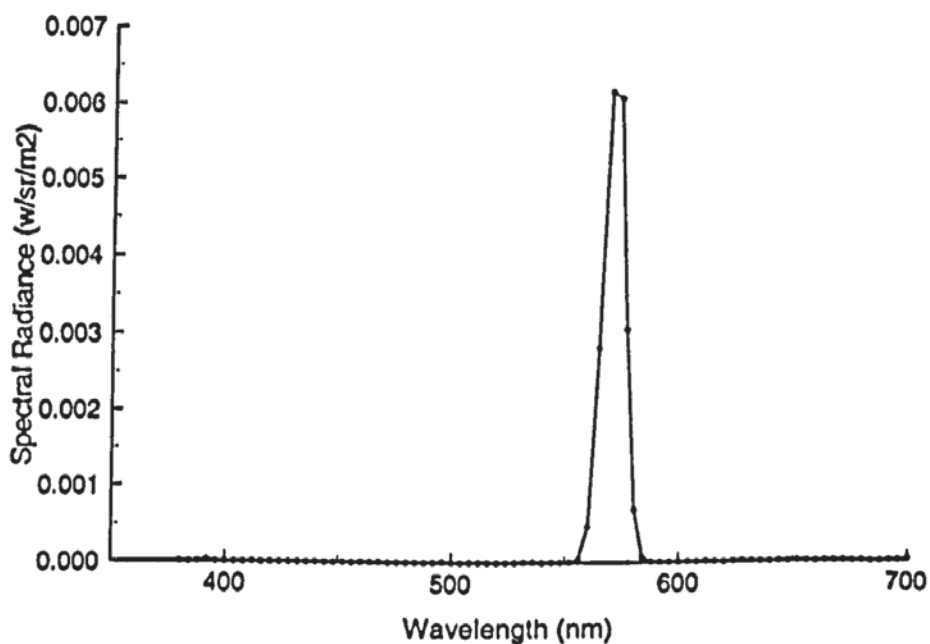


Figure 7.8. Spectral radiance as a function of wavelength for the broadband red background in combination with the infra-red absorbing filter (top) and the 570 nm narrowband stimulus filter employed in the assessment of macular pigment absorption. The broadband background transmits visible wavelengths above 645 nm and the infra-red filter absorbs wavelengths beyond 700 nm.

$$OD_{mac} = (\log S_{p_{filter}} - \log S_{f_{filter}}) + (\log S_{f_{570}} - \log S_{p_{570}}) \quad \text{Eqn 7.7.}$$

where, OD_{mac} is the individual macular pigment optical density at the short-wavelength stimulus wavelength under investigation, $\log S_{p_{filter}}$ and, $\log S_{f_{filter}}$ are the measured sensitivities at 8° and the fovea (or 5.5°) for either the 440 nm, 450 nm or 460 nm stimulus filter, and, $\log S_{p_{570}}$ and, $\log S_{f_{570}}$ are the measured 570 nm sensitivities at the fovea (or 5.5°) and at 8° respectively.

The printout from the HFA did not take into account the attenuation in stimulus luminance caused by the introduction of the narrowband filter or the magnitude of background luminance. Each threshold was therefore, recalculated according to the procedure outlined in Chapter 4 and normalised relative to the maximum stimulus luminance of 64.5 asb utilised in the commercially available SWAP. A final correction was made for the influence of ocular media absorption at all stimulus eccentricities and macular pigment absorption at the fovea and 2.2 degrees eccentricity.

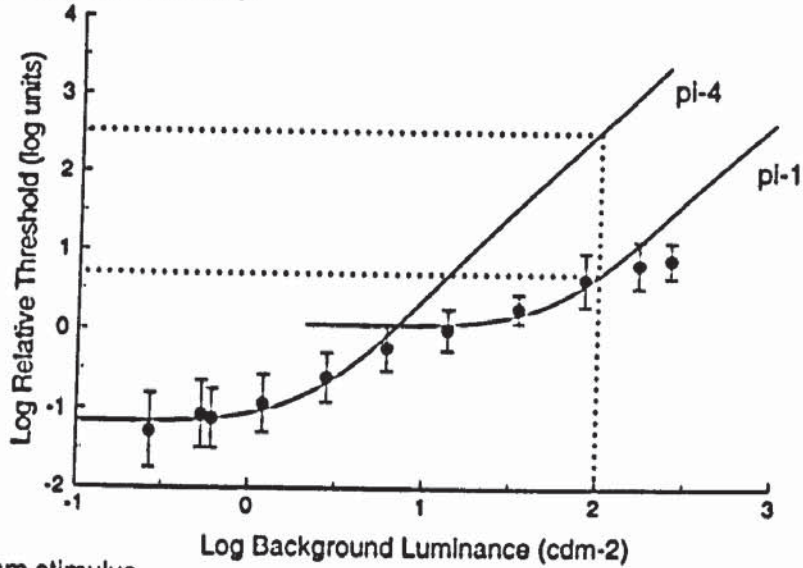
7.6. Results.

The group mean tvl functions for each stimulus wavelength at each eccentricity are illustrated in Figures 7.9 to 7.14. A Stiles template describing the pi-1 and pi-4 mechanisms was constructed from the original data of Wyszecki and Stiles (1982). Using a curve fitting software package (TableCurve for Windows v 2.03, SPSS UK Ltd, Woking, Surrey, UK), an exponential function best described the Stiles' template ($r^2 = 0.999$):

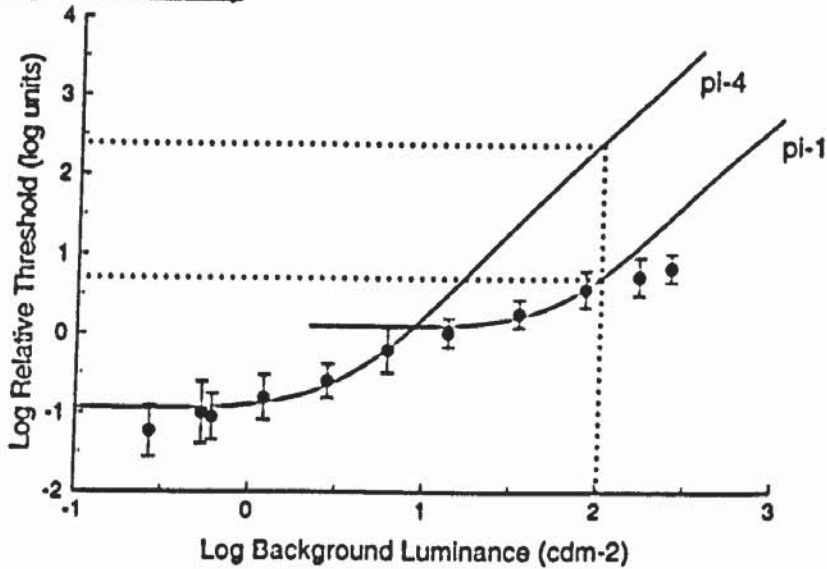
$$y = a + b \exp\left(\frac{-x}{c}\right) \quad \text{Eqn 7.8.}$$

This function was fitted to the data, and extrapolated to predict the threshold of the pi-1 and pi-4 mechanisms. The vertical dotted vertical line corresponds to the standard background luminance employed in SWAP, ie 100 cdm^2 (2 log units). The upper and lower horizontal dotted lines indicate the log threshold of the pi-4 and pi-1 mechanisms respectively at this background luminance. The difference in threshold between the pi-4 and pi-1 mechanisms represents the magnitude of SWS pathway isolation at 100 cdm^2 .

440 nm stimulus
15 degrees eccentricity



450 nm stimulus
15 degrees eccentricity



460 nm stimulus
15 degrees eccentricity

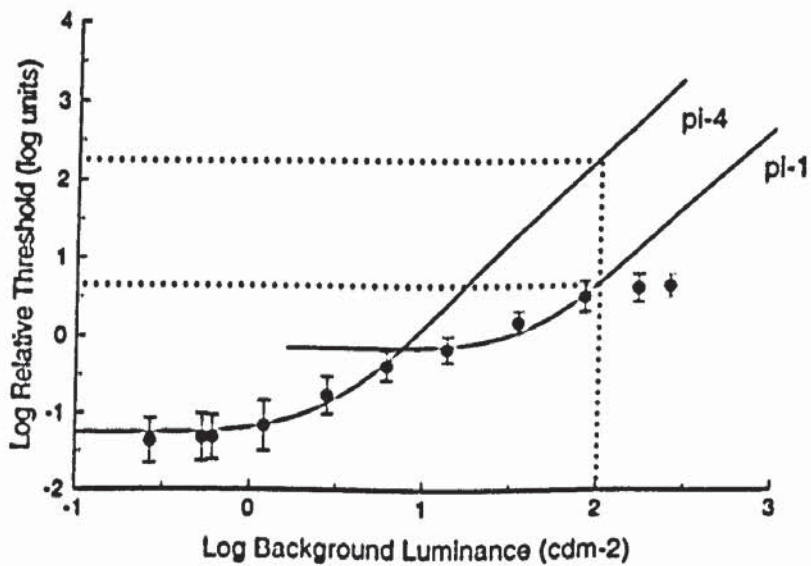
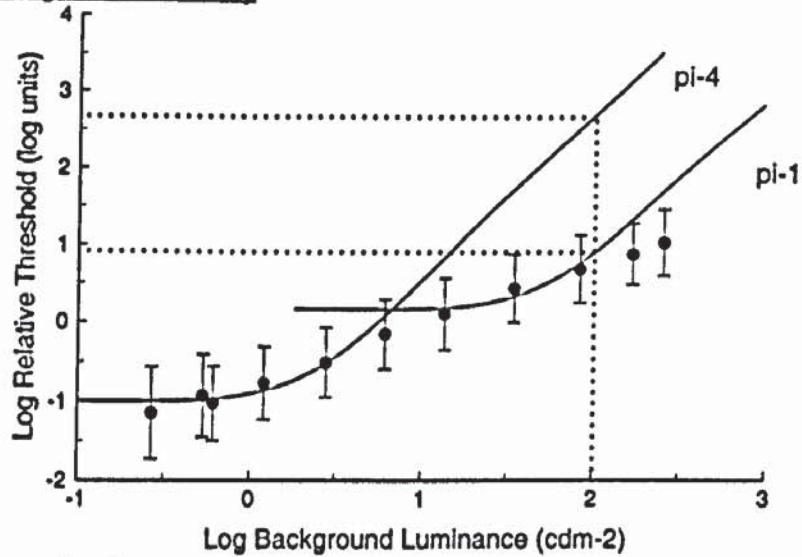
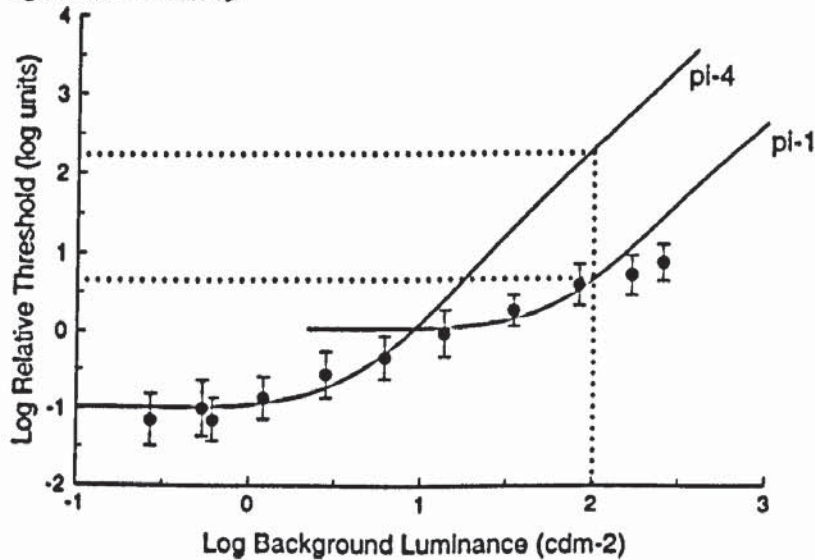


Figure 7.9. Group mean threshold versus intensity curves at the fovea for the 440 nm (top), 450 nm (middle) and 460 nm (bottom). Error bars represent ± 1 SD of the mean. Dotted lines represent the magnitude of SWS pathway isolation at 100 cdm^{-2} .

440 nm stimulus
15 degrees eccentricity



450 nm stimulus
15 degrees eccentricity



460 nm stimulus
15 degrees eccentricity

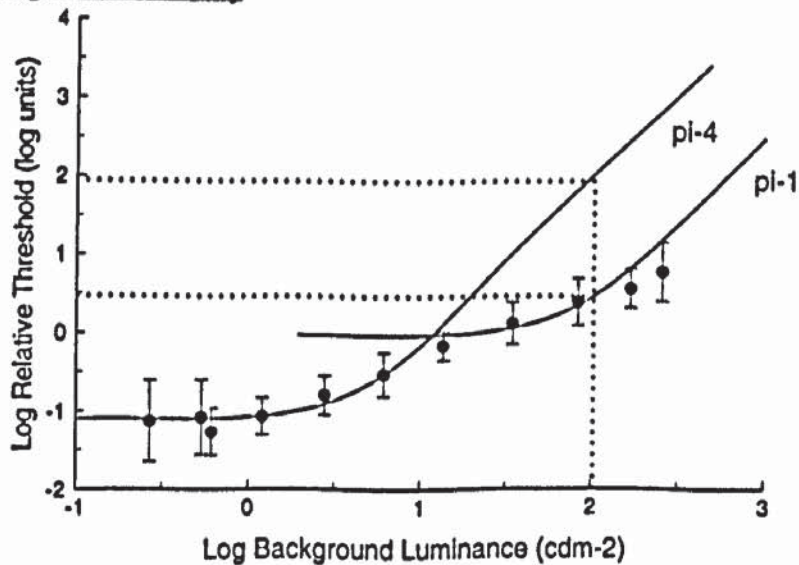


Figure 7.10. Group mean threshold versus Intensity curves at 2.2 degrees eccentricity for the 440 nm (top), 450 nm (middle) and 460 nm (bottom). Error bars represent ± 1 SD of the mean. Dotted lines represent the magnitude of SWS pathway isolation at 100 cdm².

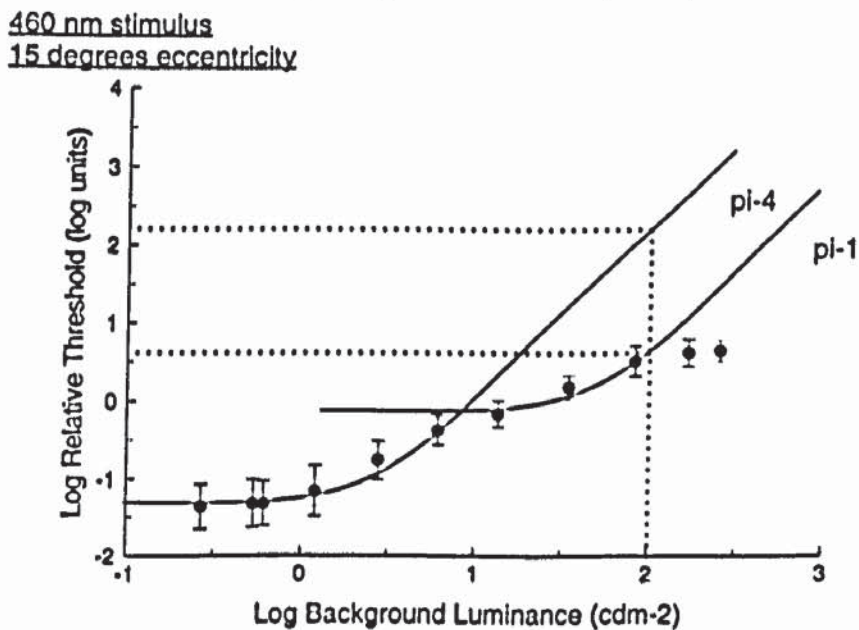
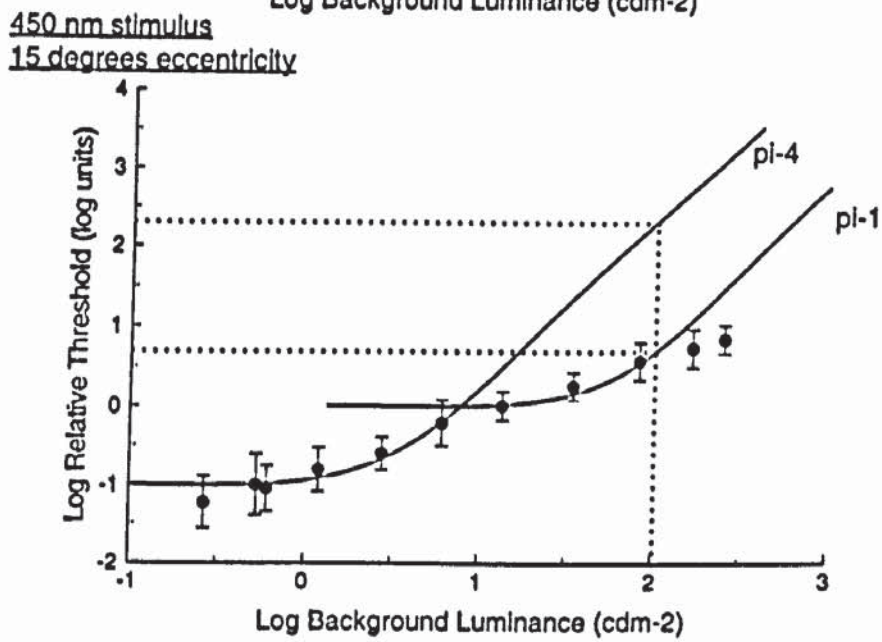
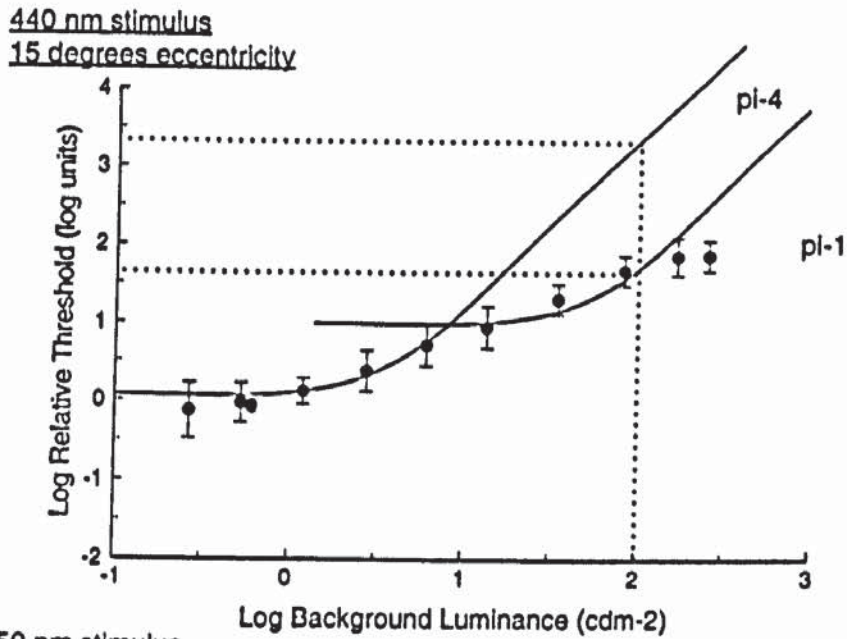


Figure 7.11. Group mean threshold versus Intensity curves at 5 degrees eccentricity for the 440 nm (top), 450 nm (middle) and 460 nm (bottom). Error bars represent ± 1 SD of the mean. Dotted lines represent the magnitude of SWS pathway isolation at 100 cdm^{-2} .

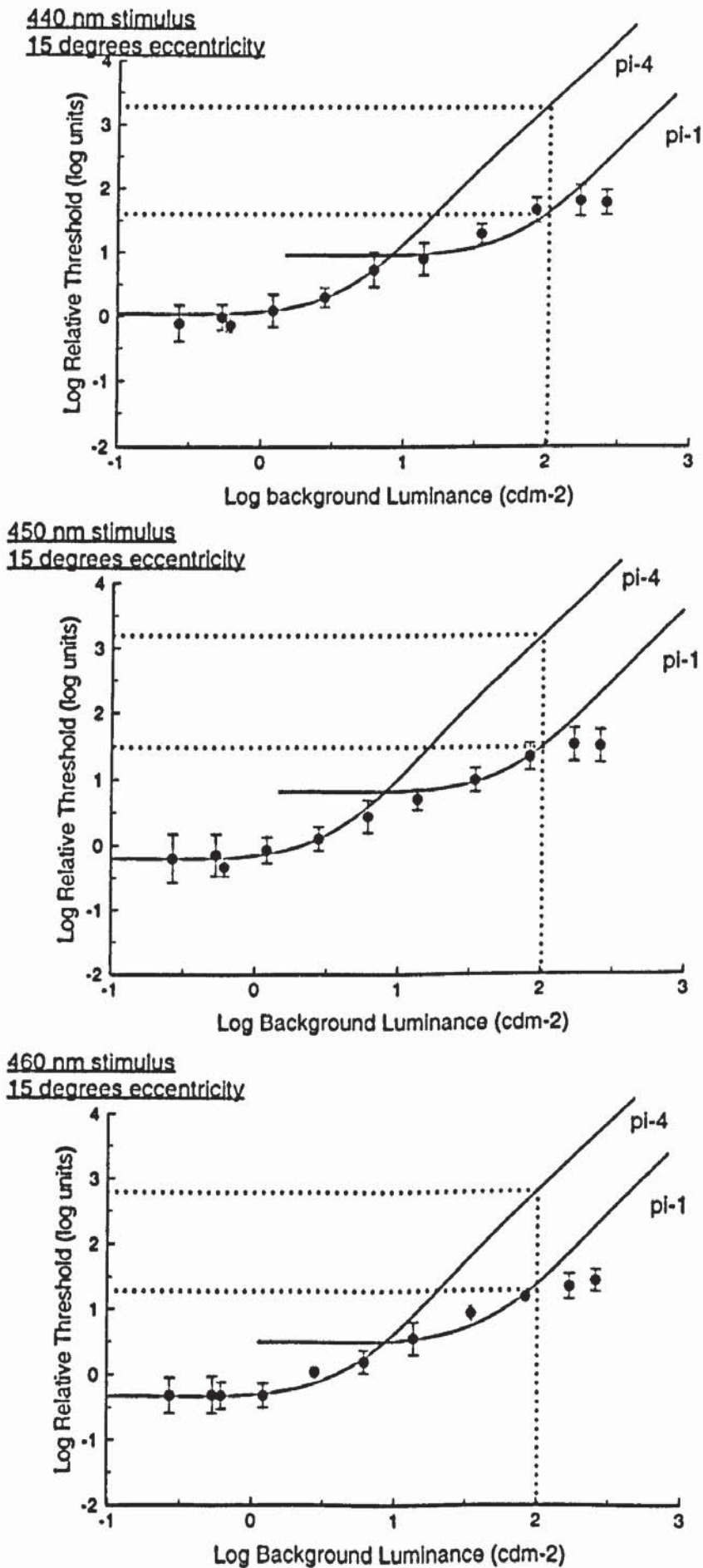
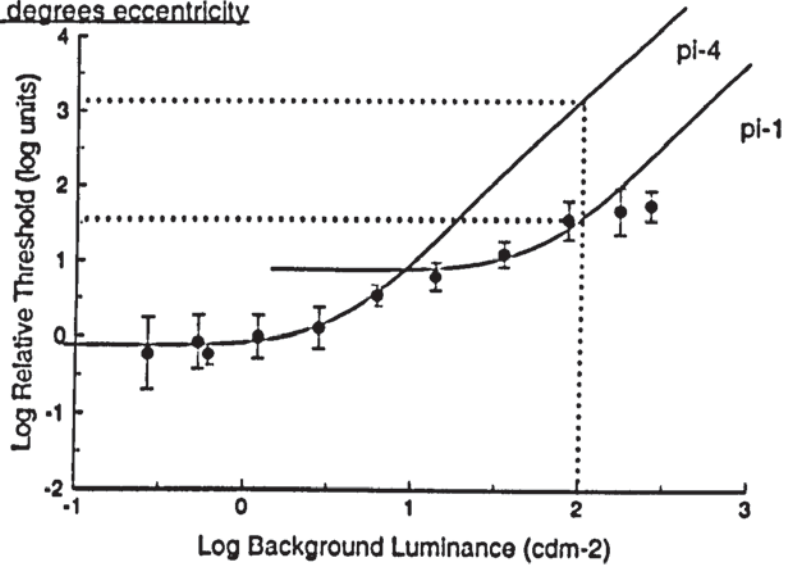
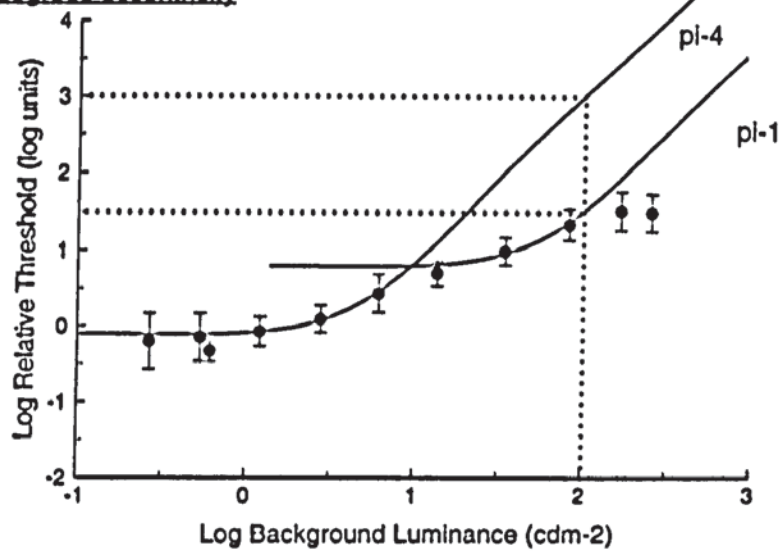


Figure 7.12. Group mean threshold versus intensity curves at 10 degrees eccentricity for the 440 nm (top), 450 nm (middle) and 460 nm (bottom). Error bars represent ± 1 SD of the mean. Dotted lines represent the magnitude of SWS pathway isolation at 100 cdm⁻².

440 nm stimulus
15 degrees eccentricity



450 nm stimulus
15 degrees eccentricity



460 nm stimulus
15 degrees eccentricity

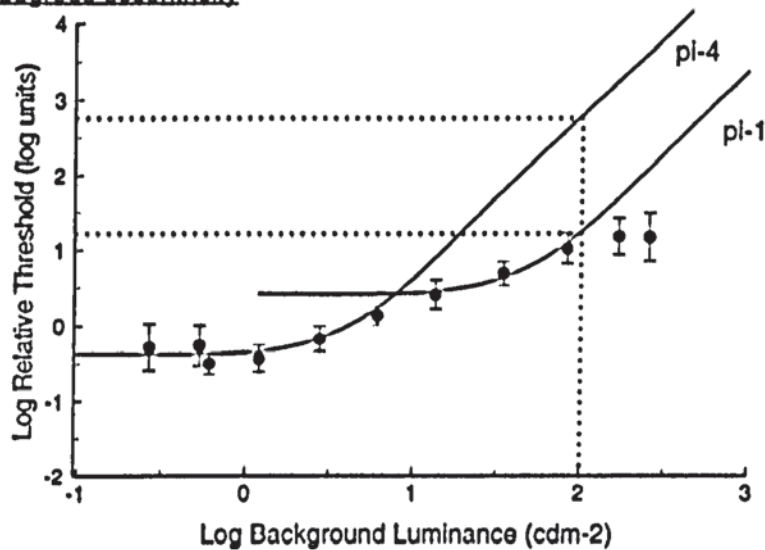
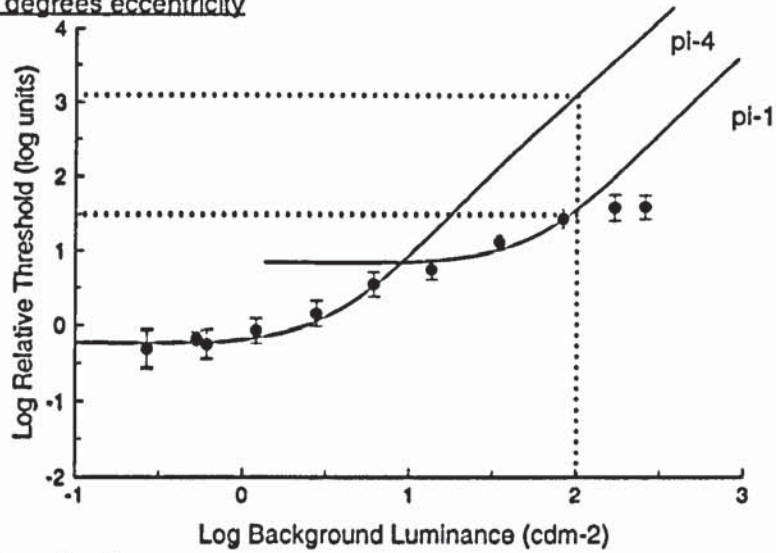
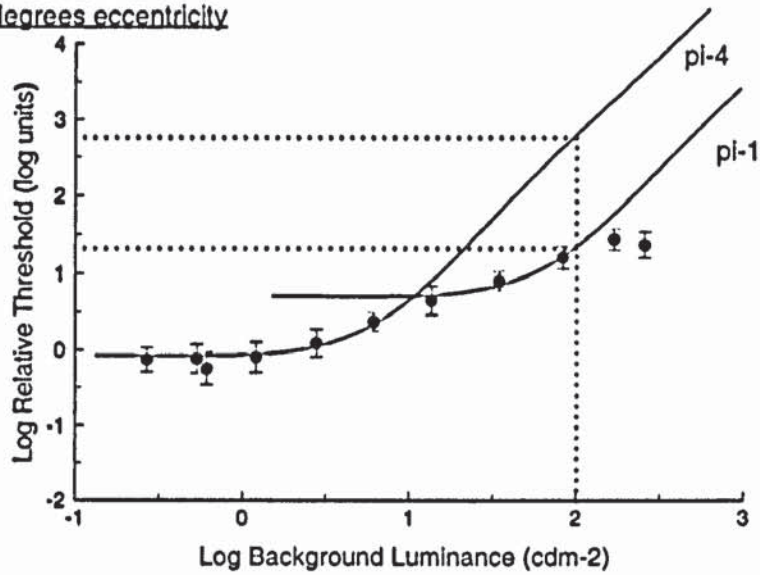


Figure 7.13. Group mean threshold versus Intensity curves at 15 degrees eccentricity for the 440 nm (top), 450 nm (middle) and 460 nm (bottom). Error bars represent ± 1 SD of the mean. Dotted lines represent the magnitude of SWS pathway isolation at 100 cdm⁻².

440 nm stimulus
15 degrees eccentricity



450 nm stimulus
15 degrees eccentricity



460 nm stimulus
15 degrees eccentricity

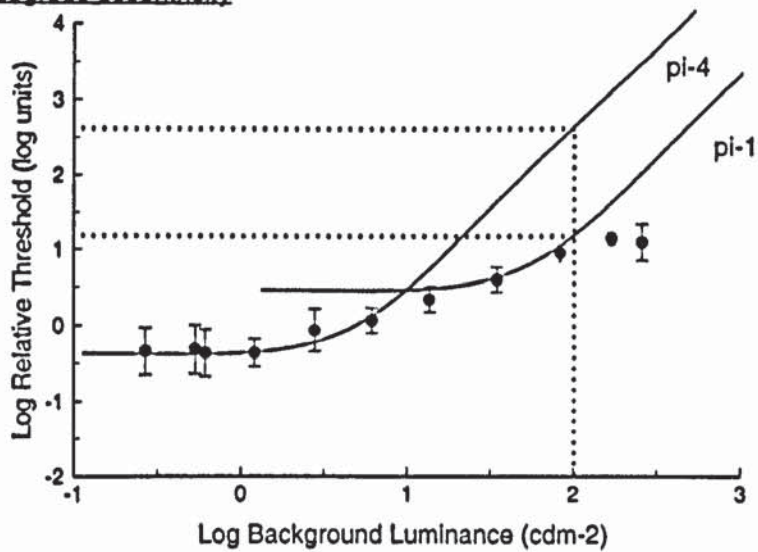


Figure 7.14. Group mean threshold versus intensity curves at 20 degrees eccentricity for the 440 nm (top), 450 nm (middle) and 460 nm (bottom). Error bars represent ± 1 SD of the mean. Dotted lines represent the magnitude of SWS pathway isolation at 100 cdm^{-2} .

As expected, SWS pathway isolation was achieved at all the stimulus eccentricities investigated. The magnitude of SWS pathway isolation was greatest for the 440 nm stimulus and least for the 460 nm stimulus. The group mean SWS pathway isolation for all stimulus eccentricities, was 1.65 log units (SD 0.09) for the 440 nm narrowband stimulus, 1.58 log units (SD 0.09) for the 450 nm narrowband stimulus and 1.53 log units (SD 0.06) for the 460 nm narrowband stimulus. The group mean SWS pathway isolation at all stimulus eccentricities, ranged between 1.52 and 1.78 log units for the 440 nm stimulus, 1.45 and 1.69 log units for the 450 nm stimulus and 1.45 and 1.62 log units for the 460 nm stimulus.

The magnitude of SWS pathway isolation was greatest at the fovea and decreased with increasing eccentricity. The difference between foveal SWS pathway isolation and SWS pathway isolation at 20 degrees eccentricity was 0.19 log units for the 440 nm stimulus, 0.24 log units for the 450 nm stimulus and 0.17 log units for the 460 nm stimulus. Univariate linear regression of SWS pathway isolation against stimulus eccentricity yielded a decrease in SWS pathway isolation of 0.10 dB per degree increase in eccentricity from the fovea for the 440 nm stimulus ($r^2 = 0.70$), and a decrease in isolation of 0.11 dB and 0.07 dB for the 450 nm stimulus ($r^2 = 0.93$) and the 460 nm stimulus ($r^2 = 0.79$) respectively (Figure 7.15). The magnitude of ocular media and macular pigment absorption is illustrated in Table 7.4. Pre-receptoral absorption decreased with increasing stimulus wavelength. Ocular media absorption ranged between 0.46 and 0.61 log units at 440 nm; 0.38 and 0.52 log units at 450 nm; and 0.33 and 0.45 log units at 460 nm. Macular pigment absorption ranged between 0.51 and 0.71 log units at 440 nm; 0.43 and 0.67 log units at 450 nm; and 0.34 and 0.61 log units at 460 nm. SWS pathway isolation was lost for all stimulus wavelengths at a background luminance of approximately 10 cdm^{-2} (1 log unit), indicated by the absolute threshold of the π_1 branch (Figures 6.10 to 6.15).

7.7. Discussion.

The greatest magnitude of SWS pathway isolation was achieved using the 440 nm narrowband stimulus and progressively decreased as the stimulus wavelength increased. This was expected since spectral sensitivity for the short-wavelength sensitive pathway is greatest

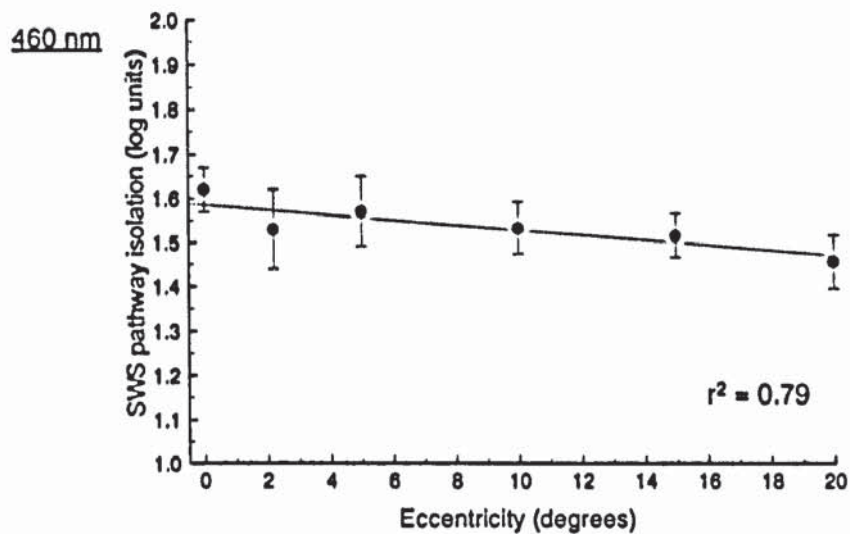
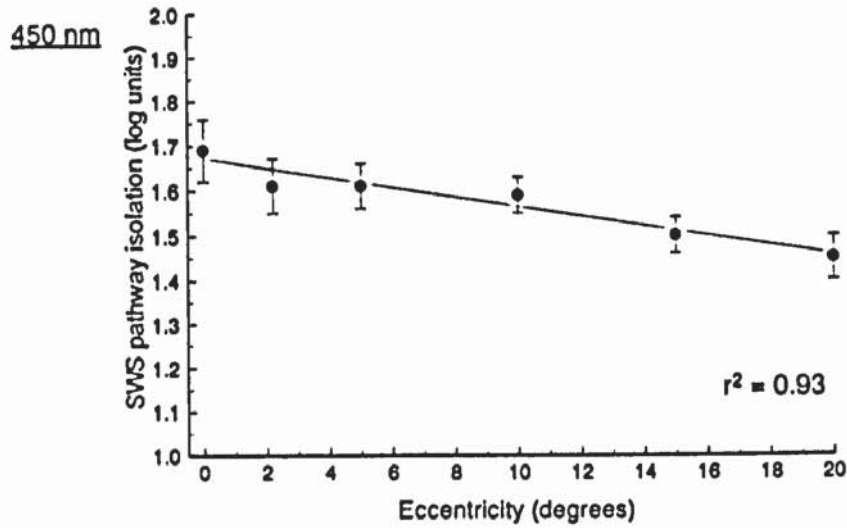
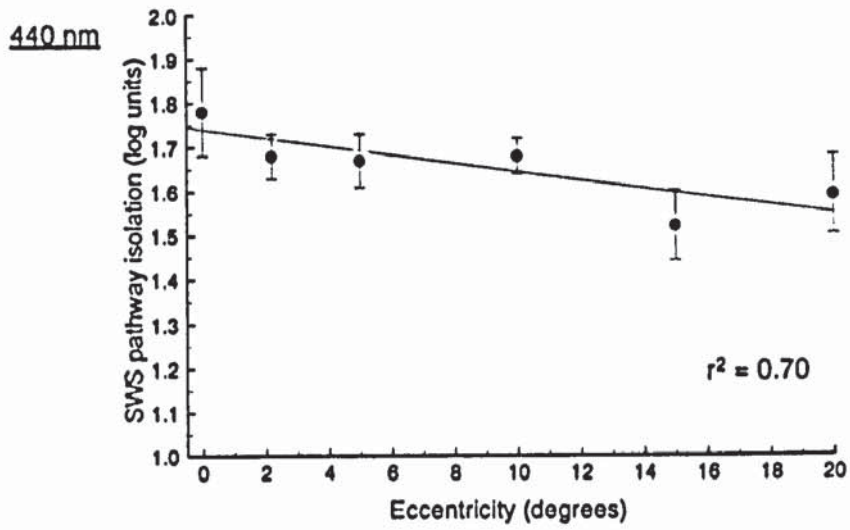


Figure 7.15. Univariate linear regression of group mean SWS pathway isolation at the standard background luminance of 100 cdm^{-2} as a function of stimulus eccentricity for the 440 nm (top), 450 nm (middle) and 460 nm (bottom) narrowband stimuli. Error bars represent ± 1 SD of the mean.

	440 nm	450 nm	460 nm
Ocular Media Absorption (log units)	0.52 (0.11)	0.44 (0.12)	0.38 (0.13)
Macular Pigment Absorption (log units)	0.63 (0.11)	0.57 (0.11)	0.50 (0.12)

Table 7.4. Group mean ocular media and macular pigment absorption (± 1 SD of the mean).

at 440 nm (Dartnall et al 1983). The Stiles template did not pass through the highest adaptation point for any of the stimulus wavelengths at any of the stimulus eccentricities investigated. This may be the origin of the short-wavelength pi-3 mechanism.

Comparisons of the magnitude of SWS pathway isolation between studies is confounded by the differing nature of the stimulus filters investigated, the background adaptation level at which isolation was assessed and therefore, differing decibel scales.

SWS pathway isolation decreased linearly with increasing eccentricity. The 440 nm narrowband stimulus yielded the lowest reduction in SWS pathway isolation with increasing eccentricity. Sample et al (1996) assessed the magnitude of SWS pathway isolation at the fovea and 20° eccentricity. They reported a reduction in SWS pathway isolation at 20° compared to the fovea of 0.42 and 0.51 log units for two 440 nm narrowband stimulus filters (HPW 28 nm and 27 nm respectively) and 0.42 log units for a 460 nm narrowband stimulus filter (HPW 28 nm). This is somewhat greater than that found in this study (0.19 log units at 440 nm and 0.17 log units at 460 nm) and may be due to the differing decibel scales between studies, combined with the greater HPW of the stimulus filters used by Sample et al (1996) which may not guarantee the same degree of isolation at peripheral stimulus locations. At the standard SWAP background and stimulus wavelength, at least of 15 dB of SWS isolation was achieved at all stimulus eccentricities investigated. This value should be treated with some caution because the 440 nm stimulus employed in this study did not possess the same transmission characteristics as the standard SWAP stimulus designed by Humphrey Instruments (440 nm HPW 27 nm) (Figure 4.2). The standard SWAP stimulus could not be incorporated into the stimulus projection system of the modified HFA. Sample et al (1996) reported a maximum of 13 dB of SWS pathway isolation at 100 cdm⁻² with the standard SWAP stimulus, although their measurements were not based upon the commercially available SWAP decibel scale.

One of the disadvantages of SWAP is the inherent reduced dynamic range over standard W-W perimetry which arises due to the reduced transmission of short-wavelength stimulus.

Indeed, the standard SWAP stimulus has a maximum luminance of 64.5 asb. Johnson et al (1993a, b) and Moss et al (1995) amongst others have advocated using a broadband stimulus filter for SWAP on the basis that spectral transmission is greater than narrowband filters. It is difficult to quantify the degree of SWS pathway isolation of a broadband stimulus filter because stimulus detection would be mediated by a combination of short-wavelength mechanisms. Clinically, all the narrowband stimuli investigated yielded an acceptable degree of SWS pathway isolation. Since the 450 nm narrowband stimulus filter possessed greater transmission than either the 440 nm or 460 nm narrowband filters (Figure 7.7), the dynamic range with this filter was the highest. A narrowband 450 nm stimulus may therefore be more applicable for SWAP since the magnitude of SWS pathway isolation is clinically comparable to that at 440 nm and the dynamic range would be greater.

Another advantage of adopting a longer wavelength stimulus than the standard 440 nm stimulus, is that the influence of ocular media absorption would be reduced (Table 7.4). Clearly, ocular media absorption is a contributory factor to the increased between-subject variability of SWAP (Chapter 4). Utilising a stimulus of longer wavelength than 440 nm may reduce this variability and yield narrower confidence intervals for normality. Nevertheless, this would be at the expense of a slight reduction in the magnitude of SWS pathway isolation. Similarly, increasing the HPW of a narrowband stimulus filter would increase the dynamic range of SWAP but would not guarantee SWS pathway isolation to the same degree as a narrowband stimulus filter. However, it should be remembered that young observers were participants in this study, and that the influence of SWS pathway isolation with age is currently unknown. It is likely that the decrease in the photoreceptor population with increase in age (Curcio et al 1993; Panda-Jonas et al 1995) would reduce the magnitude of SWS pathway isolation, in particular at peripheral stimulus locations.

Sample et al (1996) suggested that utilising a narrowband stimulus filter would have a less adverse effect upon cataract since the stimulus would be less susceptible to shifts in the peak retinal stimulus wavelength. However, such shifts in spectral sensitivity may not substantially influence the degree of SWS pathway isolation because the mean SWS pathway isolation

varied by 1.2 dB over a peak stimulus wavelength range of 20 nm. It is more likely that the reduced transmission of the stimulus filter would hinder interpretation of the short-wavelength visual field because age-related cataract yields a preferential attenuation of SWAP (Chapter 5) which may exceed the dynamic range. Furthermore, the reduction in retinal illuminance induced by cataract may reduce the retinal illuminance to less than 10 cdm^{-2} leading to a loss in SWS pathway isolation (Figures 7.9 to 7.14).

7.8. Conclusions.

The stimulus and background adaptation level chosen for SWAP is a compromise between the magnitude of SWS pathway isolation, which determines the sensitivity of the technique, and dynamic range. SWS isolation at 100 cdm^{-2} was achieved over a wide range of stimulus eccentricities and thus confirms the viability of SWAP for the investigation of glaucoma. At 100 cdm^{-2} the standard SWAP stimulus wavelength offered the highest degree of SWS pathway isolation. However, the reduced dynamic range and increased between-subject variability of SWAP may limit the clinical usefulness of the technique. The dynamic range of SWAP could be further increased by hardware modifications to the design of the optical system of the perimeter or the choice of stimulus filter. Employing a 440 nm stimulus with a wider HPW would increase transmission and hence dynamic range but may not guarantee SWS isolation. The 450 nm stimulus yielded a high magnitude of SWS isolation at all stimulus eccentricities and possessed a greater dynamic range than the 440 nm stimulus. Employing such a stimulus would also reduce the degree of ocular media absorption and therefore, may lead to a reduction in the between-subject variability in SWAP and, therefore, reduce the width of the confidence levels for normality. More detailed studies of SWAP using a 450 nm stimulus to examine the between-subject variability would reveal whether it is a superior stimulus than the standard 440 nm stimulus.

CHAPTER 8. GENERAL SUMMARY OF RESULTS AND CONCLUSIONS AND FUTURE WORK.

8.1. Summary of Results and Conclusions.

8.1.1. The Influence of Staircase Strategy on the Fatigue Effect In W-W Perimetry.

The fatigue effect associated with the 4-2 dB double reversal strategy is one of the most important factors which confound visual field interpretation. Consequently, alternative staircase strategies have been developed with the aim of reducing the overall examination time. Such strategies are being increasingly used in routine visual field examination. A study was undertaken to evaluate the fatigue effect for two short staircase strategies with respect to the standard double reversal strategy; a 4 dB single reversal strategy and a single reversal, dynamic strategy, in which the step sizes were modified according to the frequency-of-seeing psychometric function. The magnitude of the MS decreased as the examination progressed. Despite the introduction of frequent rest periods, the fatigue effect transferred to the second eye examined and was greater than for the first eye. Brief rest periods only serve to retard the fatigue effect. Although the 4 dB strategy yielded the highest MS, the efficiency was the lowest of the three strategies. The poor efficiency arose due to the greater SF of the 4 dB strategy, which is a common feature of strategies which employ single steps. Conversely, the dynamic strategy yielded the lowest SF and greatest efficiency of the three strategies. The dynamic strategy shows promise as a staircase strategy which offers reduced variability whilst simultaneously reducing examination time.

8.1.2. Staircase Strategy Variability In Short-Wavelength Automated Perimetry.

SWAP is increasingly being used in the diagnosis and monitoring of glaucoma. The normal between-subject variability of SWAP was assessed using the Full Threshold 4-2 dB double reversal and 3 dB single reversal strategies of the HFA. The hill of vision in SWAP was steeper than standard W-W perimetry. The reduction in sensitivity with age was also greater in SWAP. Correcting SWAP for the influence of ocular media absorption reduced the rate of the decline in sensitivity but the decline in corrected sensitivity was still greater than W-W perimetry. The

reduction in sensitivity with age for SWAP was less with FASTPAC than with the Full Threshold strategy; this finding may have been due to the reduced fatigue effect with FASTPAC. The short-term fluctuation was greater in SWAP than in W-W perimetry. There was little relationship between SF and age for either W-W perimetry or SWAP for either strategy. Examination time and the number of stimulus presentations was greater for SWAP than W-W perimetry for both staircase strategies. The FASTPAC staircase strategy offered an approximate saving in examination time of 40%. There was no correlation between forward light scatter and normal SWAP thresholds. Between-subject variability, defined in terms of the coefficient of variation, was greater for SWAP than for W-W perimetry. Correction of SWAP for the influence of ocular media absorption decreased the between-subject variability by approximately one third. In SWAP, the FASTPAC strategy yielded lower between-subject variability than the Full Threshold strategy. The increased between-subject variability of SWAP has profound implications for the statistical delineation of abnormality, since the reduction in sensitivity required to indicate abnormality will be greater than for W-W perimetry. The weighting function applied in SWAP for the calculation of the visual field indices will be greater than that in W-W perimetry. The greater difference in sensitivity between hemifields in SWAP, combined with wider confidence limits, may render the Glaucoma Hemifield Test ineffective. Program 24-2 for SWAP will be more appropriate in conjunction with the FASTPAC strategy since the peripheral stimulus locations of Program 30-2 which yielded greatest between-subject variability will be excluded and due to the reduced between-subject variability of the FASTPAC strategy, in combination with the saving in examination time.

8.1.3. The Influence of Examination Fatigue on Short-Wavelength Automated Perimetry,

The fatigue effect in SWAP was investigated in normal observers with particular emphasis on the hypothesis that Ganzfeld blankout was the principle contributory factor to the fatigue effect and would be eliminated by translucent occlusion. Translucent occlusion yielded a greater W-W and SWAP MS than standard opaque occlusion at all stages of the examination. The fatigue effect was greater in the second eye for W-W perimetry and SWAP. Translucent occlusion reduced the fatigue effect in W-W perimetry and SWAP. The reduction was greater in SWAP. The influence of rest periods did not eliminate the fatigue effect. The decrease in

sensitivity was greatest in SWAP regardless of the type of occluder. The fatigue effect induced a steepening in the hill of vision in W-W perimetry and SWAP which was not influenced by the type of occlusion. The examination time was greater for SWAP which may explain the greater fatigue effect. The reduced fatigue effect with translucent occlusion would indicate that Ganzfeld blankout is a major contributory factor to the reduction in sensitivity during a perimetric test. Translucent occlusion reduced the between-subject variability of W-W perimetry, but increased the between-subject variability of SWAP, possibly due to the differing effects of the veiling glare produced by the translucent occluder. The elevated sensitivity observed with such an occluder, arising from binocular summation, would necessitate caution in the interpretation of the MD_H index and the total deviation plots. In SWAP the increased between-subject variability of translucent occlusion would further confound the statistical analysis of SWAP and along with the increase in examination time, the technique should not be advocated.

8.1.4. The Influence of Age-Related Cataract on Short-Wavelength Automated Perimetry.

Age-related cataract profoundly influenced the outcome of SWAP. Cataract resulted in a general reduction in sensitivity across the visual field in W-W perimetry and in SWAP. SWAP yielded a greater attenuation in MD_H than W-W perimetry. The extent of the disparity reduced after correcting SWAP for the influence of ocular media absorption, but the magnitude of the MD_H was still greater than in W-W perimetry. This finding indicates that other factors such as forward light scatter and lens autofluorescence may influence the attenuation of SWAP by cataract. There was little correlation between forward light scatter and the attenuation in sensitivity for either W-W perimetry or SWAP. The magnitude of forward light scatter may have been underestimated due to the difference in the wavelengths of the stimuli employed in the straylight meter and in the 440 nm narrowband SWAP stimulus. The influence of backward light scatter defined by LOCS III did not appear to influence the degree of attenuation of W-W or short-wavelength sensitivity. This finding is at variance with other studies, possibly because the cataract severity was greater in this study. The degree of attenuation of sensitivity in SWAP is likely to be a complex interaction between ocular media absorption, light scatter and

autofluorescence. Cataract extraction yielded a positive SWAP MD_H in all patients which has ramifications for the statistical interpretation of SWAP since the inherently greater between-subject variability and the increased elevation of the visual field may lead to a total deviation plot not reaching statistical significance.

8.1.5. Quantification of Short-Wavelength Sensitivity Isolation in Short-Wavelength Automated Perimetry.

The utility of SWAP is dependent upon obtaining the maximum isolation of the SWS pathway. Although the stimulus and background parameters employed in SWAP have recently been standardised, they remain controversial. Threshold versus intensity curves were measured using a modified HFA. The necessary reduction in background wavelength was achieved using a system of aperture stops in order to avoid changes in the chromaticity of the background. The pupil was dilated in order to avoid changes in pupil diameter at the various adaptation levels. SWS pathway isolation was approximately 1.5 log units which did not vary significantly with eccentricity. The clinical significance of the robustness of SWS isolation in normal observers at 440 nm, 450 nm and 460 nm stimulus wavelengths would indicate that utilising a stimulus wavelength of 450 nm may be more appropriate in SWAP. The longer wavelength of the 450 nm stimulus would be less influenced by ocular media absorption and by macular pigment absorption which, in turn, would lead to a reduction in the between-subject variability of SWAP and narrower confidence limits.

8.2. Future Work.

8.2.1. The Influence of Staircase Strategy on the Fatigue Effect in W-W Perimetry.

There is a pressing need to obtain a normative database for the dynamic strategy in order for the strategy to be evaluated in the examination of patients with glaucoma and ocular hypertension. The dynamic strategy was evaluated for the sixteen stimulus locations of the first Stage of Program G1X. The MD_F was calculated from the normal database derived using the 4-2 dB strategy. The nature of the frequency-of-seeing psychometric function is known to differ in glaucoma. Consequently, the step sizes may need to be re-evaluated to avoid a loss

in efficiency. Simulations may provide an insight into the performance of the dynamic strategy particularly with respect to the standard strategy, but also to other short strategies such as the 4 dB strategy and FASTPAC. Recently, the SITA threshold strategies have been developed which depend upon *a priori* decisions about the nature of the visual field. The step sizes of the staircase strategies employed in the two SITA algorithms are 4-2 dB double reversal and 3 dB single reversal respectively. Adopting dynamic step sizes may further improve the efficiency of these new strategies. The new strategies will substantially reduce the fatigue effect such that it may become a relatively minor component of the variability of W-W perimetry because of the reduction in examination times. However, Ganzfeld blankout will still be present.

8.2.2, Short-Wavelength Automated Perimetry,

The utility of SWAP is limited by the greater short-term fluctuation and by the greater between-subject variability compared to conventional W-W perimetry. The current methods for defining focal loss used in W-W perimetry may not be applicable in SWAP due to the wider confidence limits. Image processing techniques which have been applied in W-W perimetry, detect focal loss by extracting the local spatial variability in the visual field. Such methods could be applied to SWAP. It is likely that these techniques would filter out the influence of cataract on SWAP and negate the need for ocular media absorption measurement because they do not require knowledge of the height of the hill of vision.

The reduction in the between-subject variability of SWAP after correction for ocular media absorption theoretically dictates that ocular media absorption assessment will remain a necessity. However, the difference in scotopic sensitivity method currently routinely used to correct SWAP for ocular media absorption is clinically unacceptable given that it is both time consuming and subjectively determined. Furthermore, the validity of the method in diseased eyes is questionable because rod function may be compromised. Objective methods, such as the lens absorption meter which is based upon a comparison of the luminance of the first two Purkinje images have been employed previously, could be incorporated into the design of perimeters.

The attenuation of SWAP by age-related cataract is a complex issue. Further investigations which establish the contribution of ocular media absorption, light scatter and autofluorescence to the variability of SWAP are urgently warranted. Biometric and densitometric analysis of the lens as a function of wavelength would provide an objective insight into the nature of ocular media absorption in SWAP, since the magnitude of absorption results from the optical path length through the lens and the attenuation by short-wavelength absorbing pigments present within the lens. Techniques employed to assess forward light scatter have not considered the influence of lenticular fluorescence. Densitometry may provide an insight to the magnitude of lenticular fluorescence.

The greater number of stimulus presentations required for SWAP compared to W-W perimetry, suggests that the Full Threshold and FASTPAC staircase strategies may not be appropriate in SWAP. Furthermore, the inherently greater fatigue effect of SWAP over W-W perimetry dictates that the examination time must be reduced. Knowledge of the number of stimulus presentations at each stimulus location may provide further insight to the efficiency of these strategies in SWAP. The nature of the blue-yellow frequency-of-seeing psychometric function must be evaluated in order to design novel threshold strategies optimised for SWAP. Such strategies could either adapt the step size of the strategy to the frequency-of-seeing function, or employ *a priori* criteria to estimate the threshold such as those employed by SITA. Optimisation of the staircase strategy used for SWAP should lead to a reduction in the variability, resulting from a combination of greater staircase efficiency and reduced examination time.

The clinical application of SWAP is further limited by the reduced dynamic range which arises from the high luminance background and the low transmission of the short-wavelength stimulus. Greater dynamic range is required, because the preferential attenuation of SWAP by cataract may exceed the dynamic range of the perimeter. Translucent occlusion effectively increases the dynamic range of SWAP because of the elevation in normal sensitivity. However, this method cannot be advocated presently due to the increase in between-subject

variability discussed earlier. Hardware modifications to the perimeter could increase the stimulus luminance, by a combination of increasing the light output and utilising a stimulus filter with higher transmission and longer wavelength. Several studies utilised a broadband stimulus filter because the increased transmission increased the dynamic range of the perimeter. However, narrowband stimuli encourage greater isolation of the SWS pathway. It may be appropriate to increase the standard 440 nm narrowband stimulus to 450 nm. The increased transmission of a 450 nm stimulus would increase the dynamic range and would be less influenced by ocular media and macular pigment absorption. The associated reduction in SWS pathway isolation with such a filter would not be clinically significant and, as discussed earlier, the between-subject variability would be lower. The HPW filter could be designed to optimise the spectral transmission.

Further issues relating to the variability of SWAP also need to be resolved. The degree of SWS pathway isolation as a function of age is unknown. Should SWS pathway isolation decrease with age, the utility of SWAP may be lost. The SF is greater in SWAP, and preliminary studies have shown that the LF is also greater in SWAP. Image processing techniques which have been successfully applied to W-W perimetry, could be applied to SWAP to reduce this variability. Furthermore, the influence of ocular media absorption with time to follow-up needs to be quantified in order to assess the contribution of the reduction to the LF of SWAP. The future of SWAP is assured, although until new methods are sought which simplify analysis and reduce the examination time, it will remain a relatively cumbersome procedure.

REFERENCES.

Humphrey Field Analyzer II user's guide, 1994. Humphrey Instruments, San Leandro, California, USA.

Octopus 1-2-3 Operating Instructions. Revision 1. (1990). Interzeag AG, Schlieren, Switzerland.

Peridata Manual (v. 6.3α) Interzeag AG, Schlieren, Switzerland.

Abrahamsson, M. and Sjöstrand, J. (1986). Impairment of contrast sensitivity function (CSF) as a measure of disability glare. *Invest. Ophthalmol. Vis. Sci.* **27**, 1131-1136.

Adams, A.J., Scheffrin, B. and Huie, K. (1987a). New clinical color threshold test for eye disease. *Am. J. Optom. Physiol. Opt.* **64**, 29-37.

Adams, A.J., Zisman, F., Al, E. and Bresnick, G. (1987b). Macular edema reduces B cone sensitivity in diabetics. *Appl. Optics.* **26**, 1455-1457.

Adams, A.J., Johnson, C.A. and Lewis, R.A. (1991). S cone pathway sensitivity loss in ocular hypertension and early glaucoma has nerve fiber bundle pattern. In: *Color Vision Deficiencies X*. Eds. Drum, B., Moreland, J.D. and Serra, A. Kluwer Academic Publishers. Dordrecht. pp. 535-542.

Airaksinen, P.J. , Lakowski, R., Drance, S.M. and Price, M. (1986). Color vision and retinal nerve fiber layer in early glaucoma. *Am. J. Ophthalmol.* **101**, 208-213.

Alpern, M. Thompson, S. and Lee, M.S. (1965). Spectral transmittance of visible light by the living human eye. *J. Opt. Soc. Am. A.* **55**, 723-727.

Anderson, D.R., Feuer, W.J., Alward, W.L. and Skuta, G.L. (1989). Threshold equivalence between perimeters. *Am. J. Ophthalmol.* **107**, 493-505.

Anderson, D.R. (1992). Introductory concepts. *Automated static perimetry*. Ed: Kist. K., Mosby-Year Book Inc., St Louis. pp. 10-29.

Anderson, R.S. and O'Brien, C. (1997). Psychophysical evidence for a selective loss of M ganglion cells in glaucoma. *Vision Res.* **37**, 1079-1083.

- Armaly, M.F. (1971). Visual field defects in early open-angle glaucoma. *Trans. Am. Ophthalmol. Soc.* **69**, 147.
- Åsman, P. and Heijl, A. (1988). Background luminance and detection of glaucomatous field loss. *Invest. Ophthalmol. Vis. Sci. (Suppl.)* **32**, 240.
- Åsman, P., Britt, J.M., Mills, R.P. and Heijl, A. (1988). Evaluation of adaptive spatial enhancement in suprathreshold visual field screening. *Ophthalmology*. **95**, 1656-1662.
- Åsman, P. and Heijl, A. (1992a). Glaucoma Hemifield Test. Automated visual field evaluation. *Arch. Ophthalmol.* **110**, 812-819.
- Åsman, P. and Heijl, A. (1992b). Weighting according to location in computer-assisted glaucoma visual field analysis. *Acta Ophthalmol.* **70**, 671-678.
- Åsman, P., Olsson, J. and Heijl, A. (1993). Learner's index (LI) to detect low perimetric experience. *Invest. Ophthalmol. Vis. Sci.* **34**, 1262.
- Åsman, P. and Heijl, A. (1994). The perimetric "learner's index": a pilot study. *Invest. Ophthalmol. Vis. Sci.* **35**, 2183.
- Åsman, P. (1995). Color-coded probability maps; separation of field defect types. *Perimetry Update 1994/95*. Proceedings of the XIth International Perimetric Society Meeting. Eds: Mills, R.P. and Wall, M. Amsterdam & New York. Kugler Publications. pp. 57-58.
- Åsman, P. and Olsson, J. (1995). Physiology of cumulative defect curves; consequences in glaucoma perimetry. *Acta Ophthalmol. (Scand.)* **73**, 197-201.
- Atchison, D.A. (1979). History of visual field measurement. *Aust. J. Optom.* **62**, 345-354.
- Atchison, D.A. (1987). Effect of defocus on visual field measurement. *Ophthal. Physiol. Opt.* **7**, 259-265.
- Aubert and Förster (1857) In: Atchison, D.A. (1979). History of visual field measurement. *Aust. J. Optom.* **62**, 345-354.
- Augenstein, E.J. and Pugh, E.N. (1977). The dynamics of the π_1 colour mechanism: further evidence for two sites of adaptation. *J. Physiol.* **272**, 247-281.

Aulhorn, E. and Harms, H. (1967). Early visual field defects in glaucoma. In: *Glaucoma Symposium Tutzing Castle*. Ed: Leydhecker, W. Karger Publishers. Basel & New York. pp. 151-186.

Aulhorn, E. and Harms, H. (1972). Visual perimetry. *Visual psychophysics: Handbook of sensory physiology VII*. Eds: Jameson, D. and Hurvich, L.M. Springer-Verlag, Berlin. pp. 102-145.

Ballon, B.J., Echelman, D.A., Shields, M.B. and Ollie, A.R. (1992). Peripheral visual field testing in glaucoma by automated kinetic perimetry with the Humphrey Field Analyzer. *Arch. Ophthalmol.* **110**, 1730-1732.

Barlow, H.B. (1964). Spatial and temporal summation in human vision. In: *Vision: coding and efficiency*. Ed: Blakemore, C. Cambridge University Press. pp. 378.

Barlow, H.B. (1972). Dark and light adaptation. In: *Visual psychophysics. Handbook of sensory physiology*. Vol VII, no 4. Eds: Jameson, D. and Hurvich, L.M. Berlin & New York. Springer Verlag. pp. 1-28.

Barlow, R.B. and Verrilo, R.T. (1976). Brightness sensation in a Ganzfeld. *Vision Res.* **16**, 1291-1297.

Bebié, H. and Fankhauser, F. (1981). Statistical program for the analysis of perimetric data. In: *Documenta Ophthalmologica Proceedings Series 26*. Fourth International Visual Field Symposium. Eds: Greve, E.L. and Verriest, G. The Hague. Dr. W. Junk Publishers. pp. 9-10.

Bebié, H., Fankhauser, F. and Spahr, J. (1976a). Static perimetry: accuracy and fluctuations. *Acta. Ophthalmol.* **54**, 339-348.

Bebié, H., Fankhauser, F. and Spahr, J. (1976b). Static perimetry: strategies. *Acta. Ophthalmologica.* **54**, 325-338.

Bebié, H. (1985). Computerised techniques of threshold determination. *Computerized visual fields. What they are and how to use them*. Eds: Whalen, W.R. and Spaeth, G.L. Slack Inc. New Jersey. pp. 31-44.

Bebié, H., Flammer, J. and Bebié, T. (1989). The cumulative defect curve: separation of local and diffuse components of visual field damage. *Graefe's Arch. Clin. Exp. Ophthalmol.* **227**, 9-12.

Beems, E.M. and van Best, J.A. (1990). Light transmission of the cornea in whole human eyes. *Exp. Eye Res.* **50**, 393-395.

Benedetto, M.D. and Cyrlin, M.N. (1985). The effect of blur upon static perimetric thresholds. In: *Documenta Ophthalmologica Proceedings Series 42*. Sixth International Visual Field Symposium. Eds: Heijl, A and Greve, E.L. Dr. W. Junk Publishers. Dordrecht. pp. 563-567.

Bengtsson, B., Heijl, A., Olsson, J. and Rootzén, H. (1996). Evaluation of a new interactive threshold strategy in normal subjects. Presented at the XII International Perimetric Society Meeting. 4-8 June 1996. Würzburg, Germany.

van den Berg, T.J.T.P., van Spronsen, R., van Veenendaal, W.G. and Baaker, D. (1985). Psychophysics of Intensity discrimination in relation to defect volume examination on the scoperimeter. In: *Documenta Ophthalmologica Proceedings Series 42*. Sixth International Visual Field Symposium. Eds: Heijl, A. and Greve, E.L. Dr. W. Junk Publishers. Dordrecht. pp. 147-151.

van den Berg, T.J.T.P. (1986). Importance of pathological intraocular light scatter for visual disability. *Doc. Ophthalmol.* **61**, 327-333.

van den Berg, T.J.T.P. (1987). Relation between media disturbances and the visual field. In: *Documenta Ophthalmologica Proceedings Series 49*. Seventh International Visual Field Symposium. Eds: Greve, E.L. and Heijl, A. Martinus Nijhoff / Dr. W. Junk Publishers. Dordrecht. pp. 104-107.

van den Berg, T.J.T.P., IJspeert, J.K. and deWaard, P.W.T. (1991). Dependence of intraocular straylight on pigmentation and light transmission through the ocular wall. *Vision Res.* **31**, 1361-1367.

van den Berg, T.J.T.P. and IJspeert, J.K. (1992). Clinical assessment of intraocular stray light. *Appl Optics.* **31**, 3694-3696.

van den Berg, T.J.T.P. (1993). Quantal and visual efficiency of fluorescence in the lens of the human eye. *Invest. Ophthalmol. Vis. Sci.* **34**, 3566-3573.

van den Berg, T.J.T.P., Hwan, B.S. and Delleman, J.W. (1993). The intraocular straylight function in some hereditary corneal dystrophies. *Doc Ophthalmol.* **85**, 13-20.

van den Berg, T.J.T.P. and Tan, K.E.W.P. (1994). Light transmittance of the human cornea from 320 and 700 nm for different ages. *Vision Res.* **33**, 1453-1456.

van den Berg, T.J.T.P. (1995). Analysis of intraocular straylight, especially in relation to age. *Optom. Vis. Sci.* **72**, 52-59.

van den Berg, T.J.T.P. (1996). Depth-dependent forward light scattering by donor lenses. *Invest. Ophthalmol. Vis. Sci.* **37**, 1157-1166.

Bettleheim, F.A. (1975). On the optical anisotropy of lens fiber cells. *Exp. Eye Res.* **21**, 569-578.

Bettleheim, F.A. and Chylack, L.T. (1985). Light scattering of whole excised human cataractous lenses. Relationships between different light scattering properties. *Exp. Eye Res.* **41**, 19-30.

Bickler-Bluth, M., Trick, G.L., Kolker, A.E. and Cooper, D.G. (1989). Assessing the utility of reliability indices for automated visual fields. *Ophthalmology.* **96**, 616-619.

Birch, M.K., Wishart, P.K., and O'Donnell, N.P. (1995). Determining progressive visual field loss in serial Humphrey fields. *Ophthalmology.* **102**, 1227-1235.

Blake, R. and Overton, R. (1979). The site of binocular rivalry suppression. *Perception.* **8**, 143-152.

Blake, R. (1989). A neural theory of binocular rivalry. *Psychol. Rev.* **96**, 145-167.

Blakemore, C. and Cooper, G. (1970). Development of the brain depends on the visual environment. *Nature.* **228**, 477-478.

Blakemore, C. and Vital-Durand, F. (1986). Organisation and development of the monkey's lateral geniculate nucleus. *J. Physiol.* **380**, 453-491.

Bloch (1885). Spatial and temporal summation in human vision. In: *Vision: coding and efficiency*. Ed: Blakemore, C. Cambridge University Press. pp. 376.

Boeglin, R.J., Caprioli, J., and Zulauf, M. (1992). Long-term fluctuation of the visual field in glaucoma. *Am. J. Ophthalmol.* **113**, 396-400.

Boettner, E.A. and Wolter, J.R. (1962). Transmission of the ocular media. *Invest. Ophthalmol.* **1**, 776-783.

Bolanowski, S.J. and Doty, R.W. (1987). Perceptual "blankout" of monocular homogenous fields (ganzfelder) is prevented with binocular viewing. *Vision Res.* **27**, 967-982.

Bone, R.A. and Landrum, J.T. (1984). Macular pigment in Henlé fiber membranes: a model for Hadinger's brushes. *Vision Res.* **24**, 103-108.

Bone, R.A., Landrum, J.T. and Cairns, A. (1992). Optical density spectra of the macular pigment in vivo and in vitro. *Vision Res.* **32**, 105-110.

Boynton, R.M., Das, S.R. and Gardiner, J. (1966). Interactions among chromatic mechanisms revealed by mixing conditioning fields. *J. Opt. Soc. Am.* **56**, 1775-1780.

Brenton, R.S. and Phelps, C.D. (1986). The normal visual field on the Humphrey Field Analyzer. *Ophthalmologica.* **193**, 56-74.

Brenton, R.S., Phelps, C.D., Rojas, P., and Woolston, R.F. (1986). Interocular differences of the visual field in normal subjects. *Invest. Ophthalmol. Vis. Sci.* **27**, 799-805.

Brenton, R.S. and Argus, W.A. (1987). Fluctuations on the Humphrey Field Analyzer. *Ophthalmologica.* **193**, 56-74.

Britt, J.M. and Mills, R.P. (1987). The black hole effect in perimetry. *Invest. Ophthalmol. Vis. Sci.* **29**, 795-801.

Brown, N.P. (1974). The change in the lens curvature with age. *Exp. Eye. Res.* **19**, 175-183.

Brusini, P., Della Mea, G., Miani, F. and Tosoni, C. (1990). L'indice pericentrale nella diagnosi precoce di glaucoma ad angolo aperto. *Minerva Oftalmol.* **32**, 59-62.

Brusini, P., Nicosia, S., and Weber, J. (1991). Automated visual field management in glaucoma with the PERIDATA program. In: *Perimetry Update 1990/91*. Proceedings of the IXth International Perimetric Society Meeting. Eds: Mills, R.P. and Heijl, A. Kugler & Ghedini Publications. Amsterdam, New York & Milano. pp. 273-277.

Buchsbaum, G. and Gottschalk, A. (1983). Trichromacy, opponent colours coding and optimum colour information transmission in the retina. *Proc. R. Soc. Lond. B.* **220**, 89-113.

- Budenz, D.L., Feuer, W.J. and Anderson, D.R. (1993). The effect of simulated cataract on the glaucomatous visual field. *Ophthalmology*. **100**, 511-517.
- Bynke, H. (1983). Hippocrates and homonymous hemianopsia. In: *Fifth International Visual Field Symposium*. Eds: Greve, E.L. and Heijl, A. Dr. W. Junk Publishers. The Hague, Boston & Lancaster. pp 251-256.
- Campbell, F.W. and Green, D.G. (1965). Optical and retinal factors affecting visual resolution. *J. Physiol.* **181**, 576-593.
- Caprioli, J. and Spaeth, G.L. (1985). Static threshold examination of the peripheral nasal visual field in glaucoma. *Arch. Ophthalmol.* **103**, 1150-1154.
- Caprioli, J., Sears, M. and Miller, J.M. (1987). Patterns of early visual field loss in open-angle glaucoma. *Am. J. Ophthalmol.* **103**, 512-517.
- Casson, E.J., Shapiro, L.R., and Johnson C.A. (1990). Short-term fluctuation as an estimate of variability in visual field loss. *Invest. Ophthalmol. Vis. Sci.* **31**, 2459-2463.
- Cavanagh, P., MacLeod, D.I.A., and Anstis, S.M. (1987). Equiluminance: spatial and temporal factors and the contribution of blue-sensitive cones. *J. Opt. Soc. Am. A.* **4**, 1428-1438.
- Chauhan, B.C., Drance, S.M., and Lai, C. (1989). A cluster analysis for threshold perimetry. *Graefes Arch. Clin. Exp. Ophthalmol.* **27**, 216-220.
- Chauhan, B.C., House, P.H. and Drance, S.M. (1990). A study of intra-test variability in conventional and high-pass resolution perimetry. *Invest. Ophthalmol. Vis. Sci. (Suppl.)* **30**, 15.
- Chauhan, B.C., Tompkins, J.D., LeBlanc, R.P. and McCormick, T.A. (1993). Characteristics of frequency-of-seeing curves in normal subjects, patients with suspected glaucoma, and patients with glaucoma. *Invest. Ophthalmol. Vis. Sci.* **34**, 3534-3540.
- Chen, P.P. and Budenz, D.L. (1996). The effect of cataract extraction on the glaucomatous visual field. *Invest. Ophthalmol. Vis. Sci.* **37**, S506.
- Cheng, H.M. and Chylack, L.T. (1984). Lens metabolism. In *The Ocular Lens*. Ed: Maisel, H. Marcel Decker Inc., New York. pp 223-264.

- Chester, M. (1993). In: *Neural networks: a tutorial*. PTR Prentice-Hall Inc. New Jersey. pp. 1-12.
- Choplin, N.T., Sherwood, M.B. and Spaeth, G.L. (1990). The effect of stimulus size on the measured threshold values in automated perimetry. *Ophthalmology*. **97**, 371-374.
- Chylack, L.T., Leske, C., McCarthy, D., Khu, P., Kashiwagi, T. and Sperduto, R. (1989). The lens opacities classification system II (LOCS II). *Arch. Ophthalmol.* **107**, 991-997.
- Chylack, L.T., Wolfe, J.K., Singer, D.M., Leske, C., Bullimore, M.A., Bailey, I.L., Friend, J., McCarthy, D. and Wu, S.Y. (1993a). The lens opacities classification system III. *Arch. Ophthalmol.* **111**, 831-836.
- Chylack, L.T., Wolfe, J.K., Friend, J., Khu, P.M., Singer, D.M., McCarthy, D., del Carmen, J. and Rosner, B. (1993b). Quantifying cataract and nuclear brunescence, the Harvard and LOCS systems. *Optom. Vis. Sci.* **70**, 886-895.
- Clarke, M.P., Pearson, J.C.G., Vernon, S.A. and Matthews, J.C. (1990). Influence of pupil size on measurements made with the Lens Opacity Meter 701. *Br. J. Ophthalmol.* **74**, 526-527.
- Cook, C.A., Koretz, J.F., Pfahnl, A., Hyun, J. and Kaufman, P.L. (1994). Aging of the human crystalline lens and anterior segment. *Vision Res.* **34**, 2945-2954.
- Cooper, G.F. and Robson, J.G. (1969). The yellow colour of the lens of man and other primates. *J. Physiol.* **203**, 411-417.
- Coren, S. and Girgus, J.S. (1972). Density of human lens pigmentation: In vivo measures over an extended age range. *Vision Res.* **12**, 343-346.
- Cornsweet, T.N. (1962). The staircase-method in psychophysics. *Am. J. Psychol.* **78**, 485-491.
- Cottler, E. (1987). The lens. In: *Adler's Physiology of the Eye. Clinical Application*. 8th Edition. Eds. Moses, R.A. and Hart, W.M. Mosby. St Louis, Washington D.C. and Toronto. pp. 268-290.
- Crabb, D.P., Edgar, D.F., Fitzke, F.W., McNaught, A.I. and Wynn, H.P. (1995). New approach to estimating variability in visual field data using an image processing technique. *Br. J. Ophthalmol.* **79**, 213-217.

- Crook, J.M., Lange-Malecki, B., Lee, B.B. and Valberg, A. (1988). Visual resolution of macaque retinal ganglion cells. *J. Physiol.* **396**, 205-224.
- Crosswell, H.H., Stewart, W.C., Cascairo, M.A. and Hunt, H.H. (1991). The effect of background intensity on the components of fluctuation as determined by threshold-related automated perimetry. *Graefe's Arch. Clin. Exp. Ophthalmol.* **229**, 119-122.
- Curcio, C.A., Allen, K.A., Sloan, K.R., Lerea, C.L., Hurley, J.B., Klock, I.B. and Milam, A.H. (1991). Distribution and morphology of human cone photoreceptors stained with anti-blue opsin. *J. Comp. Neurol.* **312**, 610-624.
- Curcio, C.A. and Sloan, K.R. (1992). Packing geometry of human cone photoreceptors: variation with eccentricity and evidence for local anisotropy. *Vis. Neurosci.* **9**, 169-180.
- Curcio, C.A., Millican, C.L., Allen, K.A. and Kalina, R.E. (1993). Aging of the human photoreceptor mosaic: evidence for a selective vulnerability of rods in central retina. *Invest. Ophthalmol. Vis. Sci.* **34**, 3278-3296.
- Dacey, D.M. (1993). Morphology of a small-field bistratified ganglion cell type in macaque and human retina. *Vis. Neurosci.* **10**, 1081-1098.
- Dannheim, F. (1987). First experiences with the new Octopus G1 program in chronic simple glaucoma. In: *Documenta Ophthalmologica Proceedings Series 49*. Eds: Greve, E.L. and Heijl, A. Nijhoff / Junk Publishers; Dordrecht. pp. 321-328.
- Dartnall, H.J.A., Bowmaker, J.K. and Mollon, J.D. (1983). Human visual pigments-microspectrophotometric results from the eyes of 7 persons. *Proc. Roy. Soc. Lond. B.* **220**, 115-130.
- Davson, H. (1991). Measurement of the stimulus and dioptrics of the human eye. In: *Physiology of the eye*. Ed: Davson, H. Macmillan Academic and Professional Ltd. Basingstoke and London. pp. 213.
- Delcour, J. and Papacontstantinou, J. (1970). *Physiology of the Eye*, Ed: Davson, H. Macmillan Academic and Professional Ltd, Basingstoke, London, 5th Edition pp 159.
- Delori, F.C. and Burns, S.A. (1996). Fundus reflectance and the measurement of crystalline lens density. *J. Opt. Soc. Am. A.* **13**, 215-226.

- Dengler-Harles, M., Wild, J.M., Cole, M.D., O'Neill, E.C. and Crews, S.J. (1990). The influence of forward light scatter on visual field indices in glaucoma. *Graefes Arch. Clin. Exp. Ophthalmol.* **228**, 326-331.
- Denis, D., Dezard, X., Volot, F. and Vola, J. (1993). Analytical and statistical survey of early stages of open-angle glaucoma with low luminance visual field. *Ophthalmologica.* **207**, 82-89.
- Derrington, A.M. and Lennie, P. (1984). Spatial and temporal contrast sensitivities of neurons in lateral geniculate nucleus of macaque. *J. Physiol.* **357**, 219-240.
- Dixon, W.J. and Mood, A.M. (1948). A method for obtaining and analyzing sensitivity data. *J. Am. Statist. Assoc.* **43**, 109-126.
- Drance, S.M., Wheeler, C. and Patullo, M. (1967). The use of static perimetry in the early detection of glaucoma. *Can. J. Ophthalmol.* **2**, 249-258.
- Drum, B., Armaly, M.F. and Huppert, W. (1986). Scotopic sensitivity loss in glaucoma. *Arch. Ophthalmol.* **104**, 712-717.
- Eichenberger, D., Hendrickson, P., Robert, Y. and Gloor, B. (1987). Influence of ocular media on perimetric results II: Effect of simulated cataract. In: *Documenta Ophthalmologica. Proceedings. Series. 49.* Proceedings of the VIIth International Perimetric Society. Eds: Greve, E.L. and Heijl, A. Nijhoff / Junk Publishers. Dordrecht. pp. 9-13.
- Eisner, A. and MacLeod, D.I.A. (1980). Blue-sensitive cones do not contribute to luminance. *J. Opt. Soc. Am. A.* **70**, 121-123.
- Elzenman, M., Frecker, R.C. and Hallett, P.E. (1984). Precise non-contacting measurement of eye movements using the corneal reflex. *Vision Res.* **24**, 167-174.
- Elenius, V. and Leinonen, M. (1986). Photopic tangential perimetry. *Acta. Ophthalmol.* **64**, 134-137.
- Elliott, D.B. and Hurst, M.A. (1989). Assessing the effect of cataract: a clinical evaluation of the Opacity Lensmeter 701. *Optom. Vis. Sci.* **66**, 257-263.
- Elliott, D.B., Gilchrist, J. and Whitaker, D. (1989). Contrast sensitivity and glare sensitivity with 3 types of cataract morphology. *Ophthal. Physiol. Opt.* **9**, 25-30.

Elliott, D.B., Mitchell, S. and Whitaker, D. (1991). Factors affecting light scatter in contact lens wearers. *Optom. Vis. Sci.* **68**, 629-633.

Enoch, J.M. (1972). The two-colour threshold technique of Stiles and derived component colour mechanisms. In *Handbook of Sensory Physiology*. Vol VII/4. Springer, Berlin. pp.

Fankhauser, F., Koch, P. and Roulier, A. (1972). On automation of perimetry. *Albrecht von Graefe's Arch. Klin. Exp. Ophthalmol.* **184**, 126-150.

Fankhauser, F., Spahr, J. and Bebié, H. (1977). Three years of experience with the Octopus automatic perimeter. *Documenta Ophthalmologica Proceedings Series* **14**. 7-15.

Fankhauser, F. (1979). Problems related to the design of automatic perimeters. *Doc. Ophthalmol.* **47**, 89-138.

Fankhauser, F. and Bebié, H. (1979). Threshold fluctuations, interpolations and spatial resolution in perimetry. *Documenta Ophthalmologica Proceedings Series*. **19**. Proceedings of the Third International Visual Field Symposium. Ed: Greve, E.L. Dr. W. Junk Publishers. The Hague. pp. 295-309.

Fankhauser, F. and Haeblerlin, H. (1980). Dynamic range and stray light. An estimate of the falsifying effects of stray light in perimetry. *Doc. Ophthalmol.* **50**, 143-167.

Fankhauser, F. and Jenni, A. (1981). Programs SARGON and DELTA: two new principles for the automated analysis of the visual field. *Albrecht von Graefe's Arch. Klin. Ophthalmol.* **216**, 41-48.

Fankhauser, F. (1986). Background illumination and automated perimetry. *Arch. Ophthalmol.* **104**, 1126.

Fankhauser, F. (1993). Influence of missed catch-trials on the visual field in normal subjects. *Graefe's Arch. Clin. Exp. Ophthalmol.* **231**, 58-59.

Fechner, (1860). In Treutwein, B. (1995). Adaptive psychophysical procedures. *Vision Res.* **17**, 2503-2522.

Felius, J., van den Berg, T.J.T.P. and Spekrijse, H. (1995). Peripheral cone contrast sensitivity in glaucoma. *Vision Res.* **12**, 1791-1797.

Ferree, C.E. and Rand, G. (1922). An illuminated perimeter with campimeter features. *Am. J. Ophthalmol.* **5**, 455-465.

Fisher, R.F. (1967). The influences of orbital contours and lid ptosis on the size of the peripheral visual field. *Vision Res.* **7**, 671-678.

Fitzke, F.W. and McNaught, A.I. (1994). The diagnosis of visual field progression in glaucoma. *Curr. Opin. Ophthalmol.* **5**, 110-115.

Fitzke, F.W., Crabb, D.P., McNaught, A.I., Edgar, D.F. and Hitchings, R.A. (1996). Image processing of computerized visual-field data. *Br. J. Ophthalmol.* **79**, 207-212.

Flammer, J., Drance, S.M., Fankhauser, F. and Augustiny, L. (1984a). Differential light threshold in automated static perimetry. Factors influencing short-term fluctuation. *Arch. Ophthalmol.* **102**, 876-879.

Flammer, J., Drance, S.M. and Zulauf, M. (1984b). Differential light threshold. Short- and long-term fluctuation in patients with glaucoma, normal controls, and patients with suspected glaucoma. *Arch. Ophthalmol.* **102**, 704-706.

Flammer, J. (1985). Fluctuations in the visual field. In: *Automated perimetry in glaucoma. A practical guide*. Eds: Drance, S.M. and Anderson, D. Grune and Stratton. Orlando, Florida. pp. 162-166.

Flammer, J., Drance, S.M., Augustiny, L. and Funkhouser, A.T. (1985). Quantification of glaucomatous visual field defects with automated perimetry. *Invest. Ophthalmol. Vis. Sci.* **26**, 76-81.

Flammer, J. (1986). The concept of visual field indices. *Graefes Arch. Clin. Exp. Ophthalmol.* **224**, 389-392.

Flammer, J. and Bebié, H. (1987). Lens opacity meter: a new instrument to quantify lens opacity. *Ophthalmologica.* **195**, 69-72.

Flammer, J., Bebié, J.H. and Keller, B. (1987). The Octopus glaucoma G1 program. *Glaucoma.* **9**, 67-72.

Flanagan, J.G., Moss, I.D., Wild, J.M., Hudson, C., Prokopich, L., Whitaker, D. and O'Neill, E.C. (1993a). Evaluation of FASTPAC: a new strategy for estimation with the Humphrey Field Analyser. *Graefes Arch. Clin. Exp. Ophthalmol.* **231**, 465-469.

Flanagan, J.G., Wild, J.M. and Trope, G.E. (1993b). Evaluation of FASTPAC, a new strategy for threshold estimation with the Humphrey Field Analyzer, in a glaucomatous population. *Ophthalmology.* **100**, 949-954.

Flanagan, J.G., Wild, J.M. and Trope, G.E. (1993c). The visual field indices in primary open-angle glaucoma. *Invest. Ophthalmol. Vis. Sci.* **34**, 2266-2274.

Flanagan, J.G., Wild, J.M. and Hovis, J.K. (1991). The differential light threshold as a function of retinal adaptation- the Weber-Fechner / Rose-de-Vries controversy revisited. In: *Perimetry Update 1990/91*. Eds: Mills R.P. and Heijl, A. Kugler Publications. Amsterdam / New York. pp. 551-554.

Förster (1869). In: Atchison, D.A. (1979). History of visual field measurement. *Aust. J. Optom.* **62**, 345-354.

Friedman, L.J., Yim, M.H. and Pugh, E.N. (1984). Temporal integration of the π_1 / π_3 pathway in normal and dichromatic vision. *Vision Res.* **24**, 743-750.

Fry, G.A. (1954). A re-evaluation of the scatter theory of glare. *III. Eng.* **49**, 98-102.

Fuhr, P.S., Herschner, T.A. and Daum, K.M. (1990). Ganzfeld blankout occurs in bowl perimetry and is eliminated by translucent occlusion. *Arch. Ophthalmol.* **108**, 983-988.

Fujimoto, N. and Adachi-Usami, E. (1993). Fatigue effect within 10° visual field in automated perimetry. *Ann. Ophthalmol.* **226**, 431-434.

Funkhouser, A. and Fankhauser, F. (1985). Histogram adaptation in SAPRO operation. *Documenta Ophthalmologica Proceedings Series 42*. Sixth International Visual Field Symposium. Eds: Heijl, A. and Greve, E.L. Dr. W Junk Publishers. Dordrecht. pp. 95-100.

Funkhouser, A.T. (1991). A new diffuse loss index for estimating general glaucomatous visual field depression. *Doc. Ophthalmol.* **77**, 57-72.

Funkhouser, A.T. and Fankhauser, F. (1991). The effects of weighting the "mean defect" visual field index according to threshold variability in the central and midperipheral visual field. *Graefe's Arch. Clin. Exp. Ophthalmol.* **229**, 228-331.

Funkhouser, A., Hirsbrunner, H.P., Fankhauser, F. and Flammer, J. (1991). OCTOSMART: a computerized aid for interpreting visual field examination results. In. *Perimetry Update 1990/91*. Proceedings of the IXth International Perimetric Society Meeting. Eds: Mills, R.P. and Heijl, A. Kugler & Ghedini publications. Amsterdam, New York & Milano. pp. 279-280.

Funkhouser, A.T., Fankhauser, F. and Weale, R.A. (1992). Problems related to diffuse versus localized loss in the perimetry of glaucomatous visual fields. *Graefe's Arch. Clin. Exp. Ophthalmol.* **230**, 243-247.

Gao, H. and Hollyfield, J.G. (1992). Aging of the human retina. *Invest. Ophthalmol. Vis. Sci.* **33**, 1-17.

Gilpin, L.B., Stewart, W.C., Hunt, H.H. and Broom, C.D. (1990). Threshold variability using different Goldmann stimulus sizes. *Acta Ophthalmol.* **68**, 674-676.

Glass, E., Schaumberger, M. and Lachenmayr, B.J. (1995). Simulations for FASTPAC and the standard 4-2 dB full-threshold strategy of the Humphrey Field Analyzer. *Invest. Ophthalmol. Vis. Sci.* **36**, 1847-1854.

Glovinsky, Y., Quigley, H.A. and Pease, M.E. (1993). Foveal ganglion cell loss is size dependent in experimental glaucoma. *Invest. Ophthalmol. Vis. Sci.* **34**, 395-400.

Goldbaum, M.H., Sample, P.A., White, H., Côté, B., Raphaelian, P., Fechtner, R.D. and Weinreb, R.N. (1994). Interpretation of automated perimetry for glaucoma by neural network. *Invest. Ophthalmol. Vis. Sci.* **35**, 3363-3373.

Goldman, J.N. and Benedeck, G.B. (1967). The relationship between morphology and transparency of the non-swelling stroma of the shark. *Invest. Ophthalmol.* **6**, 574-600.

Goldmann, H. (1945a). Grundlagen exacter perimetrie. *Ophthalmologica.* **109**, 57-70.

Goldmann, H. (1945b). Grundlagen exacter perimetrie. *Ophthalmologica.* **109**, 77-79.

Gollamundi, S.R., Liao, P. and Hirsch, J. (1988). Evaluation of corrected loss variance as a visual field index II. Corrected loss variance in conjunction with mean defect may identify stages of glaucoma. *Ophthalmologica*. **197**, 144-150.

Gouras, P. (1968). Identification of cone mechanisms in monkey ganglion cells. *J. Physiol.* **199**, 533-547.

von Graefe, A. (1856). In: Atchison, D.A. (1979). History of visual field measurement. *Aust. J. Optom.* **62**, 345-354.

Gramer, E., Steinhäuser, B. and Kriegelstein, G.K. (1982). The specificity of the automated suprathreshold perimeter Fieldmaster 200. *Græfe's Arch. Clin. Exp. Ophthalmol.* **218**, 253-255.

Greenstein, V.C., Hood, D.C., Ritch, R., Steinberger, D. and Carr, R.E. (1989). S (blue) cone pathway vulnerability in retinitis pigmentosa, diabetes and glaucoma. *Invest. Ophthalmol. Vis. Sci.* **30**, 1732-1737.

Greenstein, V.C., Halevy, D., Zaidi, Q. and Koenig, K.L. (1996). Chromatic and luminance systems deficits in glaucoma. *Vision Res.* **36**, 621-629.

Greve, E.L. (1972). Single stimulus and multiple stimulus threshold. *Vision Res.* **12**, 1533-1543.

Greve, E.L. and Wijnans, M. (1972). The statistical evaluation of measurements in static campimetry and its consequences for multiple stimulus campimetry. *Ophthalmic Res.* **4**, 355-366.

Greve, E.L. (1973). Single and multiple stimulus static perimetry in glaucoma; the two phases of perimetry. *Doc. Ophthalmol.* **36**, 1-355.

Greve, E.L. (1975). Static perimetry. *Ophthalmologica*. **171**, 26-38.

Greve, E.L. and Verduin, W.M. (1977). Detection of early glaucomatous damage. Part 1. Visual Field Examination. *Documenta Ophthalmologica Proceedings Series 14*. Second International Visual Field Symposium. Ed: Greve, E.L. The Hague. Dr. W. Junk Publishers. pp. 103-114.

- Greve, E.L. (1980). Peritest. Glaucoma Symposium. Diagnosis and Therapy. *Documenta Ophthalmologica Proceedings Series 22*. Ed: Greve, E.L. The Hague. Dr. W. Junk Publishers. pp. 71-74.
- Griffin, J.R. (1980). Historical summary of visual fields methods. *J. Am. Optom. Assoc.* **51**, 833-835.
- Gur, M. (1989). Color and brightness fade-out in the ganzfeld is wavelength dependent. *Vision Res.* **29**, 1335-1341.
- Gur, M. (1991). Perceptual fade-out occurs in the binocularly viewed ganzfeld. *Perception.* **20**, 645-654.
- Guthauser, U., Flammer, J. and Niesel, P. (1987). Influence of cataracts on visual fields. *Documenta Ophthalmologica Proceedings Series 49*. Proceedings of the Seventh International Visual Field Symposium. Eds Greve, E.L. and Heijl, A. Martinus Nijhoff / Dr. W. Junk Publishers. Dordrecht. pp. 39-41.
- Guthauser, U. and Flammer, J. (1988). Quantifying visual field damage caused by cataract. *Am. J. Ophthalmol.* **106**, 480-484.
- Gutteridge, I.F. (1984). A review of strategies for screening of the visual fields. *Aust. J. Optom.* **67**, 9-18.
- Guilford, J.P. (1954). In: *Psychometric methods*. New York. McGraw-Hill Publishers. pp. 101-117.
- Haas, A., Flammer, J. and Schneider, U. (1986). Influence of age on the visual fields of normal subjects. *Am. J. Ophthalmol.* **101**, 199-203.
- Haeberlin, H. and Fankhauser, F. (1980). Adaptive programs for analysis of the visual field by automatic perimetry- basic problems and solutions. *Doc. Ophthalmol.* **50**, 123-141.
- Hallet, P.E., Marriott, F.H.C. and Rodger, F.C. (1962). The relationship of visual threshold to retinal position and area. *J. Physiol.* **160**, 364-373. Cited in: Dark adaptation and the minimum visual stimulus. *Physiology of the eye*. Ed: Davson, H. Macmillan Academic and Professional Ltd. Basingstoke and London. pp. 275.

Haley, M.J. (1987). The field analyzer primer. Ed: Haley, M.J. Humphrey Allergan, San Leandro.

Hård, A.L., Beckman, C. and Sjöstrand, J. (1993). Glare measurements before and after cataract surgery. *Acta Ophthalmol.* **71**, 471-476.

Hardy, K.J., Lipton, J., Scase, M.O., Foster, D.H. and Scarpello, J.H.B. (1992). Detection of colour vision abnormalities in uncomplicated type I diabetic patients with angiographically normal retinas. *Br. J. Ophthalmol.* **76**, 461-464.

Harms and Aulhorn (1959). In: Atchison, D.A. (1979). History of visual field measurement. *Aust. J. Optom.* **62**, 345-354.

Hart, W.M., Yablonski, M., Kass, M.A. and Becker, B. (1979). Multivariate analysis of the risk of glaucomatous visual field loss. *Arch. Ophthalmol.* **97**, 1455-1458.

Hart, W.M. and Becker, B. (1982). The onset and evolution of glaucomatous visual field defects. *Ophthalmology.* **89**, 268-279.

Hart, W.M. and Hartz, R.K. (1982). Computer-generated display for three-dimensional static perimetry. *Arch. Ophthalmol.* **100**, 312-318.

Hart, W.M., Silverman, S.E., Trick, G.L., Nesher, R. and Gordon, M.O. (1990). Glaucomatous visual field damage. Luminance and color-contrast sensitivities. *Invest. Ophthalmol. Vis. Sci.* **31**, 359-367.

Hartinger (1936). In *Visual Psychophysics. Handbook of sensory physiology Vol VII Part 4*. Eds: Jameson D. and Hurvich, L.M. Springer-Verlag. Berlin, Heidelberg and New York 1972. pp 104.

Heijl, A. and Krakau, C.E.T. (1975a). An automatic perimeter for glaucoma visual field screening and control. *Albrecht von Graefe's Arch. Klin. Exp. Ophthalmol.* **197**, 13-23.

Heijl, A. and Krakau, C.E.T. (1975b). An automatic static perimeter, design and pilot study. *Acta Ophthalmol.* **53**, 293-310.

Heijl, A. (1977). Time changes of contrast thresholds during automated perimetry. *Acta Ophthalmol.* **55**, 696-708.

Heijl, A. and Drance, S.M. (1983). Changes in differential threshold in patients with glaucoma during prolonged perimetry. *Br. J. Ophthalmol.* **67**, 512-516.

Heijl, A. (1984). Computerised perimetry. *Trans. Ophthalmol. Soc. UK.* **104**, 76-87.

Heijl, A. (1985). The Humphrey Field Analyser, construction and concepts. *Documenta Ophthalmologica Proceedings Series 42*. Eds: Heijl, A and Greve, E.L. Dr. W. Junk. Dordrecht. pp. 77-84.

Heijl, A., Lindgren, G. and Olsson, J. (1987a). Normal variability of static perimetric threshold values across the central visual field. *Arch. Ophthalmol.* **105**, 1544-1549.

Heijl, A., Lindgren, G. and Olsson, J. (1987b). A package for the statistical analysis of visual fields. *Documenta Ophthalmologica Proceedings Series 49*. Proceedings of the Seventh International Visual Field Symposium. Eds Greve, E.L. and Heijl, A. Martinus Nijhoff / Dr. W. Junk Publishers. Dordrecht. pp. 593-600.

Heijl, A. and Åsman, P. (1989). A clinical study of perimetric probability maps. *Arch. Ophthalmol.* **107**, 199-203.

Heijl, A., Lindgren, G. and Olsson, J. (1989). The effect of perimetric experience in normal subjects. *Arch. Ophthalmol.* **107**, 81-86.

Heijl, A., Lindgren, G., Lindgren, A., Olsson, J., Åsman, P., Myers, S. and Patella, M. (1991). Extended empirical statistical package for evaluation of single and multiple fields in glaucoma: Statpac 2. In: *Perimetry Update 1990/91*. Proceedings of the IXth International Perimetric Society Meeting. Eds: Mills, R.P. and Heijl, A. Kugler & Ghedini Publications. Amsterdam, New York & Milano. pp. 303-315.

Heijl, A., Lindgren, G., Olsson, J. and Åsman, P. (1992). On weighted visual field indices. *Graefe's Arch. Clin. Exp. Ophthalmol.* **230**, 397-400.

Heijl, A. (1993). Perimetric point density and detection of glaucomatous visual field loss. *Acta Ophthalmologica.* **71**, 445-450.

Heijl, A. and Bengtsson, B. (1996). The effect of perimetric experience in patients with glaucoma. *Arch. Ophthalmol.* **114**, 19-22.

Henson, D.B. and Bryson, H. (1986). Clinical results with the Henson-Hamblin CFS2000. *Documenta Ophthalmologica Proceedings Series 49*. Seventh International Visual Field Symposium. Eds: Greve, E.L. and Heijl, A. Dr. W. Junk Publishers. Dordrecht, Boston and Lancaster. 233-238.

Henson, D.B. and Anderson, R. (1989). Thresholds using single and multiple stimulus presentations. *Perimetry Update 1988/89*. Ed: Heijl, A. Kugler & Ghedini Publications. Amsterdam, Berkley, Milano. pp. 191-196.

Henson, D.B. and Bryson, H. (1991). Is the variability in glaucomatous field loss due to poor fixation control? *Perimetry Update 1990/91*. Proceedings of the IXth International Perimetric Society Meeting. Eds Mills, R.P. and Heijl, A. Kugler and Ghedini Publications. Amsterdam, New York & Milano. pp. 217-220.

Heron, G., Adams, A.J. and Husted, R. (1988). Central visual fields for short-wavelength sensitive pathways in glaucoma and ocular hypertension. *Invest. Ophthalmol. Vis. Sci.* **29**, 64-72.

Herse, P.R. (1992). Factors influencing normal perimetric thresholds obtained using the Humphrey Field Analyzer. *Invest. Ophthalmol. Vis. Sci.* **33**, 611-617.

Heuer, D.K., Anderson, D.R., Feuer, W.J. and Gressel, M.G. (1987). The influence of refraction accuracy on automated perimetric threshold measurements. *Ophthalmology.* **94**, 1550-1553.

Heuer, D.K., Anderson, D.R., Knighton, R.W., Feuer, W.J. and Gressel, M.G. (1988). The influence of simulated light scattering on automated perimetric threshold measurements. *Arch. Ophthalmol.* **106**, 1247-1251.

Hills, J.F. and Johnson, C.A. (1988). Evaluation of the t-test as a method of detecting visual field changes. *Ophthalmology.* **95**, 261-266.

Hirsbrunner, H.P., Fankhauser, F., Jenni, A. and Funkhouser, A. (1990). Evaluating a perimetric expert system: experience with Octosmart. *Graefes Arch. Clin. Exp. Ophthalmol.* **228**, 237-241.

Hirvelä, H., Luukinen, H. and Laatikainen, L. (1995). Prevalence and risk factors of lens opacities in the elderly in Finland. *Ophthalmology.* **102**, 108-117.

- Holladay, L.L. (1926). The fundamentals of glare and visibility. *J. Opt. Soc. Am.* **12**, 271-319.
- Holladay, L.L. (1927). Action of a light source in the field of view in lowering visibility. *J. Opt. Soc. Am.* **14**, 1-15.
- Holmin, C. and Krakau, C.E.T. (1979). Variability of glaucomatous visual field defects in computerized perimetry. *Græfe's Arch. Clin. Exp. Ophthalmol.* **210**, 235-250.
- Hood, D.C. and Greenstein, V.C. (1988). Blue (S) cone pathway vulnerability: a test of the fragile receptor hypothesis. *Appl. Opt.* **27**, 1025-1029.
- Huag, B.A. Kolle, R.U., Trenkwalder, C., Oertel, W.H. and Paulus, W. (1995). Predominant affection of the blue cone pathway in Parkinson's disease. *Brain.* **118**, 771-778.
- Hudson, C. and Wild, J.M. (1992). Assessment of physiologic statokinetic dissociation by automated perimetry. *Invest. Ophthalmol. Vis. Sci.* **33**, 3162-3168.
- Hudson, C. and Wild, J.M. (1993). The influence of pre-receptor absorption on blue/yellow automated perimetry. In *Perimetry Update 1992/93* Ed: Mills, R.P. Kugler Publications Amsterdam and New York. pp. 451-457.
- Hudson, C., Wild, J.M. and O'Neill, E.C. (1993). Fatigue effects during a single session of automated static threshold perimetry. *Invest. Ophthalmol. Vis. Sci.* **35**, 268-280.
- IJspeert, J.K., de Waard, P.W.T., van den Berg, T.J.T.P. and de Jong, P.T.V.M. (1990). The intraocular straylight function in 129 healthy volunteers; dependence on angle, age and pigmentation. *Vision Res.* **30**, 699-707.
- Ingling, C.R. and Tsou, B.H.P. (1977). Orthogonal combinations of the three visual channels. *Vision Res.* **17**, 1075-1082.
- Jaffe, G.J., Alvarado, J.A. and Juster, R.P. (1986). Age-related changes of the normal visual field. *Arch. Ophthalmol.* **104**, 1021-1025.
- Johnson, C.A., Keltner, J.L. and Balestrery, F. (1978). Effects of target size and eccentricity on visual detection and resolution. *Vision Res.* **18**, 1217-1222.
- Johnson, C.A. and Keltner, J.L. (1981). Computer analysis of visual field loss and optimization of automated perimetric test strategies. *Ophthalmology.* **88**, 1058-1065.

Johnson, C.A. and Keltner, J.L. (1987). Optimal rates of movement for kinetic perimetry. *Arch. Ophthalmol.* **105**, 73-75.

Johnson, C.A., Adams, C.W. and Lewis, R.A. (1988a). Fatigue effects in automated perimetry. *Appl. Optics.* **27**, 1030-1037.

Johnson, C.A., Adams, A.J., Twelker, J.D. and Quigg, J.M. (1988b). Age-related changes in the central visual field for short-wavelength sensitive pathways. *J. Opt. Soc. Am. A.* **5**, 2131-2139.

Johnson, C.A., Adams, A.J. and Lewis, R.A. (1989). Evidence for a neural basis of age-related visual field loss in normal observers. *Invest. Ophthalmol. Vis. Sci.* **30**, 2056-2064.

Johnson, C.A. and Shapiro, L.R. (1991). A rapid heuristic test procedure for automated perimetry. In *Proceedings of the IXth International Perimetric Society Meeting*. Eds: Mills, R.P., Heijl, A. Kugler Publications. Amsterdam. pp. 251-256.

Johnson, C.A., Chauhan, B.C. and Shapiro, L.R. (1992). Properties of staircase procedures for estimating thresholds in automated perimetry. *Invest. Ophthalmol. Vis. Sci.* **33**, 2966-2974.

Johnson, C.A. and Nelson-Quigg, J.M. (1993). A prospective three-year study of response properties of normal subjects and patients during automated perimetry. *Ophthalmology.* **100**, 269-274.

Johnson, C.A., Adams, A.J., Casson, E.J. and Brandt, J.D. (1993a). Blue-on-yellow perimetry can predict the development of glaucomatous visual field loss. *Arch. Ophthalmol.* **111**, 645-650.

Johnson, C.A., Adams, A.J., Casson, E.J. and Brandt, J.D. (1993b). Progression of early glaucomatous visual field loss as detected by blue-on-yellow and standard white-on-white automated perimetry. *Arch. Ophthalmol.* **111**, 651-665.

Johnson, C.A., Howard, D.L., Marshall, D. and Shu, H. (1993c). A non-invasive video-based method of measuring lens transmission properties of the human eye. *Optom. Vis. Sci.* **70**, 944-955.

Johnson, C.A., Brandt, J.D., Khong, A.M. and Adams, A.J. (1995). Short-wavelength automated perimetry in low-, medium-, and high-risk ocular hypertensive eyes. Initial baseline results. *Arch. Ophthalmol.* **113**, 70-76.

- Johnson, M.A. and Choy, D. (1987). On the definition of age-related norms for visual function testing. *Appl. Optics*. **26**, 1449-1454.
- Jonas, J.B., Fernández, M.C. and Naumann, G.O.H. (1992). Glaucomatous parapapillary atrophy. *Arch. Ophthalmol.* **110**, 214-222.
- Jonas, J.B. and Dichtl, A. (1995). Advances in the assessment of optic disc changes in early glaucoma. *Curr. Opin. Ophthalmol.* **6**, 61-66.
- de Jong, L.A.M.S., Snepvangers, C.E.J., van den Berg, T.J.T.P. and Langerhorst, C.T. (1990). Blue-yellow perimetry in the detection of early glaucomatous damage. *Doc. Ophthalmol.* **75**, 303-314.
- Kaiser, H.J., Flammer, J., Bucher, P.J.M., DeNatale, R., Stümpfig, D. and Hendrickson, P. (1994). High-resolution perimetry of the central visual field. *Ophthalmologica*. **208**, 10-14.
- Kaplan, E. and Shapley, R.M. (1982). X and Y cells in the lateral geniculate nucleus of macaque monkeys. *J. Physiol.* **330**, 125-143.
- Kaplan, E. and Shapley, R.M. (1986). The primate retina contains two types of ganglion cells, with high and low contrast sensitivity. *Proc. Nat. Acad. Sci. USA*. **83**, 2755-2757.
- Katz, J. and Sommer, A. (1986). Asymmetry and variation in the normal hill of vision. *Arch. Ophthalmol.* **104**, 65-68.
- Katz, J. and Sommer, A. (1987). A longitudinal study of the age-adjusted variability of automated visual fields. *Arch. Ophthalmol.* **105**, 1083-1086.
- Katz, J. and Sommer, A. (1988). Reliability indexes of automated perimetric tests. *Arch. Ophthalmol.* **106**, 1252-1254.
- Katz, J. and Sommer, A. (1990). Reliability of automated perimetric tests. *Arch. Ophthalmol.* **108**, 777-778.
- Katz, J., Sommer, A. and Witt, K. (1991). Reliability of visual field results over repeated testing. *Ophthalmology*. **98**, 70-75.
- Katz, J., Quigley, H.A. and Sommer, A. (1995). Repeatability of the Glaucoma Hemifield Test in automated perimetry. *Invest. Ophthalmol. Vis. Sci.* **36**, 1658-1664.

Kaufmann, H. and Flammer, J. (1989). Clinical experience with the Bebié-curve. In: *Perimetry Update 1988/89*. Ed: Heijl, A. Kugler & Ghedini Publications. Amsterdam, Berkley and Milano. pp. 235-238.

Kelman, S.E., Perell, H.F., D'Autrechy, L. and Scott, R.J. (1991). A neural network can differentiate glaucoma and optic neuropathy visual fields through pattern recognition. *Perimetry Update 1990/91*. Eds: Mills, R.P. and Heijl, A. Amsterdam / New York. Kugler Publications. pp. 287-290.

Keltner, J.L., Johnson, C.A. and Balestrery, F.G. (1979). Suprathreshold static perimetry. Initial clinical trials with the Fieldmaster automated perimeter. *Arch. Ophthalmol.* **97**, 260-272.

Keltner, J.L. and Johnson, C.A. (1981). Capabilities and limitations of automated suprathreshold static perimetry. *Documenta Ophthalmologica Proceedings Series 26*. Ed: Greve, E.L. Junk Publishers. Amsterdam. pp. 49-55.

Keltner, J.L. and Johnson, C.A. (1995). Short-wavelength automated perimetry in neuro-ophthalmologic disorders. *Arch. Ophthalmol.* **113**, 475-481.

Khu, P.M and Kashiwagi, T. (1993). Quantitating nuclear opacification in color Scheimpflug photographs. *Invest. Ophthalmol. Vis. Sci.* **34**, 130-136.

Khu, P.M., Karbassi, M., Singer, D.M. and Chylack, L.T. (1994). Effect of type and severity on lens grading. *Ophthalmic Res.* **26** (Suppl 1), 61-67.

King-Smith, P.E. and Carden, D. (1976). Luminance and opponent-color contributions to visual detection and adaptation and to temporal and spatial integration. *J. Opt. Soc. Am.* **66**, 709-716.

King-Smith, P.E., Grigsby, S.S., Vingrys, A.J., Benes, S.C. and Supowit, A. (1994). Efficient and unbiased modifications of the QUEST threshold method: theory, simulations, experimental evaluation and practical implementation. *Vision Res.* **34**, 885-912.

Klein, R.E. and Klein, R. (1984). Cataracts and macular degeneration in older Americans. *Arch. Ophthalmol.* **100**, 571-573.

Klein, R.E.K., Klein, R. and Linton, K.L.P. (1992). Prevalence of age-related lens opacities in a population. The Beaver Dam Eye Study. *Ophthalmology.* **99**, 543-552.

- Klewin, K.M. and Radius, R.L. (1986). Background illumination and automated perimetry. *Arch. Ophthalmol.* **104**, 395-397.
- Klewin, K.M. and Radius, R.L. (1987). Static threshold determination and kinetic perimetry. *Glaucoma.* **9**, 61-63.
- Krakau, C.E.T. (1978). Aspects on the design of an automatic perimeter. *Acta Ophthalmol.* **56**, 389-405.
- Kulze, J.C., Stewart, W.C. and Sutherland, S.E. (1990). Factors associated with a learning effect in glaucoma patients using automated perimetry. *Acta Ophthalmol.* **68**, 681-686.
- Kudrna, G.R., Stanley, M.A. and Remington, L.A. (1995). Pupillary dilation and its effects on automated perimetry results. *J. Am. Optom. Assoc.* **66**, 675-680.
- Kupfer, C. (1984). The conquest of cataract: a global challenge. *Trans. Ophthal. Soc. U.K.* **104**, 1-10.
- Lagerlöf, O. (1991). Color vision in diabetics. In *Color Vision Deficiencies X*. Eds. Drum, B., Moreland, J.D. and Serra, A. Kluwer Academic Publishers. Dordrecht. pp.517-522.
- Lam, B.L., Alward, W.L.M. and Kolder, H.E. (1991). Effect of cataract on automated perimetry. *Ophthalmology.* **98**, 1066-1070.
- Lakowski, R., Bryett, J. and Drance, S.M. (1972). A study of colour vision in ocular hypertensives. *Can. J. Ophthalmol.* **7**, 86-95.
- Langerhorst, C.T., van den Berg, T.J.T.P. and van Spronsen, R. (1985). Results of a fluctuation analysis and defect volume program for automated static threshold perimetry with the Scotoperimeter. *Documenta Ophthalmologica Proceedings Series 42*. Proceedings of the Sixth International Visual Field Symposium. Eds: Heijl, A. and Greve, E.L. Dr W Junk Publishers. Dordrecht. pp. 1-6.
- Langerhorst, C.T., Berg, V.D., Veldman, E. and Greve, E.L. (1987). Population study of global and local fatigue with prolonged threshold testing in automated perimetry. *Documenta Ophthalmologica Proceedings Series 49*. Eds: Greve, E.L. and Heijl, A. Nijhoff / Junk Publishers. Dordrecht. pp. 657-662.

Langerhorst, C.T., van den Berg, T.J.T.P. and Greve, E.L. (1989). Is there general reduction of sensitivity in glaucoma? *Int. Ophthalmol.* **13**, 31-35.

Lauber (1932). In *Handbook of sensory physiology Vol VII. Part 4. Visual psychophysics*. Eds: Jameson, D. and Hurvich, L.M. Springer-Verlag. Berlin, Heidelberg and New York. 1972. pp. 104.

Lee, B.B. (1996). Receptive field structure in the primate retina. *Vision Res.* **36**, 631-644.

Lehmann, D. and Skrandies, W. (1979). Multichannel evoked potential fields show different properties of human upper and lower hemiretina systems. *Exp. Brain Res.* **35**, 151-159.

Lerman, S. and Borkman, R. (1976). Spectroscopic evaluation and classification of the normal aging, and cataractous lens. *Ophthalmic Res.* **8**, 335-353.

Lerman, S., Kuck, J.F., Borkman, R.F. and Saker, E. (1976). Induction, acceleration and prevention (in vitro) of an aging parameter in the ocular lens. *Ophthalmic Res.* **8**, 213-226.

Lewis, R.A., Johnson, C.A. and Adams, A.J. (1993). Automated perimetry and short wavelength sensitivity in patients with asymmetric intraocular pressures. *Graefe's Arch. Clin. Exp. Ophthalmol.* **231**, 274-278.

Li, Y. and Mills, R.P. (1992). Kinetic fixation improves threshold sensitivity in the central visual field. *J. Glaucoma.* **1**, 108-116.

Liao, P.M., Gollamudi, S.R. and Hirsch, J. (1988). Evaluation of corrected loss variance as a visual field index I. CLV exceeds RMS in discriminating between glaucoma-suspect patients with no loss of visual sensitivity and normal observers. *Ophthalmologica* **197**, 136-143.

Lieberman, M.F. and Drake, M.V. (1987). Fundamentals of computerized perimetry. In: *A simplified guide to computerized perimetry*. Slack Inc. New Jersey. pp. 19-31.

Lindenmuth, K.A., Skuta, G.L., Rabbani, R. and Musch, D.C. (1989). Effects of pupillary constriction on automated perimetry in normal eyes. *Ophthalmology.* **96**, 1298-1301.

Lindenmuth, K.A., Skuta, G.L., Rabbani, R., Musch, D.C. and Bergstrom, T.J. (1990). Effects of pupillary dilation on automated perimetry in normal patients. *Ophthalmology.* **97**, 367-370.

Lutze, M. and Bresnick, G.H. (1994). Lens-corrected visual field sensitivity and diabetes. *Invest. Ophthalmol. Vis. Sci.* **35**, 649-655.

Lynn, J.R. (1969). Examination of the visual field in glaucoma. *Invest. Ophthalmol.* **8**, 76-86.

Lynn, J.R., Swanson, W.H. and Fellman, R.L. (1991). Evaluation of automated kinetic perimetry (AKP) with the Humphrey Field Analyzer. In: *Perimetry Update 1990/91*. Eds: Mills, R.P. and Heijl, A. Kugler & Ghedini Publications. Amsterdam, Berkley and Milano. pp. 433-452.

Mackworth, J.F. (1969). In: *Vigilance and habituation. A neuropsychological approach*. Penguin Books Inc. Baltimore. pp. 13-107.

Magno, B.V., Datiltes, M.B. and Lasa, S.M. (1993). Senile cataract progression studies using the lens opacities classification system II. *Invest. Ophthalmol. Vis. Sci.* **34**, 2138-2141.

Mann, C.G., Orr, A.C., Rubilowicz, M. and Le Blanc, R.P. (1989). Automated static perimetry in chloroquine and hydroxychloroquine therapy. In: *Perimetry Update 1988/89*. Proceedings of the VIIIth International Perimetric Society Meeting. Ed. Heijl, A. Kugler and Ghedini Publications. Amsterdam, Berkeley and Milano. pp. 417-421.

Maraini, G., Pasquini, P., Tomba, M.C., Bonacini, M., Stazi, M.A., Rosmini, F., Sperduto, R.D. and the Italian-American Cataract Study Group. (1989). An independent evaluation of the lens opacities classification system II (LOCS II). *Ophthalmology.* **96**, 611-615.

Marchini, G., Pisano, F., Bertagnin, F., Marraffa, M. and Bonomi, L. (1991). Perimetric learning effect in glaucoma patients. *Glaucoma.* **13**, 102-106.

Marra, G. and Flammer, J. (1991). The learning and fatigue effect in automated perimetry. *Graefe's Arch. Clin. Exp. Ophthalmol.* **229**, 501-504.

Maurice, D.M. (1957). The structure and transparency of the cornea. *J. Physiol.* **136**, 263-286.

Mellerio, J. (1971). Light absorption and scatter in the human lens. *Vision Res.* **11**, 129-141.

Mellerio, J. (1987). Yellowing of the cortical human lens: nuclear and cortical contributions. *Vision Res.* **27**, 1581-1587.

- Merigan, W.H. and Maunsell, J.H.R. (1990). Macaque vision after magnocellular lateral geniculate lesions. *Vis. Neurosci.* **5**, 347-352.
- Merigan, W.H., Katz, L.M. and Maunsell, J.H.R. (1991). The effects of parvocellular lateral geniculate lesions on the acuity and contrast sensitivity of macaque monkeys. *J. Neurosci.* **11**, 994-1001.
- Merigan, W.H. and Maunsell, J.H.R. (1993). How parallel are the primate visual pathways? *Annu. Rev. Neurosci.* **16**, 369-402.
- Meyer, D.R., Stern, J.H., Jarvis, J.M. and Liniger, L.L. (1993). Evaluating the visual field effects of blepharptosis using automated static perimetry. *Ophthalmology.* **100**, 651-659.
- Mikelberg, F.S. and Drance, S.M. (1984). The mode and progression of visual field defects in glaucoma. *Am. J. Ophthalmol.* **98**, 443-445.
- Miller, K.N. and Quigley, H.A. (1988). The clinical appearance of the lamina cribrosa as a function of the extent of glaucomatous optic nerve damage. *Ophthalmology.* **95**, 135-138.
- Miller, K.N., Shields, M.B. and Ollie, A.R. (1989). Automated kinetic perimetry with two peripheral isopters in glaucoma. *Arch. Ophthalmol.* **107**, 1316-1320.
- Mitchell, E.S. and Hurst, M.A. (1993). The relationship between forward light scatter and cataract. *Invest. Ophthalmol. Vis. Sci. (Suppl.)* **34**, 1414.
- de Monasterio, F.M. and Gouras, P. (1975). Functional properties of ganglion cells of the rhesus monkey retina. *J. Physiol.* **251**, 167-195.
- de Monasterio, F.M. (1978). Properties of concentrically organised X and Y ganglion cells of the macaque retina. *J. Neurophysiol.* **41**, 1394-1417.
- de Monasterio, F.M., Schein, S.J. and McCrane, E.P. (1981). Staining of blue-sensitive cones of the macaque retina by a fluorescent dye. *Science.* **213**, 1278-1281.
- de Monasterio, F.M., McCrane, E.P., Newlander, J.K. and Schein, S.J. (1985). Density profile of blue-sensitive cones along the horizontal meridian of macaque retina. *Invest. Ophthalmol. Vis. Sci.* **26**, 289-302.

Moore, A.T., Fitzke, F.W., Kemp, C.M., Arden, G.B., Keen, T.J., Inglehearn, C.F., Bhattacharya, S.S. and Bird, A.C. (1992). Abnormal dark adaptation kinetics in autosomal dominant sector retinitis pigmentosa due to rod opsin mutation. *Br. J. Ophthalmol.* **76**, 465-469.

Morgan, J.E. (1994). Selective cell death in glaucoma: does it really occur? *Br. J. Ophthalmol.* **78**, 875-880.

Morgan, R.K., Feuer, W.J. and Anderson, D.R. (1991). Statpac 2 glaucoma change probability. *Arch. Ophthalmol.* **109**, 1690-1692.

Moss, I.D., Wild, J.M. and Whitaker, D. (1993). The effect of forward light scatter on chromatic sensitivity thresholds. In: *Perimetry Update 1992/93*. Ed: Mills, R.P. Kugler Publications Amsterdam / New York. pp. 477-483.

Moss, I.D. and Wild, J.M. (1994). The influence of forward light scatter on the normal blue-on-yellow perimetric profile. *Graefe's Arch. Clin. Exp. Ophthalmol.* **232**, 409-414.

Moss, I.D., Wild, J.M. and Whitaker, D.J. (1995). The influence of age-related cataract in blue-on-yellow perimetry. *Invest. Ophthalmol. Vis. Sci.* **36**, 764-773.

de Natale, R., Flammer, J., Zulauf, M. and Bebie, T. (1988). Influence of age on transparency of the lens in normals: a population study with the help of the Lens Opacity Meter 701. *Ophthalmologica.* **197**, 14-18.

Nagata, S., Kani, K. and Sugiyama, A. (1991). A computer-assisted visual field diagnosis system using a neural network. In: *Perimetry Update 1990/91*. Mills, R.P. and Heijl, A. Amsterdam / New York. Kugler Publications. pp. 291-295.

Nelson-Quigg, J.M., Johnson, C.A., Casson, E.J. and Adams, A.J. (1990). Long and short-term variability for perimetry of short-wavelength sensitive (SWS) mechanisms. *Invest. Ophthalmol. Vis. Sci. (Suppl)*. **31**, 190.

Nelson-Quigg, J.M., Johnson, C.A., Morse, L.S. and Chu, T.G. (1994). Comparison of lens transmission properties in diabetics and non-diabetics using the lens absorption monitor (LAM). *Invest. Ophthalmol. Vis. Sci. (Suppl)*. **35**, 1823.

- Niesel, P, Ramel, C. and Weidmann, B.O.S. (1978). Das Verhalten von perimetrischen Untersuchungsbefunden bei Entwicklung einer Katarakt. *Klin. Mbl. Augenheik.* **172**, 477-4803.
- Niesel, P. and Wiher, U. (1982). Modellexperimente zum Verhalten glaukomatöser Gesichtsfeldausfälle bei Kataraktentwicklung. *Klin. Mbl. Augenheik.* **180**, 461-463.
- Norren, D.V. and Vos, J.J. (1974). Spectral transmission of the human ocular media. *Vision Res.* **14**, 1237-1244.
- Noureddin, B.N., Poinosawmy, D., Fitzke, F.W. and Hitchings, R.A. (1991). Regression analysis of visual field progression in low tension glaucoma. *Br. J. Ophthalmol.* **75**, 493-495.
- O'Brien, C., Poinosawmy, D., Wu, J. and Hitchings, R. (1994). Evaluation of the Humphrey FASTPAC threshold program in glaucoma. *Br. J. Ophthalmol.* **78**, 516-519.
- Okuyama, S., Matsumoto, C., Uyama, K. and Otori, T. (1993). Reappraisal of normal values of the visual field using the Octopus 1-2-3. *Perimetry Update 1992/93*. Ed: Mills, R.P. Amsterdam / New York. Kugler Publications. pp.
- Olsson, J., Rootzén, H. and Heijl, A. (1989). Maximum likelihood estimation of the frequency of false positive and false negative answers from the up-and-down staircases of computerized perimetry. In: *Perimetry Update 1988/89*. Proceedings of the VIIIth International Perimetric Society Meeting. Ed: Heijl, A. Kugler & Ghedini Publications. Amsterdam, Berkeley & Milano. pp. 245-251.
- Olsson, J. (1991). *Statistics in perimetry*. Doctoral Dissertation. Department of Mathematical Statistics. NFMS-3145, University of Lund, Sweden.
- Olsson, J., Heijl, A., Bengtsson, B. and Rootzén, H. (1993). Frequency-of-seeing in computerized perimetry. *Perimetry Update 1992/93*. Proceedings of the Xth International Perimetric Society Meeting. Ed: Mills, R.P. Amsterdam / New York. Kugler Publications. pp. 551-556.
- Olsson, J. and Rootzén, H. (1994). An image model for the quantal response analysis in perimetry. *Scand. J. Statist.* **21**, 375-387.
- Olsson, J., Bengtsson, B., Heijl, A. and Rootzén, H. (1995). Improving estimation of false-positive and false-negative response in computerized perimetry. In: *Perimetry Update*

1994/95. Proceedings of the Xith International Perimetric Society Meeting. Eds: Mills, R.P. and Wall, M. Amsterdam & New York. Kugler Publications. pp. 219.

Olsson, J., Bengtsson, B., Heijl, A. and Rootzén, H. (1997). An improved method to estimate frequency of false positive answers in computerized perimetry. *Acta Ophthalmol. (Scand.)* **75**, 181-183.

Panda-Jonas, S., Jonas, J.B., Jakobczyk, M. and Schneider, U. (1994). Retinal photoreceptor count, retinal surface area, and optic disc size in normal human eyes. *Ophthalmology*. **101**, 519-523.

Panda-Jonas, S., Jonas, J.B. and Jakobczyk-Zmija, M. (1995). Retinal photoreceptor density decreases with age. *Ophthalmology*. **102**, 1853-1859.

Pardhan, S. (1997). A comparison of binocular summation in the peripheral visual field in young and older patients. *Curr. Eye Res.* **16**, 252-255.

Paulsson, L.E. and Sjöstrand, J. (1980). Contrast sensitivity in the presence of a glare light. *Invest. Ophthalmol. Vis. Sci.* **19**, 401-406.

Pearson, P.A., Baldwin, L.B. and Smith, T.J. (1989). The Q-statistic in glaucoma and ocular hypertension. In: *Perimetry Update 1988/89*. Proceedings of the VIIIth International Perimetric Society Meeting. Ed: Heijl, A. Kugler and Ghedini Publications. Amsterdam, Berkeley and Milano. pp. 229-233.

Pearson, P.A., Baldwin, L.B. and Smith, T.J. (1990). The relationship of mean defect to corrected loss variance in glaucoma and ocular hypertension. *Ophthalmologica*. **200**, 16-21.

Pease, P.L. and Adams, A.J. (1983). Macular pigment difference spectrum from sensitivity measures of a single cone mechanism. *Am. J. Optom. Physiol. Opt.* **60**, 667-672.

Pease, P.L., Adams, A.J. and Nuccio, E. (1987). Optical density of human macular pigment. *Vision Res.* **27**, 705-710.

Pennebaker, G.E., Stewart, W.C., Stewart, J.A. and Hunt, H.H. (1992). The effect of stimulus duration upon the components of fluctuation in static automated perimetry. *Eye*. **6**, 353-355.

Pokorny, J., Smith, V.C. and Lutze, M. (1987). Aging of the human lens. *Appl. Optics*. **26**, 1437-1440.

Pugh, E.N. (1976). The nature of the π_1 colour mechanism of W. S. Stiles. *J. Physiol.* **257**, 713-747.

Pugh, E.N. and Mollen, J.D. (1979). A theory of the π_1 and π_3 color mechanisms of Stiles. *Vision Res.* **19**, 293-312.

Purpura, K., Tranchina, D., Kaplan, E. and Shapley, R.M. (1990). Light adaptation in the primate retina: analysis of the changes in gain and dynamics of monkey retinal ganglion cells. *Vis. Neurosci.* **4**, 75-93.

Quigley, H.A., Addicks, E.M., Green, W.R. and Maumenee, A.E. (1981). Optic nerve damage in human glaucoma II. The site of injury and susceptibility to damage. *Arch. Ophthalmol.* **99**, 635-649.

Quigley, H.A., Addicks, E.M. and Green, W.R. (1982). Optic nerve damage in human glaucoma. Quantitative correlation of nerve fiber loss and visual field defect in glaucoma, ischemic neuropathy, papilledema, and toxic neuropathy. *Arch. Ophthalmol.* **100**, 135-146.

Quigley, H.A., Hohman, R.M., Addicks, E.M., Massof, R.W. and Green, W.R. (1983). Morphologic changes in the lamina cribrosa correlated with neural loss in open-angle glaucoma. *Am. J. Ophthalmol.* **95**, 673-691.

Quigley, H.A. (1987). Are some ganglion cells killed by glaucoma before others? In: *Glaucoma Update III*. Ed: Kriegelstein, G.K. Springer-Verlag; Berlin / Heidelberg. pp. 23-26.

Quigley, H.A., Sanchez, R.M., Dunkelberger, G.R., L'Hernault, N.L. and Baginski, T.A. (1987). Chronic glaucoma selectively damages large optic nerve fibers. *Invest. Ophthalmol. Vis. Sci.* **28**, 913-920.

Quigley, H.A., Dunkelberger, G.R. and Green, W.R. (1988). Chronic human glaucoma causing selectively greater loss of large optic nerve fibers. *Ophthalmology.* **95**, 357-363.

Quigley, H.A., Dunkelberger, G.R. and Green, W.R. (1989). Retinal ganglion cell atrophy correlated with automated perimetry in human eyes with glaucoma. *Am. J. Ophthalmol.* **107**, 453-464.

Quigley, H.A. (1994). Comment. *Br. J. Ophthalmol.* **78**, 879-880.

Quigley, H.A., Enger, C., Katz, J., Sommer, A., Scott, R. and Gilbert, D. (1994). Risk factors for the development of glaucomatous visual field loss in ocular hypertension. *Arch. Ophthalmol.* **112**, 644-649.

Radius, R.L. (1978). Perimetry in cataract patients. *Arch. Ophthalmol.* **96**, 1574-1579.

Radius, R.L. (1987). Anatomy of the optic nerve head and glaucomatous optic neuropathy. *Surv. Ophthalmol.* **32**, 35-44.

Reed, H. and Drance, S.M. (1972). *The essentials of perimetry. Static and Kinetic.* 2nd Edition. Oxford University Press. London, New York and Toronto. pp. 24-25.

Rebolleda, G., Munoz, F.J., Fernández Victorio, J.M., Pellicer, T. and Castillo, J.M. (1992). Effects of pupillary dilation on automated perimetry in glaucoma patients receiving pilocarpine. *Ophthalmology.* **99**, 418-423.

Reynolds, M., Stewart, W.C. and Sutherland, S. (1990). Factors that influence the prevalence of positive catch-trials in glaucoma patients. *Graefe's Arch. Clin. Exp. Ophthalmol.* **228**, 338-341.

Ricco (1887). In *Vision: coding and efficiency.* Spatial and temporal summation in human vision. Ed: Blakemore, C. Cambridge University Press, Cambridge. pp. 376

Robinson, D.A. (1964). The mechanics of human saccadic eye movement. *J. Physiol.* **174**, 245-264.

Robbins, H. and Monro, S. (1951). A stochastic approximation method. *Annals of Mathematical Statistics.* **22**, 400-407.

Rønne (1909). In: Atchison, D.A. (1979). History of visual field measurement. *Aust. J. Optom.* **62**, 345-354.

Ruddock, K.H. (1965). The effect of age upon colour vision-II. Changes with age in light transmission of the ocular media. *Vision Res.* **5**, 47-58.

Rutishauser, C. and Flammer, J. (1988). Retests in static perimetry. *Graefe's Arch. Clin. Exp. Ophthalmol.* **226**, 75-77.

- Rutishauser, C., Flammer, J. and Haas, A. (1989). The distribution of normal values in automated perimetry. *Graefes Arch. Clin. Exp. Ophthalmol.* **227**, 513-517.
- Said, F.S. and Weale, R.A. (1959). The variation with age of the spectral transmissivity of the living human crystalline lens. *Gerontologica.* **3**, 213.
- Sakkitt (1971) In *Physiology of the eye*. Dark adaptation and the minimum visual stimulus. Ed: Davson, H. Macmillan Academic and Professional Ltd. Basingstoke and London. pp. 275.
- Sample, P.A., Weinreb, R.N. and Boynton, R.M. (1986). Blue-on-Yellow color perimetry. *Invest. Ophthalmol. Vis. Sci. (Suppl.)* **35**, 1823.
- Sample, P.A., Esterson, F.D., Weinreb, R.N. and Boynton, R.M. (1988). The aging lens: in vivo assessment of light absorption in 84 human eyes. *Invest. Ophthalmol. Vis. Sci.* **29**, 1306-1311.
- Sample, P.A. and Weinreb, R.N. (1989). Color perimetry in glaucoma: Isolation of short-wavelength sensitive mechanisms. *Invest. Ophthalmol. Vis. Sci. (Suppl.)* **30**, 56.
- Sample, P.A., Esterson, F.D. and Weinreb, R.N. (1989). A practical method for obtaining an index of lens density with an automated perimeter. *Invest. Ophthalmol. Vis. Sci.* **30**, 786-787.
- Sample, P.A. and Weinreb, R.N. (1990). Color perimetry for assessment of primary open angle glaucoma. *Invest. Ophthalmol. Vis. Sci.* **31**, 1869-1875.
- Sample, P.A., Quirante, J.S. and Weinreb, R.N. (1991). Age-related changes in the human lens. *Acta Ophthalmol.* **69**, 310-314.
- Sample, P.A. and Weinreb, R.N. (1992). Progressive color visual field loss in glaucoma. *Invest. Ophthalmol. Vis. Sci.* **33**, 2068-2071.
- Sample, P.A., Taylor, J.D.N., Martinez, G.A., Lusky, M. and Weinreb, R.N. (1993). Short-wavelength color visual fields in glaucoma suspects at risk. *Am. J. Ophthalmol.* **115**, 225-233.
- Sample, P.A., Martinez, G.A. and Weinreb, R.N. (1994). Short-wavelength automated perimetry without lens density testing. *Am. J. Ophthalmol.* **118**, 632-641.
- Sample, P.A., Johnson, C.A., Haegerstrom-Portnoy, G. and Adams, A.J. (1996). Optimum parameters for short-wavelength automated perimetry. *J. Glaucoma.* **5**, 375-393.

- Sanabria, O., Feuer, W.J. and Anderson, D.R. (1990). Pseudo-loss of fixation in automated perimetry. *Ophthalmology*. **98**, 76-78.
- Sasaki, K., Fujisawa, K. and Sakamoto, Y. (1992). Quantitative evaluation of nuclear cataract using image analysis. *Ophthalmic Res.* **24** (Suppl. 1.), 26-31.
- Savage, G.L., Haegerstrom-Portnoy, G., Adams, A.J. and Hewlett, S.E. (1993). Age changes in the optical density of human ocular media. *Clin. Vis. Sci.* **8**, 97-108.
- Schaumberger, M., Schäfer, B. and Lachenmayr, B.J. (1995). Glaucomatous visual fields. FASTPAC versus full threshold strategy of the Humphrey Field Analyzer. *Invest. Ophthalmol. Vis. Sci.* **36**, 1390-1397.
- Schaumberger, M., Glass, E., Ebel, G.K. and Lachenmayr, B. (1996). A new strategy for automated perimetry. Presented at the XII International Perimetric Society Meeting. 4-8 June 1997. Würzburg, Germany.
- Schmied, U. (1980). Automated (Octopus) and manual (Goldmann) perimetry in glaucoma. *Albrecht von Graefe's Arch. Klin. Ophthalmol.* **213**, 239-244.
- Schober (1958). In *Handbook of sensory physiology Vol VII. Part 4. Visual psychophysics*. Eds: Jameson, D. and Hurvich, L.M. Springer-Verlag. Berlin, Heidelberg and New York. 1972. pp. 103
- Schouten, J.F. and Ornstein, L.S. (1939). Measurements on direct and indirect adaptation by means of a binocular method. *J. Opt. Soc. Am.* **29**, 168-182.
- Schulzer, M., Mills, R.P., Hopp, R.H., Lau, W. and Drance, S.M. (1990). Estimation of the short-term fluctuation from a single determination of the visual field. *Invest. Ophthalmol. Vis. Sci.* **31**, 730-735.
- Schwartz, B. and Nagin, P. (1985). Probability maps for evaluating automated visual fields. *Documenta Ophthalmologica Proceedings Series 42. Proceedings of the Sixth International Visual Field Symposium*. Eds: Heijl, A. and Greve, E.L. Dr. W. Junk Publishers. Dordrecht. pp. 39-48.
- Searle, A.E.T., Wild, J.M., Shaw, D.E. and O'Neill, E.C. (1991). Time related variation in normal automated static perimetry. *Ophthalmology*. **98**, 701-707.

- Shapiro, L.R., Johnson, C.A. and Kennedy, R.L. (1989). KRAKEN. A computer simulation procedure for static, kinetic, suprathreshold static and heuristic perimetry. In: *Perimetry Update 1988/89*. Proceedings of the VIIIth International Perimetric Society Meeting. Ed. Heijl A. Kugler & Ghedini Publications. Amsterdam, Berkeley and Milano. pp. 431-438.
- Shiga, S. (1968). Visual field changes with loaded illumination. *Am. J. Ophthalmol.* **66**, 245-263.
- Sigel, C. and Brousseau, L. (1982). Pi-4: adaptation of more than one class of cone. *J. Opt. Soc. Am.* **72**, 237-245.
- Simpson, T.L., Barbeito, R. and Bedell, H.E. (1986). The effect of optical blur on visual acuity for targets of different luminances. *Ophthalm. Physiol. Opt.* **6**, 279-281.
- Sloan, L.L. (1939). Instruments and techniques for the clinical testing of the light sense III - an apparatus for studying regional differences in light sense. *Arch. Ophthalmol.* **22**, 233-251.
- Sloan, L.L. (1961). Area and luminance of test object as variables in examination of the visual field by projection perimetry. *Vision Res.* **1**, 121-138.
- Smith, S.D., Katz, J. and Quigley, H.A. (1996). The effect of cataract extraction on the results of automated perimetry in glaucoma. *Invest. Ophthalmol. Vis. Sci. (Suppl.)* **37**, S509.
- Smith, V.C. and Pokorny, J. (1975). Spectral sensitivity of the foveal cone photopigments between 400 and 500 nm. *Vision Res.* **15**, 161-171.
- Snodderley, D.M., Brown, P.K., Delori, F.C. and Auran, J.D. (1984a). The macular pigment 1. Absorbance spectra, localization, and discrimination from other yellow pigments in primate retinas. *Invest. Ophthalmol. Vis. Sci.* **25**, 660-673.
- Snodderley, D.M., Auran, J.D. and Delori, F.C. (1984b). The macular pigment 2. Spatial distribution in primate retinas. *Invest. Ophthalmol. Vis. Sci.* **25**, 674-685.
- Sokolov, Y.N. (1963). In: *Perception and the conditioned reflex*. Macmillan Publishers, New York.
- Sommer, A., Katz, J., Quigley, H.A., Miller, N.R., Robin, A.L., Richer, R.C. and Witt, K.A. (1991). Clinically detectable nerve fiber atrophy precedes the onset of glaucomatous field loss. *Arch. Ophthalmol.* **109**, 77-83.

- Spahr, J. (1975). Optimization of the presentation pattern in automated static perimetry. *Vision Res.* **15**, 1275-1281.
- Spector, A., Roy, D. and Stauffer, J. (1975). Isolation and characterization of an age-dependent polypeptide from human lens with non-tryptophan fluorescence. *Exp. Eye. Res.* **1**, 9-24.
- Spenceley, S.E., Henson, D.B. and Bull, D.R. (1994). Visual field analysis using artificial neural networks. *Ophthal. Physiol. Opt.* **14**, 239-248.
- Sperling, H.G., Johnson, C. and Harwerth, R.S. (1980). Differential spectral photic damage to primate cones. *Vision Res.* **20**, 1117-1125.
- Stewart, W.C., Rogers, G.M., Crinkley, C.M.C. and Carlson, A.N. (1995). Effect of cataract extraction on automated fields in chronic open-angle glaucoma. *Arch. Ophthalmol.* **113**, 875-879.
- Stiles, W.S. (1929). The effect of glare on the brightness difference threshold. *Proc. Roy. Soc. Series B.* **104**, 322-355.
- Stiles, W.S. (1930). The scattering theory of the effect of glare on the brightness difference threshold. *Proc. Roy. Soc. Series B.* **105**, 131-141.
- Stiles, W.S. and Crawford, B.H. (1937). The effect of a glaring light source on extrafoveal vision. *Proc. Roy. Soc. Series B.* **122**, 255-280.
- Stiles, W.S. (1939). The directional sensitivity of the retina and the spectral sensitivities of the rods and cones. *Proc. Royal Soc. Lond. Series B.* **127**, 64-105.
- Stiles, W.S. (1959). Colour vision: the approach through increment-threshold sensitivity. *Proc. Nat. Acad. Sci. USA.* **45**, 100-114.
- Tan, K.E.W.P. (1971). Cited in: Pokorny, J., Smith, V.C. and Lutze, M. (1987). Aging of the human lens. *Appl. Optics.* **26**, 1437-1440.
- Taylor, M.M. and Creelman, C.D. (1967). PEST: efficient estimates on probability functions. *J. Acoust. Soc. Am.* **41**, 782-787.

- Taylor, M.M. (1971). On the efficiency of psychophysical measurement. *J. Acoust. Soc. Am.* **49**, 505-508.
- Teesalu, P., Airaksinen, P.J., Tuulonen, A., Nieminen, H. and Alanko, H. (1997). Fluorometry of the crystalline lens for correcting blue-on-yellow perimetry results. *Invest. Ophthalmol. Vis. Sci.* **38**, 697-703.
- Thorn, F. and Boynton, R.M. (1974). Human binocular summation at absolute threshold. *Vision Res.* **14**, 445-458.
- Traquair, H.M. (1938). In: *An introduction to clinical perimetry*. London. Henry Kimpton Publishers.
- Treutwein, B. (1995). Adaptive psychophysical procedures. *Vision Res.* **17**, 2503-2522.
- Trokel (1962). The physical basis for the transparency of the crystalline lens. *Invest. Ophthalmol.* **1**, 493-501.
- Trope, G.E. and Britton, R. (1987). A comparison of Goldmann and Humphrey automated perimetry in patients with glaucoma. *Br. J. Ophthalmol.* **71**, 489-493.
- Trope, G.E., Eizenman, M. and Coyle, E. (1989). Eye movement perimetry in glaucoma. *Can. J. Ophthalmol.* **24**, 197-199.
- Tuulonen, A. and Airaksinen, P.J. (1991). Statpac 2 compared to clinical evaluation of visual fields. In: *Perimetry Update 1990/91*. Proceedings of the IXth International Perimetric Society Meeting. Eds: Mills, R.P. and Heijl, A. Kugler and Ghedini Publications. Amsterdam, Berkeley and Milano. pp. 231-233.
- Urner-Bloch, U. (1987). Simulation of the influence of lens opacities on the perimetric results, investigated with orthoptic occluders. *Doc. Ophthalmol, Proc. Ser.* **49**. Ed: Greve, E.L. Nijhoff / Junk Publishers. Dordrecht. pp. 3-8.
- Vingrys, A.J. and Demirel, S. (1993). The effect of fixation loss on perimetric thresholds and reliability. *Perimetry Update 1992/93*. Ed: Mills, R.P. Kugler Publications. Amsterdam and New York.
- Vos, J.J. and Walraven, P.L. (1971). On the derivation of the foveal receptor primaries. *Vision Res.* **11**, 799-818.

- Vos, J.J. (1984). Disability glare - a state of the art report. *CIE Journal*. **3**, 39-53.
- de Waard, P.W.T., IJspeert, J.K., van den Berg, T.J.T.P. and de Jong, P.T.V.M. (1992). Intraocular light scattering in age-related cataracts. *Invest. Ophthalmol. Vis. Sci.* **33**, 618-625.
- Wall, M., Kardon, R. and Moore, P. (1993). Effects of stimulus size on test-retest variability. In: *Perimetry Update 1992/93*. Ed: Mills, R.P. Amsterdam and New York. Kugler Publications. pp. 371-376.
- Wall, M., Kutzko, K.E. and Chauhan, B.C. (1997). Variability in patients with glaucomatous visual field damage is reduced using size V stimuli. *Invest. Ophthalmol. Vis. Sci.* **38**, 426-435.
- Wandell, B.A. and Pugh, E.N. (1980a). A field-additive pathway detects brief-duration, long-wavelength incremental flashes. *Vision Res.* **20**, 613-624.
- Wandell, B.A. and Pugh, E.N. (1980b). Detection of long-duration, long-wavelength incremental flashes by a chromatically coded pathway. *Vision Res.* **20**, 625-636.
- Watkins, R.D. (1969). Foveal increment thresholds in normal and deutan observers. *Vision Res.* **9**, 1185-1196.
- Watson, A.B. and Pelli, D.G. (1983). QUEST: a Bayesian adaptive psychometric method. *Percept. Psychophys.* **33**, 113-120.
- Weale, R.A. (1954). Light absorption by the lens of the human eye. *Optica Acta.* **1**, 107-110.
- Weale, R.A. (1961). Notes on the photometric significance of the human crystalline lens. *Vision Res.* **1**, 183-191.
- Weale, R.A. (1988). Age and transmittance of the human crystalline lens. *J. Physiol.* **395**, 577-587.
- Weale, R.A. (1991). The lenticular nucleus, light, and the retina. *Exp. Eye Res.* **53**, 213-218.
- Weale, R.A. (1992). In: *The senescence of human vision*. Oxford Press. Oxford, New York, Tokyo.

- Weber, A.J., Kaufman, P.L., Hubbard, W.C. and Stanford, L.R. (1994). Glaucoma-related neuronal degeneration in the primate retina and lateral geniculate nucleus (LGN). *Invest. Ophthalmol. Vis. Sci. (Suppl)*. **35**, 1573.
- Weber, J. and Geiger, R. (1989). Grey scale display of perimetric results - the influence of different interpolation procedures. In: *Perimetry Update 1988/89*. Proceedings of the VIIth International Perimetric Society. Ed: Heijl, A. Kugler & Ghedini. Amsterdam, Berkeley & Milano. pp. 447-454.
- Weber, J. and Krieglstein, G.K. (1989). Graphical analysis of topographical trends (GATT) in automated perimetry. *Int. Ophthalmol.* **13**, 351-356.
- Weber, J., Krieglstein, G.K. and Papoulis, C. (1989). Die graphische analyse topographischer trends (GATT) in der perimetrischen verlaufskontrolle des glaukoms. *Klin. Mbl. Augenheilk* **195**, 319-322.
- Weber, J. (1990). Eine neue strategie für die automatisierte statische perimetrie. *Fortschr. Ophthalmol.* **87**, 37-40.
- Weber, J. and Diestelhorst, M. (1992). Perimetric follow-up in glaucoma with a reduced set of test points. *Ger. J. Ophthalmol.* **1**, 409-414.
- Weber, J. and Rau, S. (1992). The properties of perimetric thresholds in normal and glaucomatous eyes. *Ger. J. Ophthalmol.* **1**, 409-414.
- Weber, J. (1993). Quantification of congruence between the right and left visual fields. *Graefe's Arch. Clin. Exp. Ophthalmol.* **231**, 704-710.
- Weber, J. and Klimaschka, T. (1995). Test time and efficiency of the dynamic strategy in glaucoma perimetry. *Ger. J. Ophthalmol.* **4**, 25-31.
- Webster, A.R., Luff, A.J., Canning, C.R. and Elkington, A.R. (1993). The effect of pilocarpine on the glaucomatous visual field. *Br. J. Ophthalmol.* **77**, 721-725.
- Weinreb, R.N. and Sample, P.A. (1991). Short-wavelength visual field testing in eyes with primary open-angle glaucoma. In *Glaucoma Update V*. Ed. Krieglstein, G.K. Springer-Verlag. Berlin and Heidelberg. pp. 146-155.

Werner, E.B. and Drance, S.M. (1977). Early visual field disturbances in glaucoma. *Arch. Ophthalmol.* **95**, 1173-1175.

Werner, J.S. (1982). Development of scotopic sensitivity and the absorption spectrum of the human ocular media. *J. Opt. Soc. Am.* **72**, 247-258.

Werner, J.S. and Hardenbergh, F.E. (1983). Spectral sensitivity of the pseudophakic eye. *Arch. Ophthalmol.* **101**, 758-760.

Werner, J.S., Donnelly, S.K. and Kliegl, R. (1987). Aging and human macular pigment density. *Vision Res.* **27**, 257-268.

Whitaker, D., Steen, R. and Elliott, D.B. (1993). Light scatter in the normal young, elderly, and cataractous eye demonstrates little wavelength dependency. *Optom. Vis. Sci.* **70**, 963-968.

Wiesel, T.N. and Hubel, D.H. (1966). Spatial and chromatic interactions in the lateral geniculate body of the rhesus monkey. *J. Neurophysiol.* **29**, 1115-1156.

Wild, J.M., Wood, J.M., Worthington, F.M. and Crews, S.J. (1987). Some concepts on the use of three-dimensional isometric plots for the representation of differential sensitivity. *Documenta Ophthalmologica Proceedings Series* 49. Eds: Greve, E.L. and Heijl, A. Nijhoff / Junk Publishers. Dordrecht. pp. 423-432.

Wild, J.M., Dengler-Harles, M., Hussey, M.K. et al (1989a). Regression techniques in the analysis of visual field loss. In: *Perimetry Update 1988/89*. Proceedings of the IXth International Perimetric Society Meeting. Ed Heijl, A. Kugler and Ghedini Publications. Amsterdam, Berkeley and Milano. pp. 207-216.

Wild, J.M., Betts, T.A., Ross, K. and Kenwood, C. (1989b). Influence of antihistamines on central visual field assessment. In: *Perimetry Update 1988/89*. Ed: Heijl, A. Amsterdam, Berkeley and Milano. Kugler and Ghedini Publications. pp. 439-445.

Wild, J.M., Dengler-Harles, M., Searle, A.E., O'Neill, E.C. and Crews, S.J. (1989c). The influence of the learning effect on automated perimetry in patients with suspected glaucoma. *Acta Ophthalmol.* **67**, 537-545.

Wild, J.M., Betts, T.A. and Shaw, D.E. (1990). The influence of a social dose of alcohol on the central visual field. *Jpn. J. Ophthalmol.* **34**, 291-297.

- Wild, J.M., Hussey, M.K., Flanagan, J.G. and Trope, G.E. (1993). Pointwise topographical and longitudinal modelling of the visual field in glaucoma. *Invest. Ophthalmol. Vis. Sci.* **34**, 1907-1916.
- Wild, J.M., Moss, I.D., Whitaker, D. and O'Neill, E.C. (1995). The statistical interpretation of blue-on-yellow visual field loss. *Invest. Ophthalmol. Vis. Sci.* **36**, 1398-1410.
- Wilson, M.E. (1967). Spatial and temporal summation in impaired regions of the visual field. *J. Physiol.* **189**, 189-208.
- Witmer, F.K. van den Brom, H.J.B., Kooijman, A.C. and Blanksma, L.J. (1989). Intra-ocular light scatter in pseudophakia. *Doc. Ophthalmol.* **72**, 335-340.
- Wolf, E. (1960). Glare and age. *Arch. Ophthalmol.* **64**, 502-514.
- Wolf, E. and Gardiner, J.S. (1965). Studies on the scatter of light in the dioptric media of the eye as a basis of visual glare. *Arch. Ophthalmol.* **74**, 338-345.
- Wong, A.Y., Dodge, R.M. and Remington, L.A. (1995). Comparing threshold visual fields between the Dicon TKS 4000 automated perimeter and the Humphrey Field Analyzer. *J. Am. Optom. Assoc.* **66**, 706-711.
- Wood, J.M., Wild, J.M. and Crews, S.J. (1987a). Induced intraocular light scatter and the sensitivity gradient of the normal visual field. *Graefe's Arch. Clin. Exp. Ophthalmol.* **225**, 369-373.
- Wood, J.M., Wild, J.M., Hussey, M.K. and Crews, S.J. (1987b). Serial examination of the normal visual field using Octopus automated projection perimetry: Evidence for a learning effect. *Acta Ophthalmol.* **65**, 326-333.
- Wood, J.M., Wild, J.M., Bullimore, M.A. and Gilmartin, B. (1988). Factors affecting the normal perimetric profile derived by automated static threshold LED perimetry. I. Pupil size. *Ophthalm. Physiol. Opt.* **8**, 26-31.
- Wood, J.M., Wild, J.M., Smerdon, D.L., and Crews, S.J. (1989). Alterations in the shape of the automated perimetric profile arising from cataract. *Graefe's Arch. Clin. Exp. Ophthalmol.* **227**, 157-161.

Wright, W.D. (1951). The visual sensitivity of normal and aphakic observers in the ultra-violet. *Ann. Psychol.* **50**, 169-177.

Wu, J., Cheng, G., Poinosawmy, D., Liu, X. and Hitchings, R. (1994). Improved reliability estimates in the Humphrey visual field test in glaucoma using a knowledge based system. Presented as a paper at the Xith International Perimetric Society Meeting, Washington DC, USA. July 3-7th 1994: 25.

Wynanski, T., Desatnik, H., Quigley, H.A. and Glovinsky, Y. (1995). Comparison of ganglion cell loss and cone loss in experimental glaucoma. *Am. J. Ophthalmol.* **120**, 184-189.

Wyszecki, G. and Stiles, W.S. (1982). In: *Colour Science. Concepts and methods, quantitative data and formulae*. 2nd Ed; John Wiley and Sons Inc. pp. 514-549.

Yager, D., Yuan, R. and Mathews, S. (1992). What is the utility of the psychophysical "light scattering factor"? *Invest. Ophthalmol. Vis. Sci.* **33**, 688-690.

Yeh, T., Smith, V.C. and Pokorny, J. (1989). The effect of background luminance on cone sensitivity functions. *Invest. Ophthalmol. Vis. Sci.* **30**, 2077-2086.

Zalta, A.H. and Burchfield, J.C. (1990). Detecting early glaucomatous field defects with the size I stimulus and STATPAC. *Br. J. Ophthalmol.* **74**, 289-293.

Zalta, A.H. (1991). Use of a central 10° field and size V stimulus to evaluate and monitor small central islands of vision in end stage glaucoma. *Br. J. Ophthalmol.* **75**, 151-154.

Zeimer, R.C. and Noth, J.M. (1984). A new method for measuring in vivo the lens transmittance, and study of lens scatter, fluorescence and transmittance. *Ophthalmic Res.* **16**, 246-255.

Zeimer, R.C., Lim, H.K. and Ogura, Y. (1987). Evaluation of an objective method for the in vivo measurement of changes in light transmittance of the human crystalline lens. *Exp. Eye. Res.* **45**, 969-976.

Zeyen, T.G., Zulauf, M. and Caprioli, J. (1993). Priority of test locations for automated perimetry in glaucoma. *Ophthalmology.* **100**, 518-522.

Zeyen, T., Roche, M., Brigatti, L. and Caprioli, J. (1995). Formulas for conversion between Octopus and Humphrey threshold values and indices. *Graefe's Arch. Clin. Exp. Ophthalmol.* **233**, 627-634.

Zulauf, M., Flammer, J. and Signer, C. (1986). The influence of alcohol on the outcome of automated static perimetry. *Graefe's Arch. Clin. Exp. Ophthalmol.* **224**, 525-528.

Zulauf, M., Caprioli, J., Hoffman, D.C. and Tressler, C.S. (1991). Fluctuation of the differential light sensitivity in clinically stable glaucoma patients. In: *Perimetry Update 1990/91*. Proceedings of the IXth International Perimetric Society Meeting. Eds: Mills, R.P. and Heijl, A. Kugler and Ghedini Publishers. Amsterdam, New York and Milano. pp. 183-188.

Zulauf, M., LeBlanc, R.P. and Flammer, J. (1994). Normal visual fields measured with Octopus-Program G1. II. Global visual field indices. *Graefe's Arch. Clin. Exp. Ophthalmol.* **232**, 516-522.

APPENDIX: A1.

Abstracts

Cubblidge, R.P., and Wild, J.M. (1995). The influence of different thresholding strategies on the fatiguing perimetric profile. *Invest. Ophthalmol. Vis. Sci. (suppl)*. **36**, 942.

Cubblidge, R.P., Wild, J.M., Robinson, R. and O'Neill, E.C. (1996). The attenuation of the short-wavelength perimetric response by age-related cataract. *Invest. Ophthalmol. Vis. Sci. (suppl)*. **37**, 3465.

Wild, J.M., Cubblidge, R.P., Pacey, I. and Robinson, R. (1996). Pointwise analysis of short-wavelength automated perimetry thresholds in a normal population. *Invest. Ophthalmol. Vis. Sci. (suppl)*. **37**, 4998.

Publications.

Wild, J.M., Cubblidge, R.P., Pacey, I.E. and Robinson, R. Statistical aspects of the normal visual field derived by short-wavelength automated perimetry. *Invest. Ophthalmol. Vis. Sci.* In Press.